

## University of Bradford eThesis

This thesis is hosted in [Bradford Scholars](#) – The University of Bradford Open Access repository. Visit the repository for full metadata or to contact the repository team



© University of Bradford. This work is licenced for reuse under a [Creative Commons Licence](#).

# **ASSESSMENT OF LIME-TREATED CLAYS UNDER DIFFERENT ENVIRONMENTAL CONDITIONS**

**Hatim Farag Adem ALI**

**Submitted for the Degree of Doctor of Philosophy**

**Faculty of Engineering and Informatics  
University of Bradford**

**2019**

## **Abstract**

Hatim Farag Adem ALI

Assessment of lime-treated clays under different environmental conditions

**Keywords:** Expansive clay, Lime stabilisation, Compaction delay, ambient temperature, Swelling pressure, unconfined compressive strength, and permeability coefficient.

Natural soils in work-sites are sometimes detrimental to the construction of engineering projects. Problematic soils such as soft and expansive soils are a real source of concern to the long-term stability of structures if care is not taken. Expansive soils could generate immense distress due to their volume change in response to a slight change in their water content. On the other hand, soft soils are characterised by their low shear strength and poor workability. In earthwork, replacing these soils is sometimes economically and sustainably unjustifiable in particular if they can be stabilised to improve their behaviour. Several techniques have evolved to enable construction on problematic soils such as reinforcement using fibre and planar layers and piled reinforced embankments.

Chemical treatment using, e.g. lime and/or cement is an alternative method to seize the volume change of swelling clays. The use of lime as a binding agent is becoming a popular method due to its abundant availability and cost-effectiveness. When mixed with swelling clays, lime enhances the mechanical properties, workability and reduces sensitivity to absorption and release of water. There is a consensus in the literature about the primary mechanisms, namely cation exchange, flocculation and pozzolanic reaction, which cause the changes in the soil characteristics after adding lime in the presence of water.

The dispute is about whether these mechanisms occur in a sequential or synchronous manner. More precisely, the controversy concerns the formation of cementitious compounds in the pozzolanic reaction, whether it starts directly or after the cation exchange and flocculation are completed.

The current study aims to monitor the signs of the formation of such compounds using a geotechnical approach. In this context, the effect of delayed compaction, lime content, mineralogy composition, curing time and environmental temperature on the properties of lime-treated clays were investigated.

The compaction, swelling and permeability, and unconfined compression strength tests were chosen to evaluate such effect. In general, the results of the geotechnical approach have been characterised by their scattering. The sources of this dispersion are numerous and include sampling methods, pulverisation degree, mixing times and delay of compaction process, a pre-test temperature and humidity, differences in dry unit weight values, and testing methods. Therefore, in the current study, several precautions have been set to reduce the scattering in the results of such tests so that they can be used efficiently to monitor the evolution in the properties that are directly related to the formation and development of cementitious compounds. Four clays with different mineralogy compositions, covering a wide range of liquid limits, were chosen. The mechanical and hydraulic behaviour of such clays that had been treated by various concentrations of lime up to 25% at two ambient temperatures of 20 and 40°C were monitored for various curing times.

The results indicated that the timing of the onset of changes in mechanical and hydraulic properties that are related to the formation of cementitious compounds depends on the mineralogy composition of treated clay and ambient



temperature. Moreover, at a given temperature, the continuity of such changes in the characteristics of a given lime-treated clay depends on the lime availability.

## **Dedication**

Dedicated to my mother (Mariam Helal) my father (Farag), my wife (Hind), my children Mariam, Faraj, Mohmmud, and Maria, my brothers Hosam and Hamza, and My sisters Manal, Marwa, Monia and Safa.

## **Acknowledgement**

I want to express my honest gratitude to my supervisor Dr Mostafa Mohamed for his continuous support, encouragement and guidance.

I am indebted to Dr Mostafa Mohamed for facilitating my study from the beginning by giving me beneficial support and pieces of advice.

Dr Mohamed's broad knowledge and his valuable advice in geotechnical engineering gave me the chance to command successful research. I would also like to express my gratitude to Dr Mehdi Mizrababei for his help to improve the readability of my thesis.

Without doubt, big thanks to all technicians in the Faculty of Engineering and Informatics for their support throughout my laboratory work.

## Contents

|   |      |
|---|------|
| Abstract.....   | i    |
| Dedication.....                                       | iv   |
| Acknowledgement.....                                  | v    |
| List of figures.....                                  | xi   |
| List of tables.....                                   | xvii |
| Chapter 1 Introduction.....                           | 1    |
| 1.1 Motivation and background.....                    | 1    |
| 1.2 Aims and objectives:.....                         | 2    |
| 1.3 Structure of the thesis:.....                     | 3    |
| Chapter 2 Literature review.....                      | 4    |
| 2.1 Clay and clay minerals.....                       | 4    |
| 2.1.1 Kaolinite minerals.....                         | 9    |
| 2.1.2 Smectite minerals.....                          | 10   |
| 2.2 Lime stabilisation.....                           | 12   |
| 2.2.1 Hydration.....                                  | 16   |
| 2.2.2 Cation exchange and flocculation.....           | 16   |
| 2.2.3 Carbonisation.....                              | 18   |
| 2.2.4 Crystallisation and solidification.....         | 20   |
| 2.3 Effectiveness of lime stabilisation.....          | 24   |
| 2.3.1 Mixing techniques.....                          | 25   |
| 2.3.2 Mellowing period and mellowing temperature..... | 28   |
| 2.3.3 Curing time and curing temperature.....         | 30   |

|           |  |    |
|-----------|--|----|
| 2.3.4     | Type of clay mineral.....  | 34 |
| 2.4       | Summary:.....  | 39 |
| Chapter 3 | Materials and Methodology.....   | 41 |
| 3.1       | Materials.....   | 41 |
| 3.1.1     | Soil.....  | 41 |
| 3.1.2     | Lime.....  | 43 |
| 3.2       | Testing techniques.....  | 44 |
| 3.2.1     | Specimen preparation.....  | 44 |
| 3.2.2     | Unconfind compressive strength.....  | 46 |
| 3.2.3     | Compaction tests.....  | 52 |
| 3.2.4     | Swelling and permeability tests.....   | 59 |
| 3.3       | Testing programme.....   | 64 |
| 3.3.1     | Series 1: Effect of deficiency of wetting on the evolution of swelling<br>pressure.....  | 66 |
| 3.3.2     | Series 2: Impact of compaction delay and environmental<br>temperature.....   | 68 |
| 3.3.3     | Series 3: Effects of lime content and environmental temperature on<br>the properties of extremely high plastic clay.....                     | 71 |
| 3.3.4     | Series 4: Short and long term assessment of lime treatment of<br>expansive clays with different mineralogy at low and high temperatures..... | 73 |
| 3.3.5     | Series 5: Short term assessment of lime treatment of expansive<br>clays with different mineralogy at low and high temperature.....           | 76 |
| 3.4       | Summary.....   | 77 |

|           |  |     |
|-----------|--|-----|
| Chapter 4 | Experimental results and discussion.....   | 79  |
| 4.1       | Series 1: Effect of deficiency of wetting on the evolution of swelling pressure.....   | 79  |
| 4.1.1     | Introduction.....  | 79  |
| 4.1.2     | Effect of initial dry unit weight and moisture content.....  | 79  |
| 4.1.3     | Swelling behaviour using a modified approach.....  | 89  |
| 4.1.4     | Summary.....   | 95  |
| 4.2       | Series 2: Impact of compaction delay and environmental temperature.....  | 96  |
| 4.2.1     | Introduction.....  | 96  |
| 4.2.2     | Dry unit weight.....   | 96  |
| 4.2.3     | Swelling pressure and permeability.....  | 98  |
| 4.2.4     | Unconfined Compressive Strength.....   | 105 |
| 4.2.5     | Summary.....   | 112 |
| 4.3       | Series 3: Effects of lime content and environmental temperature on the properties of extremely high plastic clay.....                | 114 |
| 4.3.1     | Introduction.....  | 114 |
| 4.3.2     | Dry unit weight.....   | 114 |
| 4.3.3     | Unconfined Compression Strength.....   | 118 |
| 4.3.4     | Permeability coefficients.....   | 122 |
| 4.3.5     | Summary.....   | 125 |
| 4.4       | Series 4: Short-long term assessment of lime treatment of expansive clays with different mineralogy at low and high temperature..... | 127 |
| 4.4.1     | Introduction.....  | 127 |

|           |   |     |
|-----------|---|-----|
| 4.4.2     | Evolution of unconfined compression strength of lime treated M1 (bentonite clay).....   | 127 |
| 4.4.3     | Evolution of unconfined compression strength of lime treated M2 (ball clay).....  | 132 |
| 4.4.4     | Evolution of unconfined compression strength of lime-treated M3 (mix of 1 portion of bentonite to 3 portions of ball clay)..... | 135 |
| 4.4.5     | Evolution of unconfined compression strength of lime treated M4 (Mix of 1 portion of bentonite to 1 portion of ball clay).....  | 138 |
| 4.4.6     | Mineralogical effects.....  | 141 |
| 4.4.7     | Collapse pattern and desiccation cracks.....  | 145 |
| 4.4.8     | Summary.....  | 150 |
| 4.5       | Series 5: Short term assessment of lime treatment of expansive clays with different mineralogy at low and high.....             | 152 |
| 4.5.1     | Introduction.....   | 152 |
| 4.5.2     | Swelling and permeability characteristics of untreated clays.....   | 152 |
| 4.5.3     | Impact of mineralogy composition, lime content mellowing time and temperature on permeability coefficients.....                 | 156 |
| 4.5.4     | Impact of mineralogy composition, lime content, mellowing time and temperature on swelling tendency.....                        | 174 |
| 4.5.5     | Summary.....  | 189 |
| Chapter 5 | Conclusions and future recommendations.....   | 190 |
| 5.1       | Conclusions.....  | 190 |
| 5.1.1     | Conclusions of series 1.....  | 190 |

|       |                              |     |
|-------|------------------------------|-----|
| 5.1.2 | Conclusions of series 2..... | 191 |
| 5.1.3 | Conclusions of series 3..... | 2   |
| 5.1.4 | Conclusions of series 4..... | 3   |
| 5.1.5 | Conclusions of series 5..... | 6   |
| 5.1.6 | Main conclusion.....         | 8   |
| 5.2   | Future work.....             | 9   |
|       | References:.....             | 11  |



## List of figures

|   |    |
|---|----|
| Figure 2.1: 1:1 mineral layer, adopted from Brigatti et al. (2006).....   | 8  |
| Figure 2.2: 1:2 mineral layer, adopted from Brigatti et al. (2006).....   | 9  |
| Figure 3.1: Fine hydrated lime which was passed through a 425 $\mu$ m sieve.....  | 43 |
| Figure 3.2: Preparation stages of lime treated clay mixtures for testing.....   | 46 |
| Figure 3.3: Compaction equipment for preparation of UCS specimens.....  | 47 |
| Figure 3.4: Cross-section diagram illustrates the dimensions of compaction<br>equipment for UCS specimens.....                                  | 48 |
| Figure 3.5: hydraulic Jack press.....   | 48 |
| Figure 3.6: UCS specimen preparation steps (to form the first third of<br>specimen's height).....   | 50 |
| Figure 3.7: UCS specimen preparation steps (to form second third of<br>specimen's height).....  | 51 |
| Figure 3.8: Final stage in preparing UCS specimens.....   | 52 |
| Figure 3.9: Mini compaction apparatus.....  | 54 |
| Figure 3.10: Dimensions of the mini-compaction tools.....   | 55 |
| Figure 3.11: Hammering pattern for compaction.....  | 56 |
| Figure 3.12: Effect of changing the number of compacted layers from 3 layers (a)<br>to 6 layers (b).....  | 56 |
| Figure 3.13: Fabricated mould to compact the specimens used for swelling and<br>permeability tests.....   | 61 |
| Figure 3.14: GDS oedometer system equipped with a conventional cell.....  | 63 |
| Figure 3.15: GDS oedometer system equipped with a hydraulic cell and GDS<br>digital pressure/volume controller.....                             | 63 |
| Figure 3.16: Cross section of the hydraulic cell.....   | 64 |
| Figure 4.1: Maximum swelling pressures as a function of dry unit weights at<br>different moisture contents (11, 20, 27, and 35%).....           | 80 |
| Figure 4.2: Evolution of swelling pressure for specimens at an initial moisture<br>content of 35% (i.e., tested using a conventional cell)..... | 87 |
| Figure 4.3: Evolution of swelling pressure for specimens at an initial moisture<br>content of 27% (i.e., tested using a conventional cell)..... | 87 |
| Figure 4.4: Evolution of swelling pressure for specimens at an initial moisture<br>content of 20% (i.e., tested using a conventional cell)..... | 88 |

|  |     |
|--|-----|
| Figure 4.5: Evolution of swelling pressure for specimens compacted at an initial moisture content of 11% (i.e., tested using a conventional cell).....                                 | 88  |
| Figure 4.6: Evolution of swelling pressure for specimens at an initial moisture content of 11% (i.e., tested for 24h using a conventional cell).....                                   | 89  |
| Figure 4.7: Cylindrical sections extracted from the specimen prepared at shipped moisture content and tested for 24h.....  | 89  |
| Figure 4.8: Maximum swelling pressures against corresponding dry unit weights for specimens (i.e., tested using hydraulic cell and conventional cells).....                            | 90  |
| Figure 4.9: Maximum applied forces versus corresponding dry unit weights for specimens (i.e., tested using hydraulic and conventional cells).....                                      | 91  |
| Figure 4.10: Maximum unit volume swelling force versus specimen density for specimens at an initial moisture content of 11% (i.e., tested using hydraulic and conventional cells)..... | 91  |
| Figure 4.11: a) A prepared specimen with moisture content of 11% b) Vertical section of the specimen at the end of test using hydraulic cell.....                                      | 92  |
| Figure 4.12: Evolution of swelling pressure for specimens at an initial moisture content of 11% (i.e., tested using a hydraulic cell).....   | 94  |
| Figure 4.13: Effect of mellowing and temperature on the dry unit weight.....   | 97  |
| Figure 4.14: Swelling pressures of specimens tested directly after compaction.....   | 98  |
| Figure 4.15: Swelling pressures of specimens tested after 24h from mixing...   | 101 |
| Figure 4.16: Coefficient of permeability versus submersion period for a group I at 20°C with 7% lime.....  | 104 |
| Figure 4.17: Coefficient of permeability versus submersion period for a group I at 40°C with 7% lime.....  | 104 |
| Figure 4.18: Coefficient of permeability versus submersion period for a group 2 at 20°C with 7% lime.....  | 105 |
| Figure 4.19: Coefficient of permeability versus submersion period for a group 2 at 40°C with 7% lime.....  | 105 |
| Figure 4.20: Effect of mellowing periods on development of strength gain at 20°C with 7% lime.....   | 107 |
| Figure 4.21: Effect of mellowing periods on development of strength gain at 40°C with 7% lime.....   | 108 |
| Figure 4.22: Effect of the mellowing period on UCS after 1 and 28 days at different temperature with 7% lime.....  | 109 |

|  |     |
|--|-----|
| Figure 4.23: Strain behaviour a function of mellowing period after a 1 day.....  | 111 |
| Figure 4.24: Strain behaviour a function of mellowing period after 7 days.....   | 111 |
| Figure 4.25: Strain behaviour a function of mellowing period after 28 days.....  | 112 |
| Figure 4.26: Dry unit weight against mellowing periods at 40°C for various lime contents.....                                  | 115 |
| Figure 4.27: Dry unit weight against mellowing periods at 20°C for various lime contents.....                                  | 116 |
| Figure 4.28: UCS against curing time at 40°C for various lime contents.....  | 119 |
| Figure 4.29: UCS against curing time at 20°C for various lime contents.....  | 120 |
| Figure 4.30: Correlations for the strength gain rate during stage 1 at both temperatures.....                                  | 121 |
| Figure 4.31: Coefficient of permeability on specimens mellowed at 40°C for various lime contents.....                          | 124 |
| Figure 4.32: Coefficient of permeability on specimens mellowed at 20°C for various lime contents.....                          | 125 |
| Figure 4.33: Evolution of strength gain with time for lime treated M1 specimens cured at 20°C.....                             | 128 |
| Figure 4.34: Evolution of strength gain with time for lime treated M1 specimens cured at 40°C.....                             | 129 |
| Figure 4.35: Comparison between the presumed and measured strength after curing for 672h at 20°C and 40°C on M1 specimens..... | 132 |
| Figure 4.36: Evolution of strength gain with time for lime treated M2 specimens at 20°C.....                                   | 133 |
| Figure 4.37: Evolution of strength gain with time for lime treated M2 specimens at 40°C.....                                   | 133 |
| Figure 4.38: Evolution of strength gain with time for lime treated M3 specimens at 20°C.....                                   | 137 |
| Figure 4.39: Evolution of strength gain with time for treated M3 specimens at 40°C.....  | 137 |
| Figure 4.40: Comparison between the presumed and measured strength after curing for 672h at 20°C and 40°C on M3 specimens..... | 138 |
| Figure 4.41: Evolution of strength gain with time for M4 specimens at 20°C...  | 139 |
| Figure 4.42: Evolution of strength gain against curing time for M4 specimens at 40°C.....                                      | 140 |

|   |     |
|---|-----|
| Figure 4.43: Comparison between the presumed final strength and measured strength after curing for 672h at 20°C and 40°C for treated M4 clay.....           | 141 |
| Figure 4.44: Impact of bentonite Content (BC) on the kinetic of strength gain during the first phase at the different curing temperatures.....              | 143 |
| Figure 4.45: Typical cone-split failure pattern on lime treated clays after 28 days .....   | 146 |
| Figure 4.46: Stress-strain relationships on lime treated clays: L = 13%, T = 40°C and C = 672h.....   | 147 |
| Figure 4.47: Type of collapse patterns over the curing time on M1 specimens .....   | 148 |
| Figure 4.48: Stress-strain relationships on lime treated M1 specimens as a function of curing time.....   | 149 |
| Figure 4.49: Behaviour of desiccation cracks during the drying process of M1 and M4 at zero h.....  | 150 |
| Figure 4.50: Influence of bentonite content on the liquid limit, optimum moisture content, and maximum dry unit weight.....                                 | 153 |
| Figure 4.51: Evolution of swelling pressure for four clay types over the testing time.....  | 154 |
| Figure 4.52: Evolution of volume of water flow for four clay types over the testing time.....   | 155 |
| Figure 4.53: Evolution of permeability coefficients of lime treated bentonite (M1) specimens that were previously cured for 24h at 20°C.....                | 159 |
| Figure 4.54: Evolution of permeability coefficients of lime treated bentonite (M1) specimens that were previously cured for 24h at 40°C.....                | 160 |
| Figure 4.55: Evolution of permeability coefficients of lime treated (M2) ball specimens that were previously mellowed for 24h at 20°C.....                  | 162 |
| Figure 4.56: Evolution of permeability coefficients of lime treated M2 ball specimens that were previously mellowed for 24h at 40°C.....                    | 162 |
| Figure 4.57: Evolution of permeability coefficients of lime treated ball (M2) specimens that were previously cured for 24h at 20°C.....                     | 164 |
| Figure 4.58: Evolution of permeability coefficients of lime treated ball (M2) specimens that were previously cured for 24h at 40°C.....                     | 164 |
| Figure 4.59: Evolution of permeability coefficients of lime treated 1:3 bentonite to ball (M3) specimens that were previously mellowed for 24h at 20°C..... | 165 |

|   |     |
|---|-----|
| Figure 4.60: Evolution of permeability coefficients of lime treated 1:3 bentonite to ball (M3) specimens that were previously mellowed for 24h at 40°C..... | 166 |
| Figure 4.61: Evolution of permeability coefficients of lime treated 1:3 bentonite to ball specimens that were previously cured for 24h at 20°C.....         | 167 |
| Figure 4.62: Evolution of permeability coefficients of lime treated 1:3 bentonite to ball (M3) specimens that were previously cured for 24h at 40°C.....    | 168 |
| Figure 4.63: Evolution of permeability coefficients of lime treated 1:1 bentonite to ball (M4) specimens that were previously mellowed for 24h at 20°C..... | 170 |
| Figure 4.64: Evolution of permeability coefficients of lime treated 1:1 bentonite to ball (M4) specimens that were previously mellowed for 24h at 40°C..... | 171 |
| Figure 4.65: Evolution of permeability coefficients of lime treated 1:1 bentonite to ball (M4) specimens that were previously cured for 24h at 20°C.....    | 173 |
| Figure 4.66: Evolution of permeability coefficients of lime treated 1:1 bentonite to ball (M4) specimens that were previously cured for 24h at 40°C.....    | 173 |
| Figure 4.67: Evolution of swelling pressures of lime treated bentonite (M1) specimens that were previously mellowed for 24h at 40°C.....                    | 177 |
| Figure 4.68: Evolution of swelling pressures of lime treated bentonite (M1) specimens that were previously cured for 24h at 40°C.....                       | 177 |
| Figure 4.69: Evolution of swelling pressures of lime treated bentonite (M1) specimens that were previously mellowed for 24h at 20°C.....                    | 178 |
| Figure 4.70: Evolution of swelling pressures of lime treated bentonite (M1) specimens that were previously cured for 24h at 20°C.....                       | 178 |
| Figure 4.71: Evolution of swelling pressures of lime treated ball (M2) specimens that were previously mellowed for 24h at 40°C.....                         | 180 |
| Figure 4.72: Evolution of swelling pressures of lime treated ball (M2) specimens that were previously cured for 24h at 40°C.....                            | 181 |
| Figure 4.73: Evolution of swelling pressures of lime treated ball (M2) specimens that were previously mellowed for 24h at 20°C.....                         | 181 |
| Figure 4.74: Evolution of swelling pressures of lime treated ball (M2) specimens that were previously cured for 24h at 20°C.....                            | 182 |
| Figure 4.75: Evolution of swelling pressures of lime treated M3 specimens that were previously mellowed for 24h at 40°C.....                                | 183 |
| Figure 4.76: Evolution of swelling pressures of lime treated M3 specimens that were previously cured for 24h at 40°C.....                                   | 184 |

|   |     |
|---|-----|
| Figure 4.77 Evolution of swelling pressures of lime treated (M3) specimens that were previously mellowed for 24h at 20°C..... | 184 |
| Figure 4.78: Evolution of swelling pressures of lime treated (M3) specimens that were previously cured for 24h at 20°C.....   | 185 |
| Figure 4.79: Evolution of swelling pressures of lime treated M4 specimens that were previously mellowed for 24h at 40°C.....  | 187 |
| Figure 4.80: Evolution of swelling pressures of lime treated M4 specimens that were previously cured for 24h at 40°C.....     | 188 |
| Figure 4.81: Evolution of swelling pressures of lime treated M4 specimens that were previously mellowed for 24h at 20°C.....  | 188 |
| Figure 4.82: Evolution of swelling pressures of lime treated M4 specimens that were previously cured for 24h at 20°C.....     | 189 |

## List of tables

|   |     |
|---|-----|
| Table 2.1: Units and sheets of clay minerals.....   | 7   |
| Table 3.1: Chemical analysis of bentonite and ball as provided by the supplier.....   | 41  |
| Table 3.2: Geotechnical properties for utilised clay materials.....   | 43  |
| Table 3.3: Overall view on the testing programme.....   | 65  |
| Table 3.4: Swelling pressure tests schedule with conventional cell (first phase in series 1 tests).....   | 67  |
| Table 3.5: Swelling pressure tests schedule with hydraulic cell (second phase in series 1 tests).....   | 68  |
| Table 3.6: Testing programme for series 2.....  | 71  |
| Table 3.7: Testing programme for series 3.....  | 73  |
| Table 3.8: Testing programme for series 4.....  | 75  |
| Table 3.9: Testing programme for series 5.....  | 77  |
| Table 4.1: Analysis of strength gain after 24h from mixing at 20°C and 40°C.....  | 109 |
| Table 4.2: Exponential equations that govern the permeability coefficient of lime treated M1 specimens that were previously mellowed for 24h..... | 156 |
| Table 4.3: Exponential equations that govern the permeability coefficient of M1 specimens that were previously cured for 24h.....                 | 159 |
| Table 4.4: Exponential equations that govern the permeability coefficient of M3 specimens that were previously mellowed for 24h.....              | 166 |
| Table 4.5: Exponential equations that govern the permeability coefficient of M3 specimens that were previously cured for 24h.....                 | 168 |
| Table 4.6: Exponential equations that govern the permeability coefficient of M4 specimens that were previously mellowed for 24h.....              | 171 |
| Table 4.7: Exponential equations that govern the permeability coefficient of M4 specimens that were previously cured for 24h.....                 | 174 |
| Table 4.8: Resulting Maximum swelling pressures for all lime treated M1 specimens.....  | 175 |
| Table 4.9: Resulting Maximum swelling pressures for all lime treated M2 specimens.....  | 180 |
| Table 4.10: Resulting Maximum swelling pressures for all lime treated M3 specimens.....   | 183 |

Table 4.11: Resulting Maximum swelling pressures for all lime treated M4  
specimens..... 187



## **Chapter 1 Introduction**

### **1.1 Motivation and background**

The presence of expansive clays in construction sites poses significant concerns to both design and site engineers due to their substantial volumetric changes with drying and wetting cycles. Montmorillonite minerals group that has a voracity to absorb water is responsible for the volumetric behaviour of such expansive clay (Estabragh et al., 2014, Thyagaraj et al., 2016, Sridharan and Prakash, 2000). Problematic soils such as expansive soils are characterised by their significant volume changes (Swelling/shrinkage) upon a change in the moisture content. Ground movements due to their volume change could cause severe distress to structures erected above or within the expansive soil layers if appropriate measures are not undertaken. Expansive soils are encountered in arid and semiarid regions (Al-Rawas and Goosen, 2006) in more than 60 worldwide countries, including the UK (Shi et al., 2002). The Association of British Insurers estimated that losses caused by expansive soils are in the region of £400M per year in the UK (Driscoll and Crilly, 2000). Thus, it is imperative that treatment/stabilisation measures are implemented to suppress the severity and consequences of potential ground movement associated with the swelling and shrinkage behaviour of expansive clays.

Over the past few decades, several preventative techniques have been proposed and implemented to reduce or limit potentially destructive impacts of the volumetric change of expansive clays on structures. These techniques such as; replacement of near-surface expansive clay, control of compaction and moisture content, addition of fibrous materials (Mirzababaei et al., 2013), stabilisation using chemical agents (Mirzababaei et al., 2009, Soltani et al.,

2017) and traditional chemical treatment using lime, cement and fly ash (Schanz and Elsawy, 2015, Thyagaraj et al., 2016). Due to its low cost, technical efficiency and abundant availability; lime treatment is by far the most common way to suppress volumetric change and enhance the strength of expansive clays

## **1.2 Aims and objectives:**

The principal aim of this investigation is to provide a deeper understanding of the effect of lime treatment on medium to extremely plastic clays. Five comprehensive series of testing programmes are designed to assess the impact of lime treatment on compaction, strength, swelling, and permeability of clays under different conditions. In this context, the following objectives were set:

- 1- Developing testing techniques to enhance the accuracy and repeatability of the chosen tests results
- 2- Studying the effect of delayed compaction under two surrounding temperatures.
- 3- Monitoring the short- and long-term lime-clay reaction through the impact of different lime contents on the evolution of strength of four clays at two different ambient temperatures using the evolution of strength gain as an indication about the development of such reaction.
- 4- Observing the evolution of lime-clay reaction in the short term using the swelling and permeability tests under several designed conditions including two delayed compaction times, various mineral composition, temperature, and lime contents.

### **1.3 Structure of the thesis:**

In this research, an extensive examination of the influence of lime addition on the mechanical behaviour of clay soils has been performed. The thesis has been organised in 5 chapters. Following the introduction, chapter 2 includes a critical review of the technical literature in the area of lime stabilised clays.

Chapter 3 provides details of the materials and methodology that were used in this research. The experimental work was divided into five series to achieve the objectives of the research

According to this organisation, the results of the five experimental series have been presented, discussed and analysed in chapter 4. Chapter 5 presents the conclusions for each experimental series in addition to suggestions for conducting future investigation works.

## **Chapter 2 Literature review**

The first section of this chapter introduces the definitions of clays and clay minerals. The following section begins with an introduction on the lime stabilisation, followed by a general description of the main reactions accompanying the lime added to the clay in the presence of water. In the third section, a critical review of the factors impacting the resulting characteristics of lime treated clay and thus on the efficiency of lime treatment is presented. Finally, a summary of controversial issues in lime stabilisation is presented.

### **2.1 Clay and clay minerals**

“Clay” indicates to a natural matter which mainly contains fine-grained minerals. Such minerals convert from solid state to plastic state at determined moisture content and become hard if fired or dried. The clays contain mainly phyllosilicates minerals besides other substances. These substances bring plasticity when hydrated and hardness when dehydrated to clay (Guggenheim and Martin, 1995). According to Guggenheim and Martin (1995) this definition has four conditions as follow:

- 1- Clays are nature, inorganic matters; therefore, the term of clay cannot be used for synthetic clay and clay-like materials. Based on that, the peat and muck are not considered as clay, although both contain nature matters. The reason behind the exclusion of peat, muck, and some other soils is their high amount of organic materials, and the definition determines "mainly contains fine-grained minerals" and it is well known that minerals are inorganic matters.
- 2- Clay particles are classed as fine-grained. Here it is worth noting that fine-grain indicate to the size of the crystal not to the size of aggregate.

- 3- Plasticity is considered one of the main criteria in the above definition of clay. However, it should be mentioned that the plasticity characteristic is profoundly affected by the chemical composition of substances and their aggregates size.
- 4- Phyllosilicates are primary minerals besides the non-clay minerals such as quartz, feldspar, and calcite or non-crystalline matters such as colloidal silica, organic gels, and iron hydroxide gels.

"clay minerals" include the phyllosilicate minerals, in addition to other minerals provided that these minerals bring the plasticity upon hydration and the hardness upon dehydration to clay Guggenheim and Martin (1995). According to Bergaya and Lagaly (2006), there are some differences between the term "clay" and "clay minerals" that can be summarised as follow:

- 1- Unlike definition of clay, description of clay minerals does not indicate the source of minerals (whether they are natural or synthetic). Therefore, the term clay mineral could be used for natural or artificial minerals.
- 2- Unlike definition of clay, the size of crystalline is not essential for the definition of clay minerals.
- 3- Non-phyllosilicate minerals are considered clay minerals as well if they bring the plasticity if hydrated and the hardness if dehydrated to clay.

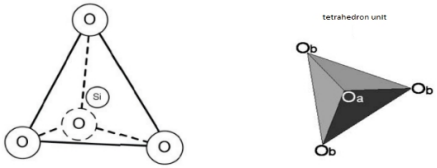
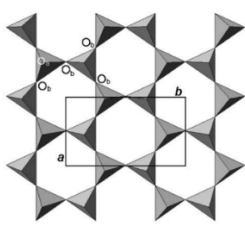
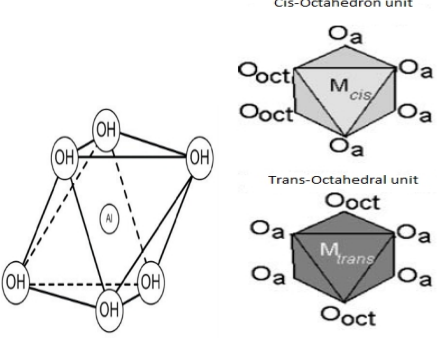
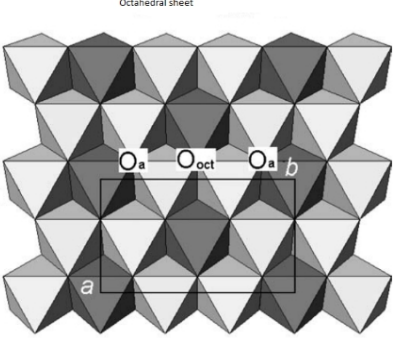
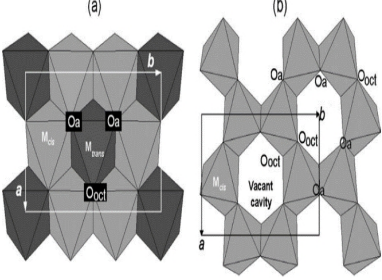
Generally, mineral structures contain two kinds of sheets called the tetrahedral sheet and octahedral sheet. The tetrahedral sheet comprises of a number tetrahedron units, and each tetrahedron contains a cation. This cation is likely to be silicon or might be  $\text{Al}^{3+}$  or  $\text{Fe}^{3+}$  (Brigatti et al., 2006), surrounded by 4 oxygen atoms. Three of the four oxygen atoms form the base of a tetrahedron unit are called basal oxygen atoms ( $\text{O}_b$ ). Basal oxygen atoms in each tetrahedron unit

are shared with the adjacent tetrahedron units infinitely in both crystal graphic directions. Such sharing leads to form hexagonal rings in the tetrahedral sheets as illustrated in Table 2.1. The fourth oxygen atom is called the apical atom ( $O_a$ ). Apical oxygen atoms in each tetrahedral sheet head in the same direction of tetrahedral sheets as seen in Figures 2.1 and 2.2.

Regarding octahedral sheets, the octahedron units form the octahedral sheet where each neighbouring octahedron units are sharing one edge. This sharing leads to form the hexagonal or pseudo-hexagonal symmetry structure as illustrated in Table 2.1. The octahedron unit contains six oxygen or six hydroxyl ions that octahedrally surrounded a central ion of  $Al^{3+}$  or  $Mg^{2+}$  cation. In addition to the aforementioned cations  $Fe^{3+}$ ,  $Fe^{2+}$ ,  $Li^+$ ,  $Mn^{2+}$ ,  $Co^{2+}$ ,  $Ni^{2+}$ ,  $Cu^{2+}$ ,  $Zn^{2+}$ ,  $V^{3+}$ ,  $Cr^{3+}$ , and  $Ti^{4+}$  cations were identified by Brigatti et al. (2006).

It is worth noting that in the octahedral sheet if  $Mg^{2+}$  cations occupy central positions in all constituent octahedron units of the octahedral sheet, the layer is called “Brucite” layer. In contrast, if the two third of the central position is occupied by Al cation, the layer is called the “Gibbsite layer” (Barnes, 2000). Table 2.1 illustrates the units and sheets that form clay minerals.

Table 2.1: Units and sheets of clay minerals

|   |   |   |
|---|---|---|
| Tetrahedron unit  |    | <p>It comprises of 4 oxygen ions (O), three basal (<math>O_b</math>) and one apical (<math>O_a</math>), tetrahedrally nestled around a cation of <math>Si^{4+}</math> or other ions such as <math>Al^{3+}</math> or <math>Fe^{3+}</math>.</p>   |
| Tetrahedral sheets  |    | <p>It can be seen that each tetrahedron unit share its basal oxygen atoms with neighbouring tetrahedron unit in two directions. Moreover, it can be noted the hexagonal ring that forming between the tetrahedron units. <i>a</i> and <i>b</i> symbolise the unit-cell parameters.</p>  |
| Octahedron unit with its two topologies                     |   | <p>It contains 6 oxygen or hydroxyl ions, nestled around a <math>Al^{3+}</math> or <math>Mg^{2+}</math> cation, in addition to the aforementioned cations <math>Fe^{3+}</math>, <math>Fe^{2+}</math>, <math>Li^+</math>, <math>Mn^{2+}</math>, <math>Co^{2+}</math>, <math>Ni^{2+}</math>, <math>Cu^{2+}</math>, <math>Zn^{2+}</math>, <math>V^{3+}</math>, <math>Cr^{3+}</math>, and <math>Ti^{4+}</math>. According to the hydroxyl ions position, the topology of octahedron can be trans-oriented or cis-oriented. It is worth noting that the position of <math>O_{oct}</math> can be occupied by OH, Cl, F, or O. This position is located near the centre of the hexagonal ring of the tetrahedral sheet, but it is not linked with the tetrahedral sheet.</p> |
| Octahedral sheet  |  | <p>Each octahedron unit shares its edges with neighbouring octahedron units as in the figure forming the octahedral sheet. This sharing leads to forming the hexagonal or pseudo-hexagonal symmetry. Note that, in the building of mineral unit cell, the octahedral sheet participated by six sites. The topology of Four of six sites is cis-oriented, whereas the topology of the rest remains as trans-oriented.</p>  |
| Trioctahedral sheet(Bricut) and Diocahedral sheet(Gibbsite) |  | <p>In the unit-cell, if the six sites are occupied, the sheet is called Trioctahedral sheet, whereas, if just four are occupied, the sheet is called Diocahedral (Brigatti et al., 2006). Whitlow (2001) stated that, if four of the six central positions are aluminium cations, the sheet is called Gibbsite. If all central position is occupied by magnesium cation, the sheet is called Brucite sheet.</p>   |

Source: the figures were adopted from (Whitlow, 2001, Brigatti et al., 2006)

Nevertheless, if the apical oxygen atoms in one tetrahedral sheet link their sheet to an octahedral sheet forming a layer, this layer is called a 1:1 mineral layer as in Figure 2.1. Repetition of this mineral layer builds the quasicrystal of the 1:1 clay mineral. In contrast, if two tetrahedral sheets sandwiched an octahedral sheet they form the 1:2 layer clay minerals as in Figure 2.2. Repetition of this layer forms the quasicrystal of 1:2 clay mineral (Brigatti et al., 2006).

1:1 and 1:2 clay minerals can be divided into Trioctahedral or Dioctahedral depending on the category of central ions. To be more precise, if the octahedral sheet is a Gibbsite sheet, the mineral belongs to the Dioctahedral subgroup. In contrast, if the octahedral sheet is Brucite, the mineral belongs to the Trioctahedral sheet subgroup (Budhu, 2000).

It is worth noting that the oxygen  $O^{2-}$  and hydroxyl  $OH^-$  ions have a dominant role in the structure of minerals due to their number and size. They usually cause the existence of a slight negative charge although the stratification of their negative charge occurs due to their presence in the surface of the sheets. Moreover, the other cause of a net negative charge could appear if the aluminium ion  $Al^{3+}$  substitutes the  $Si^{4+}$  in tetrahedral sheet or if  $Mg^{2+}$  substitutes the  $Al^{3+}$  in the octahedral sheet (due to their abundance at the time of occurrence) (Fang and Daniels, 2006).

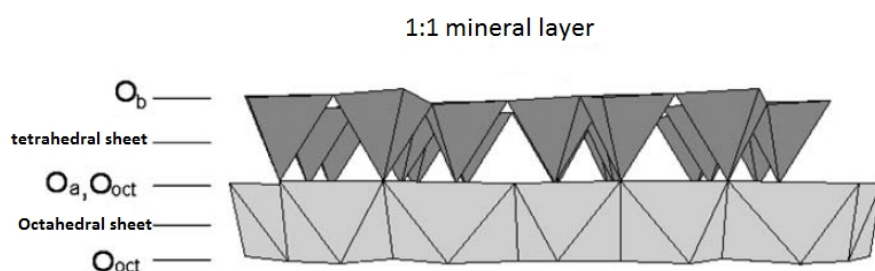


Figure 2.1: 1:1 mineral layer, adopted from Brigatti et al. (2006)



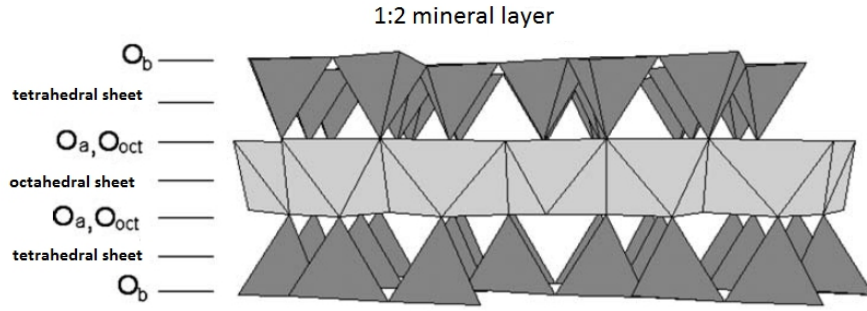


Figure 2.2: 1:2 mineral layer, adopted from Brigatti et al. (2006)

Clay minerals can be classified depending on the type of layer structure (two or three layers), the category of interlayer atoms, the character of octahedral sheets, and the value of the net layer charge (Zhang et al., 2010). In the context of classification of the clay minerals, Whitlow (2001) classified the clay minerals into four groups depending on the arrangement of layers and the type of linkage between stacked layers, in addition to the specific surface area and cation exchange capacity. According to Whitlow (2001), clay mineral groups are kaolinite, illite, montmorillonite (smectite), and vermiculite. However, Details of kaolinite and smectite are discussed below as they form primary minerals in the clays that are used in this investigation:

### 2.1.1 Kaolinite minerals

Kaolinite minerals belong to the Serpentine-kaolin group under the dioctahedral sub-group (Martin et al., 1991). The formula 2.1 represents the chemical composition of kaolinite minerals:



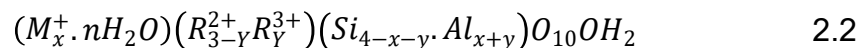
Kaolinite minerals are the main mineral in kaolin, China clay (Barnes, 2000) and ball clay (Bergaya and Lagaly, 2006). They have a flaky shape with a size reaching to 3 microns (Whitlow, 2001). Barnes (2000) stated that they have a

regular structure. In contrast, Brigatti et al. (2006) indicated existence of both ordered and disordered structures in kaolinite mineral. Kaolinite minerals comprise of up to 100 of 1:1 mineral layers linked tightly by hydrogen bonds (Whitlow, 2001). Barnes (2000) stated that the cation exchange capacity of kaolinite is low and ranges from 3 to 15 me/100. Whitlow (2001) reported that the kaolinite minerals have a small specific surface area ranging between 10 to 30 m<sup>2</sup>/g. Further, the periodicity between two mineral layers is about 0.7 nm (Brigatti et al., 2006). Their low swelling and shrinkage ability characterise kaolinite minerals. Concerning Atterberg limits, unlike the diffuse double layer (DDL) that govern the plasticity in montmorillonite minerals, repulsive and attractive forces between particles govern the arrangement of the kaolinite particles which in turn controls the liquid limit (Sridharan et al., 1988).

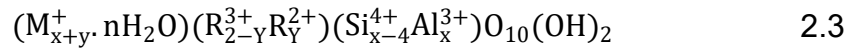
### 2.1.2 Smectite minerals

Brigatti et al. (2006) stated that smectite minerals belong to 2:1 phyllosilicate minerals which are characterised as carrying a negative layer charge ranging from 0.2 to 0.6 per half unit cell as reported by Martin et al. (1991). Depending on the Dioctahedral or Trioctahedral layer, the chemical composition of the octahedral layer, and position of layer charge, the smectite can be categorised into Trioctahedral and Dioctahedral smectite (Martin et al., 1991).

Trioctahedral smectite is characterised by all sites of the octahedral sheet that are occupied by the divalent cation. Saponite, Hectorite, and Sauconite represent the most common minerals in this group. The formula 2.2 represents Trioctahedral smectite group:

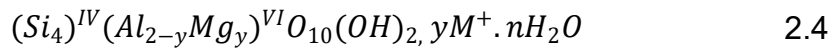


In contrast, if two of the three sites are occupied by trivalent cations, the mineral can be classified as Dioctahedral smectite and follow the formula 2.3:



where; X and y represent layer charges resulting from tetrahedral and octahedral respectively, M represents the interlayered cations and R the substituted cations in octahedral sheet and tetrahedral sheet.

The Montmorillonite minerals belong to Dioctahedral smectite group with the formula 2.4:



A broad spectrum of cations can occupy Tetrahedral, octahedral, and interlayer positions. In tetrahedral sites, the substitution of  $R^{3+}$  for  $Si^{4+}$  generates a surplus of negative charges on the three basal oxygen atoms and the apical oxygen atom, with an impact on the total charge of the 2:1 layer in addition to the local charge at the surface of the layer. Octahedral sites are generally occupied by  $Al^{+3}$ ,  $Fe^{3+}$ ,  $Fe^{2+}$ ,  $Mg^{2+}$ ,  $Ni^{2+}$ ,  $Zn^{2+}$ , and  $Li^{+}$ . Substitution of  $R^{2+}$  for  $R^{3+}$  in Dioctahedral smectite generates a surplus of negative layer charge, whereas, in Tri-octahedral smectite, a substitution of  $R^{3+}$  for  $R^{2+}$  creates an excess of positive charges. Brigatti et al. (2006) stated that hydration of interlayer cations, the interactions take place between interlayer cations, water molecules, surfaces of clay minerals, and activity of water in the system of water-clay minerals are considered the key factors affecting the hydration in interlayer regions and thus the swelling in smectite minerals.

## **2.2 Lime stabilisation**

According to the National Lime Association (NLA, 2007), the commercial lime is divided into two groups, quick lime, and hydrated lime. The quick lime is generated from calcination of limestone, which comprises of calcium and magnesium oxides. Depending on the content of magnesium carbonate in the limestone, the quick lime can be classified into high calcium quicklime and dolomitic quicklime. However, addition of enough moisture content to satisfy affinity of quick lime to water leads to the formation of hydrated lime. The hydrated lime could be classified into high calcium hydrated lime, dolomitic hydrated lime-normal, and dolomitic hydrated lime- pressure. The three types can be derived from quicklime depending on the rate of hydration, the category of quicklime and the percentage of quicklime (Mohd Yunus et al., 2014).

Hydrated lime is more popular than the quicklime, although the latter is more effectual than hydrated lime due to its higher content of lime oxide and its role in the disposal of excess water by evaporating such water due to the heat that generates during its hydration (Ingles and Metcalf, 1972). Unlike the ease of use of hydrated lime and its safety, dealing with quick lime requires care and taking precautions so as not to touch the skin in addition to its harmful impact on machinery and equipment in the workplace. It is worth noting that the hydrated lime, due to its fine particles and its larger surface compared to quick lime, offers more close contact with soil particles (Mohd Yunus et al., 2014).

Lime as a chemical stabiliser has been used to improve the properties of soils. The effect of lime is evident in that it reduces the plasticity index, swelling and shrinkage potential in the short-term; whereas, in the long term, it increases the strength properties and durability of the stabilised soil. In order to ensure

reliability and durability of earthwork treated with lime, the designed treatment should determine the following: 1) appropriateness of lime to treat the soil; 2) the water content-dry unit weight relationship; 3) initial lime consumption.

### **1- Appropriateness of lime to treat soils**

Plasticity index, swelling characteristics, clay content, distribution of grain size, organic material content and sulphate content are used to assess the suitability of a given soil to lime treatment (Little et al., 1995, McNally, 1998).

Ingles and Metcalf (1972) stated that each 10% of clay in the soil should be treated by 1% of lime by weight of dry soil. However, Bell (1996) added that the lime content should not exceed 8% even if the clay content is more than 80%. Bell (1996) stated that the excess addition of lime can have a harmful impact in the strength characteristics; attributing this behaviour to the lime, which is considered as a lousy fill and does not have marked cohesion or friction. Similarly, Dash Sujit and Hussain (2012) noted that strength gain declines on lime stabilised bentonite specimens if they were treated with more than 9% of lime. In contrast, (Al-Mukhtar et al., 2010b) observed that as the lime content increase as the strength increase with the bentonite clay treated by lime contents reach up to 20%.

### **2- Moisture content-dry unit weight relationship**

Head (1992) abbreviated the advantages of using the compaction in five points:

1) It renders the soil more stable because of the expected improvement in the value of shear strength; 2) It reduces the potential settlement in the soil by reducing the ability the compressibility of soil to a limit level. 3) It declines the voids ratio, which in turn reduces the ability of the soil to absorb water, resulting in the decline in the permeability of the soil; 4) it reduces the deformation

resulting from repeated loads through an increase in the value resulting from CBR to lower levels; 5) it reduces the effect of the frost heave. The British Standard BS1377: Part 4:1990:3.3 for Proctor compaction and BS1377: Part 4:1990:3.5 for modified Proctor compaction test are used to define the compaction curve and to determine optimum moisture content (OMC) and maximum dry unit weight (MDU). Soil characteristics such as grain size distribution, texture, Atterberg limits, particle shape, and moisture content control the quality of the compaction process.

Generally, addition of lime leads to a decline in the maximum dry unit weight and increase in the optimum moisture content (Sweeney et al., 1988, Mitchell and Hooper, 1961, Osinubi and Nwaiwu, 2006). Bell (1996) concluded that the lime addition renders the water-dry unit weight curve tend to flatten.

In terms of the mineralogy composition, Bell (1996) noted that lime-treated kaolinite clays achieve higher densities than the lime-treated montmorillonite clay attributing that to the higher affinity of expansive soils to water compared to non-expansive soils. Holt and Freer-Hewish (1998) interpreted the changes in OMC by the hydration process and increase in the voids ratio as a result of the flocculation process; whereas the changes in MDU were attributed to the flocs that arise during flocculation and agglomeration processes.

### **3- Initial lime consumption (ILC)**

Engineers must determine the percentage of lime necessary to ensure long term reaction. Initial consumption of lime test (ICL) aims to define the least percentage of lime needed to bring about long-term strength alterations. Depending on the changes in the pH value, Grim and Eades (1966) set a test for ICL in order to determine the minimum percentage of lime required to begin

the pozzolanic reaction. According to (ASTM D6276 -19), ICL or Lime Fixation Point is the smallest percentage of lime required to generate a soil pH of 12.4. The pH of 12.4 represents the degree of alkaline required to generate a pozzolanic reaction. Therefore, the smallest amount of lime added to the soil, causing a pH of 12.4, is considered as the least percentage needed for soil stabilisation (Davidson et al., 1965).

However, Rogers and Roff (1997) pointed out that there are two problems regarding the fulfilment of the test of ICL and interpretation of its outcomes. Concerning the interpretation, the test assumes that the stabilisation stage (induced by pozzolanic reaction) will only begin if the modification stage (induced by cation exchange and flocculation) is completed. Regarding the fulfilment of the test, Rogers and Roff (1997) referred that some clays inherently seem to act in a way that the pH value of 12.4 is never reached. Rogers and Roff (1997) also indicated to the existence of various ways of pH measurements can give uneven results. Moreover, impurity of lime, temperature, and amount of water might lead to uneven pH measurements (Tran et al., 2014). Therefore, Rogers and Roff (1997) introduced the modified initial lime consumption test using the changes in the plastic limit as an indicator, considering that the minimum percentage of lime that after which there is no further changes in the plastic limit as the modified initial lime consumption. However, the concept of initial lime is still used in the British standard (BS1924-2:1990). Further, the pH value has been used to monitor the development of lime-clay reaction (Boardman et al., 2001, Al-Mukhtar et al., 2014, Di Sante et al., 2014).

The reactions that take place after the lime addition to the soil in the presence of water are widely described by many researchers such as (Diamond and Kinter, 1965, Diamond and Kinter, 1966, Grim and Eades, 1966, Boardman et al., 2001, Bell, 1996, Rogers and Roff, 1997, Di Sante et al., 2014, Zhao et al., 2015, Vitale et al., 2017, Vitale et al., 2016b, Chemedda et al., 2018). These reactions are as follow:

### **2.2.1 Hydration**

The Hydration process takes place immediately when quicklime is added to the soil in the presence of water. This process works on eliminating superfluous water from the soil system. Thus, it improves the workability by consuming the excessive water through the reaction between quicklime and water in process so-called (slaking) to produce hydrated lime and the hydration's exothermic heat that causes evaporation of water (Di Sante et al., 2014, Tran et al., 2014). The exothermic energy resulting during the hydration might reach up to 65 kJ/mol (Rogers and Roff, 1997).

Quicklime hydration has a side effect that can cause an increase in the volume of treated soil leading to the generation of harmful distress in confining condition (Beetham et al., 2015). Such a potential increase in the volume might lead to appearance of cracks and thus a reduction in strength (Holt et al., 2000).

### **2.2.2 Cation exchange and flocculation**

The hydrated lime decomposes partially into hydroxyl ions and calcium ions (Beetham et al., 2015). Hydroxyl increases the pH of the pore water to nearly 12.4, and as the pH value increases, the number of negatively charge sites rises (Al-Mukhtar et al., 2014), whereas, calcium ions tend to replace the monovalent cations on the surface of the clay particles such as sodium or any



native cations in the process called cation exchange. However, it is well known that the surfaces of clay particles have instability in charges, appearing a negative charge that is inherently balanced by native hydrated cations such as sodium, potassium, and the adsorbed water molecules. These ions circle a clay particle, creating a layer called the diffuse double layer (DDL). Beetham et al. (2015) stated that the primary factor influencing the thickness of the diffuse double layer is a valence of incoming cations. The incoming cations generate attractive forces toward the clay surface higher than those between monovalent cations on the clay surface. Thus, the surface of the clay particle could be balanced by a lesser number of hydrated cations (Strawn et al., 2015). Instantly, adjacent clay particles become closer due to the reduced thickness of a double layer, interacting with each other and reconfiguring within clusters of clay flocs which in turn agglomerate together forming an open flocculated clay fabric (Zhao et al., 2015). The short term reaction gives the clay the silt character and reduces the specific surface area of clay mineral in touch with water (Bell, 1996).

The concept of the initial lime consumption test is based on the non-participation of hydroxyl ions in the reaction in the short term. However, Verhasselt (1990) reported that calcium chloride generates practically none of the immediate impacts of calcium hydroxide in concern with flocculation, though the calcium itself is considered a vigorous flocculant. The fact that calcium chloride has a higher solubility than calcium hydroxide and thus if the immediate effects of lime were just due to the adsorption calcium cations, calcium chloride should be more efficient than calcium hydroxide. Verhasselt (1990) also found that addition of sodium hydroxide alone to the soil has also no impact on the same soil. On the other hand, Verhasselt (1990) observed that there was an

immediate impact similar to the effect of lime on the soil in the case of using sodium hydroxide and calcium chloride together to treat the same soil. Aforementioned indicates that the concurrent existence of calcium cation and hydroxyl anions is indispensable to modify the soil characteristics in short and long term.

Chemeda et al. (2018) investigated the interfacial chemistry of lime-kaolinite reaction in short term and the impact of short term reaction on long term reaction through its impact on dissolution of alumina and silica from the surface of kaolinite particles. Chemeda et al. (2018) concluded that there are two critical roles played by the aggressive alkaline environment in the short-term reaction. Firstly, it dictates the prevalent species of calcium obtainable for adsorption, i.e.  $\text{CaOH}^+$ , which neutralises one charge site per calcium ion. Secondly, its role in the deprotonation of the three active sites that cause an increase in the potential negative surface. The accumulation of such calcium species works on isolating the surface of kaolinite minerals from the aggressive alkaline environment so that it inhibits the release of silica and alumina ions and further prevents the formation of cementitious compounds in the short term.

On the other hand, with the montmorilinitic clay, (Diamond and Kinter, 1965, Vitale et al., 2017) observed formation of cementitious compounds in a short time. Diamond and Kinter (1965) referred to the role of such cementitious compounds during the modification stage in linking the flocculated particles at their contact, preventing the reverse of the outcome of the modification stage.

### **2.2.3 Carbonisation**

Exposure of lime to carbon dioxide spurs the carbonisation reaction. The exposure of lime to carbon dioxide is difficult to avoid since it might take place

during manufacturing of lime, storage processes, or even when the lime is mixed with the soil in the laboratory or on site (Jucai, 2014). Bagoniza et al. (1987) investigated to the effect of carbonisation on lime stabilised soil and concluded the following:

- 1- Carbonation harms the development of the pozzolanic compounds and even ceases their formation, causing a reduction in the strength value of lime treated soil.
- 2- Carbonation might occur even after a successful stabilisation process.

Zhao et al. (2015) indicated that carbon dioxide reacts with calcium or magnesium hydroxide continuously in presence of air, forming solid particles or crystal of calcium or magnesium carbonate namely calcite, characterised by their strength. Zhao et al. (2015) pointed out to the possibility of forming these components even after long periods, considering the carbonation as a competitor consumer for calcium ions in pore water during pozzolanic reaction.

Al-Mukhtar et al. (2012) observed formation of such calcite crystals ( $\text{CaCO}_3$ ), considering them as weak cementitious matters and pointed out that at the higher content of lime of 10%, formation of calcium carbonate was more noticeable. Concerning its harmful effect on the pH value and strength, Paige-Green (2009) stated that pH value gradually declines from 12.4 to 8.3 as a result of lime consumption in the carbonation. Moreover, carbonation is accompanied by a growth in the volume in short term, whereas it is accompanied by the drop in the amount of cementitious matters in long term. Carbonisation leads to disturbance in cementitious compounds, causing a reduction in strength properties (Paige-Green, 2009).

It is worth noting that there is an indirect harmful effect of intensive carbonation on lime stabilisation because it causes formation of calcium carbonate-silicate sulphate hydrated minerals (Köhler et al., 2006) if the soil contains sulphate component (Little et al., 2010).

#### **2.2.4 Crystallisation and solidification**

Solidification or stabilisation in terms of lime treatment is believed to be caused by the long-term reaction, so-called the pozzolanic reaction. Temperature, unconsumed lime and mineralogy of the soil play critical roles in controlling the kinetics of the pozzolanic reaction (Al-Mukhtar et al., 2014).

In brief, hydroxyl ions, that disassociate from calcium hydroxide, increase the pH value in pore water to nearly 12.4 and as the pH value increases the number of negatively charged sites rises (Al-Mukhtar et al., 2014). The aggressive alkaline environment in the pore water partially destroys the clay layers launching silica and alumina anions in the pore water. Concentration and availability of silica and alumina ions are dependent upon the mineralogy of soil (Cristelo et al., 2012). Cristelo et al. (2012) stated that, chemically, the hydroxyl ions tend to attack molecular bonds between Si-O-Si, Al-O-Al, and Al-O-Si producing both alumina and silica anions in the surrounding medium. Alumina and silica anions react with calcium and hydroxyl ions forming desirable cementitious compounds in the form of calcium-silicate-hydrates (CSH), calcium-aluminate-silicate hydrates (CASH) and calcium-aluminate-hydrates (CAH). Many researchers have widely reported formation of these cementitious compounds, see for example (Diamond and Kinter, 1965, Bell, 1996, Tran et al., 2014, Zhao et al., 2015, Boardman et al., 2001, Vitale et al., 2017, Vitale et al., 2016c, Maubec et al., 2017, Di Sante et al., 2014, Al-Mukhtar et al., 2010b, Al-

Mukhtar et al., 2010a, Grim and Eades, 1966). Formation of the cementitious compounds strengthens convergence points between particles within the flocs and between the flocs within the aggregates. Immediate formation of such compounds and their role in enhancing the flocculation and agglomeration were reported by (Diamond and Kinter, 1965, Vitale et al., 2017). Immediate formation of cementitious compounds is contradictory to the outcomes of studies that refer to late formation of cementitious compounds to up to 7 days (Boardman et al., 2001). It is also debatable that whether the pozzolanic reaction takes place in the pores water (Beetham et al., 2015) or on the surface and/or edge of clay particles (Boardman et al., 2001, Al-Alwan, 2019).

Availability of alumina and silica, degree of alkalinity in the surrounding medium, and strength of molecular bonds have a direct impact on the provided rate of alumina and silica (Beetham et al., 2015). There are different opinions about the alkaline environment and its value and its continuity necessary to destroy the clay mineral layers to realise the silica and alumina. For instance, Cristelo et al. (2012) stated that the pH value of pores water should be more than 9 to create the aggressive alkaline medium capable of attacking the surface of clay minerals to launch the alumina and silica. Bell (1996) emphasised that pH value of 12.4 in the pore water should be kept nearly constant as it is to ensure maximum reactivity.

The availability of alumina and silica is fundamental to this reaction, though the amount of dissolved aluminate and/or silicate sought after to maintain the reaction is small and the clay content is not limiting if the plasticity index exceeds 10% (Beetham et al., 2015). (ASTM C618 - 19) requires that the total percentage of chemical components of silicon dioxide, aluminium oxide, and

iron oxide exceed 70% of the total components in any material to be considered as a natural pozzolan. However, He et al. (1995) stated that the amount of silicon dioxide, aluminium oxide, and iron oxide exceeds 80% of the total components in most clays.

Regarding the strength of molecular bonds, although the amount of silica in the clays is higher than alumina content, the amount of dissolved alumina is higher than dissolved silica. The higher tendency of alumina to be dissolved was attributed to the fact that the Si-O-Si bonds are stronger than Al-O-Al. Cristelo et al. (2012) chemically investigated the effect of lime on high plastic clay. They reported that dissolution of alumina ions was extremely higher compared to silica ions at the beginning of lime-soil reaction. Furthermore, as the time elapsed the dissolution of alumina ions reduced, and dissolution of silica ions gradually and continuously raised.

The availability of alumina or silica at the time when the reaction takes place controls the outputs of pozzolanic reactions. The appearance of cementitious compounds such calcium aluminate hydrate (CAH), calcium silicate hydrate (CSH), or calcium silicate aluminate hydrate (CSAH) depends on the abundant reactants during the reaction (alumina or silica) (Beetham et al., 2015).

As mentioned in the clay mineral section, the layer of 1:2 clay minerals such as illite and montmorillonite have an octahedral sheet (alumina source) located between two tetrahedral sheets (silica source). On the other hand, the layer of 1:1 clay mineral such as kaolinite mineral layer contains just octahedral and tetrahedral sheet. The expansive 1:2 clay minerals such montmorillonite with their additional silicate sheet have a higher tendency to be dissolved. They are characterised by their higher reactivity due to their higher specific surface areas

compared with specific surface areas of 1:1 clay minerals such as kaolinite. However, the specific surface area is not the only factor in the control of the rate of dissolution of alumina and silica. For example, though illite minerals have higher specific surface areas compared with kaolinite minerals the rate of dissolution of alumina and silica in case of illite minerals is smaller than in kaolinite minerals (Bell, 1988, Boardman et al., 2001).

Al-Mukhtar et al. (2014) indicated that expansive 1:2 clay minerals need less energy to open their silicate layers compared with non-expansive 1:2 clay minerals. This observation was attributed to the interlayered cations that occupy the interlayered space of expansive minerals that includes the exchangeable cations such as  $\text{Na}^+$ ,  $\text{Ca}^{2+}$ , and  $\text{Mg}^{2+}$  whereas the interlayered spaces in non-expansive 1:2 clay such illite have  $\text{K}^+$  cations that are difficult to exchange.

In contrast, Bauer and Berger (1998) reported that in highly alkaline solutions (Potassium hydroxide), the dissolved rate of kaolinite was higher than that of montmorillonite minerals. This dispute has been settled by Chemedha et al. (2018) when reported the accumulation of a kind of calcium cations on the surfaces of kaolinite minerals in the case of using calcium hydroxide. This accumulation prevents the alkaline environment from attacking the surface of kaolinite particles, leading to a delay in the release of reactants and thus a delay in the formation of cementitious compounds.

Difference in structures of clay minerals led Bauer and Berger (1998) to assume that the release of silica and alumina should be sequential; silica first, followed by alumina in the case of 1:2 clay minerals; Whereas, the launch of silica and alumina should be concurrent in the case of 1:1 clay mineral. Bauer and Berger (1998) reported that unlike preference of launching the silica in the case of

montmorillonite minerals, the preference of launching the alumina was prevalent with kaolinite minerals. This corresponds to the observation in the following studies: With lime-treated kaolinite, (Vitale et al., 2017, Maubec et al., 2017) reported the formation of calcium aluminate hydrate phase after 28 days of curing at 20°C, whereas, the calcium silicate hydrate phase was just observed by Maubec et al. (2017) after more than three months of curing at 50°C. On the other hand, (Vitale et al., 2017, Pomakhina et al., 2012) confirmed the immediate formation of calcium silicate hydrate with lime-treated bentonite, whereas the formation of calcium aluminate hydrates and calcium aluminate silicates were reported after a long time.

Further, (Al-Mukhtar et al., 2010a, Al-Mukhtar et al., 2010b) observed the evolution of cementitious compounds in a lime-treated expansive soil. This expansive soil comprised of 58% of Smectite and 38% of kaolinite minerals. The presence of calcium aluminate hydrates ( $\text{Ca}_3\text{Al}_2\text{O}_6 \cdot n\text{H}_2\text{O}$ ) was reported after 1 and 7 days at 50 and 20°C, respectively; whereas, presence of calcium silicate hydrates was just observed at 50°C after 7 days. Preference of forming the aluminate hydrates confirms the conclusion made by (Cristelo et al., 2012) about the preference of reacting with the alumina.

### **2.3 Effectiveness of lime stabilisation**

The efficiency of lime treatment was found to be dependent on many factors such as amount and type of lime, mineralogy composition of clay, moisture content, dry unit weight, temperature, compaction delay and degree of pulverization (Bozbey and Garaisayev, 2010, Beetham et al., 2014, Beetham et al., 2015).



### **2.3.1 Mixing techniques**

At a work site nowadays, unlike curing conditions and type of soil, the mixing conditions can be controlled in no small extent with the rapid development of mixing equipment. The mixing conditions include the mixing methods, mixing time, and initial and final degree of pulverisation. Toohey et al. (2013) stated that even under similar curing conditions, the individual field specimens showed significant unevenness in unconfined compression strength results. Toohey et al. (2013) attributed that to the procedures of mixing in the field are less consistent compared with the lab procedures. The better the mixing, the better the distribution and the propagation diffusion of lime and thus, the more efficient the stabilisation phase (He et al., 1995). In laboratory investigation, Grisolia et al. (2013) stated for the same binder-soil mixtures the non-standardization of mixing steps leads to the results being so varied that comparisons are not feasible.

The degree of pulverisation is an essential parameter in chemical stabilisation. Petry and Wohlgemuth (1988) conducted an experimental program investigating the impact of the degree of pulverisation on the strength of highly plastic clay (plasticity index of 60%) treated by lime and Portland cement. Petry and Wohlgemuth (1988) reported that the existence of large clay clods harms the quality of chemical stabilisation and the properties of chemically treated clay. They added that unlike expansive soil the light clays and granular soils can be effortlessly pulverised therefore pulverisation process becomes less critical. Bozbey and Garaisayev (2010) attributed the importance of pulverisation in the case of treating expansive soils to their high plasticity that make it difficult to obtain an adequate pulverisation degree.

Bozbey and Garaisayev (2010) conducted a testing programme to assess the impact of the degree of pulverisation on workability, plasticity index, swelling and compressibility, elastic module, and strength of lime treated expansive soil. The results revealed that the more significant amount of lime-treated soil passing through the 4.76 mm sieve, the higher the efficiency of lime stabilisation. In the lab, the researchers resort to adopting either the wet-regime mixing to mimic the use of lime in a slurry form in situ or the dry-regime mixing to simulate the adding of lime in a powder. Holt and Freer-Hewish (1998) conducted a study to evaluate the effect of mellowing periods on the resulting characteristics from short- and long-term reactions. In this context, the mixing methods (dry regime and wet regime) were used as parameters. With the drying regime, the soil in the dry state was mixed in a mechanical mixer with a specific quantity of lime. The mixing process continued until ensuring that lime was adequately distributed. The wet regime included the addition of a specific amount of water to the soil, followed by thoroughly mixing until obtaining a homogeneous mixture. The mixture was kept into an air-tight container for 24h, then the specific amount of lime was added and mixed thoroughly in a mechanical mixer until it gets a homogeneous mixture. The short-term effects of the mixing regime can be abbreviated as follows:

- 1- The pH values of wet-regime specimens are slightly higher than those of the dry regime. This was attributed to the existence of water in specimens of wet-regime that facilitates the dissolution of lime.
- 2- The plasticity index values of the wet-regime specimen were higher than those of dry-regime specimens. This initial difference was attributed to that the dry-regime involves adding lime to the soil in the absence of

water; therefore, the lime was appropriately distributed throughout the dry-regime specimens.

- 3- The Optimum moisture content and maximum dry unit weight of dry-regime specimens were lesser and greater respectively than those of wet regime. This is due to the increased size of clods in the wet regime, causing an increase in the demand for water and higher resistance to the compactability.

Holt and Freer-Hewish (1998) recommended that the effects of a wet mixing method could be elevated by using the mellowing and subsequent remixing to reduce the clod size and obtain a more uniform mixture. More recently, a study conducted by Pakbaz and Farzi (2015) aimed to compare between the wet-mixing way and dry-mixing way using unconfined compressive strength tests. The soil (sand bentonite mixture) were treated by various percentages of lime, cement or lime-cement reached up to 8% by dry mass. Both wet-regime specimens and dry-regime specimens were cured for 7, 14, 28 days before being subjected to unconfined compression tests. Their results revealed that the strength of dry lime treated specimens was higher than wet lime treated specimens, and this was the opposite for cement treated specimens.

In British standard (BS 1924-1:1990), untreated materials in a dry state are mixed first with intended moisture content before adding cement or lime. On the other hand, according to (ASTM D3551 - 17), untreated materials are mixed with the stabiliser in dry state before adding the designed moisture content. Unlike British standard, ASTM D3551 - 17 prescribes in detail the time required for each mixing step. Kitazume and Terashi (2013) stated that the mixing time is an indicator to reflect how passably the mixing of binder and untreated materials

has been fulfilled. Kitazume and Terashi (2013) indicated that the proportion of strength noticeably declines if the mixing period was less than 10 min. On the other hand, the proportion of strength grows just slightly when the mixing period is more than 10 min.

### **2.3.2 Mellowing period and mellowing temperature**

Compaction delay is considered as an integral step to facilitate lime treatment in many engineering standards without adequate scientifically-based justifications (Holt and Freer-Hewish, 1998). Despite receiving less attention, some studies were conducted to pinpoint scientific justification for the consequences of compaction delay such as (Mitchell and Hooper, 1961, Sweeney et al., 1988, Holt and Freer-Hewish, 1998, Holt et al., 2000, Bhattacharja et al., 2003, Osinubi, 1998, Gallage et al., 2012, Adefemi and Wole, 2013, Ocheipo et al., 2013, Di Sante et al., 2015). Compaction delay has been given different terminology, e.g. mellowing period (Holt and Freer-Hewish, 1998, Holt et al., 2000), amelioration period (Gallage et al., 2012), rotting period, and ageing period (Sweeney et al., 1988). Delaying the start of the compaction process was found necessary in declining the size of clay clods before starting the compaction in order to meet the pulverisation requirements (Holt and Freer-Hewish, 1998). Recently, the required pulverisation is easy to reach using stronger and more effective onsite plants. However, compaction delay sometimes cannot be controlled, owing to several technical and logistical on-site factors (Di Sante et al., 2015). Osinubi (1998) recommended based on his experimental results to undertake compaction immediately after the application of lime to avoid the destruction of the slowly formed cementitious compounds, while others recommended delaying the compaction process to obtain quality

workable material (Bhattacharja et al., 2003). To the best of the authors' knowledge, unlike the agreement about the role played by compaction delay in improving the workability and dry unit weight reduction, no consensus was reached on the effects of compaction delay on the hydraulic and mechanical properties of lime treated expansive soils. For instance, although several standards require compaction delay of up to 48h, Mitchell and Hooper (1961) reported that delaying compaction for 24h has a detrimental impact in curbing the swelling pressure of expansive Californian soil and leads to a reduced long-term strength.

In contrast, Sweeney et al. (1988) concluded that compaction delay of up to 24h results in no significant effect on swelling pressure(Sweeney et al., 1988). Of note, both (Sweeney et al., 1988, Mitchell and Hooper, 1961) utilised quick lime in the treatment of expansive clay soils giving rise to additional effects by the hydration process. The optimum mellowing period was introduced by Holt et al. (2000) to allow for enough reaction time between lime and soil before compaction in order to avoid appearance of cracks that could lead to loss of strength.

The focus of most of the aforementioned studies was on the duration of compaction delay regardless of the effect of temperature on the progress of interaction before and after compaction except studies by (Holt and Freer-Hewish, 1998, Holt et al., 2000) in which compaction delay impacts were assessed at temperatures of 5°C, 10°C and 20°C. They reported that there was no effect of temperature on the strength of specimens that previously were mellowed up to 12h. However, they added that with prolonger mellowing time, the temperature effect on the strength during mellowing depends on the type of

soil. The effects of the higher degree of temperatures during the mellowing time were not assessed. The impact of ambient temperature on the strength gain was reported extensively (see for example; (Bell, 1996, Rao and Shivananda, 2005, Boardman et al., 2001, Al-Mukhtar et al., 2010a, Al-Mukhtar et al., 2010b, Nasrizar et al., 2010, Nasrizar et al., 2012)).

Conflicting observations were also reported concerning the hydraulic properties of lime treated expansive clays. Addition of lime increases the permeability coefficient as found by Nalbantoglu and Tuncer (2001) and Tran et al. (2014) who attributed the increase in permeability to the increase in the size of inter-floc pores as a result of lime addition. In contrast, the results of (Metelková et al., 2011, Al-Mukhtar et al., 2012) showed an initial increase in the permeability coefficient followed by a gradual decline due to the ongoing formation of cementitious compounds that partially fill the pore voids. However, the potential effects of compaction delay on the hydraulic properties were not seriously taken into consideration except a study conducted by Di Sante et al. (2015). Di Sante et al. (2015) concluded that there is no significant change in the value of the coefficient of permeability with delayed compaction based on tests conducted on six specimens only. Further research would, therefore, be required to reach a deeper understanding and informed conclusions for the role of compaction delay on hydraulic properties.

### **2.3.3 Curing time and curing temperature**

The effects of curing temperature and curing time on the evolution of modification, solidification and the resulting properties have been examined by many researchers (Bell, 1996, Rao and Shivananda, 2005, Al-Mukhtar et al., 2014, Li et al., 2014, Boardman et al., 2001, Al-Mukhtar et al., 2010a, Al-

Mukhtar et al., 2010b, Nasrizar et al., 2012), and their studies' results emphasized the role played by curing time and temperature in lime stabilisation.

Locat et al. (1990) monitored the development of strength gain in four types of sensitive clays that were treated by different lime contents reaching up to 10%. The results showed that the strength gain passed through three distinct phases. The strength gain showed small improvement during the first phase, followed by a significant growth during the intermediate phase before slowing down or even coming to a halt through the final phase. Locat et al. (1990) attributed the behaviour of strength over the final phase to the completion of the pozzolanic reaction. Hashemi et al. (2018) observed the same strength evolution of three phases over curing time reaching up to 28 days with sand-bentonite mixtures that were treated by various percentages of quick lime ranging from 3 to 8%

Bell (1996) concluded that regardless of the percentages of lime and the soil type, as the curing time increases, the strength gain increases except at lowest percentage of moisture content of 10% where the strength reaches its peak at 7 or 14 days of curing before declining with further curing periods. Generally, as the lime content increases, the gain of strength increases, and this gain is higher with the higher temperature of 40°C than 20°C at each percentage of lime and for both soils. Another study was performed by Boardman et al. (2001) on two types of clay. One of them predominantly comprises of sodium-montmorillonite called Wyoming bentonite, and the other predominantly contains kaolinite called English China Clay. Both soils were treated with different lime contents depending on initial lime consumption. The curing periods reached up to 300 days at 11.5°C. The results indicated that no apparent pozzolanic reaction takes place before 7 days of curing. This

behaviour was due to the low temperatures which were used during the curing periods causing the delay in the pozzolanic reaction and thus increasing the period to achieve the level of pozzolanic reaction at the average temperature.

In contrast, Rao and Shivananda (2005) conducted a study on Black cotton clay treated by two different percentages of lime. Lime-treated compacted specimens cured with different curing periods ranging from 1 to 400 days under 25°C. The temperature of 25°C represents the mean temperature in semi-arid regions in India. However, the results indicated that the pozzolanic reaction takes place in an earlier time (after one day of curing). This early appearance of pozzolanic reactions can be attributed to the used curing temperature. So, it can be stated that the lower curing temperature can slow the pozzolanic reaction or even stop it, whereas the higher curing temperature quickened the pozzolanic reaction and the strength achievement and reduced the time required for curing. The conclusion as mentioned earlier is what was confirmed later (Al-Mukhtar et al., 2010a, Al-Mukhtar et al., 2010b) when studying the influence of curing temperature of 20°C and 50°C on the evaluation of pozzolanic reaction. The results in both studies indicated that the increase of curing temperature from 20°C to 50°C leads to a reduction in the pH values regardless of the percentage of lime added. This is due to an increase in curing temperature, which leads to quicken the rate of pozzolanic reaction, which in turn works on consuming lime and thus reducing hydroxyl ions concentration.

Moreover, it was demonstrated that the rate of pozzolanic reaction at a curing temperature of 50°C was six-fold higher than that at a curing temperature of 20°C. This corresponds to the finding of an experimental investigation that was conducted by De Windt et al. (2014) to evaluate the impact of curing times up to



98 days and two ambient temperatures of 20 and 50°C on lime treated bentonite. The results showed that the ambient temperature of 50°C multiplied the kinetic of pozzolanic reaction by five times compared with at 20°C.

The effect of temperature in accelerating or slowing down the rate of pozzolanic reaction has been taken into consideration to reduce the time required for the curing regime to predict the long-term performance of stabilised materials in the lab. The National Lime Association specified the curing temperature of 40°C with a curing duration of 7 days to simulate normal temperature with a curing duration of 28 days. The same protocol is adopted by (AASHTO, 2008) in the interim Mechanistic-empirical pavement design guide. However, the curing duration of 5 days with a temperature of 38°C is recommended by other organisations such as The Metropolitan Government Pavement Engineers Council (MGPEC) Pavement Design Standards of Denver, Colorado Mooney and Toohey (2010), (Toohey et al., 2013). However, this concept has been subjected to many criticisms, for example, Toohey et al. (2013) performed laboratory experiments to compare the strength gains under the normal curing regime of 28 days under 23°C and accelerated regime of curing duration ranging between 2 and 8 days under curing temperature of 41°C. Toohey et al. (2013) compared their findings with other findings from other researches in the literature and concluded that the accelerated regime gives overestimated value concerning unconfined compression strength test values. Depending on their results, Toohey et al. (2013) concluded that an accelerated regime could not be relayed on due to the percentage of error is high.

#### **2.3.4 Type of clay mineral**

The complicated nature and wide assortment of clay minerals may indicate the likely variations of the reactions and responses that take place as a result of the addition of the lime to clay in the presence of water. These variations in the reactions and responses mean that one recipe does not necessarily apply to all clays. The mechanisms that govern lime-clay-reaction have been extensively studied using chemical and microstructural approaches. Effectiveness of lime treatment is submissive to many factors such as the lime content, curing time, ambient temperature, mellowing time and mineralogical composition of clay. Reactivity of clay mineral depends on many factors, including structure of clay mineral, specific surface area, and natural pH. In terms of pH, Olphen (1963) stated that the degree of pH changes according to the prevailing clay mineral. Soils containing montmorillonite minerals show alkalinity ranging from 8 to 12. This could be explained as follows: the hydrogen cations ( $H^+$ ) that result from the disassociation of water (into  $H^+$  and  $OH^-$ ) tend to replace the sodium cation  $Na^+$ . It is worth noting that the  $Na^+$  cations are inherently held onto the surface of montmorillinitic clay particles in a weak manner by forces called “Van der Waals forces”. As a result of this cation exchange, the concentration of hydroxyl anions increases in the pore solution and thus, the alkalinity of montmorillonite mineral (Olphen, 1963).

On the other hand, kaolinitic soils are characterised by their low pH value, ranging from 3 to 6. This acidity could be attributed to the interaction between  $Al^{+3}$  cations and water molecules within the diffuse double layer that surrounds the surface of the clay particle (Olphen, 1963). Unlike the  $Na^+$  cations, the  $Al^{+3}$  cations are strongly linked to the clay particle surface, and such interaction

between the  $\text{Al}^{+3}$  cations and water molecules leads to decline in the pH value into the acidic zone owing to expelling of  $\text{H}^+$  ions from  $\text{H}_2\text{O}$  molecules into the pore solution (Olphen, 1963). Such tendency to acidic zone indicates that the kaolinite mineral required higher lime content to reach the pH of 12.4 compared with the montmorillonite minerals. However, the various compounds in the surrounding medium such, precipitation of salt from a robust base or acid, oil contamination, and organic compounds primarily take part in determining the pH value of the surrounding medium (Pansu and Gautheyrou, 2007).

The net of surface charge and specific surface area (SSA) govern the substantial soil characteristics such the swelling nature, reactivity and sorption affinity (Cherian and Arnepalli, 2015). The overall of the specific surface area comprises of external and internal surface areas; the external surfaces area includes the faces and edges of the entire crystal, whereas the area of basal surface in each layer represents the internal area (Cherian and Arnepalli, 2015). The specific surface area varies according to the type of clay mineral, for instance, montmorillonite minerals have internal and external surface areas and are characterised by high specific surface area which reaches up to  $800 \text{ m}^2/\text{g}$  (Mitchell and Soga, 2005). On the other hand, there is no internal area in the kaolinite mineral since the tetrahedral and octahedral sheets are firmly staked together in the kaolinite mineral layer and just the external areas are accounted for in the specific surface area, which ranges from 10 to  $20 \text{ m}^2/\text{g}$  (Mitchell and Soga, 2005).

Theoretically, montmorillonite minerals have higher specific area that needs more lime content to satisfy the charge deficiency, and thus, it requires higher amounts of lime to obtain the desired alteration. In contrast, kaolinite minerals

have an extremely “smaller specific surface area” and lower number of exchangeable sites that require the lesser lime amount to fulfil their charge deficiency compared with montmorillonite minerals.

The structure of clay mineral was discussed in a previous section. Hereafter, the effect of various clay mineral structures will be discussed. The layer of kaolinite mineral comprises of a tetrahedral sheet joined with an octahedral sheet. Such layers stacked together to form the kaolinite mineral and the powerful hydrogen bonds keep such structures stable and render the swelling insignificant.

In the case of montmorillonite minerals “Van der Waals forces link the neighbouring layers. The weakness of Van der Waals forces render the swelling tendency important (Cherian and Arnepalli, 2015). Cherian and Arnepalli (2015) stated that the van der Waals force, high pH and high specific surface area in montmorillonite mineral increase their capacity to provide reactive alumina and silica and thus command to high lime reactivity. Kaolinite minerals show a slow rate of lime reactivity due to the strong hydrogen bonds, low pH as well as a small specific surface that declines their capability to provide alumina and silica. On the other hand, (Bauer and Berger, 1998) found that at 35 and 80°C, the dissolution rate of kaolinite into silica and alumina in the strong base medium of potassium hydroxide is much higher than the rate of dissolution of two types of smectites. Chemed et al. (2018) conducted an investigation on the effect of lime treatment on kaolinite clays. Chemed et al. (2018) concluded that in the short term, the alkaline medium produced by lime addition works on; 1) Determining the obtainable calcium cations ( $\text{CaOH}^+$ ) for the adsorption phenomena; 2) Increasing the net negative charge on the surface of kaolinite

mineral leading the accumulation of calcium cations on the surface. This accumulation protects the surface of kaolinite mineral from the aggressive alkaline medium. This protection causes delay in release of alumina and silica and thus delays the formation of cementitious compounds.

Concerning the changes in the mechanical properties, there is a consensus regarding the immediate effect of lime on reducing plasticity and improving the workability of the soil; whereas, there is no consensus in terms of strength gain and its continuity. Bell (1996) conducted a search on kaolinite and montmorillonite clays that were treated by various percentages of lime ranging between 2 and 10%. The specimens were prepared at their standard proctor optimums and cured at 20°C for varying curing times. The results showed that even with the addition of small amounts of lime, the treated kaolinite and montmorillonite experienced notable growth in strength. Bell (1996) concluded that there was no linear relationship between the strength and the added lime contents.

Furthermore, the immoderate addition of lime causes a reduction in strength gain, which was attributed to that the lime itself lacks appreciable friction and cohesion. Instead, (Bell, 1996) launched a concept of optimum lime content, between 4 and 6% for kaolinite and 4% for montmorillonite, that after which the strength begins to decline or continues to growth at a reduced rate. (Al-Mukhtar et al., 2010a, Al-Mukhtar et al., 2010b) monitored the evolution of soil-lime reaction for highly plastic soil (contains 58% smectite and 38% kaolinite) treated by different lime contents (0-20%) and cured for 1, 7, 28 and 90 days at two temperatures of 20 and 50°C using various approaches including unconfined compressive strength tests. It was concluded that under both temperatures,

strength grows as the lime content increases and curing time extended. Strength gains over the first day were attributed to the impact of short-term reactions, i.e. cation exchange and flocculation due to the absence of formation of cementitious matters in early stages. The researchers added that the pozzolanic reaction would not begin unless the lime content exceeded the content needed to satisfy short term reactions.

In contrast, immediate initiation of pozzolanic reaction and formation of poorly crystalline cementitious compounds in the form of calcium silicate hydrates (CSH) were reported by (2017, Vitale et al., 2016a, Pomakhina et al., 2012) based on their studies conducted on montmorillonite clay. Maubec et al. (2017) observed the evolution of strength gain for kaolinite clay and bentonite treated by 10% of lime and cured for periods reaching up to 96 days under the temperature of 20 or 50°C. The results show that the strength value of lime treated kaolinite specimen tested after one hour was less than the strength value of the untreated specimen. Furthermore, it was found that at 20°C, there is a marginal growth in the strength achieved by the seventh day and then, the strength value keeps constant even after 98 days. On the other hand, a substantial growth only sees the light after the 7th day of curing at 50°C, reaching a strength value accounted for seven times the strength value of the untreated specimen.

Chemedda et al. (2018) justified the reason behind the dispute concerning the delay of dissolution of kaolinite minerals into alumina and silica and delay in the formation of cementitious compounds. The reason was the accumulation of calcium cations on the surface of clay particles that prevent surrounded alkaine from attacking the surface of koalinite minerals to release the alunmia and silica.

However, the mechanism by which the accumulation of calcium cations is eliminated so that the alkaline medium can attack the surface of clay mineral and release the reactants to produce the cementitious compounds after a week at 50°C has not been explained yet.

## **2.4 Summary:**

- 1- Most of the studies agree that addition of lime improves workability and reduces plasticity and swelling in short term; while there is no consensus concerning the effect of lime stabilisation on the permeability of the treated soil.
- 2- In the literature, there is a consensus that cation exchange, flocculation and agglomeration, carbonisation and pozzolanic reaction are in-charge of the changes in the clay properties. In contrast, there are disagreements regarding as to whether these mechanisms occur sequentially or synchronously.
- 3- Effect of mixing time, mixing method, and the degree of pulverisation on the effectiveness of lime stabilization should be put into consideration.
- 4- The impact of the mellowing periods on the acquired properties of lime stabilised soil does not seem to be thoroughly investigated. There is no agreement on its decisive and/or detrimental role. Besides, some researches neglected mellowing, considering it part of curing time.
- 5- After critically reviewing the technical literature, it is apparent that there is a disagreement amongst researchers concerning the start of strength gain and its continuity.

- 6- Although there are few studies conducted on the effect of curing temperatures, all of them have neglected the impact of temperature during the mellowing period (compaction delay).
- 7- Clay content, mineralogical composition of clay, temperature, compaction delay, and percentages of lime are factors that control the efficiency of the lime treatment.
- 8- There is a consensus in the literature on the role played by the temperature in accelerating the kinetics of the pozzolanic reaction. However, the question remains as to when this effect begins, how long it lasts, what its relation to the clay content, mineralogy composition, and the lime content.



### Chapter 3 Materials and Methodology

This chapter comprises of 3 sections. In the first section, the materials used in the current research have been described. The following section introduces the preparation methods for untreated and treated mixtures, chosen tests and the apparatuses used to conduct the tests. The testing programme in the current study has been divided into five testing series. The adopted variable and fixed parameters for each series are illustrated in the third section of this chapter.

#### 3.1 Materials

##### 3.1.1 Soil

Two different types of clay, namely bentonite and ball clay, were used in the current study and supplied by Potclays Ltd in powder form. Chemical analysis of both bentonite and ball clay, as provided by the supplier, are shown in Table 3.1.

Table 3.1: Chemical analysis of bentonite and ball as provided by the supplier

| Component %                    | bentonite clay | ball clay |
|--------------------------------|----------------|-----------|
| SiO <sub>2</sub>               | 63.02          | 52.0      |
| Al <sub>2</sub> O <sub>3</sub> | 21.08          | 31.5      |
| Fe <sub>2</sub> O <sub>3</sub> | 3.25           | 1.0       |
| K <sub>2</sub> O               | -              | 2.3       |
| Na <sub>2</sub> O              | 2.57           | 0.3       |
| MgO                            | 2.67           | 0.4       |
| CaO                            | 0.65           | 0.2       |
| FeO                            | 0.35           | -         |
| TiO <sub>2</sub>               | -              | 1.1       |
| L.O.I. @ 1000C*                | 5.64           | 11.3      |
| Carbon                         | -              | 1.6       |
| Trace                          | 0.72           | -         |

The Wyoming sodium bentonite clay (M1) is mainly comprised of montmorillonite minerals besides a small amount of non-clay minerals such as feldspar, Quartz, and calcite. Its liquid limit and plastic limit were determined according to (BS 1377-2:1990). Based on its liquid and plastic limits, The Wyoming sodium bentonite clay can be classified as extremely high plastic

Standard Proctor compaction tests showed that neither maximum optimum moisture content nor Maximum dry unit weight could be determined. Such observation could be attributed to the swelling tendency of bentonite. The moisture content of 40% was then estimated as an optimum moisture content according to the correlation developed by (Sridharan and Nagaraj, 2005). Accordingly, the corresponding dry unit weight was found to be 12.16kN/m<sup>3</sup>.

On the other hand, ball clays (M2) mainly comprises of kaolinite minerals. Both clays were mixed in different proportions to obtain two additional clay mixtures with a ratio of 1:3 and 1:1 bentonite to ball clay by mass. Geotechnical properties for the four materials used in this investigation are illustrated in Table 3.2. Ball clay can be classified as medium plastic with a liquid limit of 58%. The other two mixtures that were created by different ratios retained LL of 115 and 189% for 1:3 bentonite to ball mixture(M3) and 1:1 bentonite to ball mixture(M4), respectively. These data demonstrated that the four materials represented a vast range of liquid limit spanning from 320% down to 58%. Data for the maximum dry unit weight and optimum moisture content were obtained according to the procedure that was developed to simulate the Proctor compaction energy. Data in Table 3.2 clearly showed that with reducing liquid limit, maximum dry unit weight increased and the optimum moisture content reduced.

Table 3.2: Geotechnical properties for utilised clay materials

|  | Material |       |       |       |
|--|----------|-------|-------|-------|
|  | M1       | M2    | M3    | M4    |
| Composition of bentonite (%)                 | 100      | 0     | 25    | 50    |
| Composition of ball (%)                      | 0        | 100   | 75    | 50    |
| Liquid limit (%)                             | 320      | 58    | 115   | 189   |
| Plastic limit (%)                            | 43       | 32    | 36    | 40    |
| Maximum dry unit weight (kN/m <sup>3</sup> ) | 12.16    | 14.14 | 13.48 | 12.95 |
| Optimum moisture content (%)                 | 40       | 29    | 32.5  | 37.5  |

### 3.1.2 Lime

Non-hydraulic high calcium hydrated lime that satisfies the requirements of (BS EN 459-1:2015) was used in the current investigation. Chemically, the used hydrated lime contains 95 to 97% in the form of  $\text{Ca}(\text{OH})_2$ . In order to ensure better distribution of lime when used to treat the soil, lime powder should be fine to avoid creation of visible lime pockets, which will not disappear even during prolonged curing times. In current research, a 425 $\mu\text{m}$  sieve and pan were used to obtain fine hydrated lime. Each time, half a kilo of hydrated lime was put on a 425 $\mu\text{m}$  sieve (as seen in picture 1 in Figure 3.1). After mechanical shaking, the retained portion of lime on the 425 $\mu\text{m}$  sieve was disposed (See Figure 3.1). Whereas, the fine hydrated lime in the pan (see seen in picture 3 in Figure 3.1) was kept in a sealed bag (see seen in picture 4 in Figure 3.1) until use.



Figure 3.1: Fine hydrated lime which was passed through a 425 $\mu\text{m}$  sieve

### **3.2 Testing techniques**

In the current study, a geotechnical approach was used instead of microstructural and chemical approaches. In this context, four geotechnical tests were chosen to track formation signs of cementitious compounds through monitoring the changes in the geotechnical properties associated with the formation of such compounds. These tests are compaction, swelling and permeability, and unconfined compressive strength tests. This selection was based on the following:

- 1- With the unconfined compressive strength tests, the ongoing strength gain is indicative of the growth of cementitious compounds (Al-Mukhtar et al., 2010b);
- 2- Increased resistance of mixes to compaction shows an increased share of the input compaction energy for destructing the ongoing growth of cementitious compounds (Osinubi, 1998); and
- 3- The formation of cementitious compounds helps curb the soil swelling tendency while it reduces the permeability of the soil by growing cementitious compounds in available pores (Al-Mukhtar et al., 2012, Metelková et al., 2011, McCallister and Petry, 1992).

In this investigation, to render an efficient monitoring procedure of abovementioned mechanical parameters, mixing durations and techniques were carefully controlled.

#### **3.2.1 Specimen preparation**

In order to prepare an untreated mixture, predetermined amounts of clay and water were mixed manually to achieve a homogenous mix with a target

moisture content. The mixture was sealed in a double vinyl bag and kept in an environmental chamber at a temperature of 20°C and a humidity of 90% for 2 days to ensure a uniform distribution of moisture content.

For lime-treated mixtures, at room temperature, predetermined amount of clay and lime were mixed manually using a spatula until an even distribution of lime throughout the mixture was visually confirmed. The mixing procedure was further continued using a mechanical mixer for 1.5 minutes. A plastic cover was used to cover the mixing bowl to prevent lime-clay dust volatilisation. Afterwards, desirable amount of water was mixed with the soil-lime mixture manually. This process was continued for 5 minutes to ensure the formation of a homogenous mixture with no noticeable lumps. The processed mixture was passed through a 2mm sieve to ensure a high degree of pulverisation and uniform treatment of clay. Retained content on the sieve was mixed with some of the passing contents, kneaded by hand and returned to the rest of the mixture. Finally, the whole mixture was mixed mechanically for a minute. Figure 3.2 shows the mixing procedure.



Figure 3.2: Preparation stages of lime treated clay mixtures for testing.

### 3.2.2 Unconfined compressive strength

Determination of unconsolidated undrained shear strength of cohesive clays under unconfined condition is the primary intent of unconfined compressive strength (UCS) tests. Unconfined compressive strength of lime treated soil is chiefly utilised to assess the stabilising impact (Kitazume and Terashi, 2013). Acceptance scattering from the average of UCS values should not exceed 10% (Consoli et al., 2009). The following considerations were implemented to limit the scattering threshold of UCS data:

- 1- Adopting a cautious and thorough mixing technique to limit disparity in mixing times and to avoid the formation of lime lumps thus ensuring a high degree of pulverisation;
- 2- Selection of a feasible and an efficient compaction method to ensure the uniformity of the dry unit weight throughout specimens and thus repeatability of specimens; and

- 3- Implementing of a curing protocol that provides a stable and constant curing temperature and humidity to avoid partial drying out of specimens.

Clay-lime mixture was compacted in five layers using static compaction method. A particular mould with moveable upper and lower plungers was used for UCS specimen preparation (Figure 3.3). Compaction equipment included a steel mould and three pairs of different height steel plungers (i.e. two short, two medium and two tall plungers). Figure 3.4 illustrates dimensions of the mould and the plungers. A hydraulic jack was used to compress the mixture into the mould (Figure 3.5).



Figure 3.3: Compaction equipment for preparation of UCS specimens



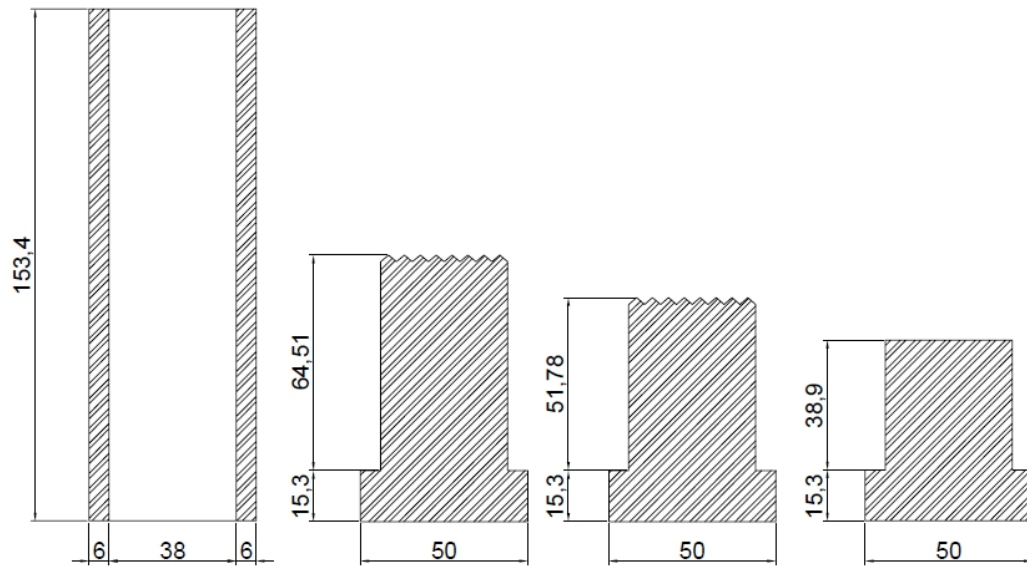


Figure 3.4: Cross-section diagram illustrates the dimensions of compaction equipment for UCS specimens



Figure 3.5: hydraulic Jack press

Tall and medium height plungers had indented surfaces, as can be seen in Figure 3.3, to ensure a kneaded surface on compacted layers for a good bond



with the layer above. This method of specimen preparation was developed by Saad et al. (2012) and was shown to minimise / eliminate discrepancy of dry unit weight along the height of the specimen.

However, the drawback in this method was that during the compaction process, the direct contact between the mixture and the surface of the plunger led to a loss of designed mixture. To overcome this disadvantage, a thin circular cling film, as seen in Figure 3.6, was used between the plunger and the soil surface to avoid sticking of materials to the surface of the plunger.

The following procedure was followed to prepare UCS specimens:

- 1- One of the tall plungers was inserted into the mould, and a circular cling film was placed on top of the plunger surface (See Figure 3.6). Then one-third of the mixture was poured carefully into the mould and levelled by a quick shaking. Another circular cling film was placed on the top, and the other tall plunger was pushed into the mould. Promptly, the mould was compressed using the hydraulic jack to form the middle part of the specimen. After that, the two tall plungers and two cling film were removed.

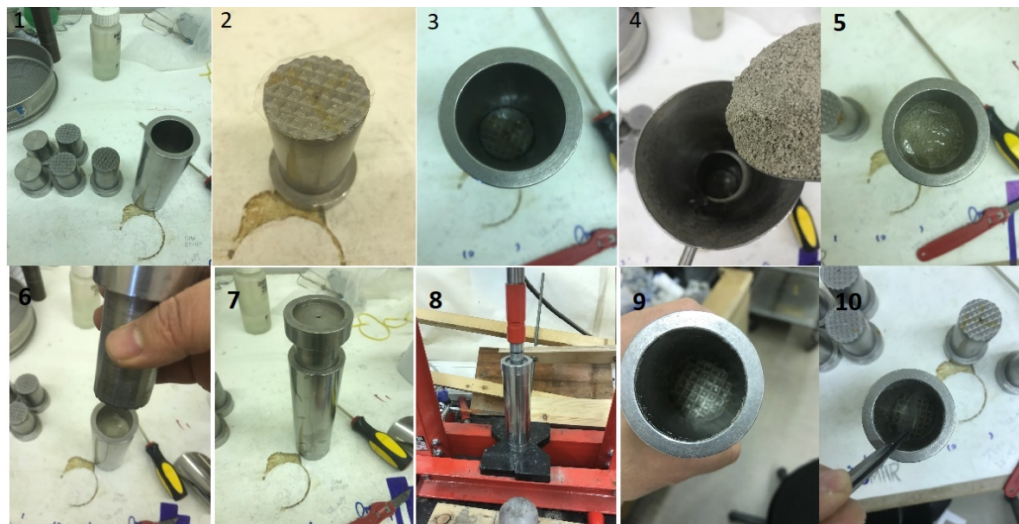


Figure 3.6: UCS specimen preparation steps (to form the first third of specimen's height)

- 2- The second third weight of the mixture was divided into two equal portions. The first part was poured into the top of the mould and was shaken slightly to level the mixture surface, followed by placing the cling-film and compressing using the medium-size plunger (see Figure 3.7). Afterwards, the mould was turned upside down, and the other part of the second third portion was poured into the mould. The mould was then

slightly shaken, and the cling-film was placed on top of the soil and compressed using the medium-size plunger.

- 3- To compact the full height of the specimen, the final two layers were compressed in the mould in a similar procedure as of step 2 using the short plunger (Figure 3.8). Finally, the specimen was extracted from the mould using a steel rod. Prepared sample was either tested accordingly or wrapped in cling-film and sealed in a double vinyl bag and stored in the environmental cupboard for curing.

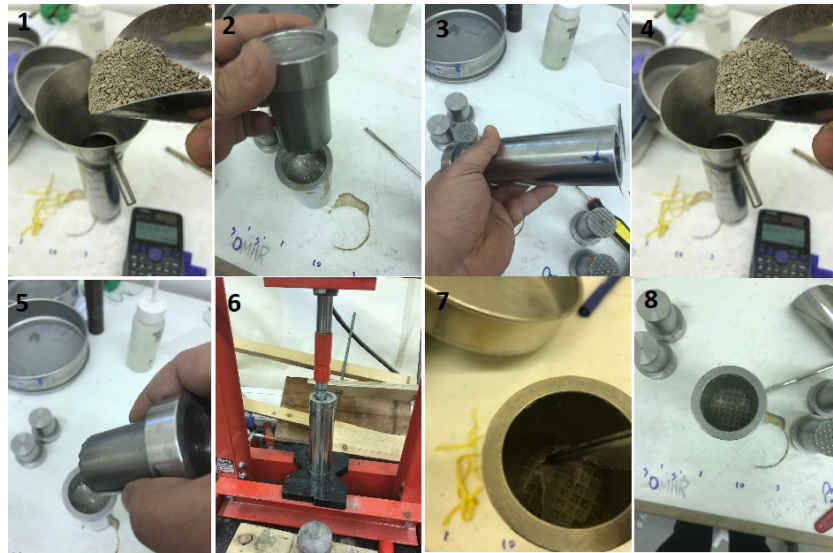


Figure 3.7: UCS specimen preparation steps (to form second third of specimen's height)

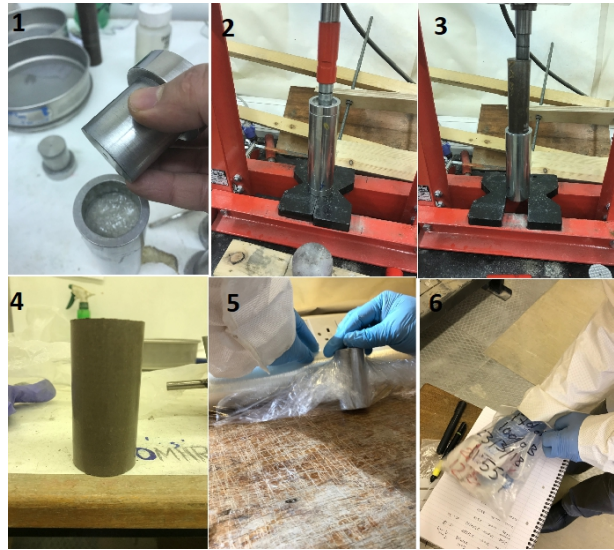


Figure 3.8: Final stage in preparing UCS specimens

An automated loading machine was used to perform UCS tests at a rate of 1mm/min. Readings of axial load and vertical deformation were recorded automatically every 1s.

### 3.2.3 Compaction tests

The main aim of performing standard Proctor compaction tests (BS 1377-4:1990) is to identify the optimum moisture content (OMC) and the maximum dry unit weight (MDU). A preliminary investigation was carried out on pure bentonite clay using the Standard Proctor Compaction test, and confirmed that:

- I. Compaction of extremely high plastic clays in a standard Proctor test is cumbersome;
- II. There is significant distortion and variation of dry unit weight along the specimen height;
- III. Proctor compaction test requires considerable effort and consumes substantive amount of materials that cannot be reused due to the

additives used. Even with untreated soil, reuse of soil leads to errors in assessment of dry unit weight since the resulting dry unit weight of reused soil is higher than that of the freshly compacted soil (ASTM D 698 - 12e2).

Results of compaction tests showed that the higher moisture content, the lower dry unit weight; so, neither optimum moisture content nor maximum dry unit weight values could be obtained. This could be attributed to the higher swelling tendency of bentonite clay. In this study, the equation 3.1 developed by Sridharan and Nagaraj (2005) was used to determine the optimum moisture content depending on the relationship between the plastic limit and optimum moisture content. Plastic limit of bentonite clay was determined as 43% according to (BS 1377-2:1990). Therefore, optimum moisture was estimated to be 40% and its corresponding maximum dry unit weight was 12.16kN/m<sup>3</sup>.

$$OMC = 0.92 \times PL \quad 3.1$$

Where: OMC is Optimum moisture content (%), and PL is Plastic limit (%).

In order to verify the estimated compaction properties, a mini-compaction apparatus was developed to simulate the compaction energy of Standard Proctor compaction. The mini-compaction apparatus shown in Figure 3.9 included a mould and a mini steel hammer.



Figure 3.9: Mini compaction apparatus

The dimensions of the mini-compaction mould and hammer are illustrated in Figure 3.10. The main body of the mould has an internal diameter of 50mm and a height of 120mm and comprises of two detached split parts with different heights. The height of the upper part in the main body is 100mm, whereas the height of the lower part is 20mm. The split form of the mould facilitates extraction of the compacted sample. The mould is also fitted with a detachable split form collar with 37mm high. A 1.25 kg hammer with a diameter of 24.8mm is used to compact the soil in the mould.

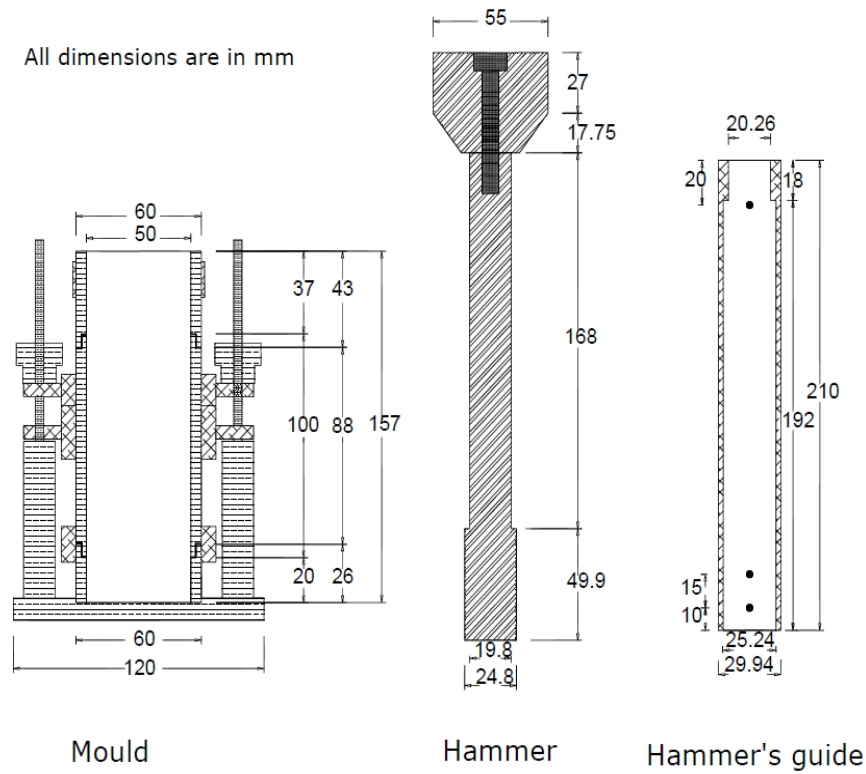


Figure 3.10: Dimensions of the mini-compaction tools

Compaction energy of the mini compaction apparatus can be calculated from Equation 3.2 (BS EN 13286-2:2010).

$$E = \frac{W \times H_f \times N_b \times N_l \times G}{V} \quad 3.2$$

Where;  $E$  is compaction energy ( $\text{MJ/m}^3$ ),  $W$  is the weight of hammer (kg),  $H_f$  is the dropping height (mm),  $N_b$  is number of blows per layer,  $N_l$  is the number of layers,  $V$  is volume of the mould ( $\text{mm}^3$ ), and  $G$  is the gravity ( $9.807 \text{ m/s}^2$ ) According to (BS EN 13286-2:2010), the compaction energy of Proctor compaction ranges between  $0.56 \text{ MJ/m}^3$  to  $0.63 \text{ MJ/m}^3$ . In the first attempt to simulate the compaction energy of Proctor compaction, the clay was compacted in three layers in which each layer received 27 blows using the 1.25kg falling weight from a height of 150mm. In order to achieve a uniform distribution of



blows, the compaction pattern shown in Figure 3.11 was adopted (Head, 1992). Although the calculated compaction energy was similar to the compaction energy of Proctor compaction, the lower part of each compacted layer appeared to be less dense than the upper part (See Figure 3.12).

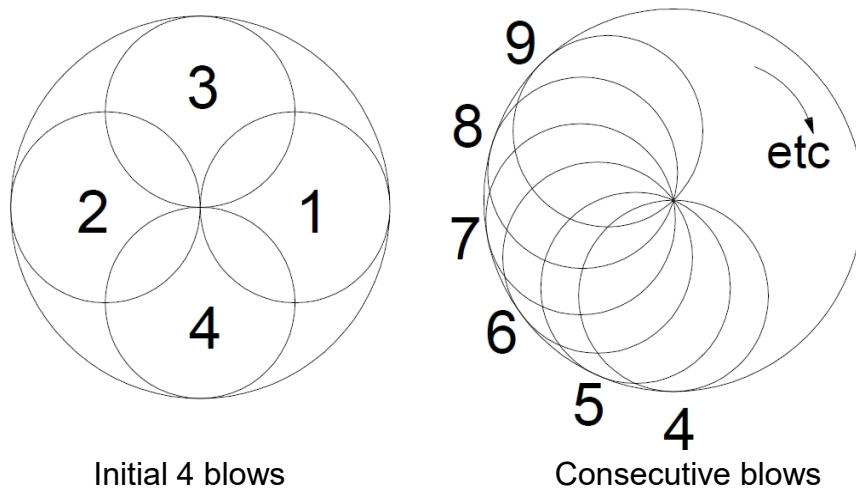


Figure 3.11: Hammering pattern for compaction

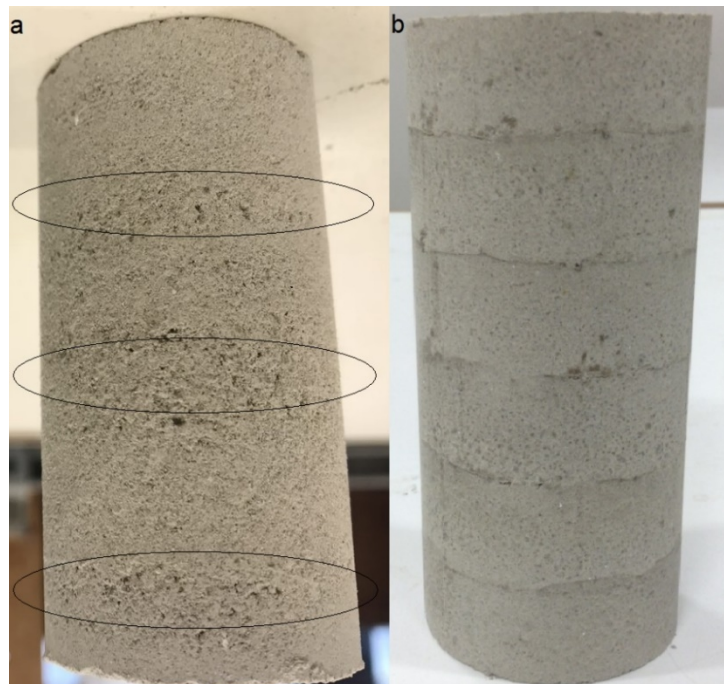


Figure 3.12: Effect of changing the number of compacted layers from 3 layers (a) to 6 layers (b)



Therefore, to overcome this issue, it was decided to increase the number of layers to 6 with each layer compacted with 13 blows. Thereafter, the number of blows was amended to 15 blows in order to obtain a dry unit weight of  $12.16 \text{ kNm}^3$  at the moisture content of 40%. With this adjustment, the compaction energy of the proposed compaction technique was calculated as shown in equation 3.3:

$$E = \frac{1.25 \times 150 \times 15 \times 6 \times 9.807}{235714} = 0.702 \text{ MJ/m}^3 \quad 3.3$$

It should be mentioned that steps of compaction test using the mini-compaction tools are very close to the steps of standard Proctor compaction. However, when using the mini-compaction tools, the following points must be considered to ensure the repeatability and the reliability of the results:

- 1- Due to the size of the mini-compaction, it is appropriate to determine the optimum dry unit weight and optimum moisture content of fine-grained soils (Size of particle < 2mm).
- 2- Hammer must drop freely from the designed height. Therefore, in the case of compacting adhesive clays, the bottom of the hammer should be covered by cling film to prevent detrimental effects of adhesion between the hammer and clay.
- 3- The mould should be cleaned every use and thus lubricated lightly using multipurpose oil to decline the friction of sidewall and to facilitate extraction of compacted specimens after completing the tests.
- 4- Separate samples of soil are prepared with different moisture content to enable the determination of optimum moisture content and maximum dry unit weight.

- 5- Samples are compacted in six layers, whilst each layer is subjected to 15 blows by 1.25-kg hammer falling from 150mm resulting in a total compaction energy of about  $0.7\text{MJ/m}^3$
- 6- The fine grained materials must be used only once for compaction as stated in (ASTM D 698 - 12e2).
- 7- It is recommended that the compaction mould must be placed on hard surface e.g. concrete or metal during the compaction tests to avoid the dissipation of compactive energy.
- 8- The surface of the compacted layer should be sacrificed before the the addition of the following layer is placed. This should be repeated with other layers until finishing the compaction of the fifth layer.
- 9- The sixth layer should not protrude more than 3mm above the top of the mould.

The primary objective of testing lime-treated samples is to monitor the evolution of lime-clay reaction with time at different ambient temperatures of  $20^{\circ}\text{C}$  or  $40^{\circ}\text{C}$  using the changes in the dry unit weight value as an indicator. For accurate assessment of the changes, specimens were prepared at a specific moisture content and initial mass of lime-clay mixture. In the current investigation, the optimum moisture content of untreated clays was chosen to prepare lime-clay mixtures. Performing compaction tests with the same initial mass of lime-clay mixtures enable the researcher to monitor the impact of temperature and lime content on the changes in dry unit weight value as the time elapsed. To determine the initial mass, the following procedure was considered:

- 1- The lime-clay mixture is split into six equal masses in order to be compacted in six layers.

- 2- Compaction test must be conducted immediately after the mixing process on lime-clay mixtures giving a zero h mellowing.
- 3- Compaction test should be repeated on zero mellowed mixtures until obtaining a mass of lime clay mixture that does not exceed 3mm from the top edge of the mould after compaction. This is to avoid loss of compactive energy on compacting excess material which will ensure consistency of compaction results. This mass of (zero mellowing) lime-clay mixture is used as a reference mass to prepare mellowed lime-clay mixtures.

Mellowed lime-clay mixtures are prepared with the same initial mass (reference mass) and then being left to mellow for the designed period of time at either 20°C or 40°C depending on the test conditions before conducting the compaction tests. All specimens are prepared under the same compaction energy. It is expected that the more time allowed for lime-clay reaction, the greater the resistance to compactability.

#### **3.2.4 Swelling and permeability tests**

The measurements of swelling pressure and the coefficient of permeability were conducted according to BS 1377-6. According to BS 1377-5 and BS 1377-6, the permeability coefficient should not be measured until tested specimens become fully saturated and reach their swelling stability.

In the current study, the time is vital since the reaction between the lime and clay starts once the lime is added to the soil in the presence of water. Therefore, adopted changes in the test procedure were introduced to accelerate the saturation and overcome the deficiency of wetting sequence. An automatic Oedometer System with hydraulic cell (GDS system) was used to conduct

swelling pressure and permeability tests simultaneously. In this regard, it was decided to run the tests on 10 mm thick specimens to shorten the flow path of water. Moreover, the base back pressure was increased to speed up the percolation of water and to ensure that all specimens were tested under comparable conditions. The base of the hydraulic cell was connected to a pressure-volume controller so that a target base back pressure of 35kPa was applied on the bottom of specimen throughout the test while the top of specimen was kept under water at atmospheric pressure. No vertical deformation was permitted during the test by increasing the axial load to prevent swelling of specimens, which means that all specimens maintained their initial dry unit weight throughout the testing period. An incremental pressure was applied to prevent swelling of the specimen so that the volume was kept constant and thus the specimen remained at its initial dry unit weight throughout the test. The maximum pressure that after which there is no further increase in the swelling is considered the maximum swelling pressure.

Regarding saturation, theoretically, it can be calculated the volume of air in the specimen at a given moisture content, volume, and dry unit weight. Hence, the base pressure controller allows measuring volume of water passing through the specimen. The specimen is considered fully saturated when the measured volume of water exceeds calculated volume of air.

The permeability coefficient of the specimen is determined frequently at 6, 12, 18, 24, 36, 48, 60 and 72h from the beginning of the test to guarantee reaching a stable swelling pressure and full saturation. The coefficient of permeability can be calculated from equation 3.4 (BS 1377-6:1990):

$$K = \frac{1.63 \times q \times RT \times 10^{-4}}{A \times ((P1 - P2) - Pc)} \quad 3.4$$

Where: K: coefficient of permeability (m/sec), q: rate of flow (ml/min), RT: correction factor for the temperature, (P1-P2): the difference between the base pressure and upper pressure (P2 is zero) (kPa), Pc: pressure loss in the system (kPa) and A: an area of the specimen (mm<sup>2</sup>)

To prepare specimens for swelling and permeability tests, a mould as seen in Figure 3.13, was fabricated to statically compact untreated or lime treated mixtures into a 50mm diameter ring. The mould was equipped with a removable base, also, a plunger to compact the specimen to the half depth of the ring (10mm). The ring placed in the allotted place between the base and the mould and fixed to the mould so that neither horizontal nor vertical movement were allowed. A predetermined amount of wet clay was placed in the mould and compacted into the ring using the plunger to achieve the target dry unit weight.

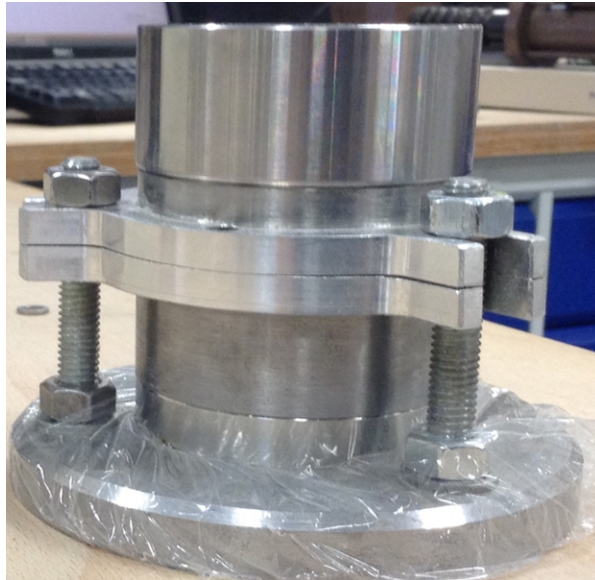


Figure 3.13: Fabricated mould to compact the specimens used for swelling and permeability tests

A GDS odometer apparatus was used to conduct swelling and permeability tests. It comprised of a load cell, digital dial gauge, loading frame and a smart keypad. The load cell in GDS odometer apparatus can apply the force reach up to 10kN. The apparatus external has a digital dial gauge can measure deformation up to 15mm with an accuracy of 0.0003mm. This device can be operated manually through its keypad or automatically using GDS Lab software. The GDS oedometer system was equipped with two types of cell, namely; conventional and hydraulic cells, as seen in Figures 3.14 and 3.15, respectively. Here it should be mentioned that the conventional cell was just used in series 1 to perform the swelling pressure tests. The hydraulic cell had two inlets to the base of the cell (Figure 3.16). A GDS digital pressure/volume controller was connected to the base inlet to apply a base back pressure as required. The pressure/volume controller could apply pressures up to 3MPa. The hydraulic cell was a watertight cell; hence, flow of water to the specimen can be monitored during the test to assess the saturation ratio of specimens as well as determining the coefficient of permeability. The 50mm diameter ring containing clay specimen was placed in the hydraulic cell in a dedicated compartment with O-rings at top and bottom to prevent ingress of water except through the specimen.



Figure 3.14: GDS oedometer system equipped with a conventional cell

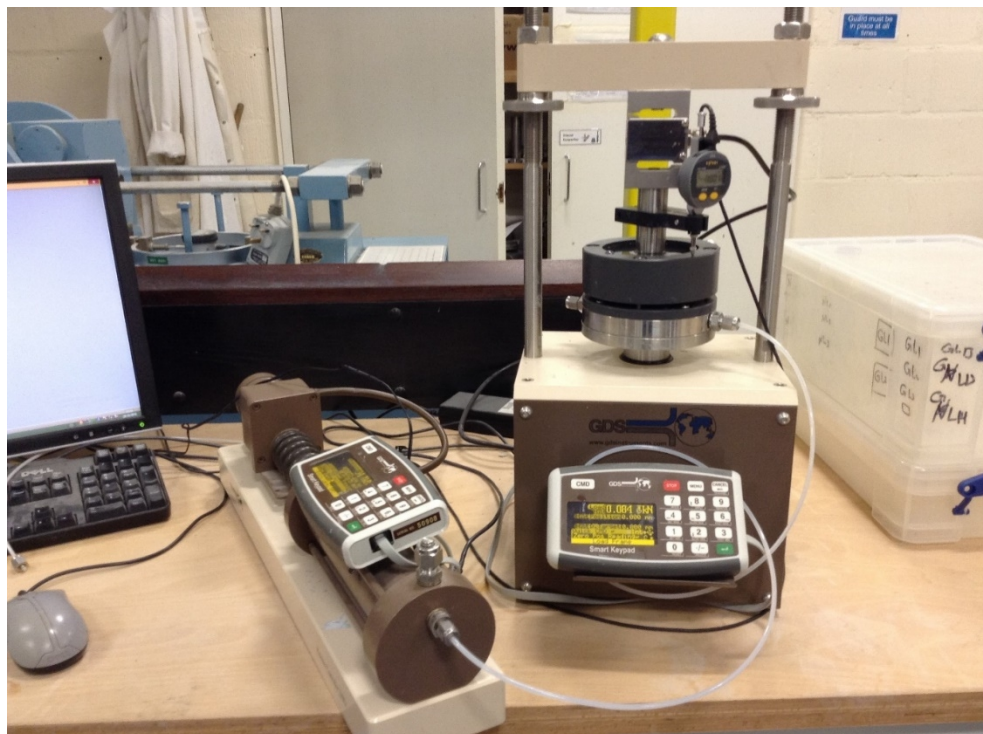


Figure 3.15: GDS oedometer system equipped with a hydraulic cell and GDS digital pressure/volume controller

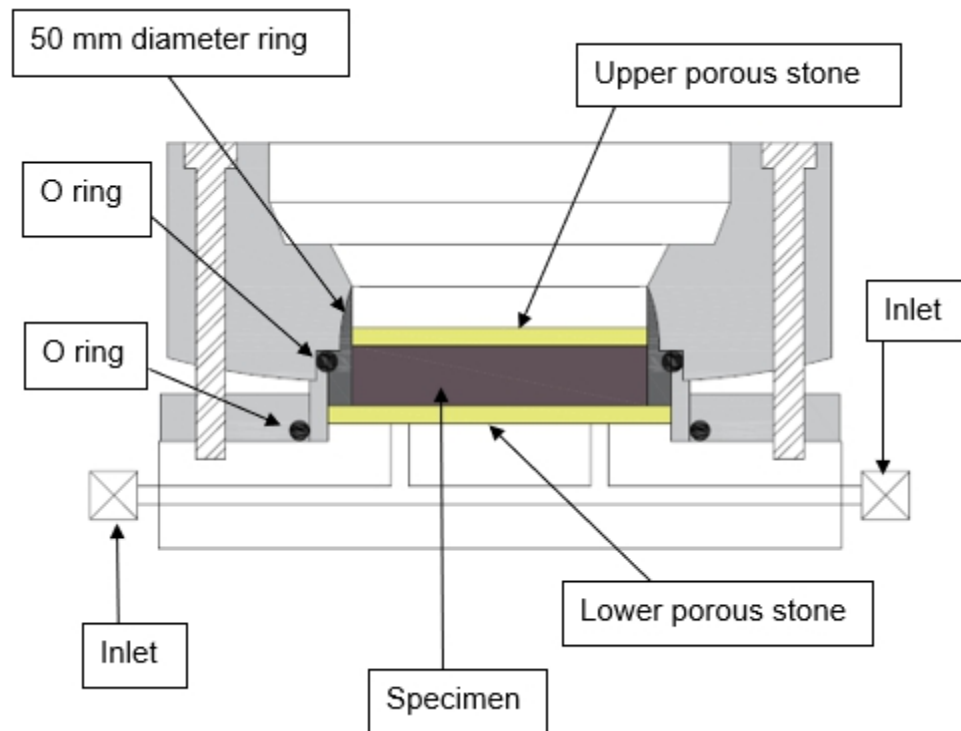


Figure 3.16: Cross section of the hydraulic cell

### 3.3 Testing programme

The testing programme was carried out in 5 series. The first series was mainly conducted to justify the adjustments on swelling and permeability tests; whereas, the second series was carried out to evaluate the impact of delayed compaction on the properties of lime-stabilised clay. Remaining three series were carried out to monitor the evolution of geotechnical characteristics of compacted clays with varying curing periods, temperature values, lime contents, and mineralogy compositions. Table gives an overall view on the experimental work in the current investigation.



Table 3.3: Overall view on the testing programme

| Series | Type of clay          | Main parameters                                      | Types of tests                             | Number of tests |
|--------|-----------------------|--|--|-----------------|
| 1      | bentonite             | Initial moisture content and Initial dry unit weight | Swelling pressure test (conventional cell) | 23              |
|        |                       | Initial dry unit weight                              | Swelling pressure test (hydraulic cell)    | 7               |
| 2      | bentonite             | Mellowing time and temperature                       | Compaction test                            | 12              |
|        |                       | Mellowing time and temperature                       | Swelling pressure test                     | 19              |
|        |                       | Mellowing time and temperature                       | Permeability test                          | 17              |
|        |                       | Mellowing time, curing time, and temperature         | Unconfind compression strength test        | 142             |
| 3      | bentonite             | Mellowing time, lime content and temperature         | Compaction test                            | 70              |
|        |                       | Curing time, lime content and temperature            | Unconfind compression strength test        | 100             |
|        |                       | Lime content and temperature                         | Permeability test                          | 10              |
| 4      | bentonite             | Curing time, lime content and temperature            | Unconfind compression strength test        | 202             |
|        |                       | Curing time, lime content and temperature            | Unconfind compression strength test        | 110             |
|        |                       | Curing time, lime content and temperature            | Unconfind compression strength test        | 82              |
| 5      | bentonite             | Curing time, lime content and temperature            | Unconfind compression strength test        | 82              |
|        |                       |  | Permeability test                          | 11              |
|        |                       | Temperature, lime content and mellowing time         | Swelling pressure test                     | 21              |
|        |                       |  | Permeability test                          | 21              |
|        |                       | Temperature, lime content and mellowing time         | Swelling pressure test                     | 21              |
|        |                       |  | Permeability test                          | 21              |
|        |                       | Temperature, lime content and mellowing time         | Swelling pressure test                     | 21              |
|        |                       |  | Permeability test                          | 21              |
|        | 1:1 bentonite to ball | Temperature, lime content and mellowing time         | Swelling pressure test                     | 21              |
|        |                       |  | Permeability test                          | 21              |

### **3.3.1 Series 1: Effect of deficiency of wetting on the evolution of swelling pressure**

The series 1 tests aimed at investigating the effect of initial wetting and initial dry unit weight on the swelling pressure of a highly reactive clay. The experimental work in series 1 was divided into two phases. The first phase aimed to investigate the impact of various initial dry unit weights and initial moisture contents on the evolution and values of swelling pressure of untreated bentonite. All swelling pressure tests in this phase were conducted using the GDS oedometer system equipped with a conventional cell. Twenty-three experiments were carried out in the first phase on specimens with a diameter of 63.5mm and a height of 20mm. Key variable parameters in this phase are illustrated in Table 3.4. It should be noted that specimens were prepared with a range of moisture content between 11% and 35% and dry unit weight values of 10.79 and 14.91kN/m<sup>3</sup>.

Table 3.4: Swelling pressure tests schedule with conventional cell (first phase in series 1 tests)

| Test No | Y <sub>d</sub> (kN/m <sup>3</sup> ) | IMC (%) | Note  |
|---------|-------------------------------------|---------|---|
| 1       | 13.73                               | 35      | Specimens were prepared at different dry unit weights and the same moisture content of 35%  |
| 2       | 13.53                               | 35      |   |
| 3       | 13.04                               | 35      |   |
| 4       | 12.36                               | 35      |   |
| 5       | 14.91                               | 27      | Specimens were prepared at different dry unit weights and the same moisture content of 27%  |
| 6       | 14.51                               | 27      |   |
| 7       | 14.02                               | 27      |   |
| 8       | 13.14                               | 27      |   |
| 9       | 12.36                               | 27      |   |
| 10      | 10.79                               | 27      |   |
| 11      | 14.51                               | 20      | Specimens were prepared at different dry unit weights and the same moisture content of 20%  |
| 12      | 14.02                               | 20      |   |
| 13      | 13.04                               | 20      |   |
| 14      | 10.98                               | 20      |   |
| 15      | 14.42                               | 11      | Specimens were prepared at different dry unit weights and the same moisture content of 11%  |
| 16      | 13.93                               | 11      |   |
| 17      | 12.75                               | 11      |   |
| 18      | 11.47                               | 11      |   |
| 19      | 15.00                               | 11      | Specimens were prepared at different dry unit weights and the same moisture content of 11%. Tests were continued for a period of 24h. |
| 20      | 14.02                               | 11      |   |
| 21      | 13.24                               | 11      |   |
| 22      | 12.65                               | 11      |   |
| 23      | 11.28                               | 11      |   |

The second phase of the experimental work in series 1 was carried out to evaluate the proposed approach to overcome the deficiency of wetting and to reduce the time required for a tested specimen to reach full saturation and maximum swelling pressure. To accomplish the second phase in series 1 experimental programme, seven constant volume tests were carried out on specimens using GDS oedometer system equipped with a hydraulic cell (See Table 3.5). Thickness of the specimen prepared for the hydraulic cell was reduced to 10 mm (i.e., half the ring height) and the back pressure of 35kPa was applied to the base of the sample for increasing the water movement rate

inside the specimen and thus quick saturation of the clay. In this phase, all tests were carried out on untreated bentonite specimens prepared at natural moisture content of 11% and various dry unit weight values. Upon completion of swelling tests, all specimens were extracted from the oedometer rings and were sliced to assess the distribution of moisture content throughout the specimens.

Table 3.5: Swelling pressure tests schedule with hydraulic cell (second phase in series 1 tests)

| Test No | $\gamma_d$ (kN/m <sup>3</sup> ) | IMC (%) | Base pressure (kPa) |
|---------|---------------------------------|---------|---------------------|
| 1       | 15.69                           | 11      | 35                  |
| 2       | 15.00                           | 11      | 35                  |
| 3       | 14.51                           | 11      | 35                  |
| 4       | 13.93                           | 11      | 35                  |
| 5       | 12.95                           | 11      | 35                  |
| 6       | 12.16                           | 11      | 35                  |
| 7       | 11.67                           | 11      | 35                  |

### 3.3.2 Series 2: Impact of compaction delay and environmental temperature

In series 2, a comprehensive experimental programme was performed with a focus on assessing the effects of compaction delay and ambient temperature on the physical and hydro-mechanical properties of lime-treated bentonite (M1). Three series of tests were conducted on lime treated bentonite clay including compaction, swelling pressure, permeability and unconfined compressive strength tests as summarised in Table 3.6.

In order to limit the number of tests, lime content was fixed to a value greater than the lime demand value (BS1924-2:1990). However, it was rather challenging to determine the initial lime consumption test for bentonite due to the formation a thick sludge of bentonite that makes pH measurement not

possible. Therefore, based on a similar observation was previously reported by Boardman et al. (2001), 7% lime was selected to induce pozzolanic reactions in sodium- bentonite clay based on lime demand test that was recommended by Boardman et al. (2001).

All specimens were prepared with the same dry unit weight of  $12.16\text{kN/m}^3$  and moisture content of 40% except for compaction tests aimed at determining dry unit weight as a function of the mellowing period. Mini compaction mould and hammer were used to conduct all compaction tests.

As illustrated in Table 3.6, swelling and permeability tests were conducted to determine the permeability characteristics and swelling pressure as a function of predetermined delayed compaction periods on specimens mellowed at two different environmental temperatures. Of note, two groups of testing (G1 and G2) were conducted on specimens that were tested: i.) Immediately after compaction and ii.) after 24h from the end of the mixing process. For the latter group, specimens were mellowed for 3, 6, 12, 24h under intended temperatures and then compacted, sealed and stored in the environmental cupboard at the same temperature for the remaining period of 24h and then tested. As a result, all specimens in this group (G2) were given 24h to chemically react until testing, which was thought to be fair. Of note, the temperature was maintained constant during mellowing and storage processes after compaction until testing.

Untreated and treated specimens were prepared at a dry unit weight of  $12.16\text{kN/m}^3$  and moisture content of 40%. This means that specimens had an initial degree of saturation of 94.7%. Measurements of water flow into the specimens indicated that the volume of water flow during the first hour was significantly higher than the volume of air in the specimens. This confirmed that

specimens had reached full saturation before determination of the permeability coefficient. Also, moisture content was measured at the end of each test. Increase in moisture content was in the range of 2 to 3%. Therefore, the specimens were fully saturated during the permeability tests. GDS Automatic Oedometer System with the hydraulic cell was used to conduct swelling pressure and permeability tests simultaneously.

UCS tests were performed to assess the impacts of mellowing periods on strength evolving of lime stabilised extremely high plastic clay specimens in short and long term as illustrated Table 3.6.

Of note, specimens for UCS were tested after 1, 7, 14 and 28 days from mixing. It should be noted that all UCS results represent the average of three replicate specimens to ensure capturing accurate trends for the gain in strength of lime stabilised clays. A total of 142 specimens were prepared and tested to capture the effect of different mellowing conditions. Mixtures of lime stabilised clays were left in the controlled temperature and humidity environmental chamber to mellow for predetermined periods before compaction, as per testing programme. Compacted specimens were extracted promptly and measurements of dimensions and mass were taken. Specimens were then wrapped in cling-film, sealed in double sealed bags and stored in the environmental chamber until the testing day.

Table 3.6: Testing programme for series 2

| Tests                                    | Parameters  |  | Notes   |
|--|---|--|---|
|  | Variables   | Fixed                                  |   |
| Compaction tests                         | MP = 0, 3, 6, 12, 24, & 48h<br>T = 20°C & 40°C  | Compaction energy<br>MC = 40%          | Additional specimen prepared of pure bentonite                        |
| Swelling pressure and permeability tests | MP = 0, 3, 6, 12, & 24h<br>T = 20°C & 40°C<br>G1 = testing upon compaction<br>G2= testing after 24h of mixing | Yd =12.16kN/m <sup>3</sup><br>MC = 40% | Two additional specimens of pure expansive clay and lime-treated clay |
| Unconfined compressive strength tests    | MP = 0, 3, 6, 12, 24 & 48h<br>T = 20°C and 40°C<br>ET = 1, 7, 14 and 28 days                                  | Yd =12.16kN/m <sup>3</sup><br>MC = 40% | Six additional specimens of pure clay and lime-treated clay           |

where; MP = Mellowing Period, T = Environmental Temperature, ET = Elapsed time from mixing, MC = Moisture Content, Yd = Dry unit weight, G1 = Group 1 and G2 = Group 2

### 3.3.3 Series 3: Effects of lime content and environmental temperature on the properties of extremely high plastic clay

The third series of tests focuses on monitoring the evolution of lime-clay reactions using geotechnical parameters as a function of lime content and environmental temperature. Lime contents of 5, 7, 9, 11 and 13% by dry weight of bentonite clay (M1) powder were added to prepare lime-clay specimens. Table 3.7 demonstrates the variable and fixed parameters in each series of tests following the initial mixing. Specimens for permeability and unconfined compressive strength tests were prepared at the same dry unit weight of

12.16kN/m<sup>3</sup> and moisture content of 40%. With unconfined compressive strength tests, the mixtures were compacted immediately upon completion of the mixing process to avoid the impact of mellowing time. Promptly, compacted specimens were extracted from the mould and measurements of specimen dimensions and mass were taken. Each specimen was then wrapped promptly in cling-film, sealed in double vinyl bags and stored for curing in the environmental chamber under the desired temperature (20°C or 40°C) and 90% relative humidity for a specific period of time (3, 6, 12, 24, 48, 72, and 168h counted from the end of the compaction process).

Permeability tests were performed to determine permeability properties as a function of lime content on specimens mellowed for 24h at two different environmental temperatures. Observations in series 2 showed that increasing mellowing period increases the initial permeability coefficient. Furthermore, specimens mellowed for 24h showed less reduction in the permeability coefficient over the testing period due to quick consumption of 7% lime. It was therefore decided in this series to select 24h mellowing period in order for the impact of lime content to be observed. Following the 24h mellowing period the mixtures were tested upon completion of the compaction process.

Compaction tests aimed at determining the dry unit weight as a function of the mellowing period. Therefore, following the preparation of lime and clay mixtures with 40% moisture content, each mixture was sealed in double vinyl bags and stored to mellow in the environmental chamber under the desired temperature (20°C or 40°C) and a relative humidity of 90% for the predetermined period of time except for the mixtures that were compacted directly after mixing (i.e., no



mellowing). Once predetermined mellowing periods elapsed, mixtures were compacted.

Table 3.7: Testing programme for series 3

| Tests                                    | Parameters  |  |
|--|---|--|
|  | Variables   | Fixed  |
| Compaction tests                         | MP = 3, 6, 12, 24, 48,<br>72 & 168h<br>T = 20°C & 40°C<br>L = 5, 7, 9, 11 & 13%   | standard compactive<br>energy<br>MC = 40%                          |
| Unconfined compressive<br>strength tests | C = 0, 3, 6, 12, 24, 48,<br>72 & 168h<br>T = 20°C & 40°C<br>L = 5, 7, 9, 11 & 13% | Y <sub>d</sub> = 12.16kN/m <sup>3</sup><br>MC = 40%<br>MP = zero h |
| Permeability tests                       | T = 20°C & 40°C<br>L = 5, 7, 9, 11 & 13%  | Y <sub>d</sub> = 12.16kN/m <sup>3</sup><br>MC = 40%<br>MP = 24h    |

where; C = curing time, MP = mellowing period, L = lime content, T = temperature, MC = moisture content and Y<sub>d</sub> = Dry unit weight

### 3.3.4 Series 4: Short and long term assessment of lime treatment of expansive clays with different mineralogy at low and high temperatures

This series of tests examines the impacts of clay mineralogy on the effectiveness of lime stabilisation at different temperatures. A comprehensive experimental programme was conducted to track the evolution of lime-clay reactions and their durations through monitoring the evolution of strength gain at specific curing times using the UCS test. This series examines clays with

different mineralogy compositions comprising Na<sup>+</sup> bentonite and ball (Kaolinite) clay. Four different clays were tested including 100% bentonite (M1), 100% ball clay and two clay mixtures with ratios of 1:1 and 1:3 by mass of bentonite to ball clay. All clays were treated using a range of lime contents up to 13% and cured for up to 672h at two different temperatures of 20°C and 40°C. Based on the observations that had been made on lime treated bentonite in series 3 showed the occurrence of two distinct stages during the evolution of strength gain. During the first stage, the strength gain was fast. The continuity of first stage seem to be dependent upon lime content and temperature. Therefore, to enhance this observation, the bentonite clay was treated by further lime content reached up to 25%. Table 3.8 presents the full details of the series 4 experimental programme. In total, 336 specimens were prepared to assess the effect of different parameters. Also, 140 specimens were prepared as replicates to confirm the effectiveness of the preparation method in alleviating the scattering in the results, especially with a curing times of 168h and 672h.

Table 3.8: Testing programme for series 4

| Materials | Parameters   |  |   |
|-----------|--|--|---|
|           | Variables  | Fixed  | Note  |
| M1        | C = 0, 3, 6, 12, 24, 48, 72, 168 and 672h<br>T = 20°C & 40°C<br>L = 5, 7, 9, 11 and 13%  | Yd = 12.16kN/m <sup>3</sup><br>MC = 40%<br>MP = 0h   | Additional specimens for L = 11% after 192 & 216h and L = 13% after 96, 216, & 240h at 40°C   |
| M1        | C = 0, 3, 6, 12, 24, 48, 72, 96, 144, 168, & 672h<br>T = 20°C & 40°C<br>L = 17, 23 & 25% | Yd = 12.16kN/m <sup>3</sup><br>MC = 40%<br>MP = 0h   | Excessive lime content<br>Additional specimens for L = 17% after 216h, L = 21% after 192 & 240h, and L = 25% after 240 & 288h at 40°C |
| M2        | C = 0, 24, 48, 72, 168 and 672h<br>T = 20°C & 40°C<br>L = 5, 7, 9, 11 & 13%              | Yd = 14.14kN/m <sup>3</sup><br>MC = 29%<br>MP = 0h   | Additional specimens for all lime contents after 3h at 40°C   |
| M3        | C = 0, 24, 48, 72, 168 & 672h<br>T = 20°C & 40°C<br>L = 5, 7, 9, 11 and 13%              | Yd = 13.48kN/m <sup>3</sup><br>MC = 32.5%<br>MP = 0h | Additional specimens for all lime contents after 3h at 40°C   |
| M4        | C = 0, 24, 48, 72, 168 & 672h<br>T = 20°C & 40°C<br>L = 5, 7, 9, 11 and 13%              | Yd = 12.95kN/m <sup>3</sup><br>MC = 37.5%<br>MP = 0h | Additional specimens for all lime content after 3h at 40°C  |

where; C = curing time, MP = mellowing period, L = lime content, T = temperature, MC = moisture content and Yd = Dry unit weight

### **3.3.5 Series 5: Short term assessment of lime treatment of expansive clays with different mineralogy at low and high temperature**

The fifth series of testing inspects the influence of clay mineralogy on the progress of lime stabilisation in the short term. An extensive testing programme was performed to investigate the progress of lime-clay reactions by observing the evolution of permeability and swelling characteristics. Sodium bentonite clay, ball clay, and two additional mixtures comprising of 1:1 and 1:3 bentonite to ball clay by weight were used in this series of tests. All clays were treated by lime contents ranging from 5% to 13% and cured or mellowed for 24h at either 20°C or 40°C before testing at room temperature. Lime treated specimens were tested at the optimum moisture content and maximum dry unit weight of untreated clays.

Table 3.9 exhibits the programme that has been set to monitor the changes in permeability coefficients and swelling pressure as a function of clay type, lime content and environmental temperatures for lime-treated specimens that were either mellowed or cured for 24h under 20 or 40°C.

After the mixing process, the mixture was either left to mellow for 24h under the desired temperature and then compacted or compacted directly and then left to cure for 24h. In the first case, the mixture was promptly put in the double sealed bag, was placed in the environmental chamber for 24h under either 20°C or 40°C and relative humidity of 90%. Immediately after 24h, the mixture was compacted statically into the ring and then tested directly. The second case involves direct compacting of the mixture into the ring. The ring containing the specimen was wrapped by cling film and sealed in double vinyl bags. The sealed bag containing the specimen was placed in the environmental chamber

to cure for 24h under either 20°C or 40°C and relative humidity of 90%. At the end of the curing time, the specimen was tested directly.

Table 3.9: Testing programme for series 5

| Materials | Variables  | Fixed  |
|-----------|--|--|
| M1        | C = 24h or MP =24h<br>T = 20°C and 40°C<br>L = 5, 7, 9, 11, and 13 % | Yd = 12.16kN/m <sup>3</sup><br>MC = 40%<br>MP = 0h   |
| M2        | C = 24h or MP =24h<br>T = 20°C and 40°C<br>L = 5, 7, 9, 11 and 13%   | Yd = 14.13kN/m <sup>3</sup><br>MC = 29%<br>MP = 0h   |
| M3        | C = 24h or MP =24h<br>T = 20°C and 40°C<br>L = 5, 7, 9, 11 and 13%   | Yd =13.48kN/m <sup>3</sup><br>MC= 32.5%<br>MP = 0h   |
| M4        | C = 24h or MP =24h<br>T = 20°C and 40°C<br>L = 5, 7, 9, 11 and 13%   | Yd =12.95kN/m <sup>3</sup><br>MC = 37.5 %<br>MP = 0h |

where; C = curing time, MP = mellowing period, L = lime content, T = temperature, MC = moisture content and Yd = Dry unit weight

### 3.4 Summary

A set of steps were adopted to avoid the scattering in the results and render the monitoring of the lime-clay reaction more efficient using the geotechnical approach. These steps could be summarised as follow:

- 1- Mixing time and mixing techniques were unified to avoid the disparity in the time allowed for lime-clay reaction between the specimens.
- 2- Mini-compaction mould was designed to minimise the variation in the resulting dry unit weight values and to reduce consumption of the materials and effort.

- 3- Curing chamber was used to avoid the dry-back and the variations in curing temperature.
- 4- A new method was utilised to prepare UCS test specimens in five layers to avoid the scattering in the results due to variations in dry unit weight values and the problems in welding points between the compacted layers.
- 5- Swelling pressure and permeability tests were performed synchronously. Depth of specimens in these tests was halved, and water pressure of 35kPa was subjected to the base of the specimen to accelerate the saturation stage and the reach to the swelling stability.

## **Chapter 4 Experimental results and discussion**

This chapter addresses a comprehensive study of the impact of lime on compaction, strength, permeability and swelling characteristics of clays. In order to evaluate such impact, five series of testing programs were performed on treated and lime-treated clays under various conditions. The results of each series of the testing program were reported, accompanied by thorough discussion and analysis on the reported behaviours.

### **4.1 Series 1: Effect of deficiency of wetting on the evolution of swelling pressure**

#### **4.1.1 Introduction**

The first series aims to i.) Investigate the role of initial moisture content and dry unit weight on the swelling pressure and its characteristics, and ii.) Propose and examine a modified testing procedure to overcome the deficiency of the wetting sequence on extremely low permeability high plastic clays e.g. bentonite. Therefore, a set of tests was performed using an automated GDS oedometer system with conventional cell on specimens that were prepared with various initial dry unit weight values and initial moisture contents. Another set of tests were also performed on specimens with half the height and being subjected to a base pressure of 35kPa to the bottom of the specimens to ensure full saturation within a reasonable time.

#### **4.1.2 Effect of initial dry unit weight and moisture content**

In order to examine the impact of initial moisture content and dry unit weight on attained swelling pressure, tests were conducted using conventional oedometer cell. Attained maximum swelling pressures were plotted against corresponding dry unit weight values of specimens, as presented in Figure 4.1.

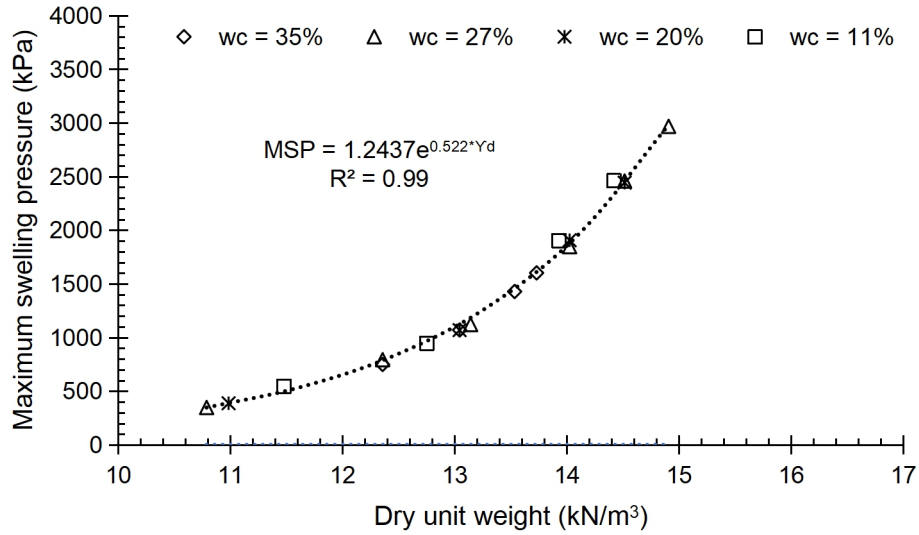


Figure 4.1: Maximum swelling pressures as a function of dry unit weights at different moisture contents (11, 20, 27, and 35%)

Results in Figure 4.1 clearly illustrate that irrespective of the initial moisture content (11, 20, 27, and 35%), the swelling pressure increased with the increase in dry unit weight. Moreover, it is evident that there is a strong exponential relationship between the maximum swelling pressure and dry unit weight. This exponential relationship is compatible with previous research outcomes (Komine and Ogata, 1994, Villar and Lloret, 2008, Jayalath et al., 2016, Yigzaw et al., 2016). Regression analysis for this exponential relationship suggested equation 4.1:

$$MSP = 1.2437e^{0.522*Yd} \quad 4.1$$

where; MSP is the maximum swelling pressure in (kPa), and Yd is the initial dry unit weight (kN/m³).

Expansive clay particles expand by imbibing water into their interlayers. Since any expansion in the volume of the specimen as a whole is restricted in the swelling test, expansion in particle volumes does not lead to an increase in the volume of tested specimens. Instead, the tendency to expansion is measured



as swelling pressure in a constant volume test. Nevertheless, owing to clay particles expansion, reduction in some of the available pores would be expected. Hence, for the same specimen volume, when the dry unit weight is higher, the higher number of particles is available in the specimen accompanied by reduced pore spaces. When the specimen is inundated with water, its pore spaces are filled quickly, accompanied by a higher swelling pressure development due to the higher number of clay particles present.

In contrast, in specimens with low dry unit weight, large pore spaces would be available due to the smaller number of clay particles leading to the measurement of a lower value of maximum swelling pressure. Increasing dry unit weight of specimens led to a reduced range of moisture content which specimens can be prepared at. On the other hand, it is assumed when the initial moisture content of the specimen is higher, lesser swelling pressure should develop compared with the specimen with lesser initial moisture content. Because in higher moisture content specimens, the particles should experience a relatively higher degree of expansion compared with lesser moisture content specimen during the preparation stage; However, there is no obvious effect of the differences in the initial moisture content on the exponential relationship between the resulting maximum swelling pressure and dry unit weight as seen in Figure 4.1.

In order to further assess the potential impact of initial moisture content on the swelling behavior of highly reactive clays, the swelling pressure evolution of specimens that were prepared with different initial moisture contents of 35%, 27%, 20%, and 11% was investigated. Figures 4.2 to 4.5 show that there exist three clear stages in the relationship between the swelling pressure evolution

and time including i. the initial response stage, ii. the intermediate stage and iii. the equalization stage. In all tests, swelling pressure showed a rapid increase during first 10h, reaching up to half of the attained maximum swelling pressure. During stage 1, the hourly change rate in the swelling pressure was determined and evaluated. It was observed that the increase in swelling pressure was slowed down when its rate reached one fifth of what was measured in the first hour. Based on this observation, it was suggested that the time at which the rate of swelling pressure declines to one fifth of measured value in the first hour, to be taken as the end of the initial stage and the beginning of the intermediate stage. The triangular symbols in Figures 4.2 to 4.5 represent end of initial stage. In order to determine end of the intermediate stage, the rate of change in the swelling pressure was calculated every five hours due to the slowdown of the swelling pressure growth during the remaining time. In this context, it was observed that when the rate of change on the swelling pressure reaches 3kPa/h, growth in swelling pressure becomes too small to the extent that it could be neglected. Therefore, end of the intermediate stage was determined when the rate of change in the swelling pressure was 3kPa/h. Square symbols refer to end of intermediate stage in Figures 4.2 to 4.5. It can be noted that the intermediate stage is characterised by a moderate change in the swelling pressure. The equalisation stage extends from the end of the intermediate stage until the end of the test. The results indicated that the change in swelling pressure during this final stage is minor in comparison with the absolute value of the attained swelling pressure.

Determining the beginning and end of the intermediate stage was found useful in distinguishing between the stages in particular on specimens prepared with

the higher moisture content of 35%. Specimens prepared with a moisture content of 35% showed an initial high rate of swelling pressure change at the beginning of the test followed by a gradual declination with time until the maximum swelling pressure was achieved within a period of 55 to 65h which was shorter compared with those observed on specimens with lower initial moisture contents. With initial moisture content of 27%, the increment in swelling pressure was prompt at the initial response stage. The rate of swelling pressure during the intermediate stage is lower and retained almost constant for a period of time past the mark which represents the end of initial stage prior to starting to decline until become difficult to distinguish by the end of the test. The exception in Figure 4.3 was noted from the specimen that was prepared with a dry unit weight of  $14.91\text{kN/m}^3$ , where the evolution of swelling pressure behaved like the specimens with 35% of moisture content because the period in which the rate of change in the swelling pressure remained constant was relatively shorter compared to all other specimens. This could be attributed to the initial degree of saturation on the specimen that was prepared at a higher dry unit weight.

With initial moisture content of 20%, the swelling pressure of specimens showed also quick growth during the initial stage. The difference in the swelling evolution was notable through the intermediate stage between specimens that were tested with initial moisture content of 20% and specimens that were tested at higher initial moisture contents. The rate of swelling pressure rate showed a gradual increase beyond the end of initial stage over a period of about 20h and then the rate of swelling pressure experienced an ongoing decline until it became difficult to distinguish after 80h.

Here it is worth noting that due to the impact of the dry unit weight on the permeability and flow of water through the specimen, the time to reach the equalisation stage on specimens that were compacted at a dry unit weight of  $10.98\text{kN/m}^3$  was shorter on specimens with similar initial moisture content of 20%. Period to reach a stable value of swelling pressure with dry unit weight less than  $11\text{kN/m}^3$  were observed to be 40 and 30h on specimens with initial moisture contents of 20% and 27% respectively.

Impressive features of the evolution of the swelling pressure were observed when specimens were prepared at an initial moisture content of 11% for various dry unit weight values. The results in Figure 4.5 showed that the swelling evolution of specimens with a dry unit weight of  $14.42$  and  $13.93\text{kN/m}^3$  were different from other specimens with higher initial moisture content. The swelling pressure shortly after the beginning of the intermediate stage reached a first peak which was observed after  $\sim 10\text{h}$  from the onset of the test before showing a gradual decline for a short period. Similar observations were recorded in earlier studies (Villar and Lloret, 2008, Villar and Lloret, 2004, Baille et al., 2010, Imbert and Villar, 2006, Yigzaw et al., 2016, Schanz and Tripathy, 2009) in which gradual decline in the evolution of swelling pressure was recorded after reaching a peak value. Unlike the higher dry unit weight specimens, the specimen that was compacted with a dry unit weight of  $12.75\text{kN/m}^3$  experienced an idle phase that lasted for about 9h rather than the declining interval. Whereas, the swelling pressure in the specimen with a dry unit weight of  $11.47\text{kN/m}^3$  showed a gradual increase at the beginning of the intermediate stage. Nevertheless, swelling pressure for the other 11% specimens began to re-evolve gradually reaching the second maximum swelling pressure at about 90,

85, 75 and 60h from the beginning of the test for specimens with 14.42, 13.93, 12.75 and 11.47kN/m<sup>3</sup> respectively. The swelling pressure evolution during the intermediate stage varied in accord with the initial moisture content of the specimen. The progress of swelling indicates an essential role for the initial moisture content in dictating the swelling evolution during the intermediate stage.

Upon completion of the test, the distribution of water in the specimen was inspected visually for specimens with an initial moisture content of 11% (i.e., natural moisture content). It was found that, although water reached all parts of the specimen, there was a slight colour difference between the upper and lower parts and the middle section of the specimen in which the later was a bit lighter. It is worth noting that, the observed colour difference was very slight but existing even after prolonged testing time (i.e., up to 20 days) for specimens that were compacted at 11% and 11.47kN/m<sup>3</sup>. This behaviour could be attributed to the deficiency of wetting as a result of the extraordinary low permeability of bentonite. It seems that during the testing time the difference in the degree of saturation along the depth of specimen renders both upper and lower parts of specimen, when both reach their fully saturation stage, work as barriers preventing the reach of water to the middle part. Both parts in direct contact with water seem to start resisting any further uptake of water hence, no further swelling pressure was recorded. This means that the specimens that have been tested using the conventional cell might have not reached their actual maximum swelling pressure.

To confirm the observed swelling behaviour additional tests were carried out on specimens with natural moisture content of 11%. Figure 4.6 shows the evolution

of the swelling pressure of specimens for a period of 24h. The results revealed that as the dry unit weight declined the swelling pressure drop from its peak value became less pronounced until being completely diminished for a specimen with a dry unit weight of  $12.65\text{kN/m}^3$ . With further reduction in the dry unit weight, the swelling pressure showed a gradual and continuous increase during intermediate stages.

After completion of the tests that lasted 24h, a cylindrical section has been taken from each specimen. Each cylindrical section was horizontally sliced into three equal thickness parts, top, middle and bottom, to determine the moisture content for each part. The cylindrical sections revealed that the middle part of specimens appeared to be slightly less saturated than the top and bottom parts as can be noticed in Figure 4.7. Moisture content of the three sections were determined and indicated that the moisture content in the middle part increased as the dry unit weight declined to range between 29% on a specimen with a dry unit weight of  $11.28\text{kN/m}^3$  to 22% on a specimen with a dry unit weight of  $15.00\text{kN/m}^3$ .

The results suggested that the moisture content in the middle section of the specimens might be responsible for the swelling pressure behaviour with time and the reduction in the swelling pressure from its first peak. These reduction intervals could be due to internal pressures arising during the absorption demand of clay particles to water. However, the swelling pressure on specimens with higher initial moisture content did not show an initial peak of swelling pressure nor a decline in the swelling pressure during intermediate stage.

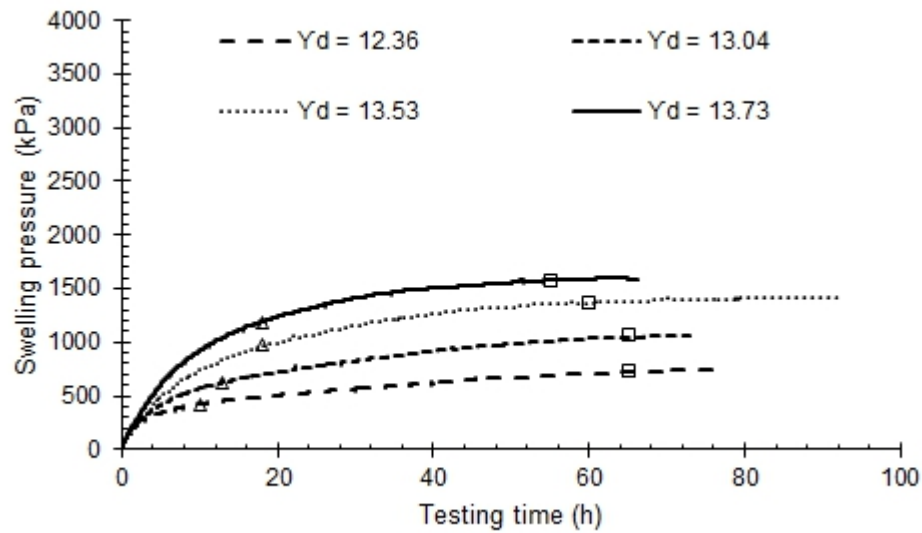


Figure 4.2: Evolution of swelling pressure for specimens at an initial moisture content of 35% (i.e., tested using a conventional cell)

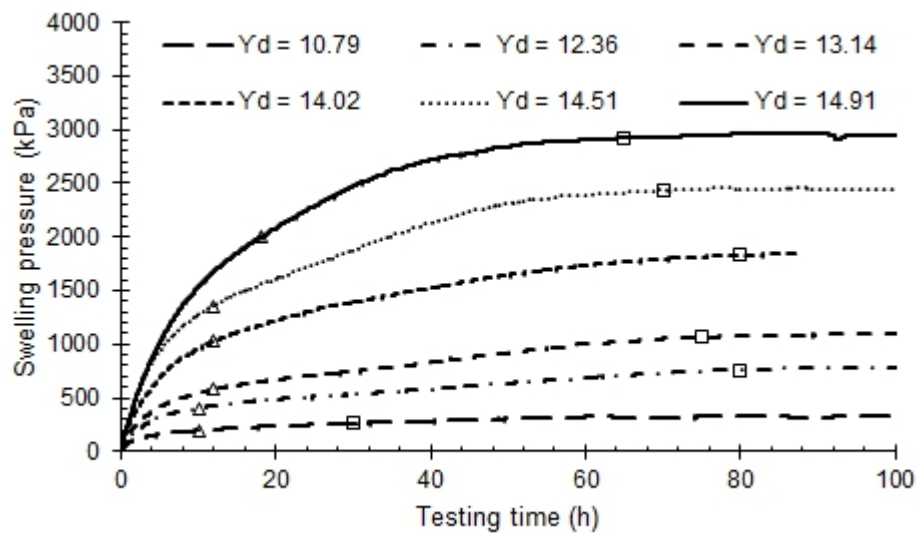


Figure 4.3: Evolution of swelling pressure for specimens at an initial moisture content of 27% (i.e., tested using a conventional cell)

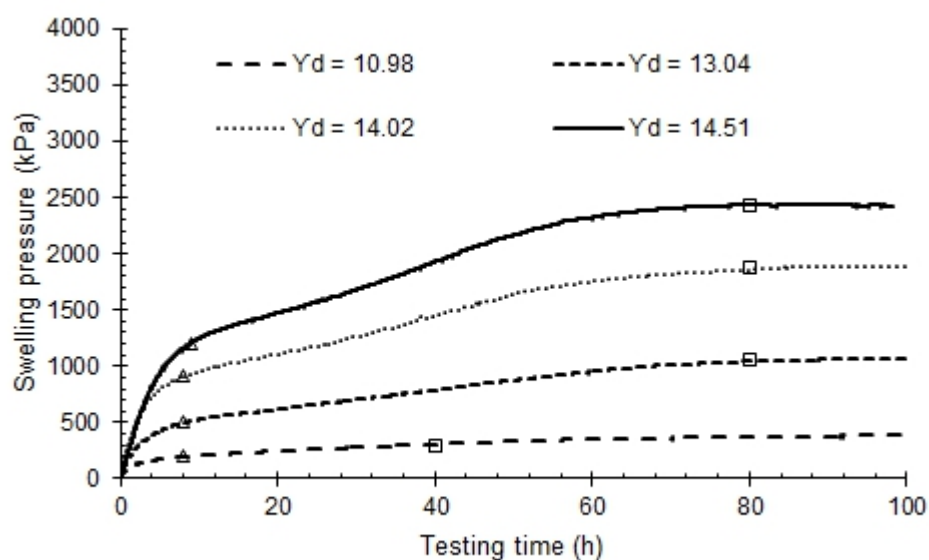


Figure 4.4: Evolution of swelling pressure for specimens at an initial moisture content of 20% (i.e., tested using a conventional cell)

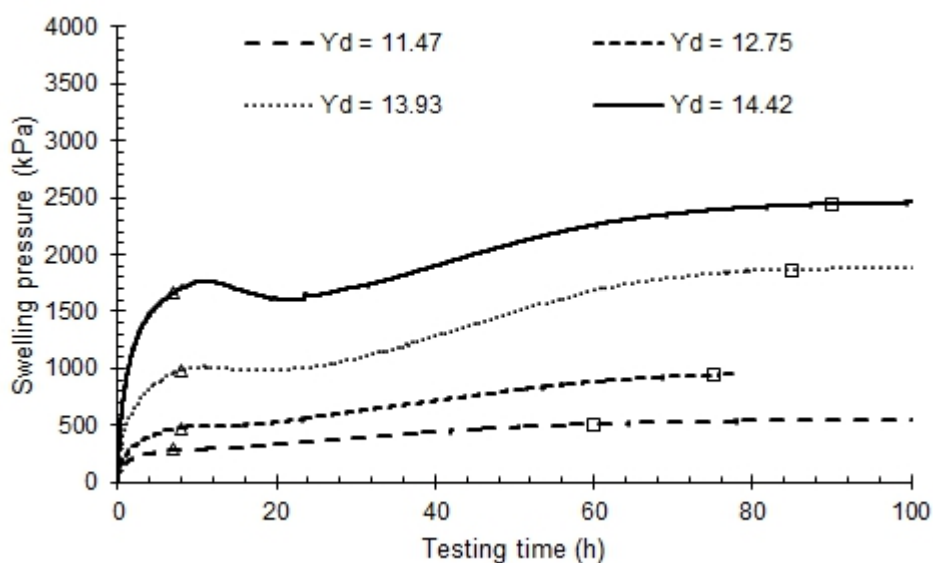


Figure 4.5: Evolution of swelling pressure for specimens compacted at an initial moisture content of 11% (i.e., tested using a conventional cell)



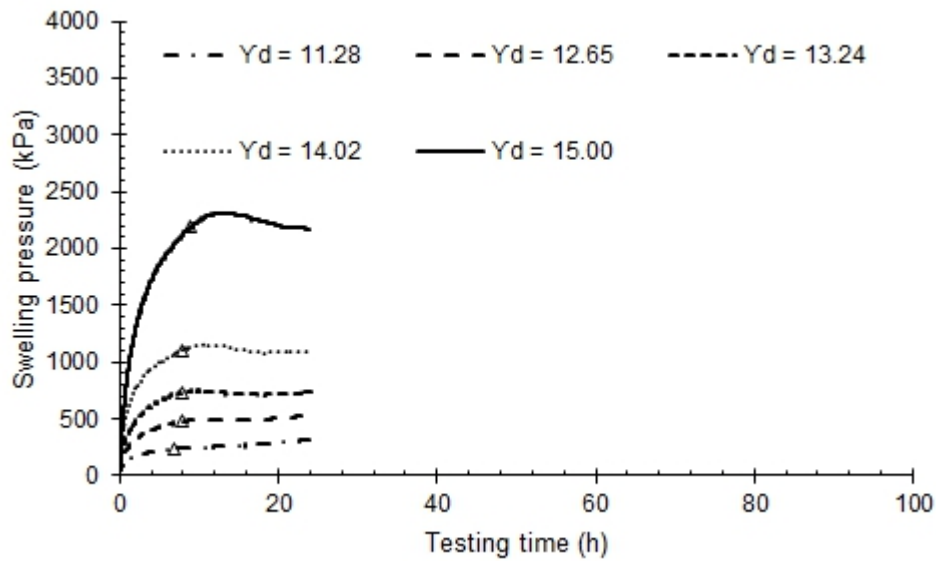


Figure 4.6: Evolution of swelling pressure for specimens at an initial moisture content of 11% (i.e., tested for 24h using a conventional cell)



Figure 4.7: Cylindrical sections extracted from the specimen prepared at shipped moisture content and tested for 24h

#### 4.1.3 Swelling behaviour using a modified approach

For the sake of comparison, the relationships for the maximum swelling pressure as a function of dry unit weight were determined for specimens that were tested using the hydraulic cell. Figure 4.8 plots the maximum swelling pressure values obtained using both conventional and hydraulic cell against the corresponding dry unit weight. As expected, there was also a strong exponential

relationship between the maximum swelling pressure and dry unit weight for specimens tested using the hydraulic cell. It is also noticeable that there was no important difference between the resulting maximum swelling pressures obtained from the hydraulic cell and with those resulting from the conventional cell for specimens with a dry unit weight of less than 13.14 kN/m<sup>3</sup>. At a similar dry unit weight, when the volume is larger the force required to curb the swelling should be higher hence the larger volume includes higher bentonite content. This consistency with Figure 4.9 that illustrates the maximum axial forces that were applied to prevent the swelling as a function of the dry unit weight values for the specimens that were tested using the hydraulic and conventional cell.

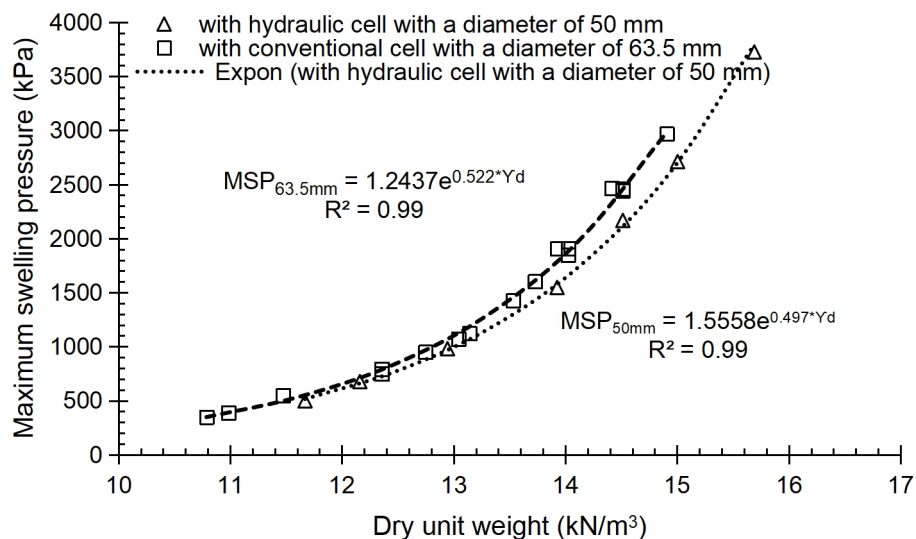


Figure 4.8: Maximum swelling pressures against corresponding dry unit weights for specimens (i.e., tested using hydraulic cell and conventional cells)

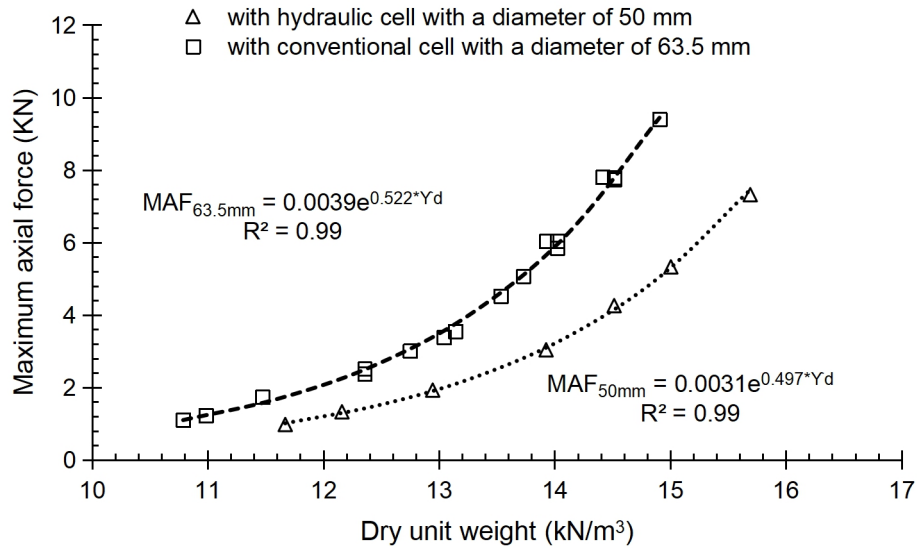


Figure 4.9: Maximum applied forces versus corresponding dry unit weights for specimens (i.e., tested using hydraulic and conventional cells)

In order to normalise the swelling pressures obtained from both conventional and the hydraulic cell, the maximum swelling pressure was divided by the thickness of the specimen (i.e., specimens compacted at a moisture content of 11%), see Figure 4.10.

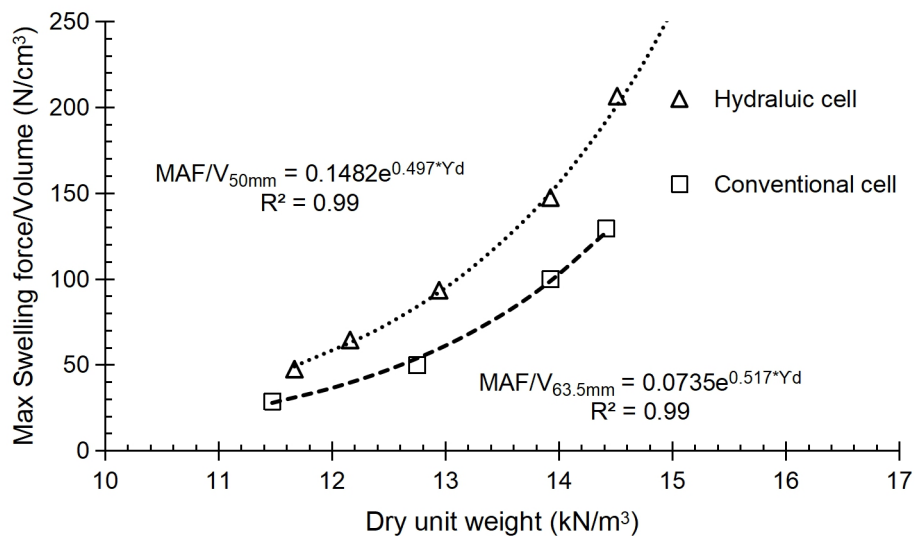


Figure 4.10: Maximum unit volume swelling force versus specimen density for specimens at an initial moisture content of 11% (i.e., tested using hydraulic and conventional cells)

Figure 4.10 shows that the maximum applied force (N) that was used to prevent the swelling of a volumetric unit ( $\text{cm}^3$ ) of the specimen was higher for the hydraulic cell than their counterparts using the conventional cell. This undoubtedly indicated the role of wetting deficiency with the use of conventional cell and therefore, the specimens that were tested at a natural moisture content of 11% using the conventional cell did not reach their actual swelling pressure. Furthermore, the observed difference between the maximum unit volume swelling force obtained from conventional cell and the hydraulic cell was increased as the dry unit weight value increased. Unlike the conventional cell, the use of hydraulic cell with the adopted approach was ensured the flow of water through the entire depth of the tested specimens. This was confirmed by the uniformity of the moisture content over the thickness of the specimens (see Figure 4.11.).

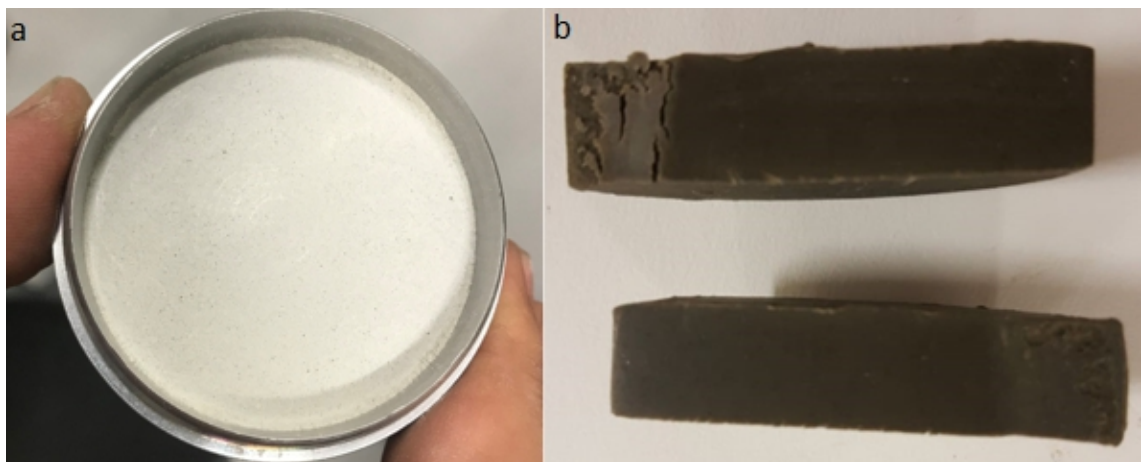


Figure 4.11: a) A prepared specimen with moisture content of 11% b) Vertical section of the specimen at the end of test using hydraulic cell

Based on the outstanding wetting efficiency with hydraulic cell, equation 4.2 can be utilised to estimate the actual maximum applied force per centimetre cube at the various dry unit weights.

$$\text{MFA}/V = 0.1482e^{0.497*Y_d} \quad 4.2$$

Where; MAF/V is the maximum applied force to prevent swelling per unit volume in (N/cm<sup>3</sup>); Y<sub>d</sub> is the initial dry unit weight (kN/m<sup>3</sup>). Equation 4.2 can be used to introduce the equation 4.3 to estimate actual swelling pressure at the utilised dry unit weight.

$$\text{MSP} = H * (0.1482e^{0.497*Y_d}) \quad 4.3$$

Where MSP is maximum swelling pressure in (kPa); Y<sub>d</sub> is the initial dry unit weight (kN/m<sup>3</sup>); H is the height of specimen in (mm)

Evolution of swelling pressure for all specimens that were tested using the hydraulic cell is depicted against the testing time in Figure 4.12. Initial rate of growth in the swelling pressure was fast during the initial stage, exceeding half of the maximum swelling pressure within 5h from the onset of the test. Concerning the intermediate stage, disappearance of intervals in which the swelling was decreasing can be observed. Disappearance of such intervals emphasised the responsibility of deficiency of the wetting sequence in the appearance of this interval with the initial moisture content of 11% and thus on the effectiveness of the proposed solution in accelerating saturation. During the intermediate stage, swelling evolution showed some concavity. At the beginning of the intermediate stage, the swelling pressure rate continued to decline for a short time ( $\leq 5h$ ) followed by a gradual increase for some time ( $\leq 20h$ ) before beginning to decline again until it becomes negligible at the end of the intermediate stage. A specimen prepared at dry unit weight of 15.69kN/m<sup>3</sup>

showed that the rate of swelling pressure kept increasing at nearly a constant value beyond the initial stage that was indicated by the triangular mark until starting to decline at about 80h.

Disappearance of the first peak during the intermediate stage using hydraulic cell confirms the role of wetting sequence in dictating the swelling evolution.

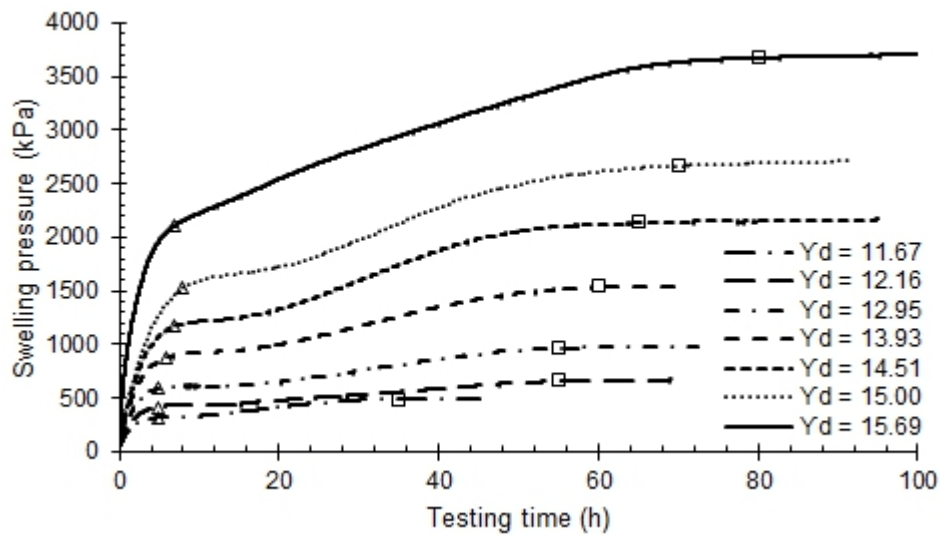


Figure 4.12: Evolution of swelling pressure for specimens at an initial moisture content of 11% (i.e., tested using a hydraulic cell)

Figure 4.12 also revealed that as the dry unit weight value increased as the time required to reach the equalisation stage become longer. For instance, at the highest dry unit weight of 15.69kN/m<sup>3</sup>, the time for specimen to reach its equilibrium was 80h whereas the equilibrium was reached in just 35h on the specimen with a dry unit weight of 11.67kN/m<sup>3</sup>. Such behaviour could be attributed to impact of dry unit weight on the permeability. Where, as the dry unit weight increases as the permeability declines (Ren et al., 2014, Gao et al., 2018). The use of hydraulic cell for measuring the maximum swelling pressure also resulted in a significant reduction of the test duration. As an example, the time required for reaching the swelling pressure equilibrium was about 90h for

the conventional cell whereas, this value was decreased to 65h for the hydraulic cell. Thus, it can be inferred that the adopted solution has remarkable influence in reducing the test duration.

#### **4.1.4 Summary**

The results revealed that the initial dry unit weight controlled the maximum swelling pressure, and the initial moisture content has no effect on the value of maximum swelling pressure. However, the initial moisture content alongside the dry unit weight was found to have an undeniable impact on swell-time behaviour. Furthermore, it was found that the proposed modification to the testing procedure was practically effective to reach full saturation, speed up the testing without adverse implication on the measurement of swelling pressure.

## **4.2 Series 2: Impact of compaction delay and environmental temperature**

### **4.2.1 Introduction**

In the second series, a comprehensive experimental programme was performed with the focus on assessing the effects of compaction delay and ambient temperature on the physical, mechanical and hydraulic properties of 7% lime treated bentonite. Specimens were mellowed for periods of 0, 3, 6, 12, 24 and 48h at two different temperatures of 20°C and 40°C before being compacted, then tested and/or cured for up to 28 days for evaluating the impacts on long-term strength development. All specimens were prepared with the same dry unit weight of 12.16kN/m<sup>3</sup> and moisture content of 40% except for tests aimed at determining dry unit weight as a function of the mellowing period.

### **4.2.2 Dry unit weight**

The effect of compaction delay and environmental temperatures on the dry unit weight of lime treated extremely high expansive clay is shown in Figure 4.13. It is evident that the dry unit weight of lime-treated clay specimens that were mixed and compacted immediately was found to decline appreciably to 10.95kN/m<sup>3</sup> compared to the dry unit weight of pure clay specimen (12.16kN/m<sup>3</sup>). The reduction in compactability and hence the 10% drop in the dry unit weight can primarily be attributed to the flocculation of lime treated clay caused by cation exchange processes and instant formation of cementation compounds that bind the flocs. The growing of such cementitious compounds in lime-treated bentonite was observed to occur very shortly after the addition of lime (Vitale et al., 2017). Delaying compaction of lime-clay mixtures led to a further drop in the dry unit weight, in particular, mixtures that were mellowed for up to 12h. The trend for the measured dry unit weight relationships as a function



of the mellowing period nearly flattened up with a further increase in the mellowing period. This pattern can be explained by ongoing formation of cementitious compounds in a loose state offering increased resistance to compaction in the first 12h from mixing. In other words, delay in compaction would lead to enhanced clay agglomeration and stronger bonding between clay particles, which would cause further resistance to compactability. It is worth noting that specimens mellowed at a temperature of 40°C showed a higher reduction in the dry unit weight than those mellowed at 20°C due to the higher rate of the formation of cementitious compounds as observed by (Al-Mukhtar et al., 2014, De Windt et al., 2014). The rate of reduction in dry unit weight for both temperatures slowed down after 12h of mellowing. Such slow down indicates the slow formation of cementitious compounds generally and losing the dependence on the ambient temperature after the first 12h of mellowing.

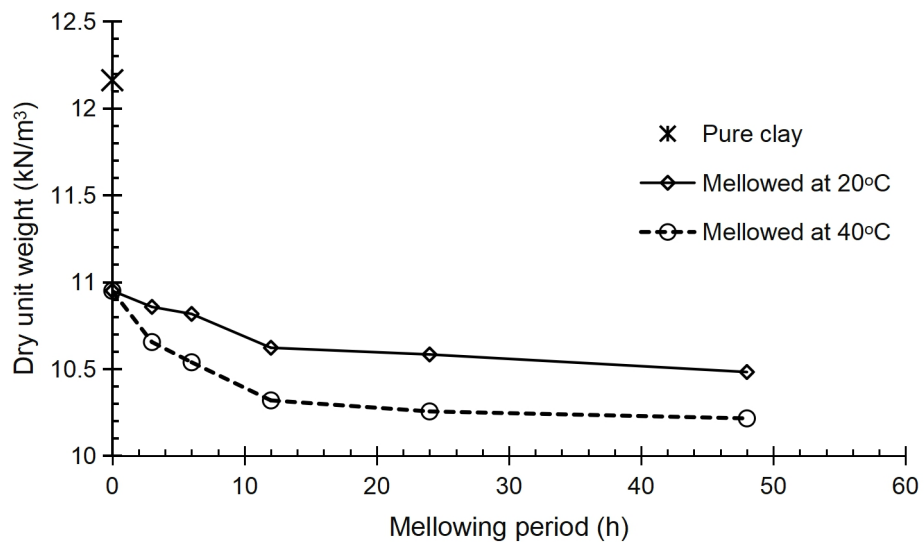


Figure 4.13: Effect of mellowing and temperature on the dry unit weight

### 4.2.3 Swelling pressure and permeability

#### 4.2.3.1 Swelling pressure

Results on untreated expansive clay specimens showed that the swelling pressure of pure clay was as high as 750kPa. However, that of lime treated specimens declined to 250kPa when the specimens were compacted without delay and directly tested, resulting in a 67% reduction in the swelling pressure irrespective of the mixture temperature. The significant reduction in the measured swelling pressure can be attributed to declining specific surface area of treated clay particles in contact with the pore water due to flocculation, agglomeration, and initial cementitious compounds (Beetham et al., 2015). Figure 4.14 shows results for the swelling pressure as a function of mellowing period for the first group of specimens that were tested immediately upon compaction as a function of compaction delay at two different temperatures.

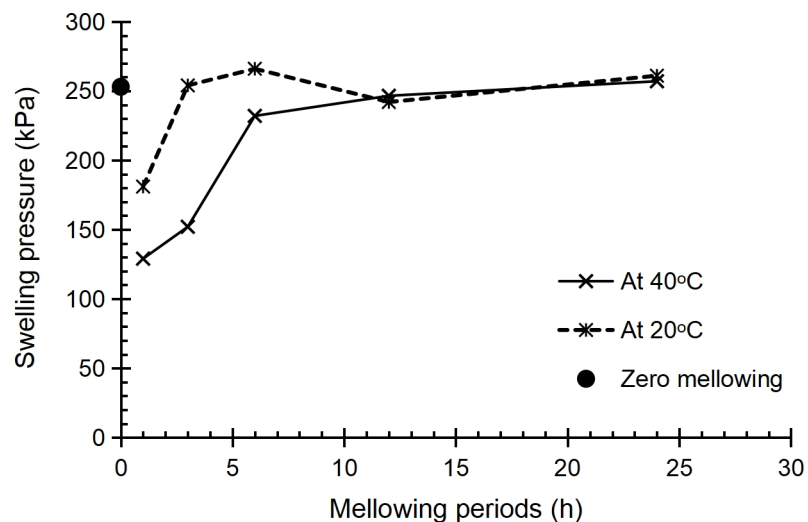


Figure 4.14: Swelling pressures of specimens tested directly after compaction

Illustrated data in Figure 4.14 revealed that measured swelling pressure of the treated specimens which had been mellowed at 20°C and 40°C reached comparable values after 12h of mellowing. The swelling pressure of the lime-treated specimens showed a substantial reduction in the first 12h in particular for specimens mellowed at 1h at 40°C. This substantial decline could be attributed to the rapid rate of formation of cementitious compounds during the first 12h, which enabled a substantial drop in the tendency to swell. Besides, formation of cementitious compounds enhances the role of flocculation and agglomeration and binds the flocs together, which would help further in curbing the swelling pressure. However, hence, the phenomenon mentioned above took place in the loose state during mellowing before compaction; subsequent compaction would cause partial destruction to the flocs and bonding between clay particles which in turn would lead to higher swelling pressure. Due to testing immediately after compaction, one would note that the time given for the chemical reaction in these specimens was different. As a result, another group of testing was performed in which all specimens were given 24h to chemically react until testing while compaction was conducted at an intermediate stage at 3h, 6h, 12h and 24h from mixing. Therefore, group 2 of testing was characterised by being fair in terms of the time given to the lime to chemically interact with the clay. Results for swelling pressure of the second group on specimens that were tested after 24h from mixing irrespective of the mellowing period are shown in Figure 4.15. Measured swelling pressure on the lime-treated specimens that were compacted immediately after mixing and cured for 24h at 20°C and 40°C before testing was found to be 26kPa and 17kPa respectively. The results show clearly that the swelling tendency of lime treated

extremely high expansive clay nearly abolished when specimens were not permitted to mellow before compaction but cured for 24h. By comparing the values of swelling pressure with no compaction delay with those measured on 24h-mellowed specimens at both temperatures, it can be stated that the formation of initial cementitious compounds shortly after the addition of lime plays a significant role in restraining the swelling tendency. In other words, disturbance of the initial cementitious compounds by delayed compaction adversely affects the ability of lime to control the expansion of expansive clay. Figure 4.15 shows remarkable reliance on the curing period after compaction for restraining the swelling pressure rather than the mellowing period. There is a potential increase in the swelling due to the breaking down of the flocs and initial cementation that formed in the loose state as a result of subsequent compaction. It is also noticeable the deviation between those mellowed for 6h. This deviation is explained by the higher rate of formation of cementitious compounds at 40°C during the first 12h which would compensate for the partial destruction of flocs and help in further curbing the swelling tendency. The results, therefore, suggest that changing environmental temperature during the mixing process, mellowing and curing would affect the swelling pressure during the first 12h.

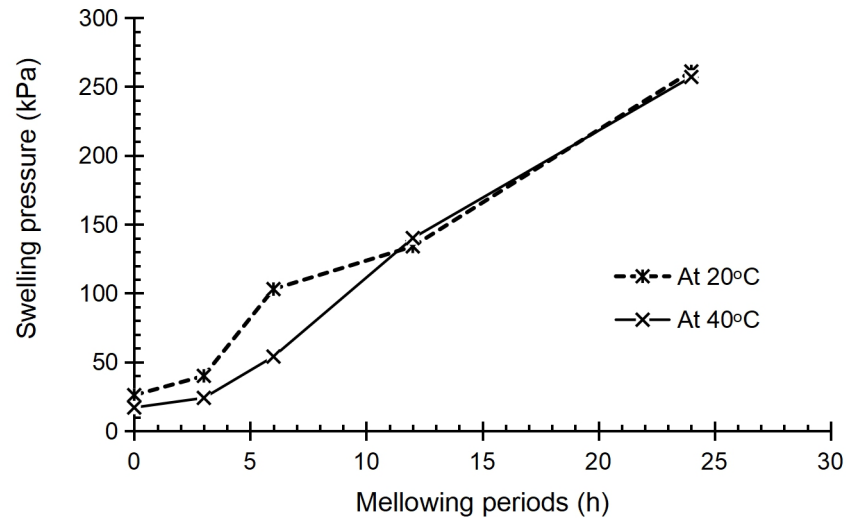


Figure 4.15: Swelling pressures of specimens tested after 24h from mixing

#### 4.2.3.2 Permeability

Of note, the untreated expansive clay specimen was found to be impermeable under the applied pressure. Hence, its coefficient of permeability could not be determined. The coefficient of permeability of the lime-treated specimen, which was compacted directly after mixing (zero h mellowing period) and then submerged directly, reached a value of  $1.7 \times 10^{-9}$  m/s. The immediate increase in permeability can be attributed to the formation of inter-particle and inter-flocs pores. Figures 4.16 and 4.17 present data for the measured coefficient of permeability of lime treated clays for G1 specimens, which were compacted and tested immediately after a period of mellowing at 20°C and 40°C respectively, versus elapsed time from submersion in the odometer cell.

Inspection of illustrated data in Figures 4.16 and 4.17 showed that there is a direct increase in the value of the coefficient of permeability with increased mellowing period shortly after testing. Nevertheless, the gradual decline in the value of the coefficient of permeability was evident for all specimens over the 3-

day measurement period reaching a relatively lowered coefficient of permeability value. The gradual decline can be explained by the ongoing formation of cementitious compounds in the available pores leading to a reduced size of interconnected pores (Wild et al., 1987, Al-Mukhtar et al., 2012). The permeability coefficient of specimen mellowed for 24h at 20°C was 1 order of magnitude higher than that measured after 3h of mellowing. Mellowing at 40°C resulted in lime-treated clay specimens being more permeable and followed by a substantial reduction in permeability coefficient over the testing period. It was noted that specimens mellowed for 24h had a permeability coefficient as high as 40 times as that measured on mellowed specimens for up to 6h before testing. The higher coefficient of permeability could be due to the rapid consumption of lime before compaction and destruction of the bond, which leads to an open structure and enhanced connectivity between the pore voids.

Results for the permeability coefficient of group 2 specimens that were tested after 24h from mixing are presented in Figures 4.18 and 4.19 at 20°C and 40°C, respectively. Generally, the results of specimens mellowed and cured at 20°C showed a gradual reduction in the coefficient of permeability with elapsed time. Among all specimens that were tested after 24h of mellowing at 20°C hrs, the specimen with no compaction delay but cured for 24h had the lowest value of the coefficient of permeability. The other prevailing observation is that the coefficient of permeability of all specimens that were tested after 24h at 20°C was one order of magnitude higher in comparison with counter specimens that were tested upon compaction.

By comparing data in Figure 4.19 with those presented in Figure 4.18 illustrates that mellowing the specimens at a temperature of 40°C resulted in a coefficient of permeability being several times higher than that measured on specimens mellowed at 20°C. Since all specimens were prepared with the same dry unit weight, the difference in the coefficient of permeability values is likely to be due to the distribution of pore size and connectivity between pores. It seems that the more open fabric is induced by, the higher rate of formation of cementitious compounds at 40°C in the loose state offering some resistance to the subsequent compaction keeping the microstructure open and leading to an increased flow of water under the same water pressure. Careful inspection of Figures 4.18 and 4.19 indicates that unlike the measured coefficient of permeability values at 20°C which showed a gradual decline over elapsed time, specimens that were mellowed and cured at 40°C and tested after 24h of mixing showed relatively stable values of coefficient of permeability after 24h of being submerged. Such stability could be due to the rapid consumption of the lime during the first 24h at 40°C. By and large, increasing the mellowing period leads to higher values of the coefficient of permeability. The results, therefore, suggest that permeability of lime treated clays are mellowing period, temperature and lime availability dependent.

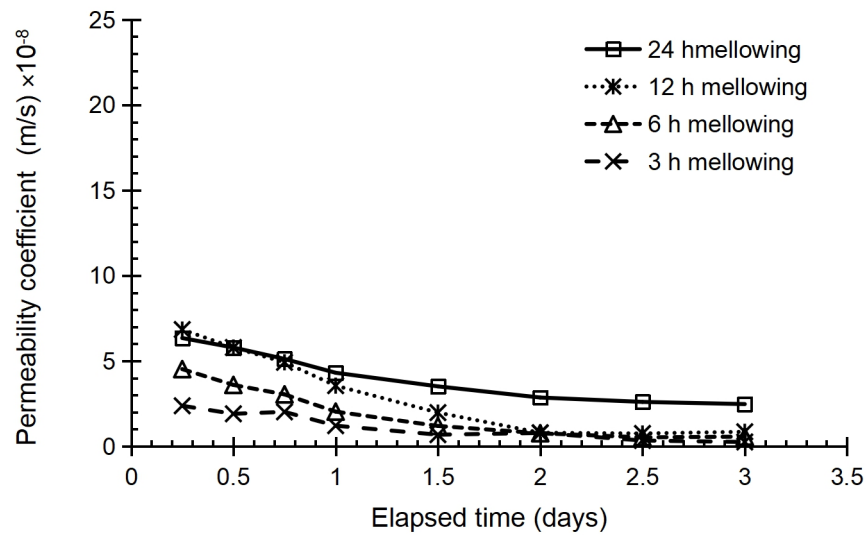


Figure 4.16: Coefficient of permeability versus submersion period for a group I at 20°C with 7% lime.

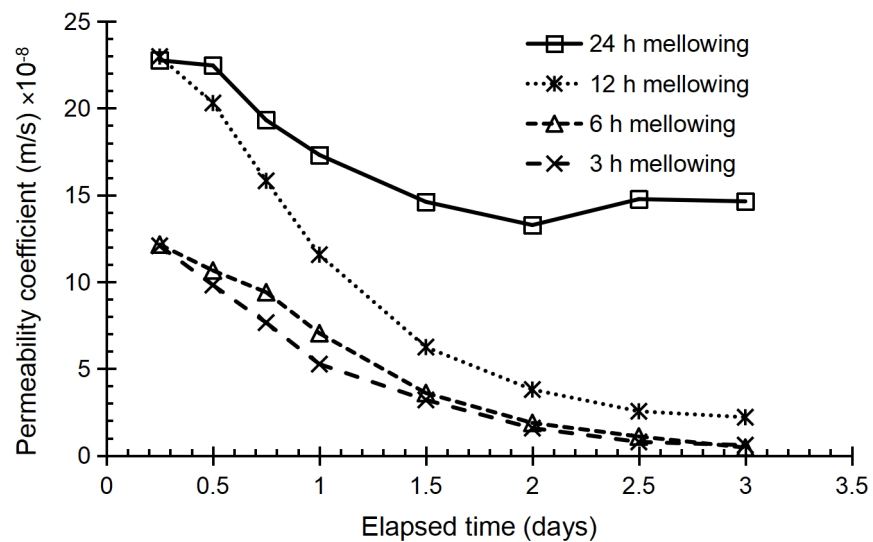


Figure 4.17: Coefficient of permeability versus submersion period for a group I at 40°C with 7% lime



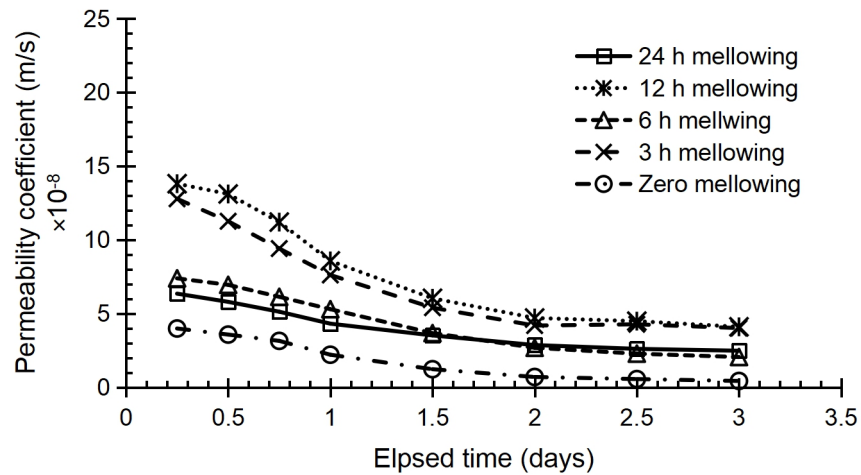


Figure 4.18: Coefficient of permeability versus submersion period for a group 2 at 20°C with 7% lime.

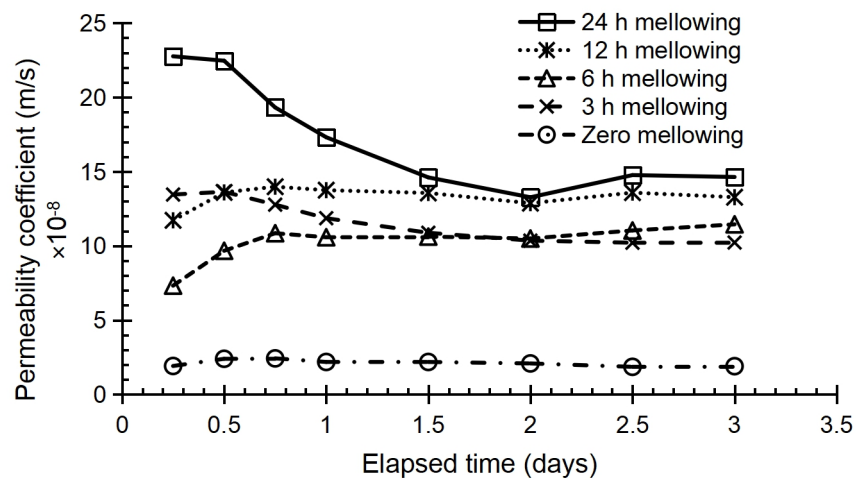


Figure 4.19: Coefficient of permeability versus submersion period for a group 2 at 40°C with 7% lime.

#### 4.2.4 Unconfined Compressive Strength

##### 4.2.4.1 Axial stress

Tests were undertaken in this section to not only investigate the immediate effects of compaction delay on Unconfined Compressive Strength (UCS) of lime treated expansive clays but also assess the gain in strength throughout curing.

Of note, identical environmental conditions were maintained during the predetermined periods of compaction delay and curing periods. It is also worth noting that the data presented hereafter for UCS represent the average peak strength that was measured on three replicate specimens. The variation of UCS from the average strength was found not to exceed  $\pm 4\%$  which was considered acceptable and reflects the effectiveness of specimen preparation method as the individual strength was not diverged from the average by more than  $\pm 10\%$  as recommended by Consoli et al. (2011). Measurements that were taken for dimensions of specimens and moisture content just before testing showed the negligible change in specimen volume and the value of moisture content.

Specimens tested under similar conditions of no mellowing and direct testing upon compaction showed that UCS of pure clay specimens was found to be  $525\text{kN/m}^2$  whereas that of lime treated expansive clay was  $1255\text{kN/m}^2$ . The immediate strength gain by lime addition indicates the speed of lime interaction and its immediate effects on soil characteristics. The immediate strength gain suggests that both cation exchange and the pozzolanic reaction would occur concurrently from the addition of lime which is supported by earlier observations made by (Diamond and Kinter, 1965, Vitale et al., 2017). The UCS values of lime treated specimens that were compacted directly after mixing and left for 24h at  $20^\circ\text{C}$  and  $40^\circ\text{C}$  were found to be  $1756\text{kN/m}^2$  and  $2009\text{kN/m}^2$  respectively. In contrast, the strength of specimens which were mellowed for 24h and then compacted and tested directly was found to be  $1156\text{kN/m}^2$  and  $1344\text{kN/m}^2$  at  $20^\circ\text{C}$  and  $40^\circ\text{C}$  respectively. The results clearly show that specimens mellowed for 24h experienced a significant loss in strength irrespective of the environmental temperature. The reduction in the strength illustrates the adverse

effects of subsequent compaction destroying the cementitious compounds that were developed over 24h of mellowing period.

Figures 4.20 and 4.21 show results for measured UCS on specimens treated with 7% of lime as a function of mellowing period at environmental temperatures of 20°C and 40°C respectively over of a period of 28 days from mixing. The results show clearly that irrespective of the ambient temperature, delaying the compaction of lime treated extremely high plastic clay mixture was found to be detrimental to achieving enhanced UCS. However, a gradual increase in the value of UCS was noticeable throughout curing. The results clearly show that UCS of specimens mellowed and cured at 40°C was higher by 25% in comparison to those mellowed and cured at 20°C.

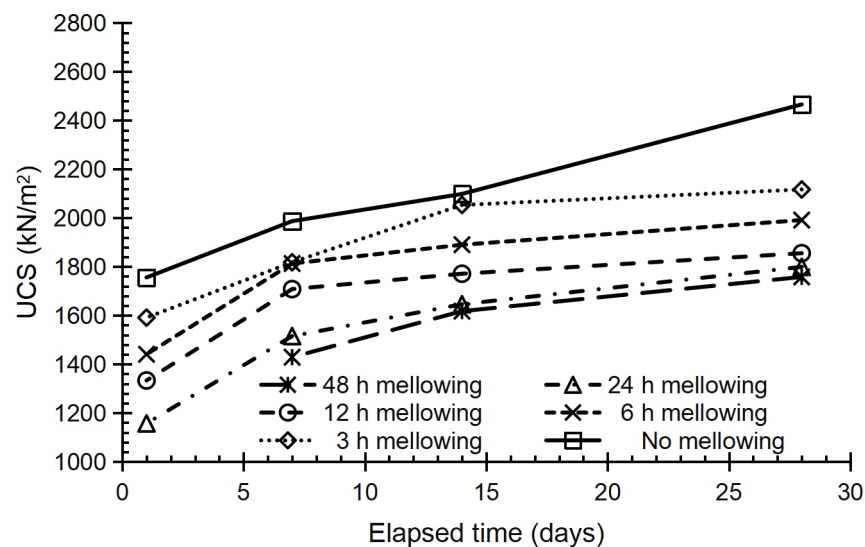


Figure 4.20: Effect of mellowing periods on development of strength gain at 20°C with 7% lime

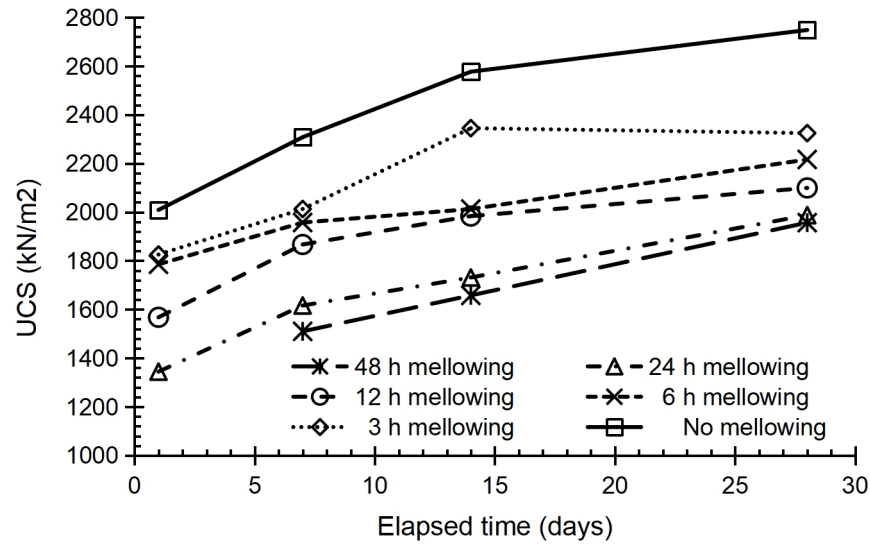


Figure 4.21: Effect of mellowing periods on development of strength gain at 40°C with 7% lime

To aid the discussion, Figure 4.22 was plotted for UCS measured after 1 and 28 days from mixing versus mellowing periods and Table 4.1 was presented to illustrate the strength gain in 24h. Of note, UCS of pure expansive clay was taken as a control. It is evident that a substantial drop in the measured values of UCS was observed as a result of increasing mellowing period in particular within the first 12h. Figure 4.22 also revealed that the difference in the strength gain occurred due to temperature appeared, to some extent, to remain the same across the 28 days of curing period. This differences in strength are likely to be due to the initial cementation compounds and their rate of formation, which is dependent on the temperature. The formation rate of cementitious compounds is sharply lower regardless of the ambient temperature with a prolonged curing period. Table 4.1 illustrates that the gain in strength after 24h from mixing was generally faster and higher at 40°C than those measured at 20°C. The results confirm that zero mellowing gave a 234% and 282% increase

in strength when cured for 24h at 20°C and 40°C respectively, whereas those mellowed for 24h showed only an increase of 120.4% and 156.4%, respectively

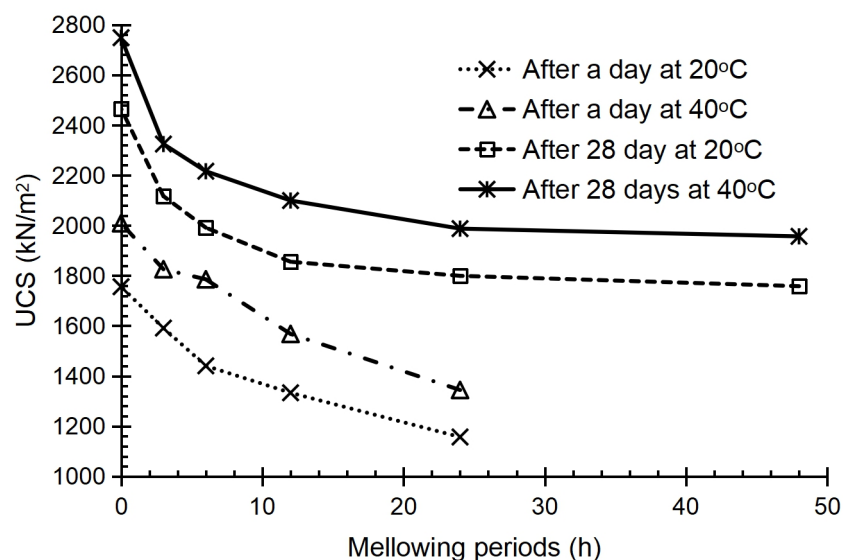


Figure 4.22: Effect of the mellowing period on UCS after 1 and 28 days at different temperature with 7% lime

Table 4.1: Analysis of strength gain after 24h from mixing at 20°C and 40°C

| Mellowing period (h) | Temperature of 20°C  |   | Temperature of 40°C  |   |
|----------------------|--|---|--|---|
|                      | Strength gain at the end of the first day (kN/m <sup>2</sup> ) | % increase in UCS after 24h from mixing | Strength gain at the end of the first day (kN/m <sup>2</sup> ) | % increase in UCS after 24h from mixing |
| 0                    | 1230.7   | 234.4                                   | 1483.7   | 282.6                                   |
| 3                    | 1066   | 203.0                                   | 1300.5   | 247.7                                   |
| 6                    | 915.5  | 174.4                                   | 1260.3   | 240.0                                   |
| 12                   | 808.1  | 153.9                                   | 1042.7   | 198.6                                   |
| 24                   | 631.87   | 120.4                                   | 819.24   | 156.0                                   |

#### **4.2.4.2 Axial strain**

Data presented hereafter represent average values of axial strain that were measured at peak strength on three replicate specimens. The variation between measured strains from the three replicate specimens did not exceed  $\pm 5\%$ . Tests with no compaction delay on specimens of pure expansive clay and lime-treated clays showed that peak strength was experienced at an axial strain of 6% and 2.4% respectively. Of note, lime-treated expansive clay specimens were compacted immediately after mixing and tested directly. The decline in measured strain would directly be related to the development of cementation material at the particles contact. On the other hand, lime-treated expansive clay specimens that were mellowed for 24h and tested directly experienced axial strains of 3.0% and 2.5% at 20°C and 40°C respectively. The slightly higher strain measured on specimen mellowed at 20°C could be interpreted by the slow formation of gel cementitious compounds.

Figures 4.23, 4.24 and 4.25 present the response of axial strain measured at peak UCS versus compaction delay on specimens tested after 1, 7 and 28 days from mixing at two different temperatures of 20°C and 40°C. The results revealed that delaying compaction leads to increased axial strain irrespective of elapsed time for testing, which means that lime treated expansive clays are ductile. The environmental temperature was found to play a significant role in the underpinning treatment process leading to changing axial strain behaviour over the curing period. For a short curing period of 1 day, the results revealed that specimens mellowed and cured at 20°C experienced higher axial strain than those managed at 40°C due to the accelerated pozzolanic reaction. This trend of behaviour was wholly altered with extended curing periods to 7 and 28

days, resulting in, specimens being mellowed and cured at 20°C experienced being brittle. This observation could be attributed to the quick consumption of lime at the higher temperature (40°C) whereas at 20°C lime stabilisation continues over the prolonged curing period which is contradictory to earlier conclusions made by Toohey et al. (2013).

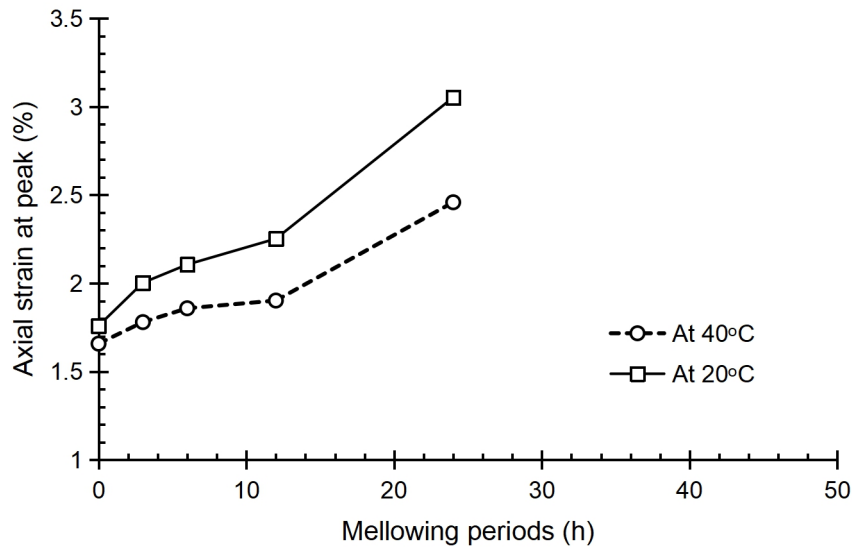


Figure 4.23: Strain behaviour a function of mellowing period after a 1 day

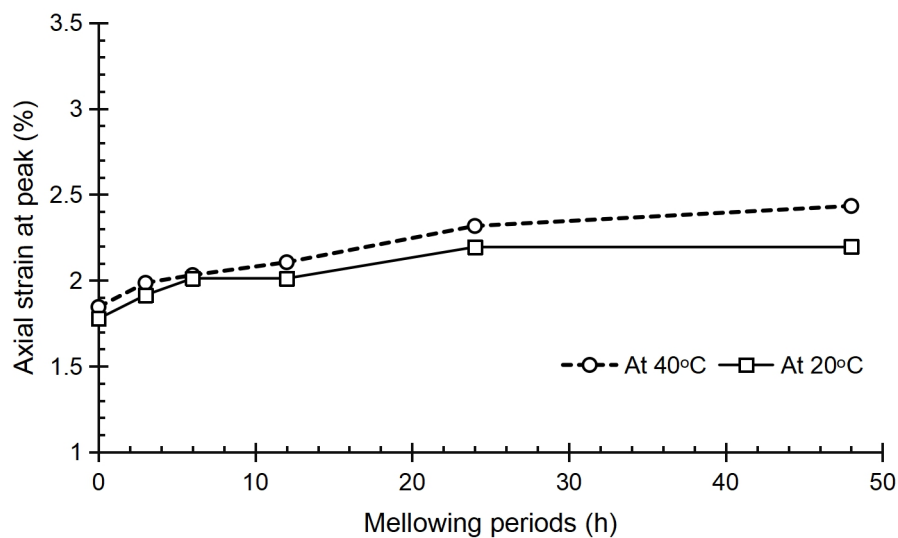


Figure 4.24: Strain behaviour a function of mellowing period after 7 days

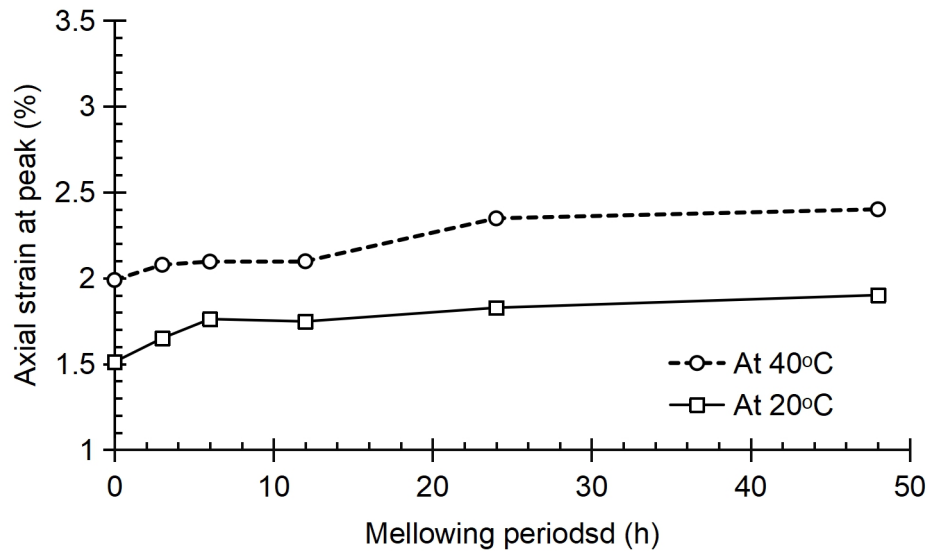


Figure 4.25: Strain behaviour a function of mellowing period after 28 days

#### 4.2.5 Summary

The results revealed that as the mellowing duration increased the dry unit weight declined remarkably at both temperatures within the first 12h. Besides, a higher reduction rate was observed when specimens were mellowed at a temperature of 40°C. A 97% reduction in swelling pressure was obtained when the specimens were compacted upon mixing (zero-hour mellowing period) and left to cure for 24h before testing. The permeability coefficient of lime treated expansive clays was increased by up to 40 times when compaction was delayed for 24h or when specimens were mellowed at 40°C. Specimens mellowed at a temperature of 40°C showed relatively stable values of permeability coefficient over the measurement period, which could be attributable to the accelerated pozzolanic reaction. The Unconfined Compressive Strength tests revealed that the strength of lime treated expansive clays is significantly affected by compaction delay. An increase of 234% and 282% in the Unconfined Compressive Strength was achieved after 24h of mixing with no



compaction delay at 20°C and 40°C respectively. A gradual long-term gain in strength was observable within the 28 days post mixing, but the rate of strength gain becomes slower and independent of temperature after the first 24h of mixing. The results suggested that the four fundamental reaction mechanisms occur concurrently within the first 12–24h after lime addition recognised as being the most crucial time. Damaging the cementitious compounds by delayed compaction is harmful to the restraining of the swelling pressure, and the strength value of lime treated expansive clays.

### **4.3 Series 3: Effects of lime content and environmental temperature on the properties of extremely high plastic clay**

#### **4.3.1 Introduction**

The third series focuses on monitoring the evolution of lime-clay reactions using geotechnical parameters as a function of lime content and environmental temperature. Lime contents of 5, 7, 9, 11 and 13% by dry weight of expansive clay powder were added to prepare lime-clay specimens. The specimens were prepared at the same dry unit weight of  $12.16\text{kN/m}^3$  and moisture content of 40% except for tests aimed at the determination of dry unit weight as a function of the mellowing period. Prepared specimens were mellowed or cured at two different ambient temperatures of  $20^\circ\text{C}$  and  $40^\circ\text{C}$

#### **4.3.2 Dry unit weight**

The dry unit weight of untreated clay specimens that were prepared with 40% moisture content was found to be  $12.16\text{kN/m}^3$ . The dry unit weight of specimens that were treated with 5, 7, 9, 11 and 13% lime and compacted and tested directly after mixing were 10.68, 10.75, 10.73, 10.70 and  $10.71\text{kN/m}^3$  respectively. These results show a decline by about 12% in the dry unit weight of treated specimens compared with that of the untreated specimen. This immediate reduction in the dry unit weight can be attributed to the immediate changes due to the flocculation that is predominantly induced by cation exchange phenomenon and the formation of initial cementitious compounds. Lime content did not play a significant role at zero h mellowing due to its quantity, which seemed sufficient to induce cation exchange. The resulting values of dry unit weight on specimens mellowed at  $40^\circ\text{C}$  and  $20^\circ\text{C}$  were plotted against the mellowing period in Figures 4.26 and 4.27, respectively. The effect of lime content on attained dry unit weight is very notable when mellowing

was conducted at 40 °C. Whereas, specimens mellowed at 20°C showed a lower declining rate in the dry unit weight with the increased mellowing period. Also, no further drop in dry unit weight was observed on specimens treated with 5% lime after 24h of mellowing, which could be due to the total consumption of lime.

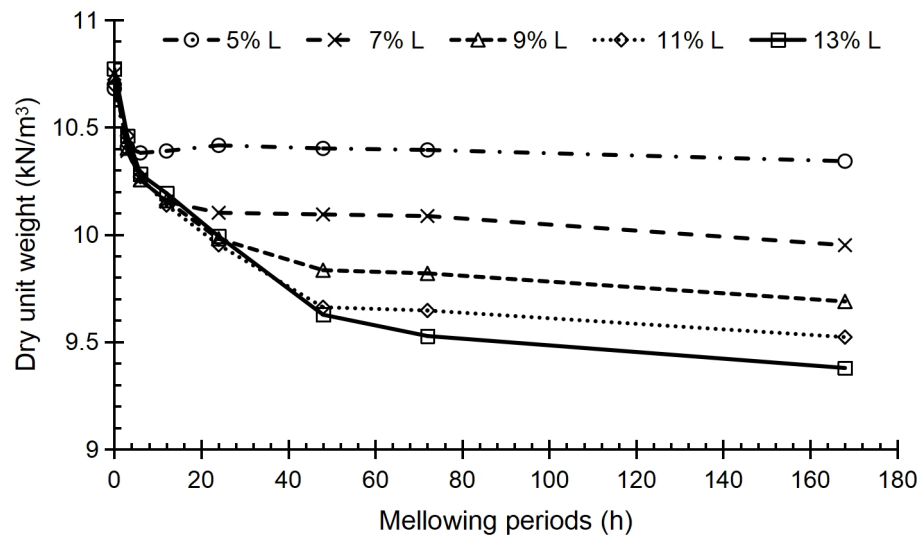


Figure 4.26: Dry unit weight against mellowing periods at 40°C for various lime contents

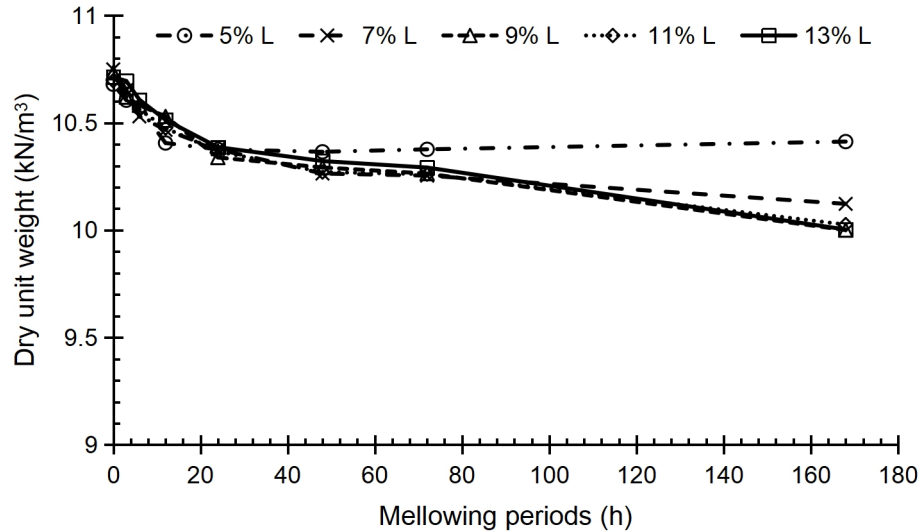


Figure 4.27: Dry unit weight against mellowing periods at 20°C for various lime contents

The data presented in Figures 4.26 and 4.27 show a significant drop in the measured dry unit weight with the increasing mellowing period up to a specific time. Beyond which a relatively reduced drop in the dry unit weight would be observed. The measured data, therefore, suggest that the declining pattern in dry unit weight is a two-stage process, namely stages 1 and 2. During stage 1, a remarkable drop in the dry unit weight was observable and accelerated at a high temperature of 40 °C, but the behaviour relied on the lime content. Subsequent stage (stage 2) was characterised by a slower rate of declining dry unit weight, which was also dependent on lime availability in particular when mellowing was conducted at 40 °C. The fast declining in the dry unit weight during stage 1 can be attributed to all chemical reactions, including pozzolanic reaction, which occurs upon the addition of lime in the presence of water. Recent results by Vitale et al. (2017) indicated that the ongoing growth of cementitious compounds starts shortly after the addition of lime. Al-Mukhtar et al. (2014) observed an accelerating rate of lime consumption with increasing

temperature. Accordingly, the mild decline in the dry unit weight in the second stage indicates that most of the lime was consumed during stage 1 in particular when mellowing was carried out at a higher temperature.

Careful inspection of the data presented in Figures 4.26 and 4.27 clearly shows that during stage 1, the decline in the dry unit weight for specimens mellowed at 20 °C is not as substantial as those measured on specimens mellowed at 40 °C. Such behaviour is due to the impact of temperature on the kinetics of the pozzolanic reaction, as suggested by De Windt et al. (2014). The pozzolanic reaction would be accelerated in the loose mixture leading to an increased amount of cementitious compounds formed at 40 °C which in turn provides more resistance to compactability than that experienced on specimens mellowed at 20 °C. As a result, a substantial drop in the dry unit weight was observable when specimens were mellowed at 40 °C. The time taken for the fast reaction (stage 1) was lime content dependent in particular when mellowing was carried out at higher temperature. Mellowing at the low temperature of 20 °C though resulted in a slight difference in the measured dry unit weight even with increasing lime content. The start of the slowdown period (stage 2) was found to occur after 6, 12, 24, 48, and 72h for specimens treated with lime content of 5, 7, 9, 11, and 13% respectively at 40 °C. Since the same compactive energy was used, the decline in dry unit weight can be attributed to increased utilisation of the compactive energy in destroying the ongoing growth of cementitious compounds with the increasing mellowing period. Therefore, the decline and subsequent steadiness in the value of dry unit weight can be used as an indicator to reflect the ongoing growth of cementitious compounds over the mellowing period.

### **4.3.3 Unconfined Compression Strength**

The measured Unconfined Compressive Strength (UCS) on untreated specimens was found to be 0.525MPa. The UCS values on specimens that were treated by 5, 7, 9, 11 and 13% of lime and tested directly after compaction were 1.35, 1.30, 1.30, 1.30 and 1.25MPa respectively. The immediate increase in strength reflects immediate changes in the clay characteristics due to fast interaction between lime and clay in the presence of water. The immediate change in strength is consistent with the observation made by Vitale et al. (2017). The results of UCS at 40°C and 20°C were plotted against the curing periods in Figures 4.28 and 4.29, respectively. From Figure 4.28, it can be clearly seen that the attained UCS values were increased substantially with the addition of more lime achieving 1.7, 2.7, 3.6, 4.4 and 5.2 MPa on specimens treated with lime content of 5, 7, 9, 11 and 13% respectively after 7 days (168 h) of curing at 40°C. It is clear that fast strength gain was experienced with increasing lime content. The rate of strength gain is nearly equal and fast during the initial stage. The initial stage can be defined as the time after which the rate of strength gain begins to slow down drastically. Increasing curing time has had a minor effect on the UCS beyond the initial stage period, which is significantly related to the lime content. The change in the strength gain behaviour was recorded to occur at 6, 12, 24, 48, 72h for specimens treated with lime content of 5, 7, 9, 11, and 13% respectively which are precisely the same periods of time for the change in declining rate of dry unit weight (see Figure 4.26). This behaviour confirms that the fast chemical reaction occurs whether in a loose state during mellowing or after compaction during curing and results in aggregation and cementation of the clay particles. It is also worth noting that elevating the environmental temperature to 40°C accelerated the consumption of available lime for

pozzolanic reaction. In contrast, curing at 20°C led to a maximum strength gain of about 2.3 MPa after 7 days as it can be seen in Figure 4.29 for specimens with lime contents of 9, 11 and 13%. The UCS measured on specimens treated with 5 and 7% of lime were even lower, achieving only UCS values of 1.7 and 2.1 MPa respectively. Specimens treated with 5% and 7% of lime showed a slower strength gain after 24 and 72h respectively. This reinforces the previous interpretation of the impact of temperature on the lime consumption and rate of pozzolanic reaction as a function of available lime.

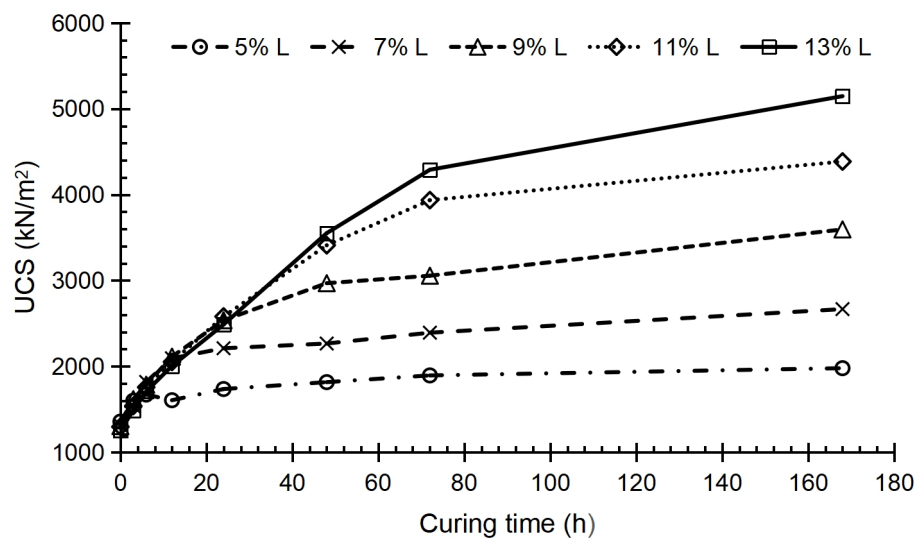


Figure 4.28: UCS against curing time at 40°C for various lime contents

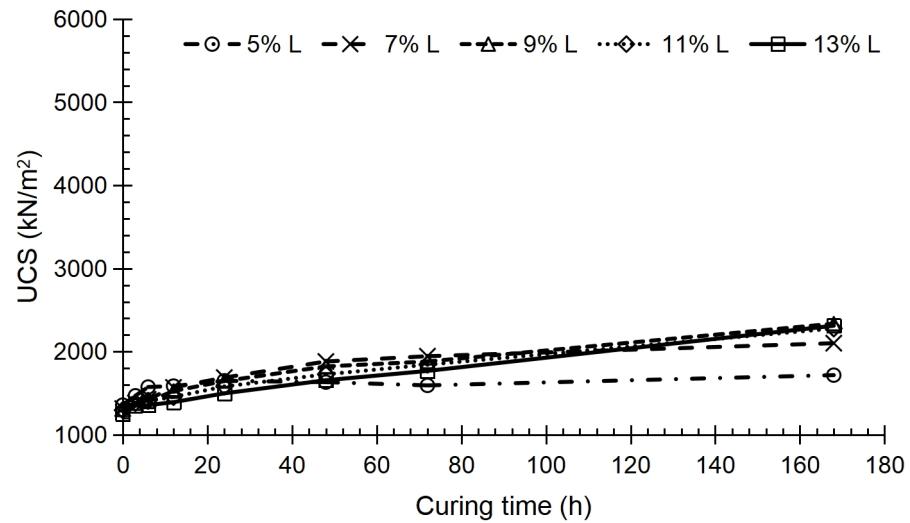


Figure 4.29: UCS against curing time at 20°C for various lime contents

The UCS values on specimens treated with various amount of lime were plotted as a function of curing time that had been recorded at the end of the initial stage (stage 1) before the beginnings of slowdown period for both curing temperatures as shown in Figure 4.30. It can be noted that linear relationships between the UCS values and the curing time at 20°C and 40°C are attainable. The rate of strength gain during stage 1 at 40°C is 8 times higher than that recorded on specimens cured at 20°C irrespective of the lime content. Lime content affected the maximum strength in the initial stage and the length of time until reaching stage 2 of the reaction in which the strength gain is characterised by its low rate. These results also confirm the effect of curing temperature in accelerating the strength gain in lime-stabilised clays as observed previously by several authors see for example; (Saldanha and Consoli, 2016, Al-Mukhtar et al., 2010b, Nasrizar et al., 2012, Toohey et al., 2013). This can be attributed to the impact of temperature on increasing the kinetic of pozzolanic reaction (De



Windt et al., 2014) and thus on the rate of formation of cementitious compounds. Moreover, the results suggest that lime content plays a vital role in the continuity of the fast rate of strength gain. Therefore, it can be stated that the accelerated rate of strength gain is evident at high curing temperature for a specific period, but it depends on the availability of lime. The patterns for the UCS gain as a function of lime content and curing time is in harmony with those observed earlier for the decline in the dry unit weight. It is, therefore, reasonable to suggest that upon addition of lime in the presence of water, all chemical reactions take place including pozzolanic reaction resulting in a fast gain in strength which becomes remarkably high with increased lime content and higher environmental temperature. Followed by another stage in which a slower reaction occurs depends on the availability of lime and temperature.

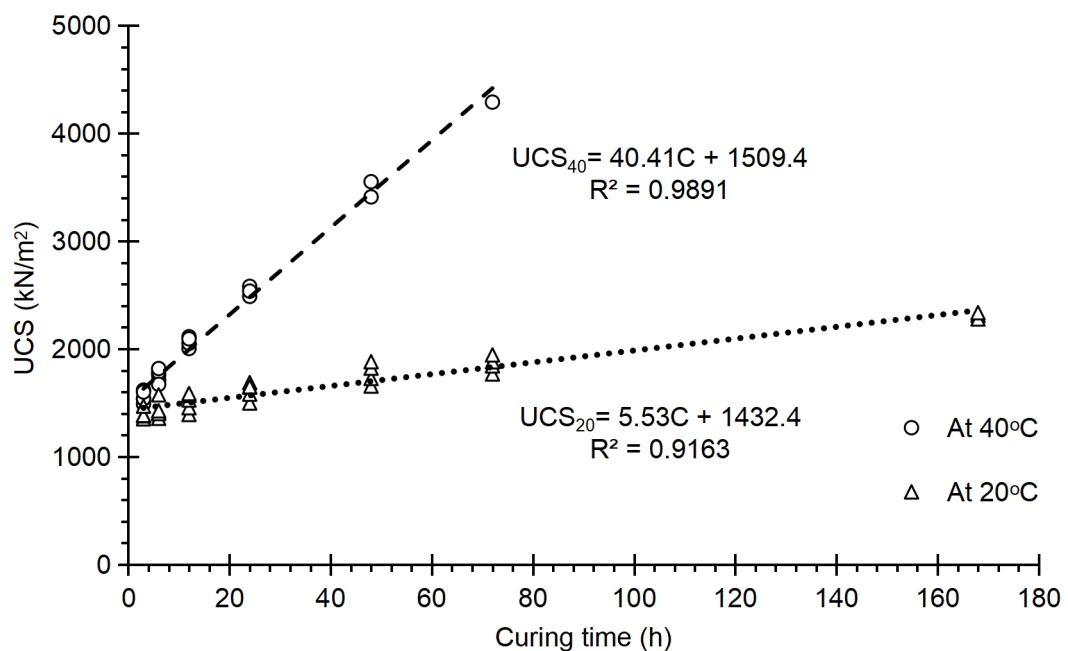


Figure 4.30: Correlations for the strength gain rate during stage 1 at both temperatures

#### **4.3.4 Permeability coefficients**

The coefficient of permeability has been measured over three days from the start of the testing on specimens that were mellowed for 24h at 40°C and 20°C. Figures 4.31 and 4.32 show data for the coefficients of permeability of lime treated specimens that previously mellowed at 40°C and 20°C against testing time, respectively. Of note, the coefficient of permeability of pure clay could not be determined, indicating that it is an exceptionally impermeable clay. Whereas, initially, the coefficients of permeability of lime treated specimens were observed to be in the order of ( $10^{-7}$  m/s). Such an increase in the permeability generally corresponds to the impact of cation exchange phenomenon that causes flocculation upon the addition of lime. Flocculation which occurs before the compaction process is enhanced by the initial cementitious compounds (Vitale et al., 2017, Diamond and Kinter, 1965) in a loose state. These cementitious compounds that have developed at the sites of contact between the particles within the flocs and between the flocs within the clusters causing the formation of intra-floc and inter-floc pores (Beetham et al., 2015). Therefore, the fabric of lime-treated specimens became more porous than the untreated specimen even after the compaction. The measured values for the coefficient of permeability for specimens that were mellowed at 40°C were higher than those mellowed at 20°C. This is due to the effect of temperature of 40°C on accelerating the kinetic of the pozzolanic reaction during the first day rendering the fabric of lime treated clay more open structure than that formed at 20°C. However, the coefficient of permeability reduced substantially as the time elapsed due to the ongoing formation of cementitious compounds. This behaviour manner was reported by (Metelková et al., 2011, Wild et al., 1987, Al-Mukhtar et al., 2012). Moreover, the microfabric investigation conducted by

Bozbey (2017) using Mercury intrusion porosimetry indicated that lime stabilised clay specimens had lesser total porosity in the long term compared with that measured in the short term due to the ongoing growth of cementitious compounds in the available pores causing a gradual reduction in the effective porosity. Data in Figures 4.31 and 4.32 show that coefficient of permeability on specimens treated with lime contents of 9, 11, and 13% declines exponentially with the elapsed time. After 72h their coefficients of permeability declined by two orders of magnitude compared to their initially permeability coefficients. The ongoing reduction over the 72h testing time could be attributed to the ongoing growth of cementitious compounds.

In contrast, the hydraulic behaviour of specimens treated by 5% and 7% at both temperatures were different from higher lime contents. With lime content of 7%, the coefficient of permeability for the specimen that previously mellowed at 20°C showed an exponential decline as seen in Figure 4.32 but the decline in the permeability slowdown after 48h. Whereas the permeability coefficient of 7% lime treated clay specimen that was mellowed at 40°C, declined remarkably during the first 24h and then became nearly steady for the rest of the testing duration. These results indicate that there is not enough amount of lime to sustain the formation of cementitious compounds during the rest of the submerging period, unlike treatment with higher lime contents. This can be attributed to the effect of temperature on accelerating the consumption of lime, which was previously reported by Al-Mukhtar et al. (2014). Moreover, the coefficients of permeability on 5% lime treated specimens at both temperatures were nearly steady during the 3-day duration. This stability indicates that the lime was consumed during the mellowing period.

Based on those mentioned above, it can be stated that the permeability results correspond to a great extent with the results of strength and dry unit weight. Furthermore, the formation of such cementitious compounds and thus, the accompanying changes in the clay characteristics is dependent on the availability of lime while the temperature controls the rate of lime consumption.

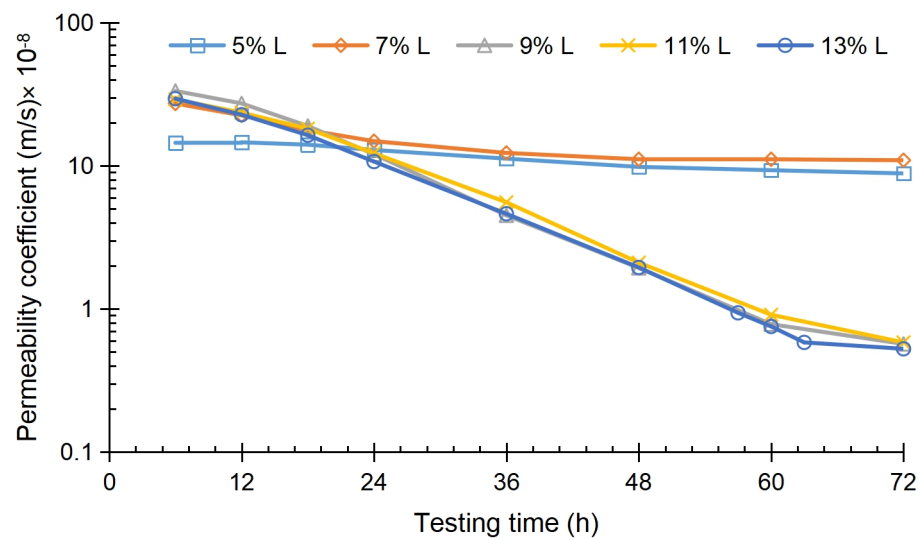


Figure 4.31: Coefficient of permeability on specimens mellowed at 40°C for various lime contents

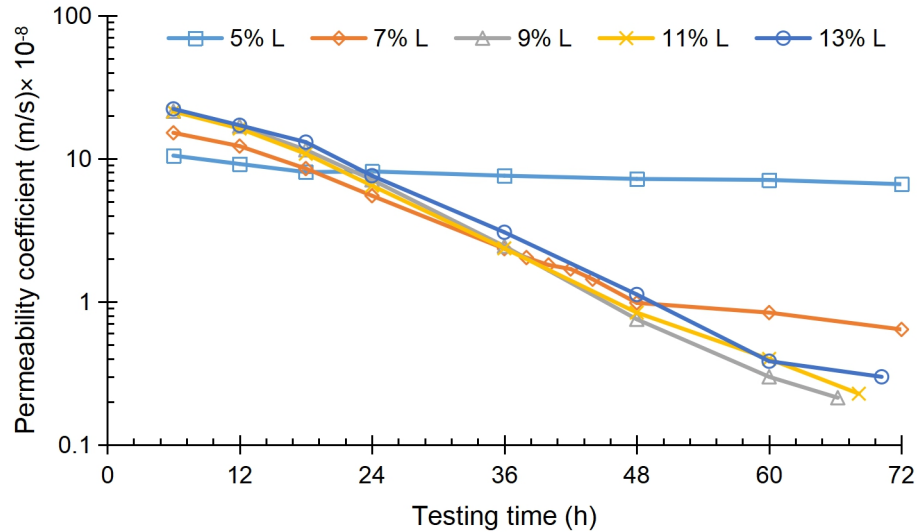


Figure 4.32: Coefficient of permeability on specimens mellowed at 20°C for various lime contents

#### 4.3.5 Summary

Results attained from Unconfined Compressive Strength, and permeability tests were employed to assess the impact of lime content on the mechanical and hydraulic properties of lime treated expansive clays. The results revealed that at the beginning, the rate of strength gain is remarkably fast for a particular time, which is dependent on lime content.

Furthermore, the strength gains on specimens cured at 40°C are 8 times higher than that observed on specimens cured at 20°C, which highlights significant effect for the environmental temperature on accelerating the chemical reactions. Reduced dry unit weight due to increased resistance to compactability is observable with increasing lime content and higher environmental temperature. The accelerated pozzolanic reaction at higher environmental temperature resulted in the permeability coefficient of specimens mellowed for 24h at 40°C to be higher than those mellowed at 20°C. The results also highlighted that the

permeability coefficient would be relatively stable when expansive clays were treated with small amounts of lime, e.g. 5%.

#### **4.4 Series 4: Short-long term assessment of lime treatment of expansive clays with different mineralogy at low and high temperature**

##### **4.4.1 Introduction**

The fourth series examines the impacts of clay mineralogy on the effectiveness of lime stabilisation at different temperatures. A comprehensive experimental programme was conducted to track down the evolution of lime-clay reactions and their durations through monitoring the evolution of strength gain at specific times using the Unconfined Compressive Strength (UCS) test. The study examined clays with different mineralogy compositions comprising Na<sup>+</sup> bentonite and ball (Kaolinite) clay. Four different clays were tested including 100% bentonite, 100% ball clay and two clay mixtures with ratios of 1:1 and 1:3 by mass of bentonite to ball clay. All clays were treated using a range of lime content up to 25% and cured up to 672h at two different temperatures of 20 and 40°C.

##### **4.4.2 Evolution of unconfined compression strength of lime treated M1 (bentonite clay)**

The strength values for all lime treated bentonite specimens that were tested immediately after compaction were higher than double the strength value of the untreated specimen, which was 0.5 MPa. The sudden increase in the strength is consistent with earlier observations by Vitale et al. (2017). This increase could be caused by a reduction in the specific surface area which can be attributed to the flocculation and aggregation mechanisms that were prompted by cation exchange phenomena and enhanced by the immediate formation of initial cementitious compounds that takes place instantly after the addition of lime in the presence of water.

The evolution of strength gain over the curing period at different temperatures of 20°C and 40°C are illustrated in Figures 4.33 and 4.34, respectively. The Figures revealed that the evolution of strength passes through two phases, depending on the rate of strength gain and can be named first and second phases. During the first phase, the rate of strength gain was extremely high compared with that recorded in the second phase in particular at the higher temperature. The first phase can then be defined as the interval of time after which the rate of strength gain commences to slacken drastically. Due to the role that the higher temperature of 40°C plays on accelerating the strength gain and thus the lime consumption, it is easier to distinguish the onset of the second phase, unlike at the temperature of 20°C.

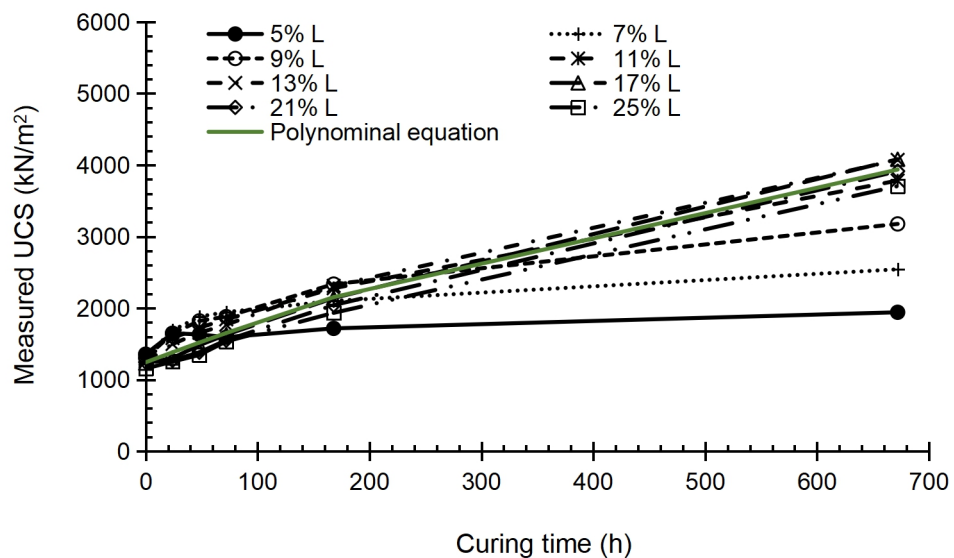


Figure 4.33: Evolution of strength gain with time for lime treated M1 specimens cured at 20°C



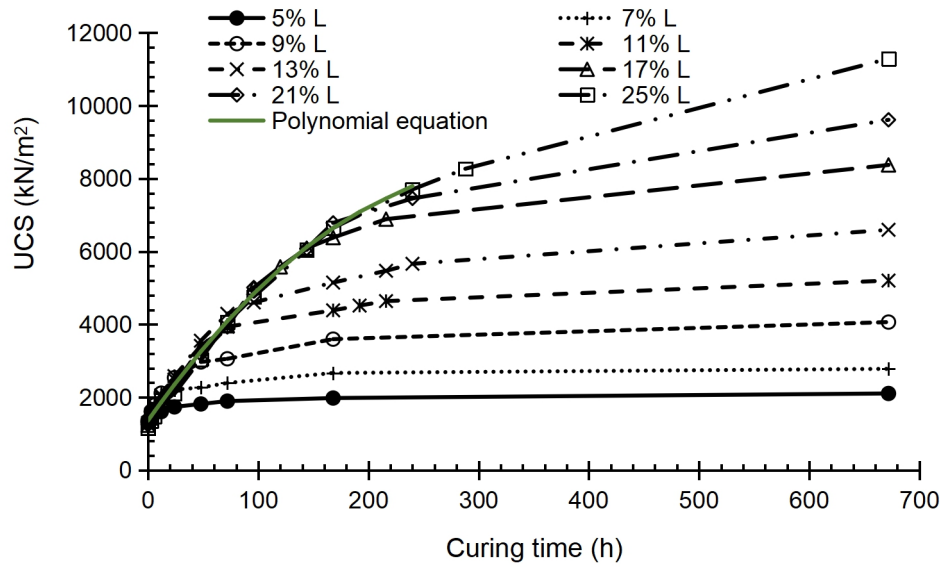


Figure 4.34: Evolution of strength gain with time for lime treated M1 specimens cured at 40°C

Although the strength gain appeared to develop linearly over the first phase, the rate of strength gain slightly decreased as time elapsed. Therefore, a polynomial equation was found to best describe the strength gain over the first phase. The green lines that are plotted in Figures 4.33 and 4.34 represent the polynomial relationships that govern the strength evolution at 20 and 40°C, respectively. At 40°C, the strength gain during the first phase evolves polynomially governing by the equation 4.4 until 6, 24, 48, 72, 96, 144, 192, and 240h for lime content of 5, 7, 8, 9, 11, 13, 17, 21 and 25% respectively.

$$UCS_{\text{Initial phase}} = -0.067C^2 + 42.762C + 1360.6 \quad 4.4$$

The data suggested that the continuity of the first phase is strongly dependent on the lime content and its duration increases with the increase in the lime content. Here it should be mentioned that higher lime contents from 17 to 25% were considered to assess the continuity of the first phase. The data showed that the strength of lime stabilised bentonite during the second phase can be represented by logarithmic relation reaching strength values of 2, 2.78, 4, 6.6,

8.37, 9.6 and 11.3 MPa after 672h of curing time for lime contents of 5, 7, 9, 11, 13, 17, 21 and 25% respectively. Unlike the relatively shorter first phase at 40°C, the results showed that the first phase at 20°C continued to 672h with the addition of the substantial amount of lime, e.g. 11, 13, 17, 21, and 25% reaching nearly the same strength value of about 4 MPa. In contrast, the first phase was shorter with the addition of 5, 7 and 9% of lime at 20°C achieving 2, 2.5 and 3.1 MPa respectively but it was reached after extremely long periods of curing time in comparison with those recorded at 40°C on specimens treated with the same lime content. During the first phase at 20°C, the strength is governed by the equation 4.5.

$$UCS_{\text{Initial phase}} = -0.0028C^2 + 5.891C + 1242.6 \quad 4.5$$

However, careful inspection of data presented in Figure 4.34 for specimens cured at 40°C suggested that most of the difference in the strength was gained during the first phase and was a function of the lime content. The rate of strength gain during the second stage was significantly lower but increased with the further addition of lime. In an attempt to describe the evolution of strength over phase 2 at 40°C the equation 4.6 was developed based on the attained data. The strength in equation 4.6 evolves logarithmly as a function of lime content (L) and curing time (C) during phase 2 at 40°C.

$$UCS = (4.015L^2 + 41.93L) \ln C + (-35.1L^2 + 464.1L - 87) \quad 4.6$$

To aid the discussion to examine lime consumption, Figure 4.35 was plotted to present the attained strength results on specimens after 672h of curing time against the lime content at 40°C and 20°C. The data for specimens cured at 40°C show that there is a linear relationship between strength and lime content up to a lime content of 13% and that the difference in the strength value

between two consecutive lime contents was about 1 MPa. This means that lime was fully consumed within the 672h of curing time under 40°C. Extrapolating the best fit line at higher lime content would assist with estimation of the final strength at the time of full consumption of lime. The best fit line for the full range of lime content used in this investigation was plotted in Figure 4.35. The resulting linear equation 4.7 from this relationship was used to predict the presumed final strength for other lime contents of 17, 21 and 25%.

$$UCS_{\text{Presumed final strength}} = 546.2 \times L - 791.03 \quad 4.7$$

The Figure 4.35 shows that at 40°C the available lime was consumed entirely during the 672h of curing time for specimens with lime content up to 17% whereas specimens with lime content of 21% and 25% might not have fully consumed the lime. Furthermore, data on specimens that were cured at 20°C indicated that just lime contents of 5 and 7% were nearly consumed whereas other lime contents would require a prolonged period of curing time more than 672h to consume the available lime. The data suggested that the addition of lime of more than 13% would remain unconsumed in the stabilised clay when cured at 20°C.

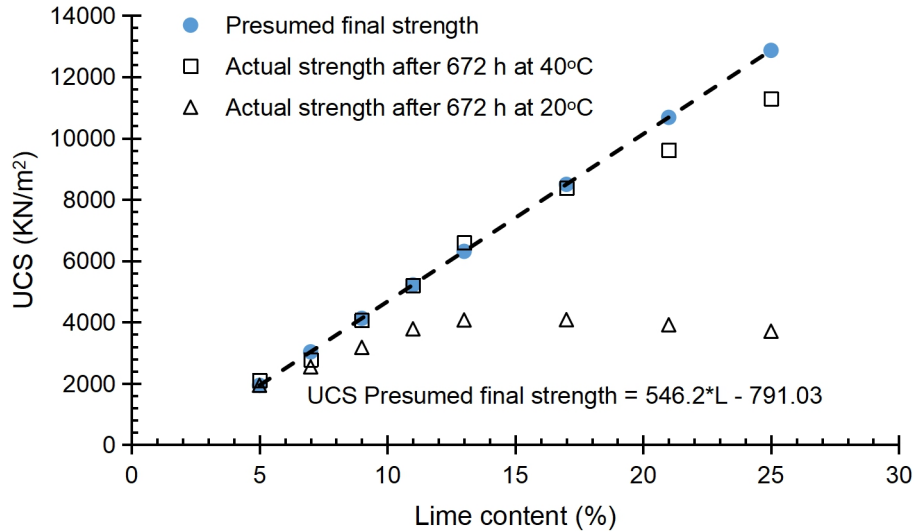


Figure 4.35: Comparison between the presumed and measured strength after curing for 672h at 20°C and 40°C on M1 specimens.

#### 4.4.3 Evolution of unconfined compression strength of lime treated M2 (ball clay)

Initially, the specimens that were tested directly after compaction process achieved a strength gain of 0.82, 0.89, 0.92, 0.95, and 1.03 MPa for 5, 7, 9, 11 and 13% of lime contents respectively compared with just 0.33 MPa for the untreated specimen. These values indicated that addition of lime enhances the strength of kaolinite material initially with up to 3 times. This sudden surge in strength could be attributed to the fast initial calcium adsorption and sodium desorption in cation exchange process within the first five minutes which was reported by (Chemedda et al., 2018, Singh et al., 1996). Chemedda et al. (2018) also observed that as the concentration of  $Ca(OH)_2$  increased, the adsorbed calcium by Kaolinite become higher based on measurements of the concentration of calcium that was taken after 3h from submerging equal amounts of Kaolinite in various concentration of  $Ca(OH)_2$ .

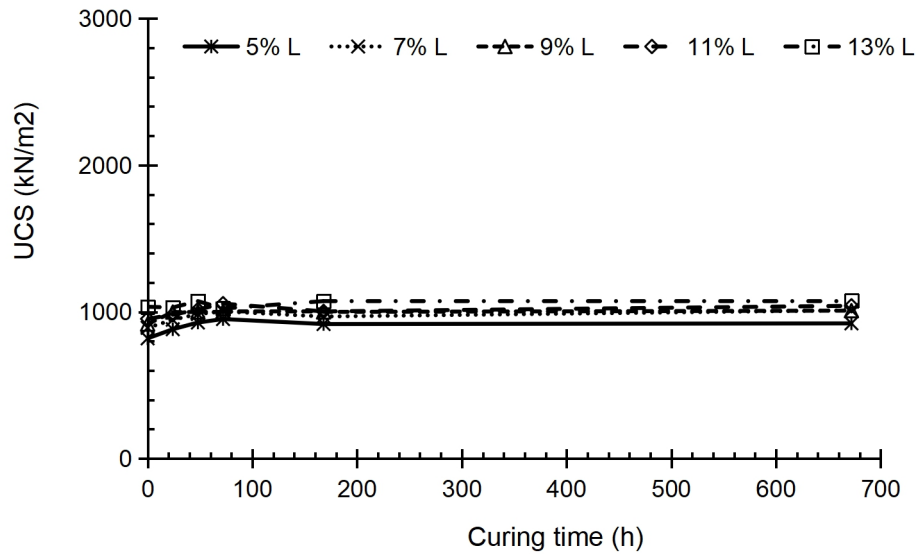


Figure 4.36: Evolution of strength gain with time for lime treated M2 specimens at 20°C

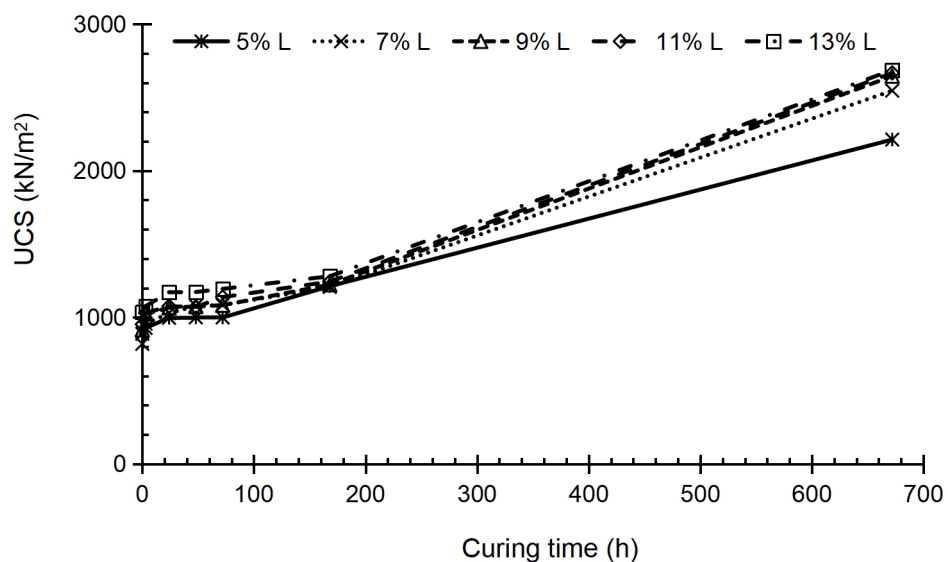


Figure 4.37: Evolution of strength gain with time for lime treated M2 specimens at 40°C

The evolution of strength gain for lime treated kaolinite specimens under a temperature of 20°C and 40°C were plotted against the curing time in Figures 4.36 and 4.37, respectively. The attained strength values on specimens that were cured at 20°C indicated a very marginal increase in the strength within the first 72h subsequently the strength remained constant irrespective of the lime

content and curing time as seen in Figure 4.36. This would be due to a delay in the consumption of lime and the absence of formation of cementitious compounds after treating kaolinite clay, which was observed by Vitale et al. (2017). Though, Bauer and Berger (1998) reported that in alkaline solution, the dissolution rate of Kaolinite was higher than its counterpart with the bentonite. (Chemedda et al., 2015, Konan et al., 2009, Chemedda et al., 2018) attributed the observed behaviour of Kaolinite to the accumulation of various adsorbed calcium species on the surfaces of kaolinite mineral forming a coating layer which isolates the surface of Kaolinite from the alkaline environment, curbs the dissolution of alumina and silica compounds and thus inhibits the pozzolanic reaction. In contrast, when curing at 40°C, the strength remained nearly stable during the first 72h followed by a gradual but remarkable gain in the strength up to reaching values of 2.2, 2.54, 2.6, 2.66 and 2.68 MPa for 5, 7, 9, 11, and 13% of lime content respectively after 672h, as illustrated in Figure 4.37. This gave a clear indication of the temperature role (40°C) in accelerating the strength gain.

Further, the lowest strength value for 5% lime content indicated that the available lime content was nearly consumed during the 28 days of curing at 40°C. The role of higher temperature, e.g. 50°C in re-initiating the strength gain in lime-treated Kaolinite after a period of stability (7 days) was also reported by Maubec et al. (2017). Maubec et al. (2017) coupled this behaviour with the re-initiation of the calcium absorption and the beginning of forming hydrates compounds, e.g. Calcium Aluminate Hydrates and Carboaluminate Hydrates. However, the mechanism by which the accumulating calcium layer is eliminated, after a long time at 20°C and shorter time at 40°C, so that the alkaline environment could attack the surface of Kaolinite, has not been clarified yet. A

possible elucidation is that the calcium disposal mechanisms depend on the specific surface area of Kaolinite over time at 20°C, which prolonged increases as observed by Vitale et al. (2017). On the other hand, relatively faster growth in the specific surface area at 40°C is likely to occur, which enables the accommodation of the calcium accumulation. Further investigation would be needed to assess the evolution of specific surface area over time at different temperature.

#### **4.4.4 Evolution of unconfined compression strength of lime-treated M3 (mix of 1 portion of bentonite to 3 portions of ball clay)**

The UCS data on M3 specimens treated with 5, 7, 9, 11 and 13% of lime and cured for a period of time up to 672h at 20°C and 40°C are shown in Figures 4.38 and 4.39, respectively. Immediately after compaction, UCS was nearly equal for all specimens with various lime content and is about double of the UCS of the untreated specimen (0.5 MPa). Unlike lime treated ball M2 specimens, the treated M3 specimens showed marginal strength gain of about 0.4 MPa after 672h at 20°C, reaching UCS value of about 1.4 MPa for all specimens. The equation 4.8 governs the evolution of strength during the initial phase at 20°C.

$$UCS_{\text{Initial phase}} = -0.0003 * C^2 + 0.7774 * C + 1031.5 \quad 4.8$$

On the other hand, the cured specimens at 40°C achieved UCS values of 1.4 MPa in only 48h which highlights the significant role for the curing temperature in accelerating the chemical reaction. After a period of curing of 168h at 40°C, the measured UCS values for all specimens with various lime contents were nearly the same at about 2.1 MPa except a specimen that was treated with 5% lime content which showed a slowdown in the strength gain entering in the

second phase after 72h of curing. The UCS values observed on specimens with 5% lime content experienced no significant change after 168h of curing, achieving a value of almost 1.9 MPa. The no significant change in the strength suggests that the addition of 5% lime is not enough to support further reactions between lime and clay after 168h of curing at 20°C. The UCS values at 40°C increased notably with the increase in lime content reaching 2.7, 3.6, 4.0 and 4.2 MPa on M3 specimens treated with lime content of 7, 9, 11 and 13% respectively after 672h of curing. The equation 4.9 governs the evolution of strength during the initial phase at 40°C

$$UCS_{Initial\ phase} = -0.0039 * C^2 + 7.1276 * C + 1072 \quad 4.9$$

Results of UCS values at 672h of curing time were plotted against lime content in Figure 4.40. The data suggested that UCS values attained at 672h at 40°C is directly related to the lime contents of 5, 7, and 9%, which means that lime was fully consumed during the curing period. Consequently, a linear relationship between UCS and lime content is obtained and used to predict the final UCS values for specimens treated with higher lime contents of 11 and 13%.

$$UCS_{Presumed\ final\ strength} = 405.7 * L - 115.92 \quad 4.10$$

Comparing estimated strength values that obtain from the equation 4.10 with measured UCS values after a period of curing of 672h at 40°C illustrated that specimens treated with 11 and 13% of lime would not have reached their maximum strength yet which means that lime is not fully consumed. Nevertheless, curing at 20°C slowed the consumption of lime and resulted in markedly lower values of strength. Besides, the relationship indicated that a 1%



increase in the lime content would result in an increase of 0.4MPa in the final strength value when cured at 40°C.

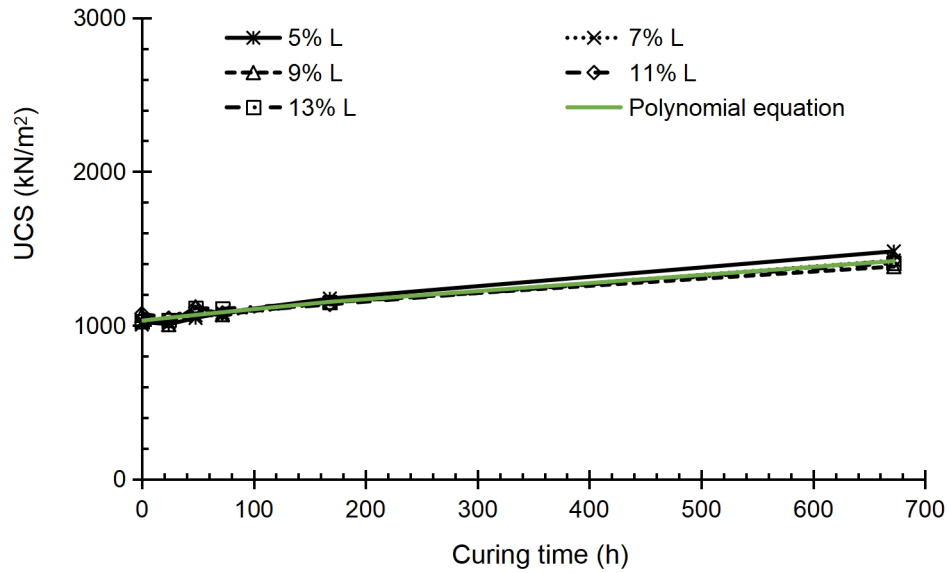


Figure 4.38: Evolution of strength gain with time for lime treated M3 specimens at 20°C

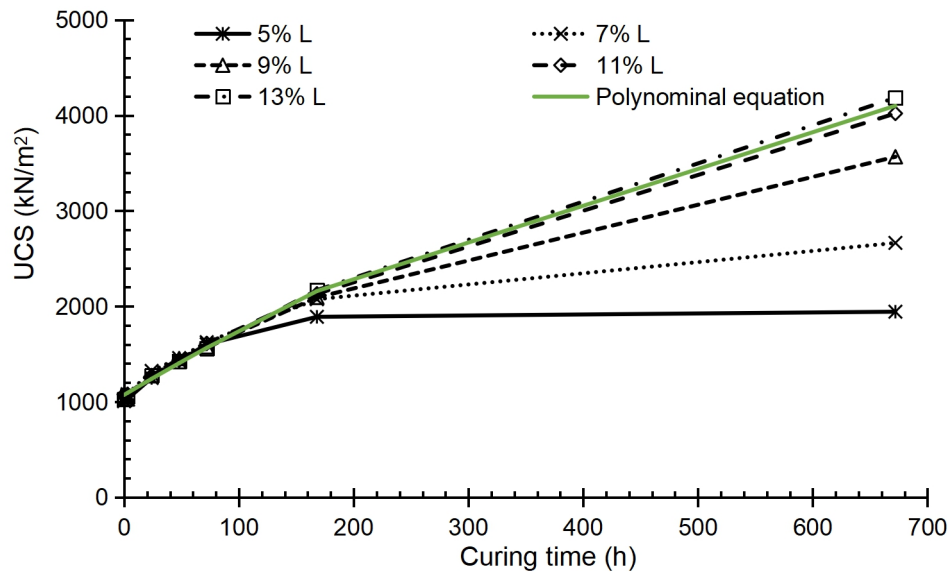


Figure 4.39: Evolution of strength gain with time for treated M3 specimens at 40°C

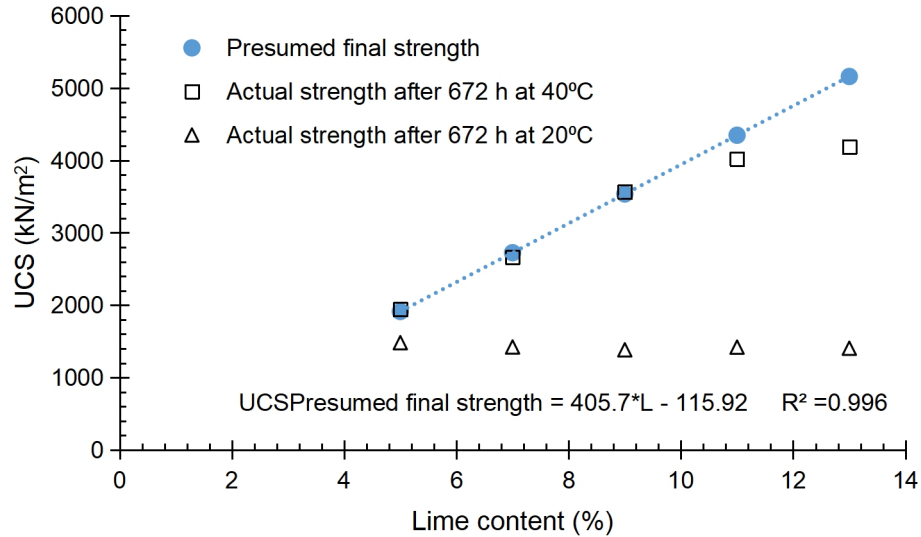


Figure 4.40: Comparison between the presumed and measured strength after curing for 672h at 20°C and 40°C on M3 specimens

#### 4.4.5 Evolution of unconfined compression strength of lime treated M4 (Mix of 1 portion of bentonite to 1 portion of ball clay)

The UCS evolution of compacted M4 specimens that were treated with 5, 7, 9, 11 and 13% of lime and cured for a period of time up to 672h at 20°C and 40°C are depicted in Figures 4.41 and 4.42, respectively. The measured UCS values for all treated specimens that tested directly after compaction were about two times that attained on the untreated specimen (0.43MPa). Results of specimens treated with 7, 9, 11 and 13% of lime and cured at 20°C showed a gradual increase in strength over the whole duration of curing. The similarity in strength growth means that the first strength phase continued until 672h for specimens with lime content 7% and higher. The relationship between strength and curing time seems to be governed by a polynomial equation 4.11, as illustrated in Figure 4.41, achieving the same UCS value of about 2.2 MPa at 672h. However, M4 specimens treated with 5% lime did not follow the same path for the

evolution of strength. The strength did not increase after 168h of curing time, indicating the commencement of the second phase.

$$UCS_{Initial\ phase} = -0.0015 * C^2 + 2.8147 * C + 1059.9 \quad 4.1$$

On the other hand, specimens cured at 40°C showed a typical relationship through which the strength gain was initially fast, followed by a slower second phase. It is clear that the continuity of the fast phase was dependent on the availability of lime. The strength gain over the initial phase at 40°C is governed by equation 4.12. The achieved strength at the end of curing period at 40°C was directly related to the lime content attaining 2, 2.9, 4.2, 4.9 and 5.8 MPa on specimens treated with lime content of 5, 7, 9, 11 and 13% respectively.

$$UCS_{Initial\ phase} = -0.0432C^2 + 22.524 * C + 1089 \quad 4.1$$

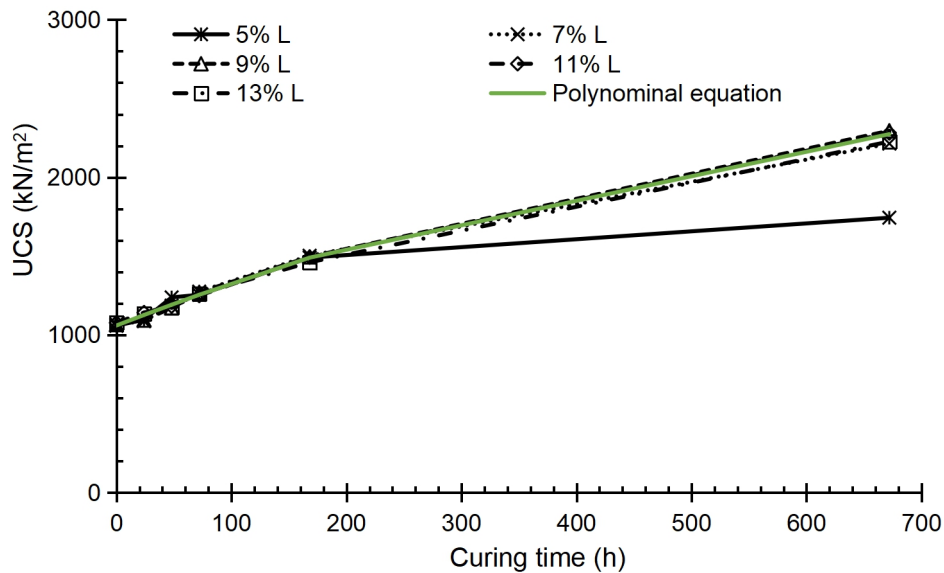


Figure 4.41: Evolution of strength gain with time for M4 specimens at 20°C

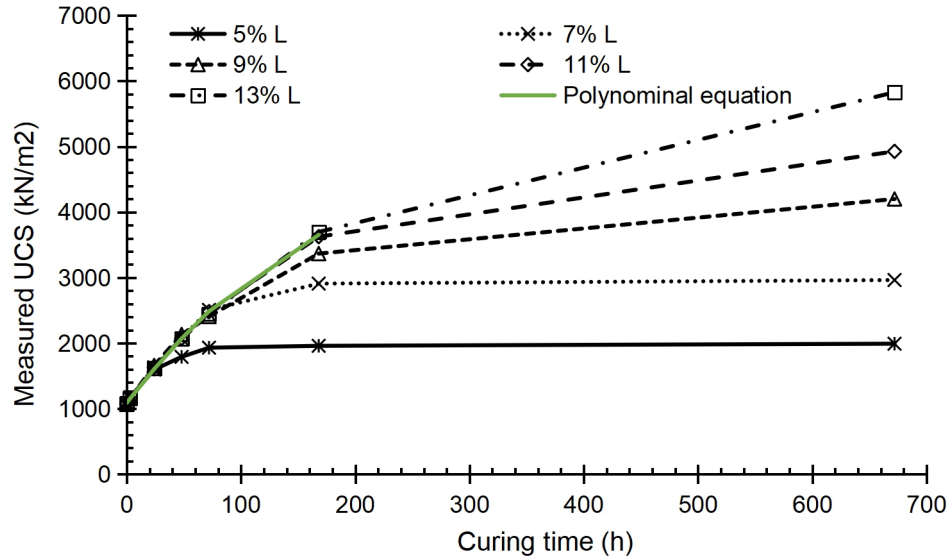


Figure 4.42: Evolution of strength gain against curing time for M4 specimens at 40°C

The attained UCS values at 20 and 40°C after 672h of curing were plotted in Figure 4.43 against the corresponding lime content. The data suggest that lime would be consumed entirely on specimens treated with lime content of 5, 7 and 9% at 40°C since a linear equation can fit the data accurately. Extending the linear equation 4.13 to higher lime contents is presented in Figure 4.43. The best fit line indicates that after 5% of lime content, an increase of 1% in the lime content would result in an increase in the final strength value by about 0.55 MPa. The data suggest that lime was not consumed when specimens were cured at 20°C. Figures 4.35, 4.40 and 4.43 highlighted the responsibility of lime content on determining the final strength value and the role of mineralogy composition and temperature on determining the time needed to reach the final value ranges from 0.4 to 0.55 MPa.

$$UCS_{\text{Presumed final strength}} = 552.15 \times L - 813.15$$

4.1

3

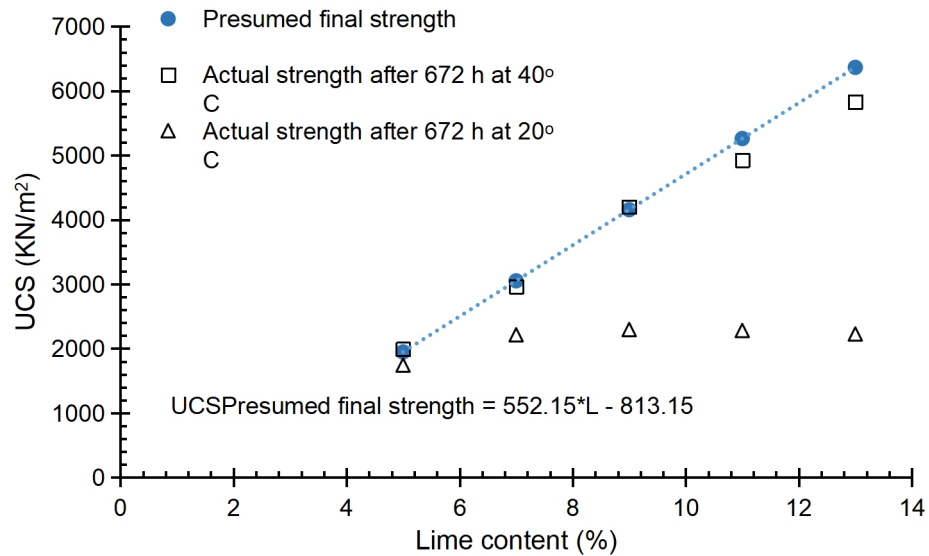


Figure 4.43: Comparison between the presumed final strength and measured strength after curing for 672h at 20°C and 40°C for treated M4 clay

#### 4.4.6 Mineralogical effects

In this investigation, four different types of clay namely; M1 of pure bentonite, M2 of pure Kaolinite, M3 which is a mix of bentonite and Kaolinite with a ratio of 1:3 by mass and M4 which is a mix of bentonite and Kaolinite with a ratio of 1:1 by mass were used to represent soils with a vast range of liquid limit from 330% down to 58%. Based on the UCS results that were presented earlier for the four different types of clay, thorough assessment and comparison were conducted to highlight the impact of clay mineralogy on the reaction process and kinetics of strength gain when mixed with hydrated lime.

The data showed that testing lime treated specimens with a range of lime contents immediately after compaction would result in a relatively narrow range of UCS. By and large, the UCS values on treated specimens were 2~3 times that achieved on untreated specimens irrespective of the amount of added lime. The UCS values increased slightly with the increase in the bentonite content in the specimens. The immediate changes in the structure and bonding between

treated particles could be attributed primarily to cation exchange, flocculation and aggregation mechanisms and enhanced by the immediate formation of initial cementitious compounds. Since the surface area of bentonite clay is much higher than that of kaolinite clay, it is likely that lime would react with bentonite particles at a higher rate resulting in a significant reduction in the surface area of bentonite and a relatively higher strength immediately after compaction. The results demonstrated that the amount of added lime at zero h curing has no impact on the evolvement of strength which could be attributed to the small amount of lime that is required to satisfy the needs for cation exchange and flocculation mechanisms.

Careful inspection of UCS data for all clays indicated that the kinetic of strength gain throughout curing is dependent on curing temperature, lime content and curing time. Two stages were very noticeable in the evolution of strength of the lime-treated clays in particular at the high temperature of 40°C. Quadratic equations were proposed for stage 1 of strength gain (fast-growing) and presented in equations 4.4, 4.5, 4.8, 4.9, 4.11 and 4.12. It is noted that during the first days of curing the equations behave mostly linear due to the small negative value of the numerical coefficient in the second order parameter compared with the higher positive numerical coefficient in the first order parameter. Discarding the minor numerical coefficients in the second order parameters, it became clear that the strength gain was a function of the clay mineralogy and increased with elevating the curing temperature as seen in Figure 4.44. So, it can be inferred that the numerical coefficients in the first order parameters reflect the kinetic of strength gain under both temperatures. Consequently, the results suggested that during the first hours (stage 1), the

kinetic of strength gain at curing temperature of 40°C was about 8 times that experienced when curing at 20°C on M1, M3, and M4 lime-treated specimens. Furthermore, at a given temperature, the rate of strength gain with M3 and M4 during stage 1 was about 15% and 50% of that recorded for M1 which highlighted a significant role of bentonite in the reaction with lime and evolution of strength.

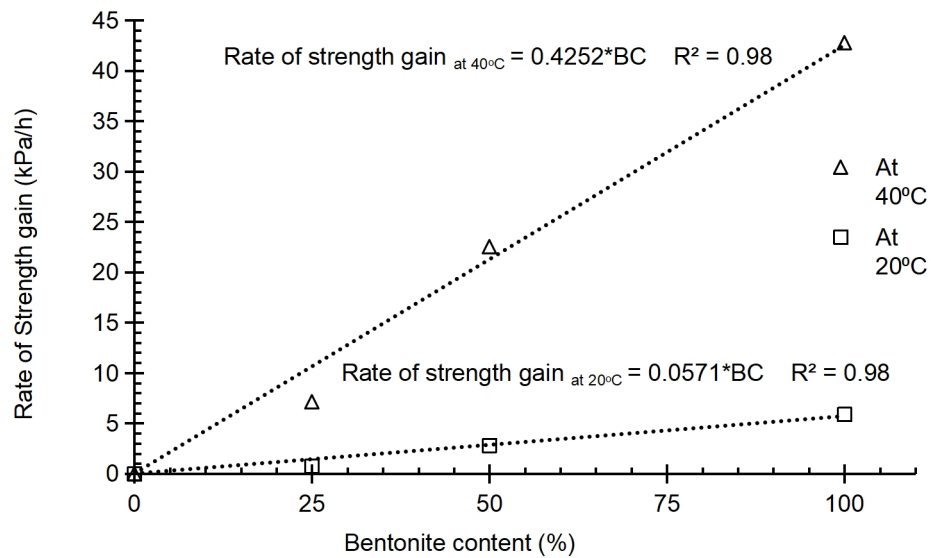


Figure 4.44: Impact of bentonite Content (BC) on the kinetic of strength gain during the first phase at the different curing temperatures

Two possible elucidations could be brought forward to clarify the changes leading to the increase in strength gain with the rise in the bentonite content; i. Increasing the amount of bentonite content pushes towards consideration that bentonite is predominantly responsible for the degree of improvement in the strength gain since the increase in strength is directly related to the proportional of bentonite in the material and ii. bentonite might act as a rival consumer for calcium ions. Consequently, the bentonite relieves the potential accumulation of calcium ions on the surface of kaolinite particles allowing the alkaline

environment access to the surface of kaolinite layer. As a result of attacking the alkaline environment to the surface of kaolinite and montmorillonite minerals, silica and alumina would be released leading to the formation of cementitious compounds in the form of Calcium Silicate Hydrates (CSH), Calcium Aluminate Hydrates (CAH) and Calcium Aluminate Silicate Hydrates (CASH). It is well known that kaolinite minerals comprise of an octahedral sheet (AL site) and tetrahedral sheet (Si site) whereas, in the case of montmorillonite, there are two tetrahedral sheets sandwiched an octahedral sheet (Brigatti et al., 2006). These differences in the structure of both minerals should make the launch order of alumina and silica different. Therefore, the release of alumina and silica should be synchronised in the case of Kaolinite.

On the other hand, the release of silica would be followed by the release of alumina in the case of montmorillonite minerals. Bauer and Berger (1998) concluded that unlike the preference of releasing the silica in the case of montmorillonite mineral, the preference of the dissolution of alumina was prevalent in the case of kaolinite minerals. Using X-ray diffraction analysis, the presence of CAH with lime-treated Kaolinite was observed by Maubec et al. (2017) and Vitale et al. (2017) after 28 days at 20°C, whereas CSH was observed by (Maubec et al., 2017) after 98 days of curing at 50°C. With respect to the montmorillonite mineral, the presence of CSH was observed since short time after lime addition whereas the presence of CAH and CASH were observed after just a prolonged period of time as reported by (Pomakhina et al., 2012, Vitale et al., 2016a, Maubec et al., 2017, Vitale et al., 2017). Bauer and Berger (1998) also reported that the rate of dissolution of Kaolinite was higher



than that in montmorillonite minerals in a robust base solution (potassium hydroxide).

On the other hand, the results of two studies conducted by (Al-Mukhtar et al., 2010a, Al-Mukhtar et al., 2010b) on expansive soils naturally contains 38% of Kaolinite and 58% of smectite minerals indicated that the formation of CAH was observed using X-ray diffraction after 1 and 7 days at 50 and 20°C respectively. In contrast, the formation of CSH was observed at 50°C after 7 days. Hence, the availability of alumina and/or silica at the time when the reaction takes place controls the outputs of the pozzolanic reactions and the development of CAH, CSH and/or CSAH depending on the abundant reactants, e.g. alumina or silica (Beetham et al., 2015). The formation of CAH; 1.) refers to the responsibility of Kaolinite in the formation of the cementitious compounds and thus on the strength gain, 2.) confirms the role that played by the smectite as competitive consumer which prevents the accumulation of calcium ions on the surface of Kaolinite and faster dissolution of Kaolinite in alkaline environment. Based on that in the current study, it can be stated that the increase in bentonite content in M3 and M4 offered faster elimination of the calcium accumulation, the earlier appearance of cementitious compounds and initiation of greater kinetic of strength gain.

#### **4.4.7 Collapse pattern and desiccation cracks**

Careful inspection of the failure pattern of all lime-stabilised clay specimens suggested that the failure mechanism was markedly dependent upon the type of material and its strength, which is a function of the curing conditions. Figure 4.45 shows pictures of specimens at failure after being cured for 672h (28 days). In all specimens, the failure pattern was in the form of a cone-split that was well

formed at one end only. The physical observations suggested that the cone-split equally occurred at either the top or the bottom of the specimens. Curing of lime stabilised clays for an extended period resulted in a brittle behaviour which can be noticed by failure at a relatively small strain, as shown in Figure 4.46. The cone-split is very similar to that classified by ASTM C39 / C39M - 18 (, type 2 for the typical collapse in the cylindrical brittle concrete specimen.

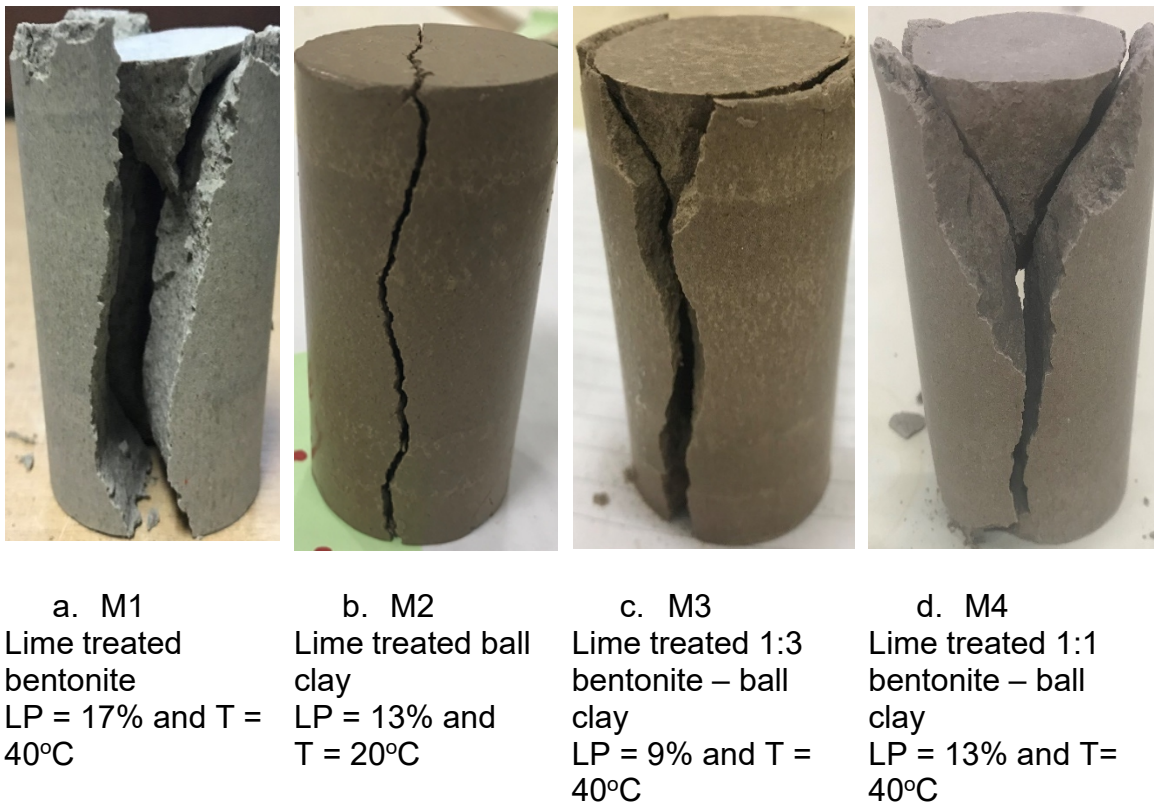


Figure 4.45: Typical cone-split failure pattern on lime treated clays after 28 days

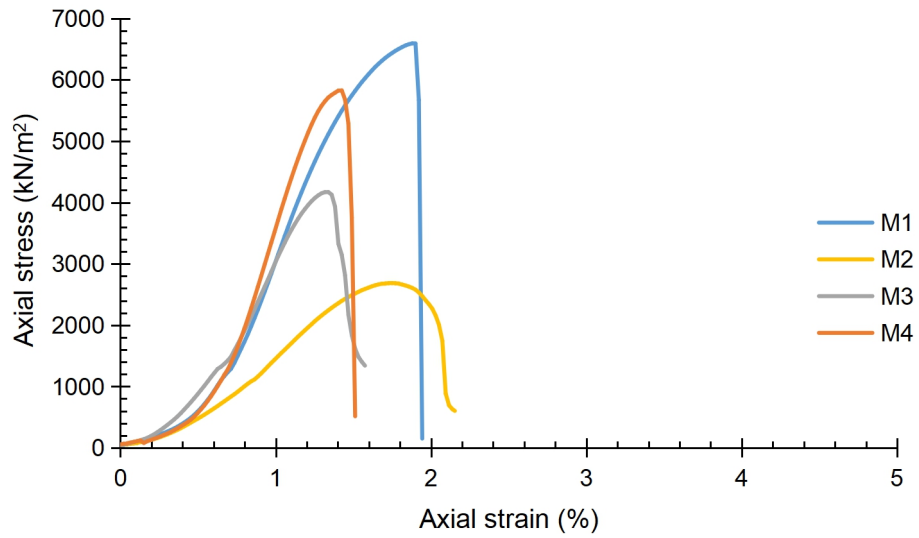
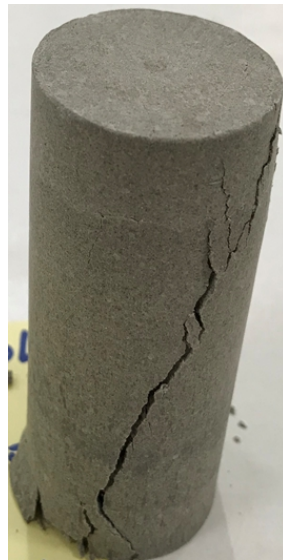


Figure 4.46: Stress-strain relationships on lime treated clays: L = 13%, T = 40°C and C = 672h



a. Shear collapse  
At zero curing time  
LP=21%



b. Cone-shear collapse  
At 24h of curing at  
40°C, LP=25%



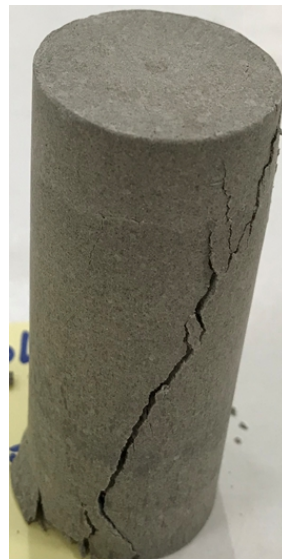
c. Cone-split  
collapse  
after 72h of curing at  
40°C, LP=21%

Figure 4.47 shows an example of the failure of the M1 at different times of curing. It was observed that a classical shear collapse was imminent on specimens that were cured for a short time up to 12h whereas a combined

cone-shear collapse appeared to occur on specimens that were cured for a period of time between 12 and 72h. Furthermore, the failure pattern on specimens cured for longer periods showed a cone-split failure. The collapse pattern is related to the strength of the specimen at the time of testing. Results for the stress-strain relationships are presented in Figure 4.48. The results confirmed that the behaviour of lime treated clay specimens changed from ductile to brittle with curing time. The ductile behaviour of lime-stabilised soil was accompanied by a classical shear failure, whereas the cone-split is dominant on high strength specimens that showed brittle behaviour.



d. Shear collapse  
At zero curing time  
LP=21%



e. Cone-shear collapse  
At 24h of curing at  
40°C, LP=25%



f. Cone-split  
collapse  
after 72h of curing at  
40°C, LP=21%

Figure 4.47: Type of collapse patterns over the curing time on M1 specimens

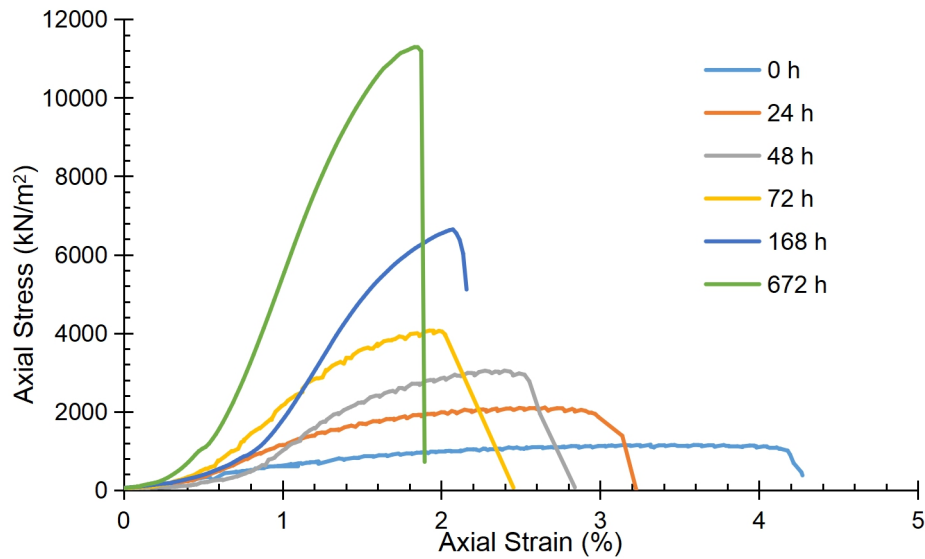
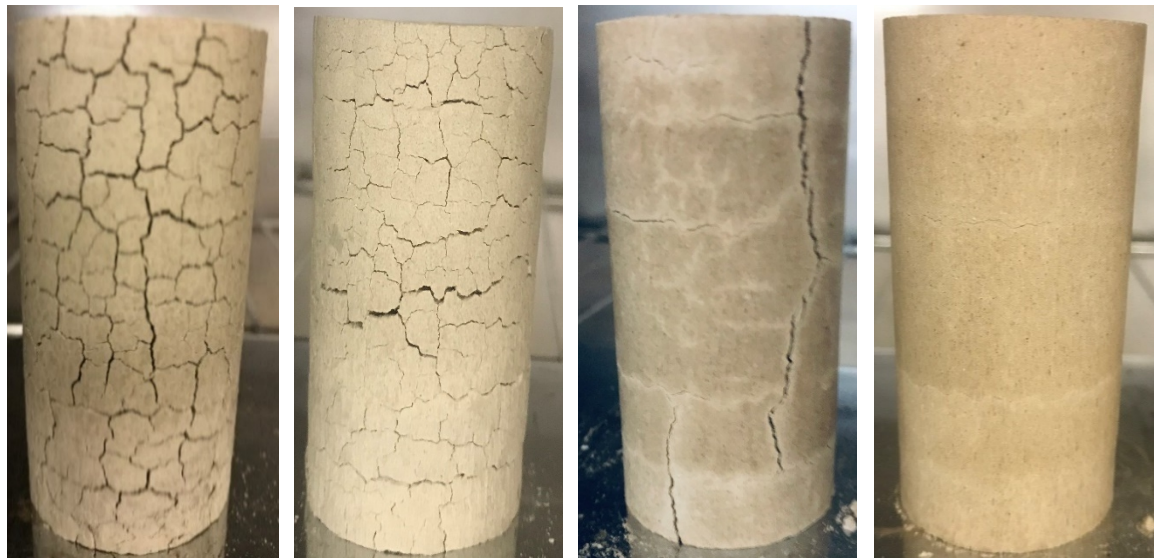


Figure 4.48: Stress-strain relationships on lime treated M1 specimens as a function of curing time

Another distinctive feature was observed during the drying process during which all tested specimens were dried in the oven at 105°C. This was a final quality assurance step that was important to ensure the effectiveness of controlling and maintain a target moisture content throughout the curing period. During the drying process, it was observed that the appearance of desiccation cracks on the surface of lime treated bentonite (M1) is different from that observed on lime treated ball clay (M2). The desiccation cracks on the lime-treated ball clay, M3 clay, and M4 clay specimens appeared at the onset of the drying process within 1h (see Figure 4.49c) and then gradually closed by the end of 24h of drying as shown in Figure 4.49d. Only some hair cracks can still be visible on the specimens. Whereas the substantial amount of cracks were generated within 1h of drying on lime treated bentonite M1 specimens (see Figure 4.49a) and some cracks were widened with time and remained after completion of drying as

shown in Figure 4.49b. Nevertheless, there was no significant volume change on the lime-treated clays.



a. Treated M1  
after 1h of  
drying

b. Treated M1  
after 24h of  
drying

c. Treated M4  
clay after 1h of  
drying

d. Treated M4  
clay after 24h  
of drying

Figure 4.49: Behaviour of desiccation cracks during the drying process of M1 and M4 at zero h

#### 4.4.8 Summary

The results showed that the continuity of the fast phase (stage 1) of strength gain was dependent on the availability of lime in particular at the higher temperature. Whereas, for the same lime content, the duration of the fast phase and the kinetic of strength gain were significantly related to the clay mineralogy and curing temperature. Except for the initial strength gain at 0h curing time, the lime-treated ball clay specimens at 20°C appeared to show no strength gain throughout curing that extended up to 672h. However, when curing occurred at 40°C, the no strength gain stage only lasted for 72h after which a gradual increase in the strength was observed over the remaining curing time. The addition of bentonite to ball clay succeeded in kicking off the strength gain after a short period of curing time at both curing temperatures.





## **4.5 Series 5: Short term assessment of lime treatment of expansive clays with different mineralogy at low and high**

### **4.5.1 Introduction**

The fifth series inspected the influence of clay mineralogy, lime content, mellowing time and temperature on the progress of lime-clay reactions in the short term. An extensive testing programme was performed to keep track of the progress of lime-clay reactions by observing the evolution of permeability and swelling characteristics. Sodium bentonite clay, ball clay, and two additional mixtures are comprising of 1:1 and 1:3 bentonite to ball clay by weight were used in series 5. All clays were treated by lime contents ranging from 5 to 13% and cured or mellowed for 24h at either 20°C or 40°C before testing at room temperature. Lime treated specimens were tested at the optimum moisture content and the maximum dry unit weight of their untreated clays.

### **4.5.2 Swelling and permeability characteristics of untreated clays**

The influence of the bentonite content on permeability and swelling characteristics was studied. Liquid limits, optimum moisture contents, and Maximum dry unit weights that had been obtained for M1, M2, M3, and M4 were depicted in Figure 4.50 against their bentonite content. The results reveal that as the bentonite content increases, both liquid limit and optimum moisture content values increase whereas, the dry unit weight declines. Figure 4.50 reveals that there are three linear equations (4.15, 4.16 and 4.17) govern the relationship between the bentonite content (BC) with each of resulting liquid limit (LL), maximum dry unit weight ( $\gamma_d$ ), and optimum moisture content (OMC) as seen in Figure 4.50.

$$\gamma_d = 2.6491 * BC + 54.6 \quad R^2 = 0.99 \quad 4.1$$



$$LL = -0.0195 * BC + 14.034 \quad R^2 = 0.98$$

4.1  
5

$$OMC = 0.1109 * BC + 29.9 \quad R^2 = 0.92$$

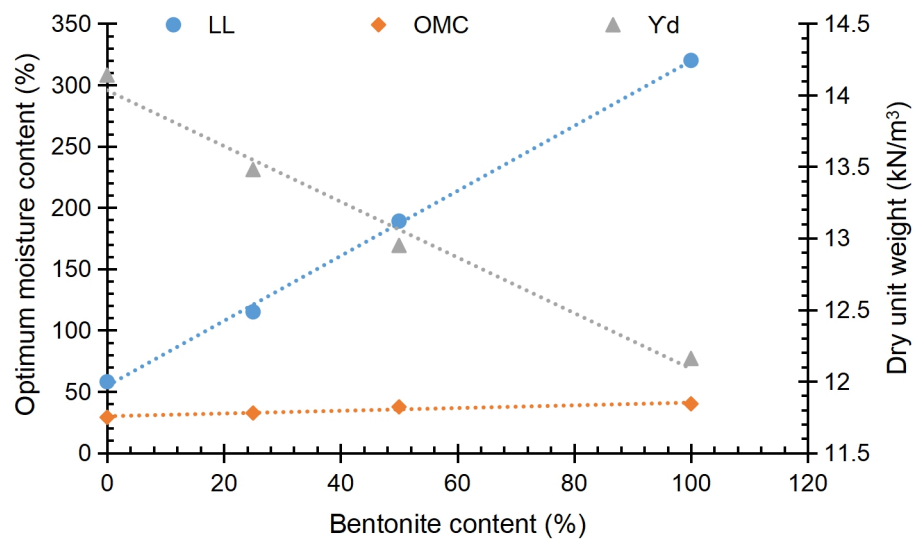
4.1  
6

Figure 4.50: Influence of bentonite content on the liquid limit, optimum moisture content, and maximum dry unit weight

The evolution of swelling pressure and the volume of water flow against the testing time for the four clays were depicted in Figures 4.51 and 4.52, respectively. The bentonite clay at its optimums is extremely impermeable to the extent that it resisted the water flow when it became fully saturated as can be recognised from the evolution of water flow with time elapse in Figure 4.52. Here it should be noted that the tested specimen reached its fully saturated stage shortly because it had been nearly saturated since its preparation. Figure 4.51 shows that the swelling pressure reached its stability shortly after 16h from the onset of the test, reaching a value of about 750kPa. In contrast, the swelling

pressure of ball clay reached its maximum of 92kPa in less than an hour and remained stable during the rest of the testing time. Unlike the pure bentonite, the flow of water was more pronounced with ball clay achieving a permeability coefficient of about  $8.22 \times 10^{-8}$  m/s at its maximum dry unit weight and optimum moisture content.

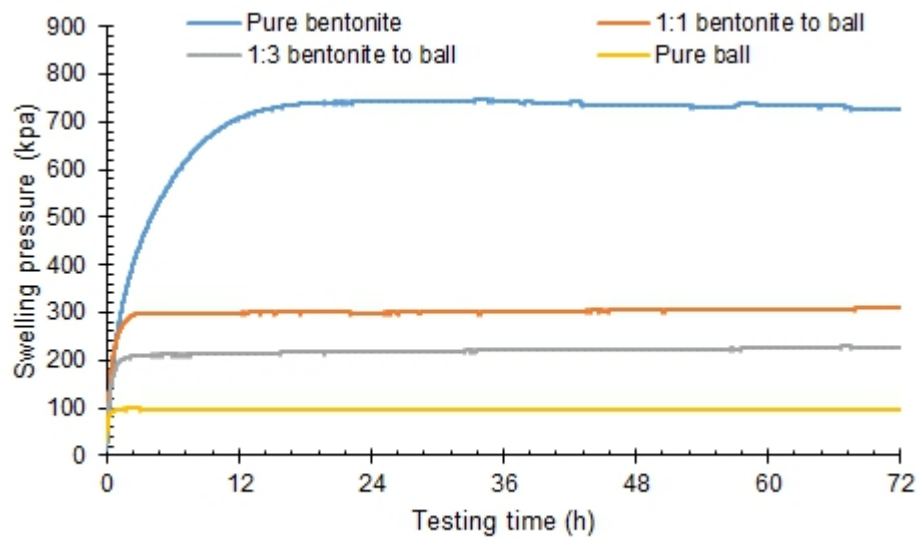


Figure 4.51: Evolution of swelling pressure for four clay types over the testing time

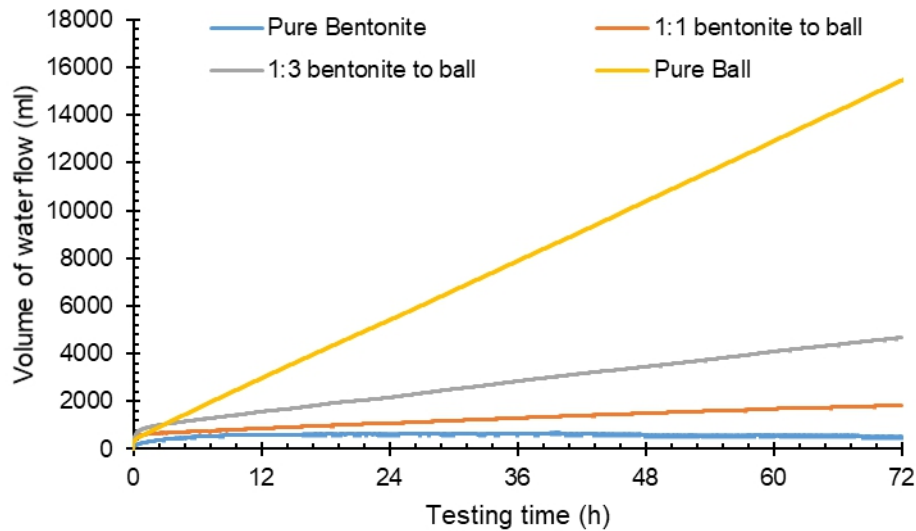


Figure 4.52: Evolution of volume of water flow for four clay types over the testing time

The coefficient of permeability declined four-time reaching to  $2.06 \times 10^{-8}$  m/s when the bentonite had been mixed with ball clay with a ratio 1:3 and compacted at their optimums compared with the coefficient permeability of ball clay. Further addition of bentonite to the ball clay resulted in a further reduction in the permeability coefficient, which declined 12 times to  $6.4 \times 10^{-9}$  m/s compared with the permeability coefficient of the ball clay when the bentonite and ball clay were mixed in equal proportions (1:1 bentonite to ball clay) at their optimums.

Regarding swelling tendency, the evolution of swelling pressure of 1:1 and 1:3 mixtures against the testing time reveals that the swelling pressure of both reached their stability just after 2h from the onset of tests reaching maximum swelling pressures of 310 and 229 kPa, respectively. Though, the dry unit weight of 1:1 clay is smaller than its counterpart with 1:3 clay. It seems that the bentonite content controls the resulting maximum swelling pressure.

### 4.5.3 Impact of mineralogy composition, lime content mellowing time and temperature on permeability coefficients

#### 4.5.3.1 Evolution of permeability coefficient of lime treated M1 specimens

In the previous series, the permeability was measured throughout 72h from the beginning of the test on lime-treated specimens that had been mellowed for 24h at 20°C and 40°C. Though, the bentonite is extremely impermeable the first measurements that have been taken after 6h from the onset of test shown a noticeable improvement in the permeability for all lime treated specimens with different lime contents (5 to 13%). The results showed that the coefficient of permeability would decline exponentially as the time elapsed if there is enough lime after the 24h mellowing to sustain substantial growth of cementitious compounds. Table 4.2 shows the exponential equations that govern the evolution of the permeability coefficients through the testing time on M1 lime treated specimens that were previously mellowed for 24h at 20 and 40°C.

Table 4.2: Exponential equations that govern the permeability coefficient of lime treated M1 specimens that were previously mellowed for 24h

| Lime content | Temperature of 40°C          |                | Temperature of 20°C          |                |
|--------------|------------------------------|----------------|------------------------------|----------------|
|              | Equation                     | R <sup>2</sup> | Equation                     | R <sup>2</sup> |
| 5            | $K = 15.7e^{-0.009 \cdot C}$ | 0.97           | $K = 9.7e^{-0.008 \cdot C}$  | 0.84           |
| 7            | $K = 23.9e^{-0.013 \cdot C}$ | 0.81           | $K = 18.6e^{-0.054 \cdot C}$ | 0.94           |
| 9            | $K = 55.8e^{-0.067 \cdot C}$ | 0.99           | $K = 43.4e^{-0.081 \cdot C}$ | 0.99           |
| 11           | $K = 50.4e^{-0.064 \cdot C}$ | 0.99           | $K = 38e^{-0.078 \cdot C}$   | 0.99           |
| 13           | $K = 49.7e^{-0.067 \cdot C}$ | 0.99           | $K = 40.5e^{-0.073 \cdot C}$ | 0.99           |

The coefficient of permeability for specimens that were treated by 9, 11, and 13% of lime showed an ongoing reduction during the testing time governed by exponential equations. The exponential rates of decay of specimens above range from -0.073 to -0.081 for specimens that were previously mellowed at 20°C and from -0.064 to -0.067 for those mellowed at 40°C. Such rates of decay show the speed at which the permeability decline during the tests due to the rapid growth of cementitious compounds.

In contrast, when the lime content is limited due to it was nearly or entirely consumed during the 24h mellowing periods as taken place with the specimens that were treated by 5% at 20 and 40°C and 7% at 40°C. The permeability showed a small decline in the measured coefficient of permeability for a limited time, followed by stability or being stable from the beginning, as seen in Figures 4.31 and 4.32 in series 3. The permeability of 7% lime content's specimen that was previously mellowed at 20°C showed an evident decline in the permeability with a rate of decay of -0.054. This decline indicates that even after 24h of mellowing at 20°C, there was adequate lime to sustain significant growth in the cementitious compound. The difference in the permeability evolution between the specimens that were treated by 7% lime is due to the role of the temperature of 40°C in accelerating the lime consumption during the 24h mellowing so that in there is not enough lime to maintain substantial growth of cementitious compounds during the testing time.

The registered coefficients of permeability for lime treated specimens that previously cured at 20 and 40°C were plotted against the testing time, as seen in Figures 4.53 and 4.54, respectively. Though the initial permeability

coefficients showed noticeable improvement, their values were lower by one order of magnitude compared with previously their counterparts, which were formerly mellowed for 24h at both temperatures.

The Permeability coefficients after which started to decline with rates of decay ranging from -0.04 to -0.57 until the end of testing time for specimens that had been treated by lime contents of 9, 11, and 13% and left to cure for 24h at 40°C. As well as the specimens that had been treated by lime contents of 7, 9, 11, and 13% and left to cure for 24h at 20°C showed rates of decay between -.035 and 0.04 as seen in Table 4.3. This observation points out that even after 24h of curing at 20 or 40°C, there is enough lime to preserve substantial growth of cementitious compounds over testing time. Here it should be mentioned that the rates of decay for the specimens with higher lime contents that previously cured at both temperatures were lesser than their counterparts that previously mellowed at both temperatures. Such observation could be attributed to the higher initial permeability coefficients for previously mellowed specimens compared with cured specimens. The higher permeability means higher pores spaces for reaction and thus higher space to accommodate the growth of cementitious compounds.

On the other hand, the significant part of lime content seems to be consumed with 5 and 7% lime treated specimens that were cured at 40°C as well as the 5% lime treated specimen that was cured at 20°C. This after which led to that the permeability coefficients either showed a slight decline followed by stability or were stable from the beginning of the test.

Table 4.3: Exponential equations that govern the permeability coefficient of M1 specimens that were previously cured for 24h

| Lime content | Temperature of 40°C          |                | Temperature of 20°C          |                |
|--------------|------------------------------|----------------|------------------------------|----------------|
|              | Equation                     | R <sup>2</sup> | Equation                     | R <sup>2</sup> |
| 5            | $K = 2.2e^{-0.007 \cdot C}$  | 0.43           | $K = 2.8e^{-0.005 \cdot C}$  | 0.64           |
| 7            | $K = 3.4e^{-0.003 \cdot C}$  | 0.7            | $K = 5e^{-0.035 \cdot C}$    | 0.96           |
| 9            | $K = 3.2e^{-0.04 \cdot C}$   | 0.96           | $K = 2.1e^{-0.03 \cdot C}$   | 0.98           |
| 11           | $K = 10.4e^{-0.057 \cdot C}$ | 0.97           | $K = 4.3e^{-0.033 \cdot C}$  | 0.98           |
| 13           | $K = 5e^{-0.051 \cdot T}$    | 0.96           | $K = 7.8.5e^{-0.04 \cdot C}$ | 0.99           |

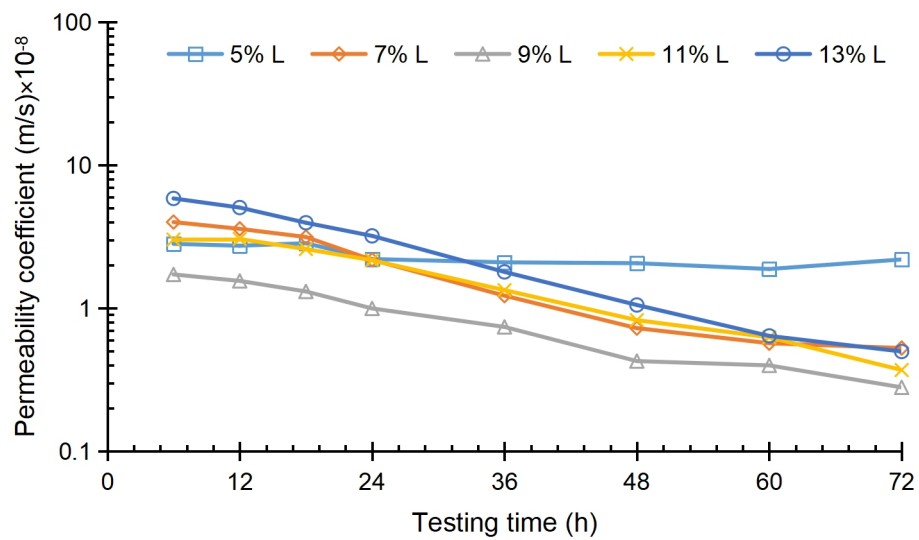


Figure 4.53: Evolution of permeability coefficients of lime treated bentonite (M1) specimens that were previously cured for 24h at 20°C

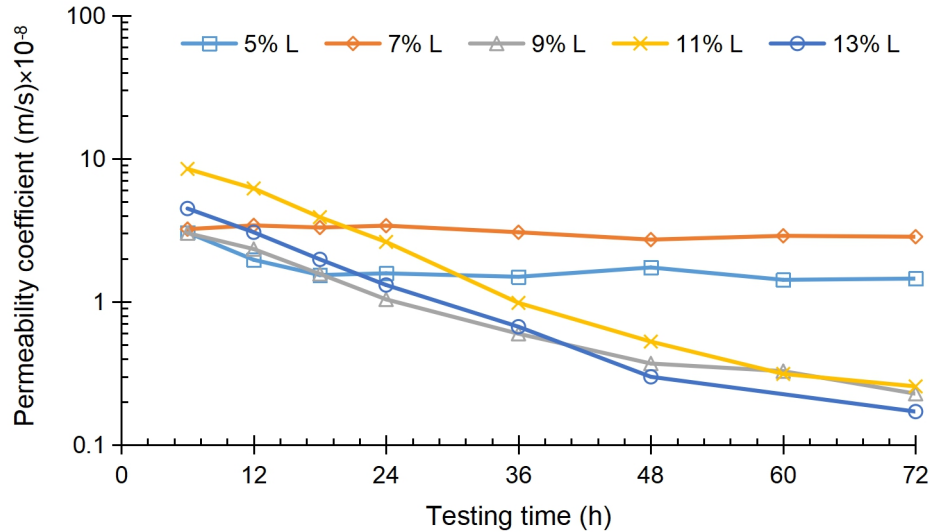


Figure 4.54: Evolution of permeability coefficients of lime treated bentonite (M1) specimens that were previously cured for 24h at 40°C

#### 4.5.3.2 Evolution of permeability coefficients of lime treated M2 specimens

The progress of coefficients of permeability against the testing time for lime treated M2 specimens that previously mellowed at 20 and 40°C were depicted in Figures 4.55 and 4.56. Initially, the permeability coefficients of lime treated specimens that were previously mellowed for 24h showed an increase by a factor of 2 to 3 compared with untreated ball clay specimen. The initial increase in the permeability coefficients could be imputed to the fast initial adsorption of calcium and desorption of sodium in the cation exchange process (during less than 5 minutes from the lime addition) that was reported by (Chemeda et al., 2018, Singh et al., 1996). Phenomena above might lead to from the flocs and cluster and renders the fabric of lime treated ball clay more porous compared with untreated one.



Furthermore, there was no significant difference in the values of initial permeability coefficients among the specimens that previously were mellowed at 20 and 40°C. Such observation giving an indication that the temperature has a limited or no effect on lime-clay reaction that take place during 24h mellowing. In general, the registered permeability coefficients after which exhibited stability or stability for 48h, followed by a marginal decline in the rest of testing time. Such manner could be attributed to the lime consumption delay and thus, the nonattendance of cementitious compounds with lime-treated kaolinite clay. It is well known that the role of alkaline environment that was induced by the addition of lime in attacking the surface of clay particles to release the reactants (alumina and silica) required for initiating the pozzolanic reaction. In the case of kaolinite, the accumulation of types of calcium cations on the surface of clay particles creating calcium cations layer preventing the alkaline environment from destructing the surfaces of clay particles to release the alumina and silica and thus leads delay of the formation of cementitious compounds (Konan et al., 2009, Chemedda et al., 2015, Chemedda et al., 2018).

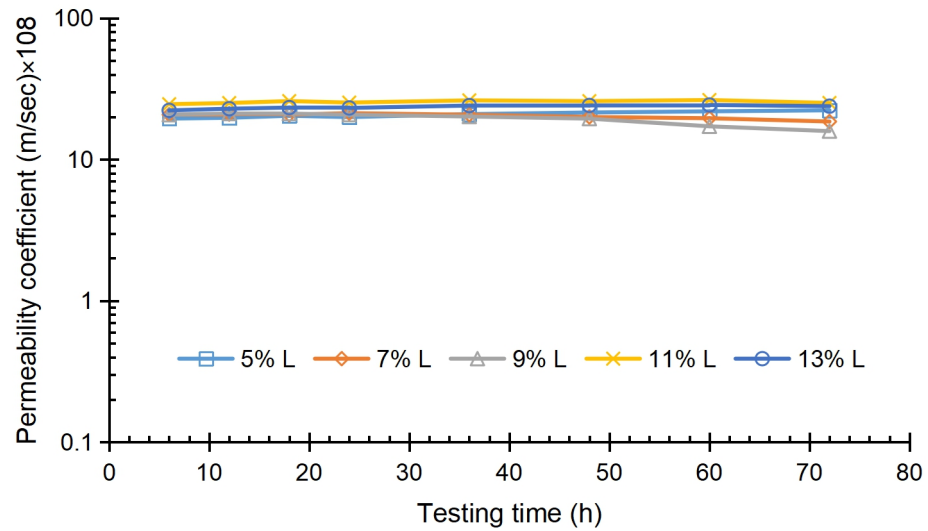


Figure 4.55: Evolution of permeability coefficients of lime treated (M2) ball specimens that were previously mellowed for 24h at 20°C

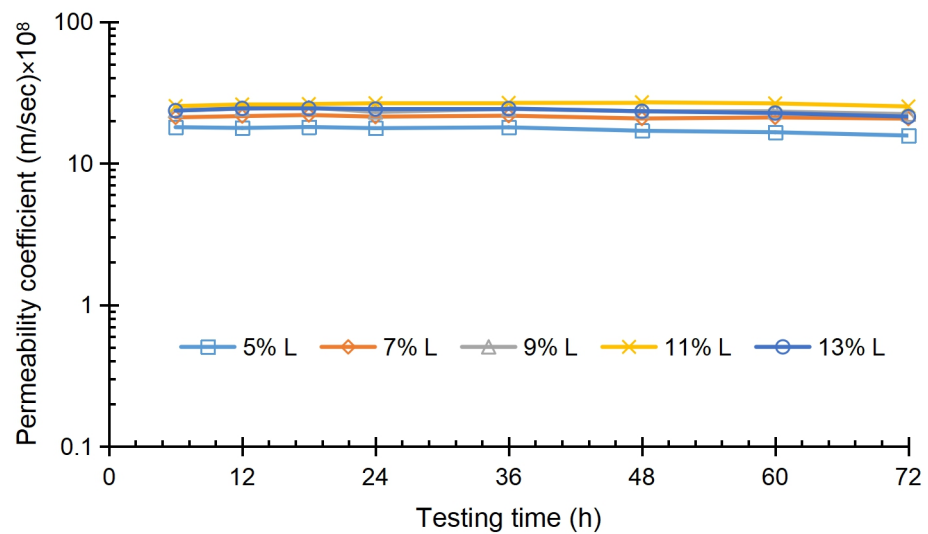


Figure 4.56: Evolution of permeability coefficients of lime treated M2 ball specimens that were previously mellowed for 24h at 40°C

Figures 4.57 and 4.58 display the reported permeability coefficients versus testing time for lime treated M2 specimens that previously were cured at 20°C and 40°C, respectively. The initial permeability coefficients of specimens

showed an increase by a factor of 1.3 to 2 and 2 to 3 for specimens that cured at 20 and 40°C. It is worth noting that comparing the initial permeability coefficients of the previously cured specimen with the previously mellowed specimens demonstrates that there is no difference regarding their values. This convergence in the initial permeability coefficient values could be attributed to that there is no vital reaction takes place except the immediate reaction that causes the initial increase in permeability.

The behaviour of permeability curves shows two manners; it sometimes remains nearly stable until the end of testing time or remains stable for a time ranging from 36 to 60h, followed by ongoing reduction. This decline after a period of stability was evident in the specimens that were previously cured at 20°C. Such decline undoubtedly indicates the formation of cementitious materials during the testing time in the available pores, which led to the reduction of effective porosity. The interpretation of such behaviour could be attributed to a rise in temperature to more than 30°C during June 2018, which we could not avoid though.

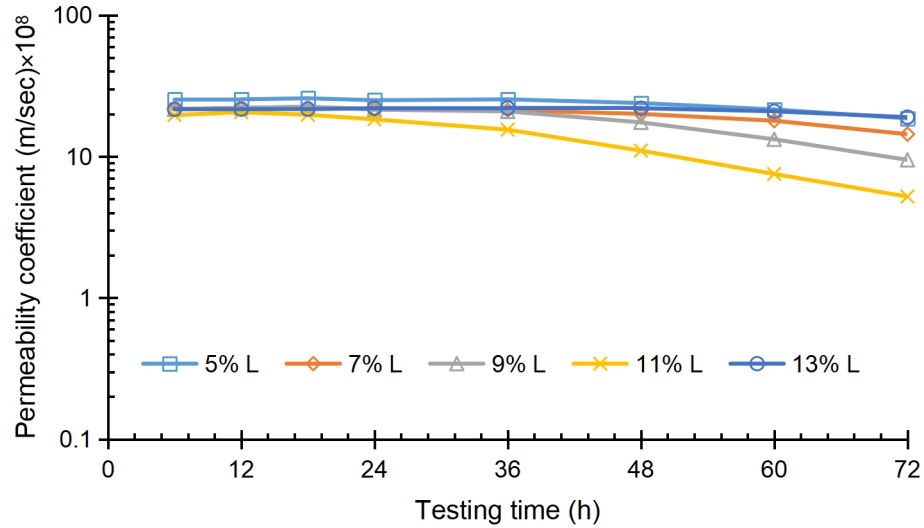


Figure 4.57: Evolution of permeability coefficients of lime treated ball (M2) specimens that were previously cured for 24h at 20°C

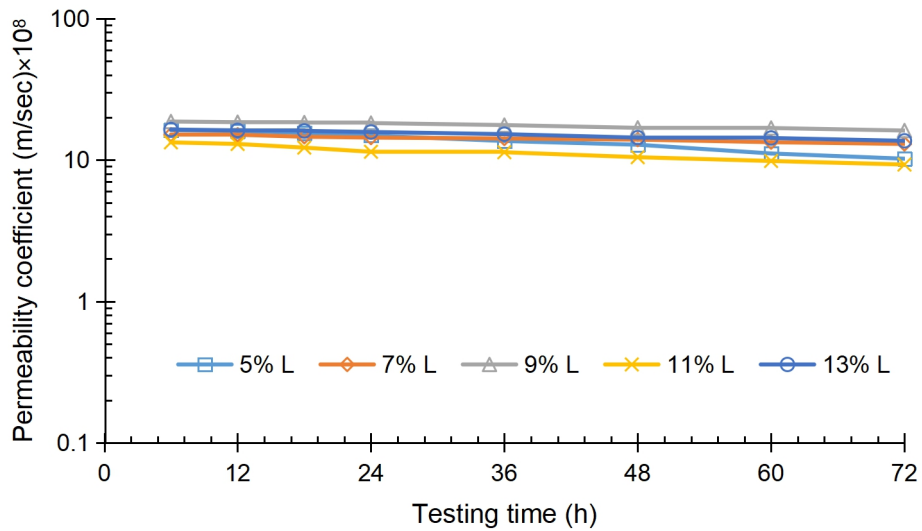


Figure 4.58: Evolution of permeability coefficients of lime treated ball (M2) specimens that were previously cured for 24h at 40°C

#### 4.5.3.3 Evolution of permeability coefficients of lime treated M3 specimens

The coefficients of permeability for lime treated M3 specimens that previously mellowed for 24h at 20 and 40°C that have been registered during the tests are plotted against the testing time as seen in Figures 4.59 and 4.60, respectively.

Initial permeability coefficients of lime treated M3 specimens showed an increase ranging from 3 to 5 and from 4.5 to 5.5 times higher with of lime treated specimens that previously had been mellowed at 20 and 40°C, respectively compared with untreated 1:3 clay. After which, the rate of water flow showed a continuous marginal decline over the rest of the testing time. Exponential equations govern the decline with marginal rates of decay ranges from -0.003 to -0.007 and – 0.004 to -.009 for the specimens that previously mellowed at 20 and 40°C, respectively (see in Table 4.4).

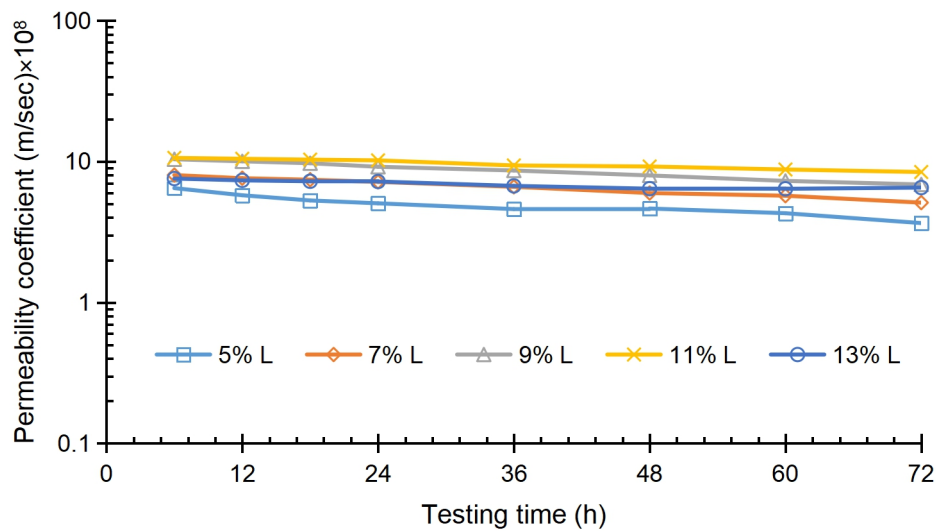


Figure 4.59: Evolution of permeability coefficients of lime treated 1:3 bentonite to ball (M3) specimens that were previously mellowed for 24h at 20°C

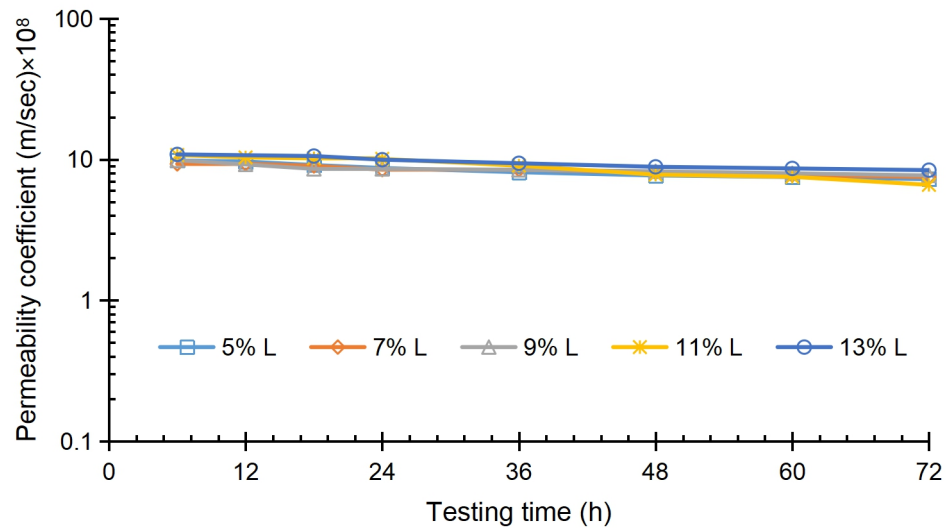


Figure 4.60: Evolution of permeability coefficients of lime treated 1:3 bentonite to ball (M3) specimens that were previously mellowed for 24h at 40°C

Table 4.4: Exponential equations that govern the permeability coefficient of M3 specimens that were previously mellowed for 24h

| Temperature of 40°C |                              |                | Temperature of 20°C           |                |
|---------------------|------------------------------|----------------|-------------------------------|----------------|
| Lime content        | Equation                     | R <sup>2</sup> | Equation                      | R <sup>2</sup> |
| 5                   | $K = 9.9e^{-0.005 \cdot C}$  | 0.97           | $K = 6.3e^{-0.007 \cdot C}$   | 0.92           |
| 7                   | $K = 9.5e^{-0.003 \cdot C}$  | 0.96           | $K = 8.3e^{-0.007 \cdot C}$   | 0.99           |
| 9                   | $K = 9.5e^{-0.003 \cdot C}$  | 0.85           | $K = 10.7e^{-0.006 \cdot C}$  | 0.99           |
| 11                  | $K = 11.5e^{-0.007 \cdot C}$ | 0.97           | $K = 10.8e^{-0.004 \cdot C}$  | 0.98           |
| 13                  | $K = 11e^{-0.004 \cdot C}$   | 0.96           | $K = 7.5.5e^{-0.009 \cdot C}$ | 0.8            |

The coefficients of permeability for specimens that previously cured for 24h at 20 and 40°C are depicted against the testing time as seen in Figures 4.61 and 4.62, respectively. Initially, the permeability coefficients exhibit an increase ranging from 3 to 5 times compared with the permeability coefficient of the untreated specimen. It seems that the formation of cementitious compounds

was not significant during the first 24h of curing or mellowing at both temperatures to create a difference in the values of initial permeability coefficients between previously mellowed specimens and previously cured specimens even at 40°C. After which, the permeability declines exponentially with rates of decay ranging from 0.002 to 0.005 for the specimen that previously cured at 40°C and from 0.006 to .01 for those previously cured at 20°C as reported in Table 4.5. Such exponential decline, even it is small, could be considered as an indicator on the growth of cementitious compounds over the testing time.

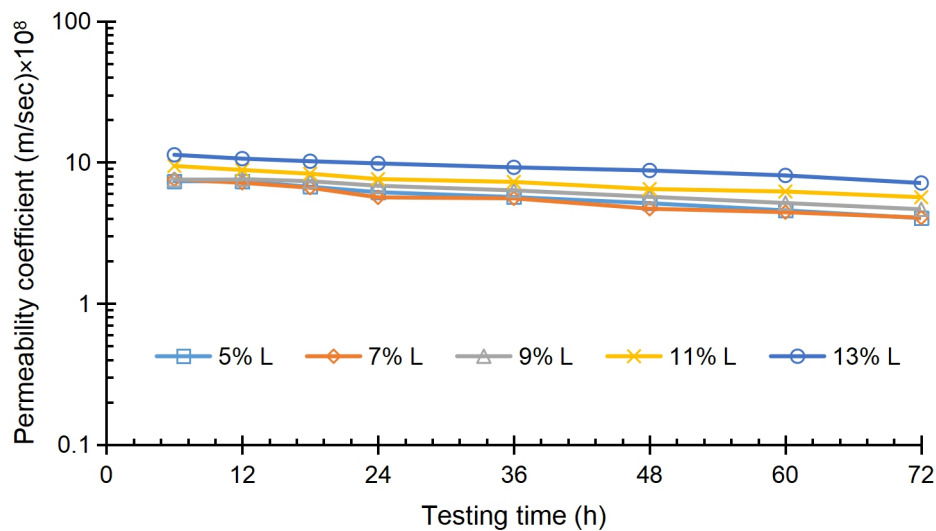


Figure 4.61: Evolution of permeability coefficients of lime treated 1:3 bentonite to ball specimens that were previously cured for 24h at 20°C

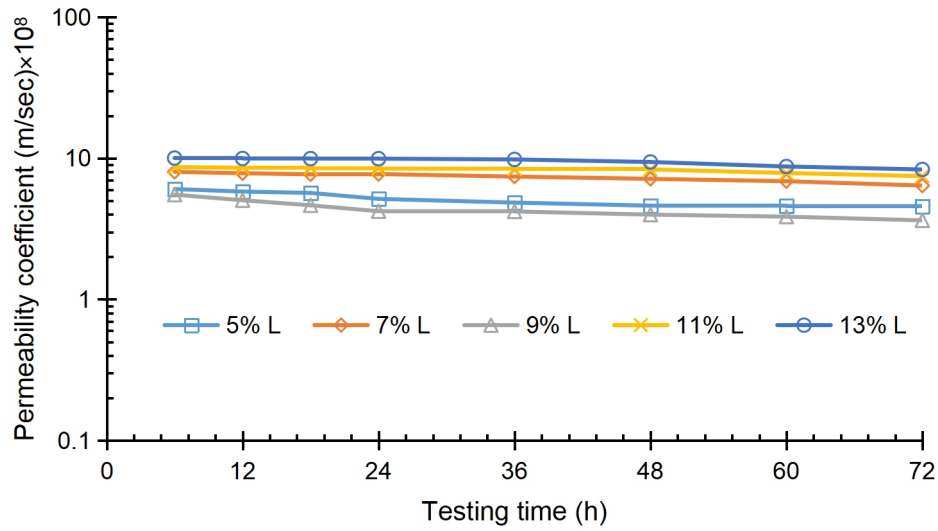


Figure 4.62: Evolution of permeability coefficients of lime treated 1:3 bentonite to ball (M3) specimens that were previously cured for 24h at 40°C

Table 4.5: Exponential equations that govern the permeability coefficient of M3 specimens that were previously cured for 24h

| Temperature of 40°C |                              |                | Temperature of 20°C           |                |
|---------------------|------------------------------|----------------|-------------------------------|----------------|
| Lime content        | Equation                     | R <sup>2</sup> | Equation                      | R <sup>2</sup> |
| 5                   | $K = 6e^{-0.005 \cdot C}$    | 0.88           | $K = 7.9e^{-0.009 \cdot C}$   | 0.99           |
| 7                   | $K = 8.2e^{-0.003 \cdot C}$  | 0.97           | $K = 7.7e^{-0.01 \cdot C}$    | 0.96           |
| 9                   | $K = 5.3e^{-0.003 \cdot C}$  | 0.87           | $K = 8.2e^{-0.008 \cdot C}$   | 0.99           |
| 11                  | $K = 8.9e^{-0.002 \cdot C}$  | 0.85           | $K = 9.5e^{-0.007 \cdot C}$   | 0.98           |
| 13                  | $K = 10.5e^{-0.003 \cdot C}$ | 0.87           | $K = 11.65e^{-0.006 \cdot C}$ | 0.98           |

#### 4.5.3.4 Evolution of permeability coefficients of lime treated M4 specimens

The rates of flow water were measured over the 72h from the beginning of the test on specimens that were previously mellowed at 40°C and 20°C for 24h. Figures 4.63 and 4.64 exhibit data for the permeability coefficients versus



testing time for specimens with different lime contents that previously mellowed at 20°C and 40°C, respectively. Of note, the permeability coefficient of untreated 1:1 is low at  $6.4 \times 10^{-9}$  m/s the initial permeability coefficients of lime treated specimens showed an increase to be in the order of ( $10^{-8}$  m/s). The initial permeability coefficients of lime treated specimens that previously mellowed at 40°C are 10 to 13 times higher compared with untreated 1:1 clay. Whereas, the coefficients of permeability increased by 7 to 9 times in the case of specimens that were previously mellowed at 20°C compared with the permeability coefficient of the untreated specimen. Such a significant increase in the permeability could be attributed to the flocculation and agglomeration that had taken place as a result of cation exchange phenomenon and enhanced by formation of cementitious compounds. The formation of such flocs and clusters leads to reduce the specific surface area in contact with water in the system leading to decline the swelling tendency and form inter- and intra- pores within and between the flocs rendering the lime-treated clay soil more porous. It seems that the occurrence of such mechanisms at 40°C in the loose state offer resistance to the compactability and thus more porous nature after subsequent compaction compared with their counterparts at 20°C. It is worth noting that the impact of temperature regarding the initial permeability coefficients was less evident with lime-treated M3 specimens that were previously mellowed at 20 and 40°C giving an indication on the vital role of bentonite content in initiating the pozzolanic reaction.

After which, the rate of water flow started to decline and continue to decline until the end of testing time. Exponential equations with rates of decay govern the rate of flow during the testing time ranged from -0.018 to -0.021 as seen in

Table 4.6 to fall by up to three-quarters of their initial values by the end of testing time. This reduction indicates the ongoing formation of cementitious compounds in the available pores due to their impact on the size of pores and the accessibility of water to these pores. The exception was the 5% lime content that was previously mellowed at 40°C, where the decline continued for 2 days, and then the rate of flow showed stability over the next 24h to fall just by half its initial value by the end of the test. This behaviour indicates that there is no sufficient amount lime to maintain the formation of cementitious compounds during the rest of testing time due to the role of the temperature of 40°C in accelerating the consumption of the available lime.

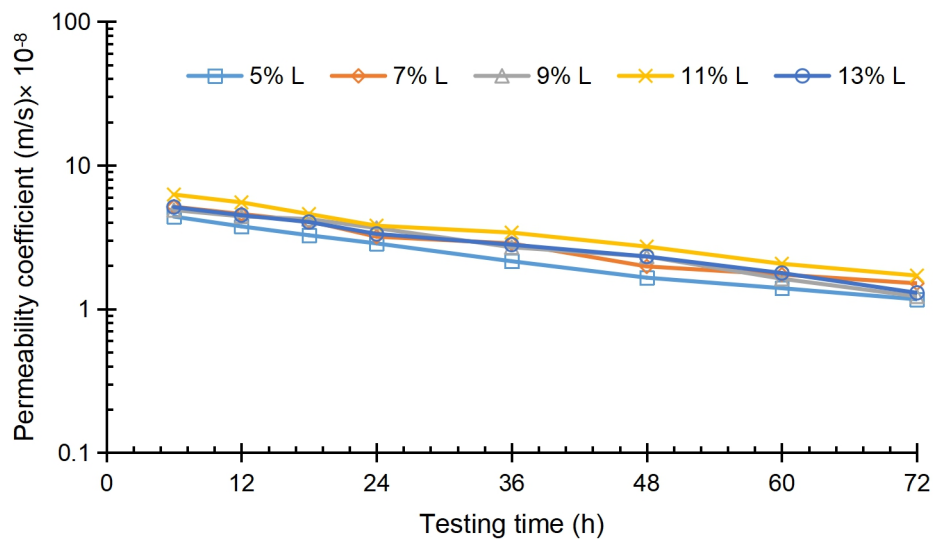


Figure 4.63: Evolution of permeability coefficients of lime treated 1:1 bentonite to ball (M4) specimens that were previously mellowed for 24h at 20°C

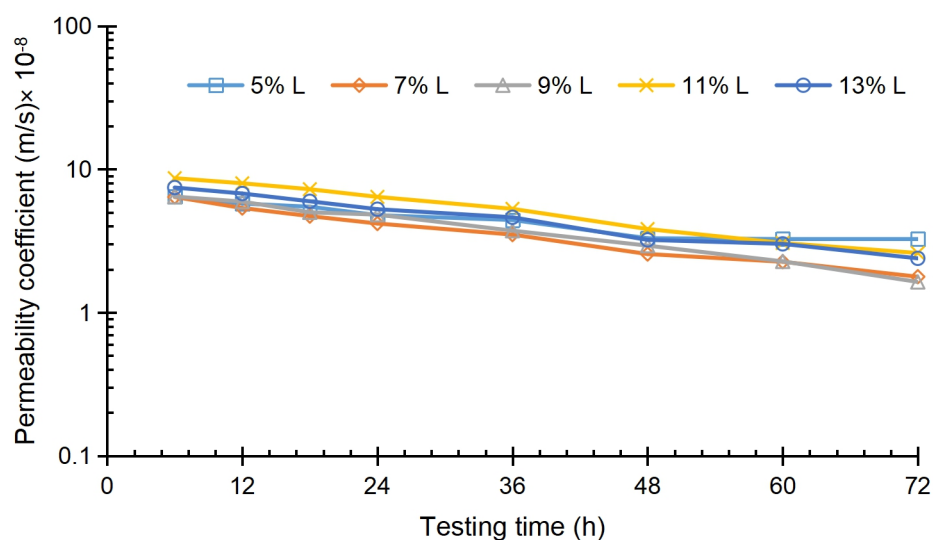


Figure 4.64: Evolution of permeability coefficients of lime treated 1:1 bentonite to ball (M4) specimens that were previously mellowed for 24h at 40°C

Table 4.6: Exponential equations that govern the permeability coefficient of M4 specimens that were previously mellowed for 24h

| Lime content | Temperature of 40°C         |                | Temperature of 20°C         |                |
|--------------|-----------------------------|----------------|-----------------------------|----------------|
|              | Equation                    | R <sup>2</sup> | Equation                    | R <sup>2</sup> |
| 5            | $K = 6.5e^{-0.011 \cdot C}$ | 0.92           | $K = 4.7e^{-0.02 \cdot C}$  | 0.99           |
| 7            | $K = 6.7e^{-0.019 \cdot C}$ | 0.99           | $K = 5.6e^{-0.019 \cdot C}$ | 0.98           |
| 9            | $K = 7.5e^{-0.02 \cdot C}$  | 0.99           | $K = 5.8e^{-0.021 \cdot C}$ | 0.99           |
| 11           | $K = 10e^{-0.019 \cdot C}$  | 0.99           | $K = 6.7e^{-0.019 \cdot C}$ | 0.99           |
| 13           | $K = 8.2e^{-0.017 \cdot C}$ | 0.99           | $K = 5.75e^{-0.02 \cdot C}$ | 0.99           |

Concerning the specimens that were previously cured for 24h at 20 and 40°C, the evolution of permeability coefficients was plotted against testing time in Figures 4.65 and 4.66, respectively. Initial permeability coefficients of

specimens that previously cured at 20 and 40°C indicate an improvement in the permeability by a factor of 3 to 4.5 and 4 to 6, respectively compared with the permeability coefficient of the untreated specimen. However, the registered initial permeability coefficients were lesser than their counterparts that were previously mellowed for 24h at 20 and 40°C. This difference in favour of mellowed specimens is due to the formation of cementitious compounds over 24h mellowing time in the loose state which offers higher resistance to the compactability and thus more porous nature after subsequent compaction compared with their counterparts that were compacted directly after mixing. After which the permeability showed an exponential reduction during the remaining time of test with a rate of decay ranges from -0.022 to -0.026 and from -0.018 to -0.021 for specimens that were previously cured at 20 and 40°C, respectively (see Table 4.7). With such ongoing decline, the permeability coefficients showed a decline reaching between 70 and 80% of their initial values by the end of the tests. The exception again was the 5% lime treated specimen that was cured at 40°C, where the permeability showed a decline before showing stability after the reading that had been taken 48h after the start of the test. This corresponds with the role of the temperature of 40°C in accelerating the major part of lime content during the first 24h and the rest of the available lime was enough to sustain the formation of cementitious compounds for just 48 from the submerging of the specimen under room temperature so that the rate of flow becomes stable after which. This also demonstrates that the rate of lime consumption was lower in the case of lime treated M4 specimen compared with lime-treated bentonite specimens. Since bentonite specimens that were treated with higher lime content (7%) behaved in

the way appearing that the available lime content was nearly consumed after 24h from submerging. In general, the rates of decay were higher with the specimens with higher bentonite content indicating that the rate of formation of cementitious compounds was higher when the bentonite content was more significant.

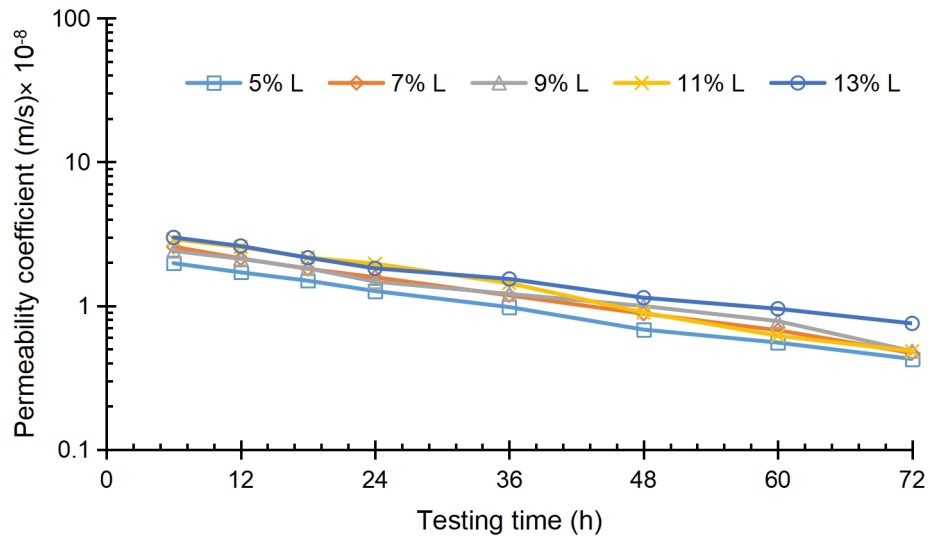


Figure 4.65: Evolution of permeability coefficients of lime treated 1:1 bentonite to ball (M4) specimens that were previously cured for 24h at 20°C

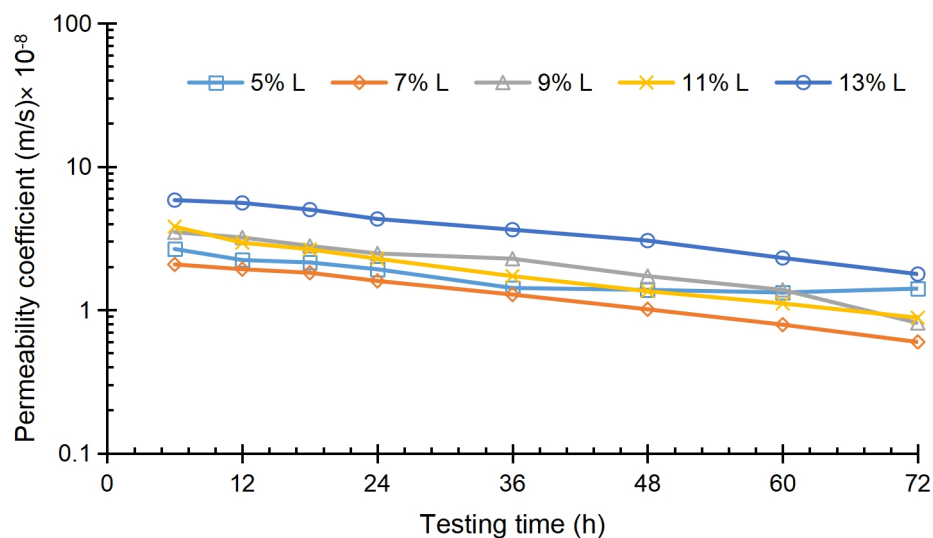


Figure 4.66: Evolution of permeability coefficients of lime treated 1:1 bentonite to ball (M4) specimens that were previously cured for 24h at 40°C

Table 4.7: Exponential equations that govern the permeability coefficient of M4 specimens that were previously cured for 24h

| Temperature of 40°C |                             |                | Temperature of 20°C           |                |
|---------------------|-----------------------------|----------------|-------------------------------|----------------|
| Lime content        | Equation                    | R <sup>2</sup> | Equation                      | R <sup>2</sup> |
| 5                   | $K = 1.1e^{-0.01 \cdot C}$  | 0.86           | $K = 2.2e^{-0.024 \cdot C}$   | 0.95           |
| 7                   | $K = 2.4e^{-0.019 \cdot C}$ | 0.99           | $K = 2.9e^{-0.025 \cdot C}$   | 0.99           |
| 9                   | $K = 4.3e^{-0.021 \cdot C}$ | 0.95           | $K = 2.7e^{-0.023 \cdot C}$   | 0.99           |
| 11                  | $K = 3.9e^{-0.021 \cdot C}$ | 0.99           | $K = 3.6e^{-0.028 \cdot C}$   | 0.99           |
| 13                  | $K = 6.8e^{-0.018 \cdot C}$ | 0.99           | $K = 3.2.5e^{-0.021 \cdot C}$ | 0.99           |

#### 4.5.4 Impact of mineralogy composition, lime content, mellowing time and temperature on swelling tendency.

##### 4.5.4.1 Swelling behaviour of lime treated M1 specimens:

The progress of swelling pressures versus the testing time for all lime treated M1 specimens are depicted in Figures 4.67, 4.68, 4.69 and 4.70. The resulting maximum swelling pressures for all lime treated M1 specimens were reported in Table 4.8. The results of maximum swelling pressures indicate that there is a significant depression in registered maximum swelling pressure values of lime-treated bentonite specimens compared to the maximum swelling pressure value of untreated bentonite specimens. This depression can be referred the reduction in the surface area of clay particles in contact with water as a result of flocculation mechanism generated by cation exchange phenomena and enhanced by initial cementitious compounds (Beetham et al., 2015).

Table 4.8: Resulting Maximum swelling pressures for all lime treated M1 specimens

|                  | Temperature of 40°C |           | Temperature of 20°C |           |
|------------------|---------------------|-----------|---------------------|-----------|
|                  | Mellowing           | Curing    | Mellowing           | Curing    |
| Lime content (%) | MSP (kPa)           | MSP (kPa) | MSP (kPa)           | MSP (kPa) |
| 5                | 294                 | 98        | 232                 | 117       |
| 7                | 257                 | 17        | 212                 | 42        |
| 9                | 199                 | 18        | 168                 | 72        |
| 11               | 187                 | 15        | 131                 | 63        |
| 13               | 242                 | 17        | 150                 | 55        |

The reported maximum swelling pressures were small for all 24h cured specimens compared with the maximum swelling pressures of mellowed specimens at both temperatures. In general, this noticeable reduction in the swelling for 24h cured specimens undoubtedly refer to the role of formation of cementitious bonds between the flocs in the compacted state in further curbing the swelling tendency. As well as, it asserts the impact of subsequent compaction in partially destructing such cementitious bonds that previously formed in the loose state during the 24h mellowing.

Growth of cementitious compounds over 24h curing at 20°C and 40°C in the compacted state was enough to decline the swelling significantly to less than 10% of the swelling pressure of untreated specimens. However, the swelling tendency was completely curbed for 24h cured (M1) specimens that were treated by 7, 9, 11 and 13% lime content. This magnitude of reduction could be

attributed to the role of temperature in accelerating the formation of cementitious compound offering a further reduction in the specific surface areas and stronger cementitious bonds enough to eliminate the tendency to swelling. Here it should be mentioned that the 24h cured specimens that were treated by 5% of lime appeared relatively higher swelling pressures compared to their counterparts that were treated by higher lime contents. It seems that the 5% lime content was not enough to generate the required amount of cementitious compounds to obtain a swelling reduction similar to with higher lime contents.



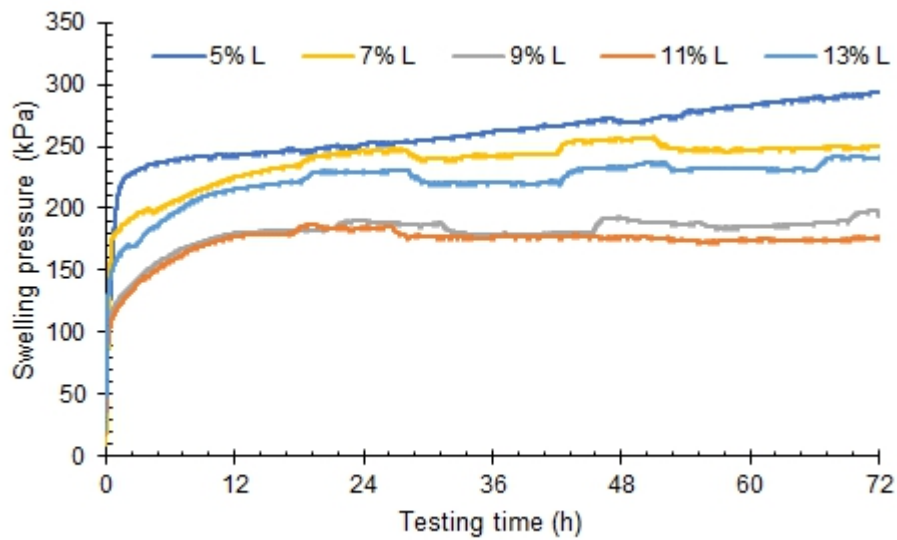


Figure 4.67: Evolution of swelling pressures of lime treated bentonite (M1) specimens that were previously mellowed for 24h at 40°C

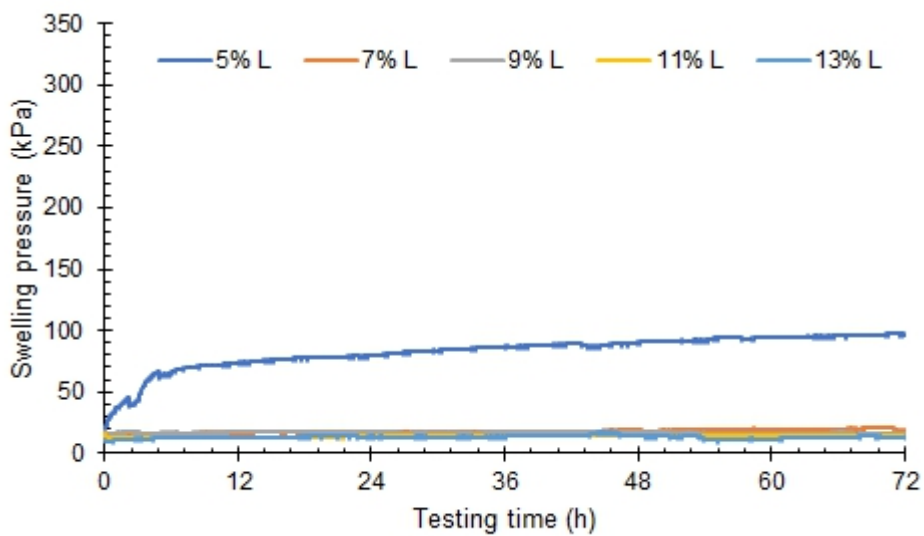


Figure 4.68: Evolution of swelling pressures of lime treated bentonite (M1) specimens that were previously cured for 24h at 40°C

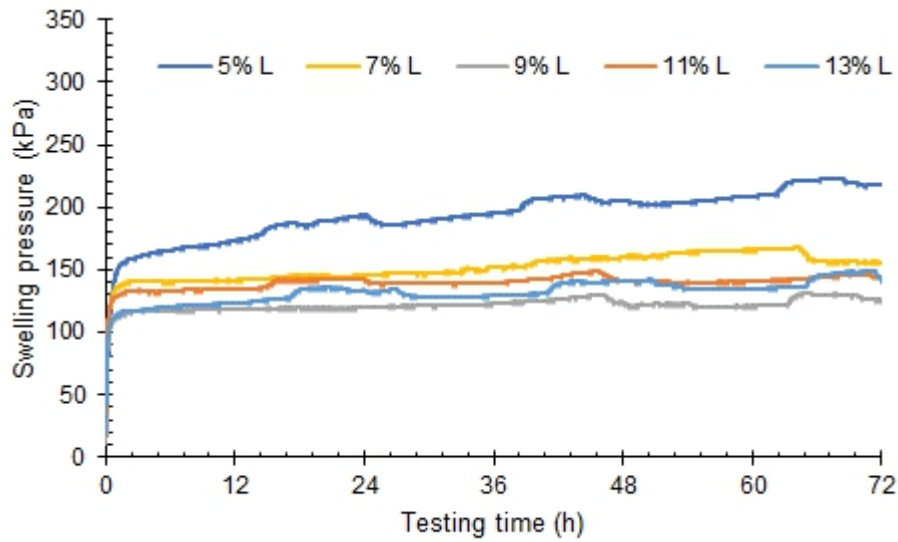


Figure 4.69: Evolution of swelling pressures of lime treated bentonite (M1) specimens that were previously mellowed for 24h at 20°C

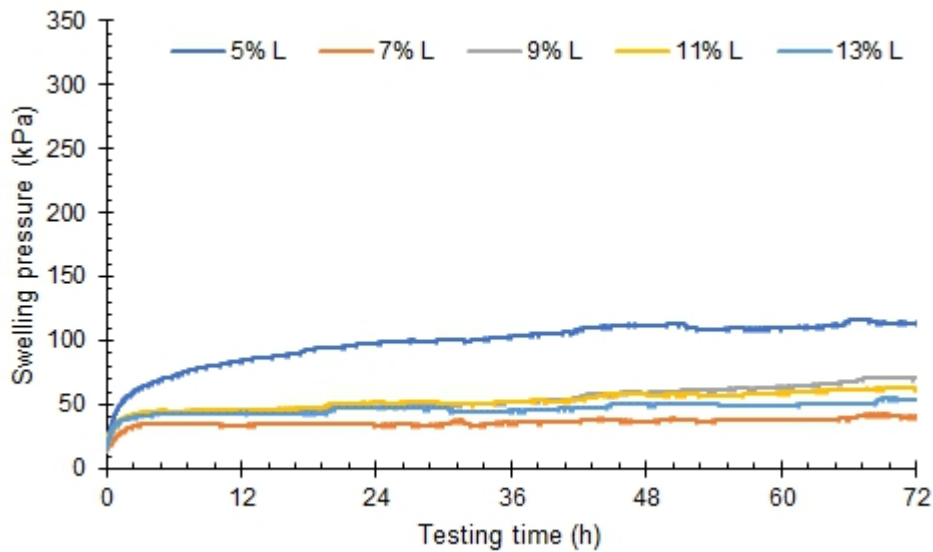


Figure 4.70: Evolution of swelling pressures of lime treated bentonite (M1) specimens that were previously curd for 24h at 20°C

#### 4.5.4.2 Swelling behaviour for lime treated M2 specimens:

Evolution of swelling pressures against the testing time for all lime treated M2 specimens are illustrated in Figures 4.71, 4.72, 4.73 and 4.74. The resulting maximum swelling pressures for all lime treated M2 specimens were shown in

Table 4.9. It is evident that there is no difference in the swelling values between treated specimens and untreated specimen as well as between mellowed and cured specimens at both temperatures. This observation indicates non-formation of cementations compounds during at least in the first 24h. No effect of lime on the swelling pressure values has two possible explanations. The first is that the swelling mechanism that governs the swelling in the M1 clay differed from its counterpart with M2 clay. The second possible explanation is that the growth of cementations compounds that are involved in reducing the tendency to swell are delayed. Such delay in the formation of cementitious compounds could be attributed to the delay of releasing the alumina and silica from the surfaces of kaolinite particles as a results of accumulation of a type of calcium cations on kaolinite surfaces. Chemedda et al. (2018) reported the role of such accumulation preventing the alkaline environment from attacking the surface kaolinite particle and thus delaying the release of alumina and silica that required to initiate the cementitious compounds. The similarity in resulting maximum swelling pressures at both temperatures indicates that even with higher temperature there is a delay in the formation of cementitious compounds at least during the first 24h.

Table 4.9: Resulting Maximum swelling pressures for all lime treated M2 specimens

|                  | Temperature of 40°C |           | Temperature of 20°C |           |
|------------------|---------------------|-----------|---------------------|-----------|
|                  | Mellowing           | curing    | Mellowing           | curing    |
| Lime content (%) | MSP (kPa)           | MSP (kPa) | MSP (kPa)           | MSP (kPa) |
| 5                | 127                 | 94        | 108                 | 86        |
| 7                | 128                 | 99        | 126                 | 100       |
| 9                | 93                  | 96        | 113                 | 103       |
| 11               | 105                 | 91        | 103                 | 98        |
| 13               | 104                 | 88        | 100                 | 96        |

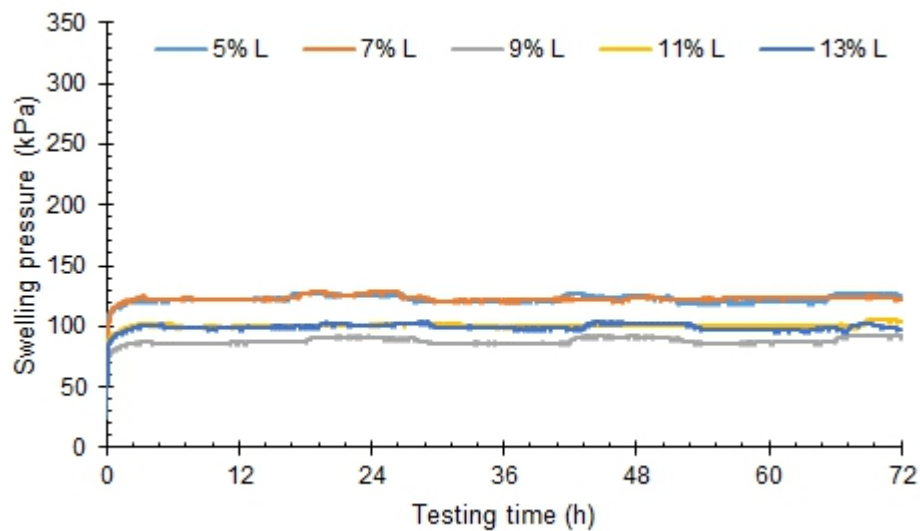


Figure 4.71: Evolution of swelling pressures of lime treated ball (M2) specimens that were previously mellowed for 24h at 40°C

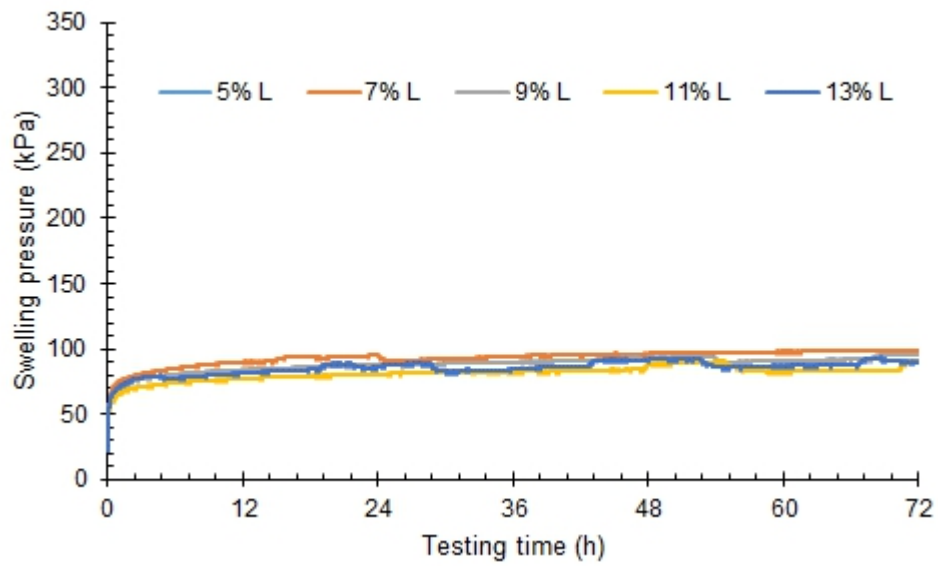


Figure 4.72: Evolution of swelling pressures of lime treated ball (M2) specimens that were previously cured for 24h at 40°C

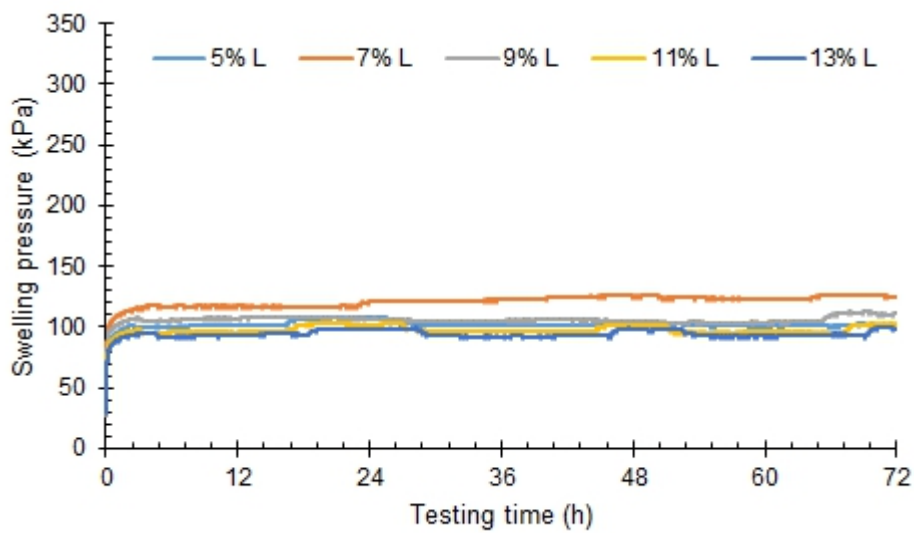


Figure 4.73: Evolution of swelling pressures of lime treated ball (M2) specimens that were previously mellowed for 24h at 20°C

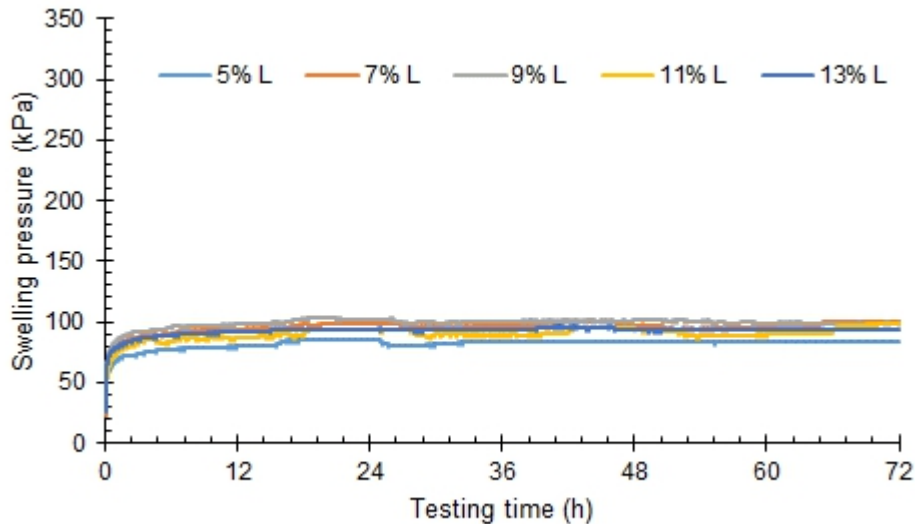


Figure 4.74: Evolution of swelling pressures of lime treated ball (M2) specimens that were previously cured for 24h at 20°C

#### 4.5.4.3 Swelling behaviour for lime treated M3 specimens:

The development of swelling pressures during the testing time for lime treated M3 specimens are presented in Figures 4.75, 4.76, 4.77 and 4.78. The resulting maximum swelling pressures for all lime treated M3 specimens were presented in Table 4.10. In general, the reduction in the maximum swelling pressures for all lime treated M3 specimens was marginal compared with the maximum swelling pressure of the untreated M3 specimen. This marginal reduction in swelling indicates the role of bentonite content in initiating the pozzolanic reaction. It seems that the formation of cementitious compounds was very marginal during the first 24h. However, the swelling pressures values of the lime-treated M3 specimens that were previously cured for 24h at 40°C are relatively smaller compared with other lime treated M3 specimens. This small difference refers to the role that was played by curing temperature of 40°C in accelerating the growth of cementitious compounds during the first 24h in the

compacted state; and thus, in partially curbing the tendency of swelling pressure compared with others lime treated M3 clay.

Table 4.10: Resulting Maximum swelling pressures for all lime treated M3 specimens

|                  | Temperature of 40°C |           | Temperature of 20°C |           |
|------------------|---------------------|-----------|---------------------|-----------|
|                  | Mellowing           | curing    | Mellowing           | curing    |
| Lime content (%) | MSP (kPa)           | MSP (kPa) | MSP (kPa)           | MSP (kPa) |
| 5                | 177                 | 121       | 183                 | 187       |
| 7                | 183                 | 137       | 154                 | 192       |
| 9                | 159                 | 142       | 166                 | 189       |
| 11               | 180                 | 132       | 150                 | 179       |
| 13               | 176                 | 126       | 160                 | 160       |

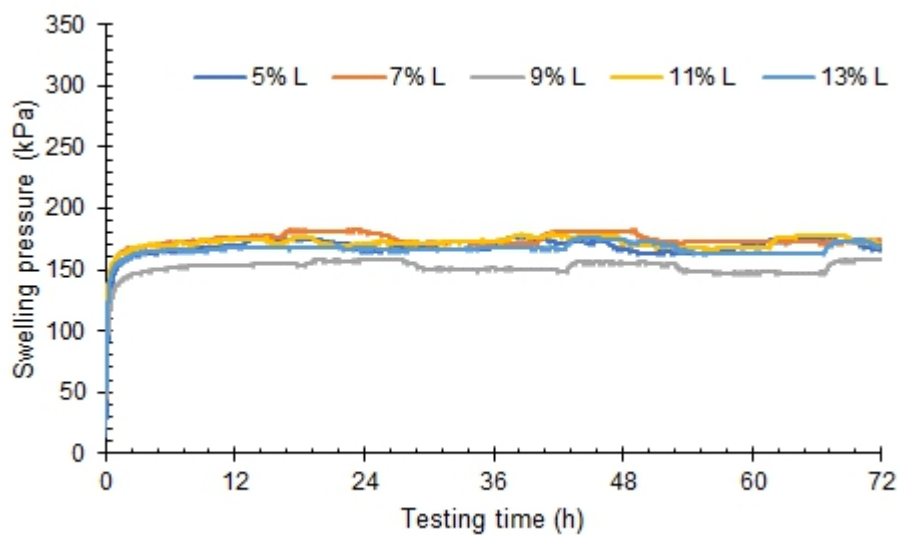


Figure 4.75: Evolution of swelling pressures of lime treated M3 specimens that were previously mellowed for 24h at 40°C

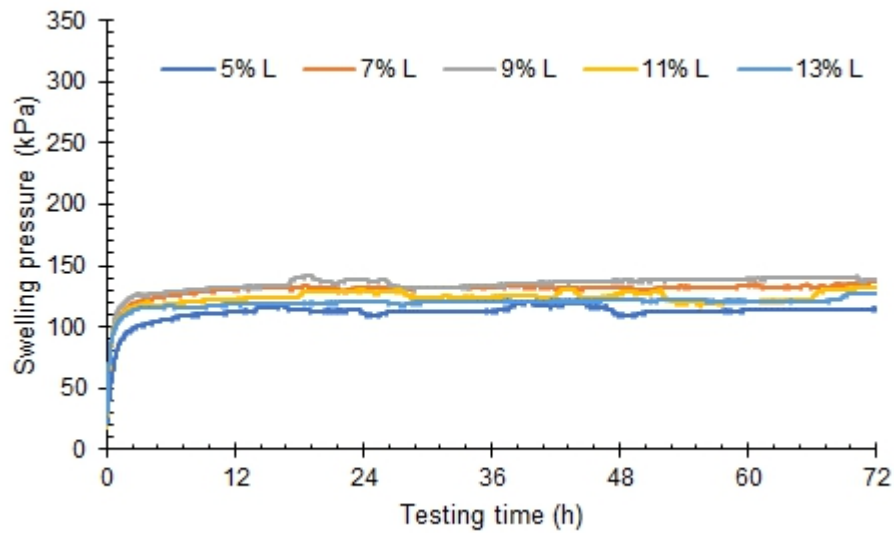


Figure 4.76: Evolution of swelling pressures of lime treated M3 specimens that were previously cured for 24h at 40°C

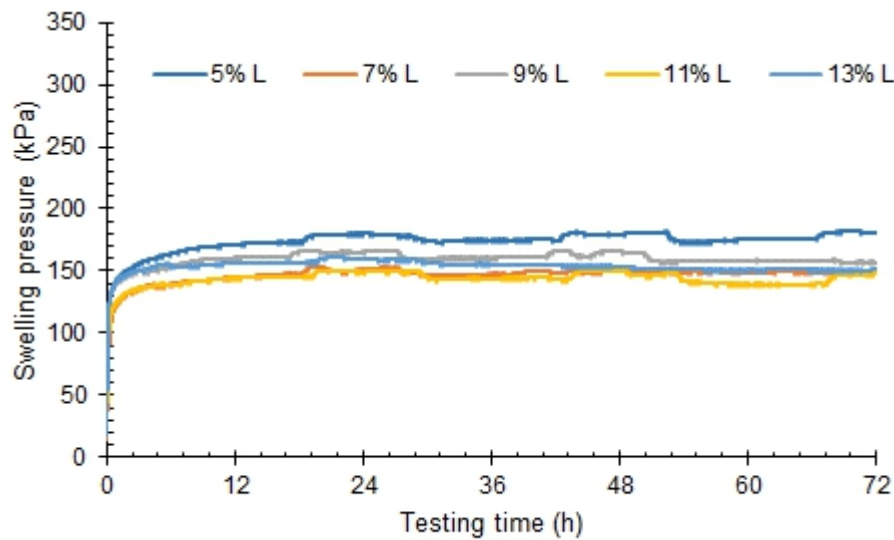


Figure 4.77 Evolution of swelling pressures of lime treated (M3) specimens that were previously mellowed for 24h at 20°C



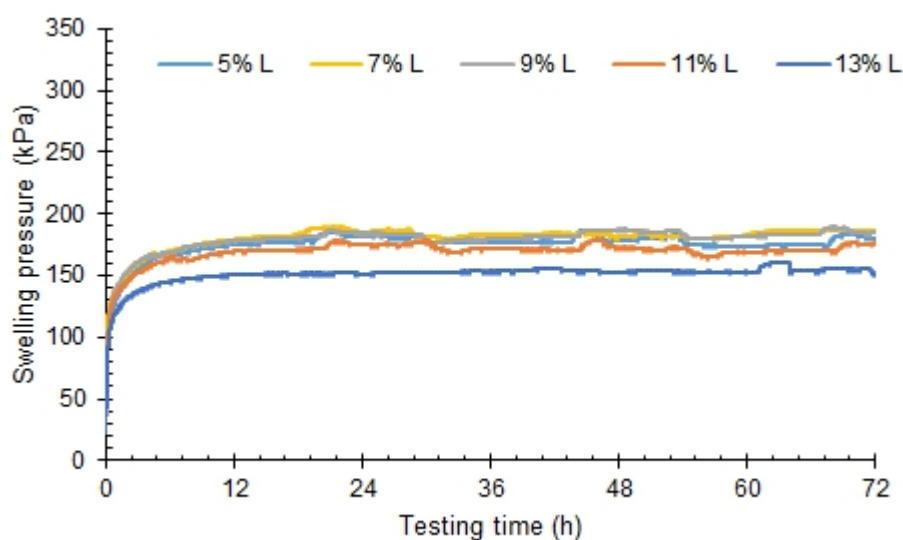


Figure 4.78: Evolution of swelling pressures of lime treated (M3) specimens that were previously cured for 24h at 20°C

#### 4.5.4.4 Swelling behaviour of lime treated M4 specimens

The evolution of swelling pressures against the testing time for all lime treated M1 specimens are depicted in Figures 4.79, 4.80, 4.81 and 4.82. The resulting maximum swelling pressures for all lime treated M1 specimens were reported in Table 4.11. Though the swelling pressure declined in general, it seems that the flocs and the cementitious bonds that formed in the loose state have been partially destroyed during subsequent compaction causing the appearance of these reported values of swelling pressure as presented in Table 4.11.

Here also, it should be mentioned that the swelling pressures of the specimens that previously were mellowed at 40°C reached its stability in less than 2h from the submerging of specimens as seen in Figure 4.79. Whereas at 20°C, the evolution of swelling pressures entered in a transition stage in which the swelling grew gradually for a period extended from the second hour of the test to about twenty-fourth, as shown in Figure 4.81. The transition stage in the swelling evolution was also observed with the previously cured specimens at

20°C, as seen in Figure 4.82. Whereas with 24h curing at 40°C, the swelling pressures reached its stability shortly in two hours from the submerging the specimen.

It worth noting that, unlike other specimens, the specimens that were previously cured at 40°C appeared the lowest tendency to the swelling. This give an indication that though the time allowed for specimens to cure for 24h at 20°C and 40°C before testing, the growth of cementitious compounds in compacted state at 20°C was not enough to show a decline in the swelling like at 40°C due to the impact of temperature of 40°C in accelerating the formation of cementitious compounds.

Regarding the swelling, the strong evidence on the role of temperature and bentonite content in accelerating the formation of cementations compounds comes from the lime-treated specimens containing 25, 50, and 100% of bentonite that were previously were cured for 24h. Such specimens showed less tendency to swelling compared with their counterparts that were cured at 20°C or those mellowed at 20 and 40°C. Furthermore, the extent to which the lime treatment is effective in curbing the potential swelling seems to depend on the bentonite content. This behaviour corresponds with the higher initial permeability coefficient with previously mellowed at 40°C compared with those mellowed at 20°C. It seems that as bentonite content increases as the rate of formation of cementitious compounds increases.

Table 4.11: Resulting Maximum swelling pressures for all lime treated M4 specimens

|                  | Temperature of 40°C |           | Temperature of 20°C |           |
|------------------|---------------------|-----------|---------------------|-----------|
|                  | Mellowing           | curing    | Mellowing           | curing    |
| Lime content (%) | MSP (kPa)           | MSP (kPa) | MSP (kPa)           | MSP (kPa) |
| 5                | 202                 | 90        | 226                 | 194       |
| 7                | 146                 | 79        | 188                 | 209       |
| 9                | 181                 | 68        | 215                 | 207       |
| 11               | 155                 | 56        | 162                 | 194       |
| 13               | 183                 | 58        | 193                 | 192       |

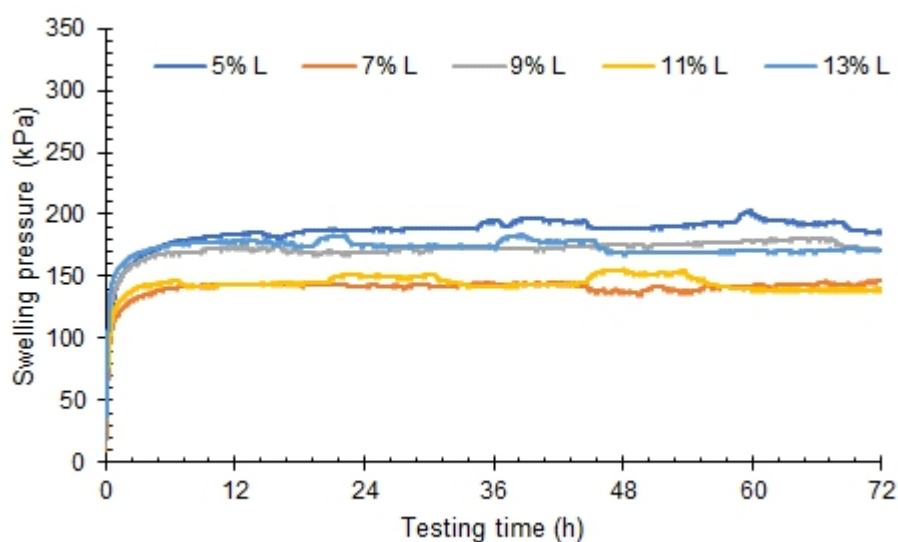


Figure 4.79: Evolution of swelling pressures of lime treated M4 specimens that were previously mellowed for 24h at 40°C

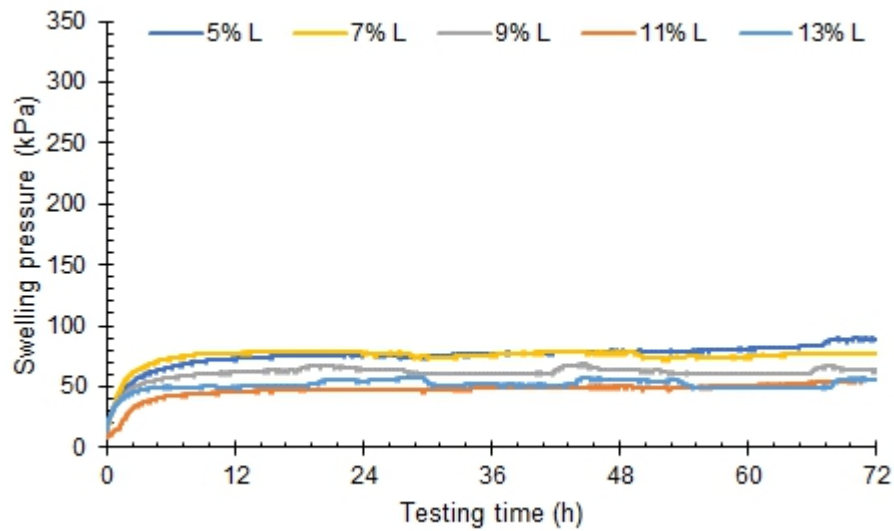


Figure 4.80: Evolution of swelling pressures of lime treated M4 specimens that were previously cured for 24h at 40°C

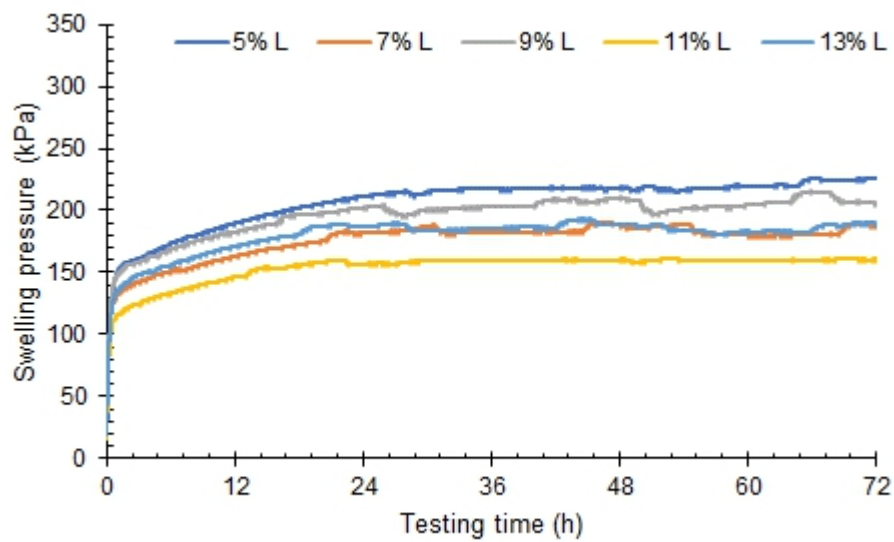


Figure 4.81: Evolution of swelling pressures of lime treated M4 specimens that were previously mellowed for 24h at 20°C

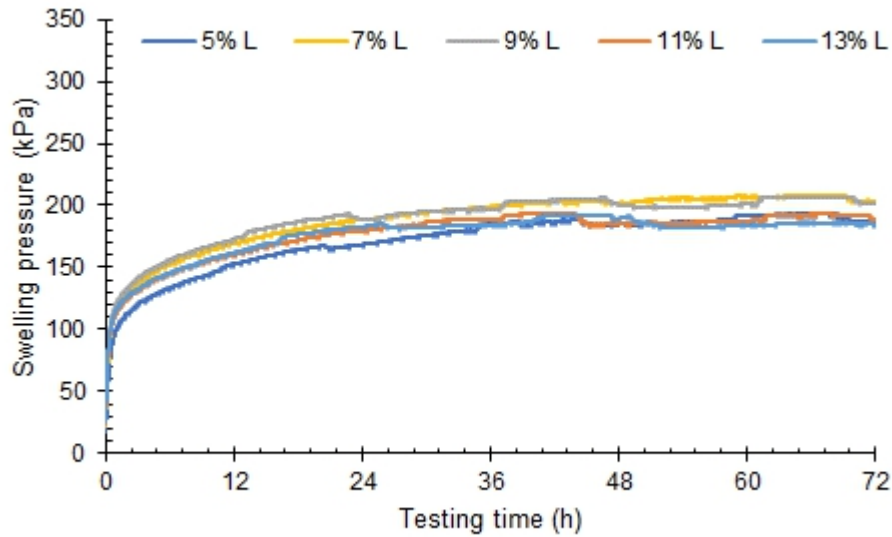


Figure 4.82: Evolution of swelling pressures of lime treated M4 specimens that were previously cured for 24h at 20°C

#### 4.5.5 Summary

The results confirm the role of 24h mellowing time in increasing the initial permeability coefficients of all lime treated specimens that contain bentonite clay. Such an increase in the permeability indicates the formation of such compounds during the first 24h render the mellowed specimens more porous compared with 24h cured specimens. The role of 24h mellowing diminishes as the bentonite content and the temperature declines. During the testing time, permeability coefficients declined exponentially as the time elapsed, and this reduction was less severe when the bentonite content was less. The strong evidence of the growth of such compounds also comes from disappearance of the swelling tendency for lime treated bentonite specimens that were previously cured at 40°C. The role of 24h curing in curbing the swelling tendency also declines as the bentonite content declines at the temperature of 20°C.

## **Chapter 5    Conclusions and future recommendations**

### **5.1    Conclusions**

The following are conclusions drawn out of each experimental series.

#### **5.1.1    Conclusions of series 1**

This series aims to i. assess the role of initial moisture content and dry unit weight on the swelling pressure and its characteristics, and ii. Propose and examine a modified testing procedure to overcome the deficiency of the wetting sequence on extremely low permeability high plastic clay, e.g. bentonite. Based on the results of this series, the following conclusions have been drawn;

- 1- Maximum swelling pressure was found to be dependent on the dry unit weight of the specimen. The relationship between dry unit weight and maximum swelling pressure took the shape of exponential. Further, the moisture content has no noticeable impact on the attained maximum swelling pressure.
- 2- The initial moisture content and dry unit weight govern the time required for the specimens to reach the maximum swelling pressure.
- 3- The swelling pressure behavior over time includes three phases (i.e., initial, intermediate, and equalization stages).
- 4- There is an interval at the beginning of the intermediate stage in which the value of the swelling pressure declined for specimens with a (hygroscopic) natural moisture content (i.e., 11%). This was attributed to the deficiency of wetting sequence using the conventional cell and was further resolved by using a hydraulic cell with a reduced specimen thickness and introduction of a back pressure at the base of the specimen during the test for carrying out the swelling pressure tests.

- 5- Both the time required to reach the equilibrium and the swelling behavior during intervals at the beginning of the intermediate stage were used as indicators to ensure the effectiveness of the adopted solution for i. accelerating the saturation of specimens, ii. decreasing the test duration and iii. removing the peak and post peak reduction in swelling pressure.

### **5.1.2 Conclusions of series 2**

In series 2, a comprehensive experimental programme was undertaken to investigate the impact of mellowing time at two different mellowed temperatures on hydraulic and mechanical properties of 7% lime-treated bentonite. Several conclusions are drawn out of the investigation;

- 1- Delaying compaction of lime treated expansive clays was found be destructive to the development of cementation compounds at particles contact and between clay flocs resulting in a substantial decline in the measured dry unit weight within the first 12h of compaction delay beyond which insignificant change in the measured dry unit weight was observed.
- 2- 7% lime treated bentonite specimens mellowed at the higher temperature of 40°C experienced an elevated reduction in the dry unit weight than those mellowed at a temperature of 20°C because higher temperature accelerates the rate of formation of cementitious compounds. The results suggest that the first 12h is the most crucial period for the development of bond and clay flocs. The decline in the dry unit weight was found to be independent of temperature after the first 12h of compaction delay.
- 3- The results illustrated that compaction delay has a harmful impact on the swelling tendency. The results illustrated that both compaction delay and ambient temperature have an impact on the swelling tendency and

attained swelling pressure when the 7% lime-treated specimens were tested without curing during the first 12h from mixing. However, the results revealed that specimens compacted immediately after mixing and left to cure for 24h experienced remarkable reduction by 97% in the observed swelling pressure.

- 4- In general, increasing mellowing period and environmental temperature led to an increased coefficient of permeability of lime treated expansive clays. However, the coefficient of permeability experienced a gradual decline with elapsed time from submersion due to the slow formation of cementitious compounds.
- 5- Coefficient of permeability experienced an increase by one order of magnitude with long compaction delay and when mellowed at 40°C.
- 6- The results illustrated that UCS is directly related to the duration of mellowing with a significant loss in UCS being occurred with a prolonged delay of compaction. The first 12h of compaction delay is being recognised as the most crucial period affecting the long term strength of lime stabilised expansive clay.
- 7- The strength gain is fast and temperature dependent during the first day, being relatively slow and time-dependent later on. Thus, enhanced strength could be achieved if the 7% lime treated specimen is cured carefully for the first 24h.
- 8- The axial strain of lime treated expansive clay was found to increase with the delay of compaction and be dependent on ambient temperature and period of curing.



Based on that, delaying the compaction of lime treated extremely high plastic clay should be avoided to preserve the cementitious compounds as it appears to be the primary contributor for enhancing strength and reducing swelling pressure of lime treated expansive clays.

### **5.1.3 Conclusions of series 3**

Series 3 was conducted to assess the impacts of lime content and environmental temperature on the physical, mechanical and hydraulic properties of lime treated bentonite clay. Several conclusions were drawn from this series;

- 1- Mellowing specimens at a temperature of 40 °C results in a higher drop in the attained dry unit weight providing availability of lime. Furthermore, drop in the dry unit weight when specimens were mellowed at 20 °C is not as substantial as that measured at 40 °C during the initial stage due to the accelerated formation of cementitious compounds at the higher temperature.
- 2- It is apparent that strength gain and dry unit weight follow a two-stage evolution irrespective of the environment temperature. Initially, a fast change occurs for a specific time depending on the availability of lime and the environment temperature. Subsequently, the change gets relatively slow and is lime-dependent after that. This behaviour should be taken into consideration when using the accelerated regime to predict the strength gain under normal condition.
- 3- The rate of strength gain on specimens cured at 40 °C is found to be significant at 8 times higher than that measured on specimens cured at 20 °C.

- 4- Results attained for the strength gain, and dry unit weight give a strong indication of concurrent chemical reactions in particular during the early stage of lime addition.
- 5- The lime content and environmental temperature have a significant impact on the hydraulic behaviour performance of lime treated clay. The decline in the permeability coefficient is found to be exponentially throughout the test

#### **5.1.4 Conclusions of series 4**

In series 4, four different types of clay with a wide range of liquid limit were mixed with different amounts of lime up to 25% by mass to examine and evaluate the mineralogical effects on the chemical process by monitoring the evolution of strength. Five sets of experiments were undertaken to test specimens with different lime contents at two different curing temperature for a period of curing time up to 28 days. A number of conclusions could be drawn out of this experimental series:

- 1- An immediate effect of lime on the strength of lime treated clays was evident in all specimens that were tested directly after compaction in comparison with those recorded on untreated specimens at the same dry unit weight. The results suggested that an increase of 2 ~ 3 times could be achieved with the addition of lime. However, the degree of improvement in the strength was not related to the amount of lime.
- 2- Lime treatment of bentonite and kaolinite clays showed recognisable differences during the period of curing and immediately after the initial strength gain at zero h of curing period. Bentonite clay reacted swiftly with lime leading to a significant and sustained degree of improvement in

the strength as time passed at 20°C and 40°C but with different rates. Nevertheless, specimens of treated ball clay (Kaolinite) showed that the strength gain entered in an idle phase in which no growth in strength was observed over the 672h of curing in particular at 20°C. Whereas the idle phase was shortened to only 72h when the curing temperature was raised to 40°C.

- 3- Since the ball clay comprised mainly of kaolinite minerals, the phenomenon of the accumulation of calcium cations species on the kaolinite surface caused obscuring the surfaces of mineral from the alkaline environment. Such accumulation led to a delay in the release of alumina and silica and thus delaying the formation of cementitious compounds. However, the mechanism by which the accumulation of calcium was reduced or eliminated at 40°C so that the alkaline environment was allowed to attack the surface of mineral and thus to launch the alumina and silica in order to form the cementitious compounds that are responsible for the strength gain, deserves further investigations.
- 4- The addition of Bentonite to ball clay with a ratio of 1:3 and 1:1 to form M3 and M4 materials was found successful in eliminating the idle phase in the strength gain over the curing period. Bentonite would act as a competing consumer for the incoming calcium ions to the system, eliminating or even reducing the accumulation of the calcium ions on the surface of kaolinite minerals. This led to a gradual improvement in the strength but at a slower rate.

- 5- The results showed that the strength gain throughout curing went through two stages process. The first stage was recognised by a fast strength gain, followed by a second stage in which a slower strength gain occurred. The two stages were very prominent at the high curing temperature of 40°C. The time for stage 1 of strength gain was dependent upon the curing temperature, lime content and mineralogy of clay. It increased with higher lime content and increased bentonite portion.
- 6- Despite the use of quadratic equations to best fit stage 1 of strength gain, the numerical coefficients for the second order term were found to be negligible. Simplifying the equations into straight lines assisted with comparing the rate of strength gain.
- 7- During stage 1 of strength gain, the rate of strength gain at the high curing temperature of 40°C was found to be about 8 times that observed at the low curing temperature of 20°C. At the same temperatures, the ratio between the rates of strength gain was very dependent upon the clay mineralogy. The kinetic of strength gain of lime treated bentonite clay was about 2 and 7 times the kinetic of strength gain of lime treated clays with 50 and 25% bentonite content, respectively.
- 8- The failure pattern was found to change throughout curing owing to the strength of treated specimens. Classical shear failure was imminent on all specimens that were cured for a short period up to 24h. A combined shear and cone-split occurred on specimens that were cured for up to 72h and then cone-split failure pattern was observed on all specimens

that were cured for long periods. This was in harmony with the change in behaviour from ductile to brittle with further curing.

#### **5.1.5 Conclusions of series 5**

In series 5, four different types of clay with a wide range of liquid limit were mixed with different lime content up to 13% by mass to inspect and assess the mineralogical effects on the chemical process in short through monitoring the evolution of swelling and permeability characteristics. Five sets of experiments were performed to test specimens that previously spent 24h in either a loose or compacted state at different curing temperature of (20 and 40°C) before testing for 72hours under room temperature. A number of conclusions could be drawn out of this experimental series:

- 1- For untreated specimens, the increase in the bentonite content results in a reduction in the permeability and an increase in the swelling pressure.
- 2- Mixing bentonite with ball clay in different proportion showed that as the bentonite content decline, liquid limit and maximum dry unit weight also decline, but the optimum moisture content increases
- 3- The initial permeability coefficients of all lime-treated specimens showed an increase compared to the permeability coefficients of untreated specimens. Such increases in the permeability coefficient values were more noticeable as the content of bentonite increased.
- 4- Previously mellowed specimens registered higher initial coefficient of permeability compared with previously cured specimens.
- 5- The magnitude of difference in the values of initial permeability coefficients between previously cured and mellowed specimens as well

as between mellowed specimens at 20 and 40°C declined as the bentonite content declined.

- 6- The permeability coefficients of the lime-treated specimens that contain bentonite showed exponential reduction till the end of testing time, giving a sign on the growth of compounds in the available pores reducing the effective porosity.
- 7- The rates of decay in the permeability become less severe as the bentonite content declines.
- 8- The permeability of lime treated ball clay showed stability or stability for a period followed by a marginal decline during the testing time.
- 9- In general, the lime treaded specimens that contain bentonite showed a reduction in the maximum swelling pressures compared with untreated specimens.
- 10-The reduction in the maximum swelling pressures was more significant with the specimens that were previously cured at 40°C compared with those previously cured at 20°C. Such behaviour gives in an indication of the formation of cementitious compounds in compacted state work on curbing the swelling tendency. The formation of such compounds seems to be much higher with lime-treated bentonite clay and decline with the decline of bentonite content.
- 11- Regarding to ball clay specimens, there is no difference in the values of maximum swelling pressures of all lime-treated specimens compared to the maximum swelling pressure of the untreated specimen. Indeed, this refers to that there is no growth of cementitious compounds during the first 24h even under 40°C with lime-treated ball clay.

#### **5.1.6 Main conclusion**

The key conclusion of the current investigation is that the timing of the beginning of changes and the vitality of such changes in mechanical and hydraulic characteristics that are accompanied by the formation of cementitious compounds and its kinetics depend mainly on the mineralogy composition of lime treated clay and the surrounding temperature. Furthermore, at a given surrounding temperature, the continuity of such changes in the characteristics of a given lime-treated clay depends on the availability of lime.

## **5.2 Future work**

The findings of the current research help to better understand the changes in the behaviour of lime treated clay using geotechnical approaches. However, there is several undiscovered points need further effort and time to be covered. These points could be abbreviated as follow:

- 1- In this research, the constant volume method was used to measure the swelling pressure of bentonite at various dry unit weights and moisture contents. In addition to introducing a successful solution to overcome the sequence of wetting deficiency and reduce the testing time. However, there is an actual need to evaluate the role that is played by a liquid limit in determining the resulting maximum swelling pressure. The liquid limit is used by the British standard as an indicator to determine the suitability of the soil for construction. In the current research, the liquid limit of bentonite was reduced by mixing the bentonite and ball clay in different proportions. To differentiate the role of liquid limit from the role of mineralogy composition, it can be chosen two types of swelling clays that naturally have two different liquid limits, for instance, 100 and 200%. The sodium bentonite and ball clay should be mixed to obtain two mixtures with two liquid limits like liquid limits of two chosen natural clays. After which, the two clays and two resulting mixtures should be tested for various dry unit weights to determine the resulting maximum swelling pressure at each dry unit weight. Then for each clay type, the resulting maximum swelling pressures are plotted against the corresponding dry unit weights, and thus it can be evaluated the role of liquid limit by comparison between the resulting curves from the natural clays and clay



mixtures that are mixed to simulate the liquid limits of the chosen natural clays.

- 2- The effect of mellowing time in term of the loss of strength gain was evaluated with 7% lime content at 20 and 40°C, and there is a need to repeat the experimental programme with higher lime contents (> 7% of lime) with sodium bentonite clay. Furthermore, it can be the same experimental programme with the non-active clay such ball clay in order to obtain a full picture on the impact of various mellowing time in the resulting strength. Regarding using the permeability as an approach to monitor the formation of cementitious compounds. All permeability tests in the current study were conducted in the room temperature, and this was considered as a drawback hence it is well known that the effect of temperature has a significant impact on the formation of cementations compounds, and the temperature was a little bit fluctuant. Therefore, in the future work, the innovative programme should be repeated so that the permeability tests should be performed at a temperature similar to the temperature during the 24h mellowing.

## References:

- AASHTO 2008. Mechanistic-empirical pavement design guide (MEPDG): A manual of practice,. Washington, DC.
- Adefemi, B. A. & Wole, A. C. 2013. Regression Analysis of Compaction Delay on CBR and UCS of Lime Stabilized Yellowish Brown Lateritic Soil.
- Al-Alwan, A. A. K. 2019. *Undrained shear strength of ultra-soft soils admixed with lime*. University of Glasgow.
- Al-Mukhtar, M., Khattab, S. & Alcover, J.-F. 2012. Microstructure and geotechnical properties of lime-treated expansive clayey soil. *Engineering Geology*, 139, 17-27.
- Al-Mukhtar, M., Lasledj, A. & Alcover, J.-F. 2010a. Behaviour and mineralogy changes in lime-treated expansive soil at 20 °C. *Applied Clay Science*, 50, 191-198.
- Al-Mukhtar, M., Lasledj, A. & Alcover, J.-F. 2010b. Behaviour and mineralogy changes in lime-treated expansive soil at 50 °C. *Applied Clay Science*, 50, 199-203.
- Al-Mukhtar, M., Lasledj, A. & Alcover, J. F. 2014. Lime consumption of different clayey soils. *Applied Clay Science*, 95, 133-145.
- Al-Rawas, A. A. & Goosen, M. F. A. 2006. *Expansive soils: recent advances in characterization and treatment*, London, Taylor & Francis.
- ASTM C39 / C39M - 18 Standard Test Method for Compressive Strength of Cylindrical Concrete Specimens. .
- ASTM C618 - 19 Standard Specification for Coal Fly Ash and Raw or Calcined Natural Pozzolan for Use in Concrete.
- ASTM D3551 - 17 Standard Practice for Laboratory Preparation of Soil-Lime Mixtures Using Mechanical Mixer.
- ASTM D6276 -19 Standard Test Method for Using pH to Estimate the Soil-Lime Proportion Requirement for Soil Stabilization.

- ASTM D 698 - 12e2 Standard Test Methods for Laboratory Compaction Characteristics of Soil Using Standard Effort (12,400 ft-lbf/ft<sup>3</sup> (600 kN-m/m<sup>3</sup>)).
- Bagoniza, S., Peete, J. M., Freer-Hewish, R. & Newill, D. 1987. Carbonation of stabilised soil-cement and soil-lime mixtures.
- Baille, W., Tripathy, S. & Schanz, T. 2010. Swelling pressures and one-dimensional compressibility behaviour of bentonite at large pressures. *Applied Clay Science*, 48, 324-333.
- Barnes, G. E. 2000. *Soil mechanics: principles and practice*, London, Macmillan.
- Bauer, A. & Berger, G. 1998. Kaolinite and smectite dissolution rate in high molar KOH solutions at 35° and 80°C. *Applied Geochemistry*, 13, 905-916.
- Beetham, P., Dijkstra, T. & Dixon, N. 2014. Lime diffusion and implications for lime stabilization practice. *Compendium of Papers from the Transportation Research Board 93rd Annual Meeting, Washington DC*. 14-5734 ed.: TRB, USA .
- Beetham, P., Dijkstra, T., Dixon, N., Fleming, P., Hutchison, R. & Bateman, J. 2015. Lime stabilisation for earthworks: a UK perspective. *Proceedings of the Institution of Civil Engineers - Ground Improvement*, 168, 81-95.
- Bell, F. G. 1988. Stabilisation and treatment of clay soils with lime. Part 1-basic principles. *Ground Engineering*, 21.
- Bell, F. G. 1996. Lime stabilization of clay minerals and soils. *Engineering Geology*, 42, 223-237.
- Bergaya, F. & Lagaly, G. 2006. General introduction: clays, clay minerals, and clay science. *Developments in clay science*. Elsevier.
- Bhattacharja, S., Bhatta, J. I. & Todres, H. A. 2003. Stabilization of clay soils by Portland cement or lime-A critical review of literature. *Research and Development Serial No. 2066, Portland Cement Association, Skokie, USA*, 60.
- Boardman, D. I., Glendinning, S. & Rogers, C. D. F. 2001. Development of stabilisation and solidification in lime-clay mixes. *Géotechnique*, 51, 533-543.

- Bozbey, İ. 2017. Microfabric Evaluation of Lime-Treated Clays by Mercury Intrusion Porosimetry and Environment Scanning Electron Microscopy. *International Journal of Civil Engineering*.
- Bozbey, I. & Garaisayev, S. 2010. Effects of soil pulverization quality on lime stabilization of an expansive clay. *Environmental Earth Sciences*, 60, 1137-1151.
- Brigatti, M. F., Galan, E. & Theng, B. K. G. 2006. Structures and mineralogy of clay minerals. *Developments in clay science*. Elsevier.
- BS1924-2:1990 1990. Stabilized Materials for Civil Engineering Purposes. *Part 2: Methods of test for cement-stabilized and lime-stabilized materials*. BSI, London, UK.
- BS 1377-2:1990 1998. Methods of test for Soils for civil engineering purposes *Part 2: Classification tests, 5: Determination of the plastic limit and plasticity index*. BSI, London, UK.
- BS 1377-4:1990 2002. Methods of test for Soils for civil engineering purposes. *Part 4: Compaction-related tests, 3: Determination of dry density/moisture content relationship, 3.3: Method using 2.5 kg rammer for soils with particles up to medium-gravel size*. BSI, London, UK.
- BS 1377-6:1990 1999. Methods of test for Soils for civil engineering purposes. *Part 2: Consolidation and permeability tests in hydraulic cells and with pore pressure measurement, 4: Determination of permeability in a hydraulic consolidation cell*. BSI, London, UK.
- BS 1924-1:1990 1998. Stabilized materials for civil engineering purposes. *Part 1: General requirements, sampling, sample preparation and tests on materials before stabilization*. BSI 389 Chiswick High Road London W4 4AL: BSI.
- BS EN 459-1:2015 2015. Building lime Part 1: Definitions, specifications and conformity criteria. BSI, London, UK.

- BS EN 13286-2:2010 2013. Unbound and hydraulically bound mixtures. *Part 2: Test methods for laboratory reference density and water content-Proctor compaction*. BSI, London, UK.
- Budhu, M. 2000. *Soil mechanics and foundations*, Chichester; New York, John Wiley.
- Chemedá, Y. C., Deneele, D., Christidis, G. E. & Ouvrard, G. 2015. Influence of hydrated lime on the surface properties and interaction of kaolinite particles. *Applied Clay Science*, 107, 1-13.
- Chemedá, Y. C., Deneele, D. & Ouvrard, G. 2018. Short-term lime solution-kaolinite interfacial chemistry and its effect on long-term pozzolanic activity. *Applied Clay Science*, 161, 419-426.
- Cherian, C. & Arnepalli, D. N. 2015. A critical appraisal of the role of clay mineralogy in lime stabilization. *International Journal of Geosynthetics and Ground Engineering*, 1, 8.
- Consoli, N. C., Lopes Jr, L. d. S., Prietto, P. D. M., Festugato, L. & Cruz, R. C. 2011. Variables Controlling Stiffness and Strength of Lime-stabilized Soils. *Journal of Geotechnical and Geoenvironmental Engineering*, 137, 628-632.
- Consoli, N. C., Lopes, L. d. S. & Heineck, K. S. 2009. Key Parameters for the Strength Control of Lime Stabilized Soils. *Journal of Materials in Civil Engineering*, 21, 210-216.
- Cristelo, N., Glendinning, S., Fernandes, L. & Pinto, A. T. 2012. Effect of calcium content on soil stabilisation with alkaline activation. *Construction and Building Materials*, 29, 167-174.
- Dash Sujit, K. & Hussain, M. 2012. Lime Stabilization of Soils: Reappraisal. *Journal of Materials in Civil Engineering*, 24, 707-714.
- Davidson, L. K., Demirel, T. & Handy, R. L. 1965. Soil pulveration and lime migration in soil-lime stabilization. *Highway Research Record*.

- De Windt, L., Deneele, D. & Maubec, N. 2014. Kinetics of lime/bentonite pozzolanic reactions at 20 and 50 C: Batch tests and modeling. *Cement and Concrete Research*, 59, 34-42.
- Di Sante, M., Fratalocchi, E., Mazzieri, F. & Brianzoni, V. 2015. Influence of delayed compaction on the compressibility and hydraulic conductivity of soil–lime mixtures. *Engineering Geology*, 185, 131-138.
- Di Sante, M., Fratalocchi, E., Mazzieri, F. & Pasqualini, E. 2014. Time of reactions in a lime treated clayey soil and influence of curing conditions on its microstructure and behaviour. *Applied Clay Science*, 99, 100-109.
- Diamond, S. & Kinter, E. B. 1965. Mechanisms of soil-lime stabilization. *Highway Research Record*.
- Diamond, S. & Kinter, E. B. 1966. Adsorption of calcium hydroxide by montmorillonite and kaolinite. *Journal of Colloid and Interface Science*, 22, 240-249.
- Driscoll, R. M. C. & Crilly, M. 2000. *Subsidence damage to domestic buildings: lessons learned and questions remaining*, CRC.
- Estabragh, A. R., Rafatjo, H. & Javadi, A. A. 2014. Treatment of an expansive soil by mechanical and chemical techniques. *Geosynthetics International*, 21, 233-243.
- Fang, H.-Y. & Daniels, J. L. 2006. *Introductory geotechnical engineering: an environmental perspective*, CRC Press.
- Gallage, C., Cochrane, M. & Ramanujam, J. 2012. Effects of lime content and amelioration period in double lime application on the strength of lime treated expansive sub-grade soils. *Advances in Transportation Geotechnics II*, 99-104.
- Gao, Y., Qian, H., Li, X., Chen, J. & Jia, H. 2018. Effects of lime treatment on the hydraulic conductivity and microstructure of loess. *Environmental Earth Sciences*, 77, 529.
- Grim, J. L. E. R. E. & Eades, J. L. 1966. A Quick Test to Determine Lime Requirements of Lime Stabilisation. *Highway Research Record*, 139, 61-72.

- Grisolia, M., Leder, E. & Marzano, I. P. Standardization of the molding procedures for stabilized soil specimens as used for QC/QA in Deep Mixing application. 2013 2013. 2481-2484.
- Guggenheim, S. & Martin, R. T. 1995. *Definition of clay and clay mineral: joint report of the AIPEA nomenclature and CMS nomenclature committees* [Online]. [Long Island City, NY]: Pergamon Press 1968-. [Accessed 2 43].
- Hashemi, M. A., Massart, T. J. & François, B. 2018. Experimental characterisation of clay-sand mixtures treated with lime. *European Journal of Environmental and Civil Engineering*, 22, 962-977.
- He, C., Osbaeck, B. & Makovicky, E. 1995. Pozzolanic reactions of six principal clay minerals: Activation, reactivity assessments and technological effects. *Cement and Concrete Research*, 25, 1691-1702.
- Head, K. H. 1992. *Manual of soil laboratory testing: Vol.1, Soil classification and compaction tests*, London, Pentech.
- Holt, C. C. & Freer-Hewish, R. J. 1998. The use of lime-treated British clays in pavement construction. Part 1. The effect of mellowing on the modification process. *Proceedings of the Institution of Civil Engineers-Transport*, 129, 228-239.
- Holt, C. C., Freer-Hewish, R. J. & Ghataora, G. S. 2000. The use of lime-treated British clays in pavement construction. Part 2: The effect of mellowing on the stabilization process. *Proceedings of the Institution of Civil Engineers - Transport*, 141, 207-216.
- Imbert, C. & Villar, M. V. 2006. Hydro-mechanical response of a bentonite pellets/powder mixture upon infiltration. *Applied Clay Science*, 32, 197-209.
- Ingles, O. G. & Metcalf, J. B. 1972. *Soil stabilization: principles and practice*, Butterworths.

- Jayalath, C. P. G., Gallage, C. & Miguntanna, N. S. 2016. Factors affecting the swelling pressure measured by the oedometer method. *International Journal*, 11, 2397-2402.
- Jucai, D. 2014. Investigation of aggregates size effect on the stiffness of lime and/or cement treated soils: from laboratory to field conditions.
- Kitazume, M. & Terashi, M. 2013. *The deep mixing method*, CRC press.
- Köhler, S., Heinz, D. & Urbonas, L. 2006. Effect of ettringite on thaumasite formation. *Cement and Concrete Research*, 36, 697-706.
- Komine, H. & Ogata, N. 1994. Experimental study on swelling characteristics of compacted bentonite. *Canadian geotechnical journal*, 31, 478-490.
- Konan, K. L., Peyratout, C., Smith, A., Bonnet, J. P., Rossignol, S. & Oyetola, S. 2009. Comparison of surface properties between kaolin and metakaolin in concentrated lime solutions. *Journal of Colloid and Interface Science*, 339, 103-109.
- Li, J., Wu, X. & Hou, L. 2014. Physical, Mineralogical, and Micromorphological Properties of Expansive Soil Treated at Different Temperature. *Journal of Nanomaterials*, 2014.
- Little, D. N., Nair, S. & Herbert, B. 2010. Addressing Sulfate-Induced Heave in lime Treated Soils. *Journal of geotechnical and geoenvironmental engineering*, 136, 110-118.
- Little, D. N., Scullion, T., Kota, P. & Bhuiyan, J. 1995. Guidelines for mixture design and thickness design for stabilized bases and subgrades.
- Locat, J., Bérubé, M.-A. & Choquette, M. 1990. Laboratory investigations on the lime stabilization of sensitive clays: shear strength development. *Canadian Geotechnical Journal*, 27, 294-304.
- Martin, R. T., Bailey, S. W., Eberl, D. D., Fanning, D. S., Guggenheim, S., Kodama, H., Pevear, D. R., Srodon, J. & Wicks, F. J. 1991. Report of the clay minerals



- society nomenclature committee; revised classification of clay materials. *Clays and Clay Minerals*, 39, 333-335.
- Maubec, N., Deneele, D. & Ouvrard, G. 2017. Influence of the clay type on the strength evolution of lime treated material. *Applied Clay Science*, 137, 107-114.
- McCallister, L. & Petry, T. 1992. Leach Tests on Lime-Treated Clays. *Geotechnical Testing Journal*, Vol. 15, pp. 106-114.
- McNally, G. 1998. *Soil and rock construction materials*, London, CRC Press.
- Metelková, Z., Bohác, J., Sedlářová, I. & Prikryl, R. Changes of pore size and of hydraulic conductivity by adding lime in compacting clay liners. Geotechnical engineering: new horizons, Proceedings of the 21st European Young Geotechnical Engineers Conference, Rotterdam, 2011 2011 Amsterdam: IOS Press; 2011. 93-8.
- Mirzababaei, M., Miraftab, M., Mohamed, M. & McMahon, P. 2013. Impact of Carpet Waste Fibre Addition on Swelling Properties of Compacted Clays. *Geotechnical and Geological Engineering*, 31, 173-182.
- Mirzababaei, M., Yasrobi, S. & Al-Rawas, A. 2009. Effect of polymers on swelling potential of expansive soils. *Proceedings of the Institution of Civil Engineers - Ground Improvement*, 162, 111-119.
- Mitchell, J. K. & Hooper, D. R. 1961. Influence of time between mixing and compaction on properties of a lime-stabilized expansive clay. *Highway Research Board Bulletin*.
- Mitchell, J. K. & Soga, K. i. 2005. *Fundamentals of soil behavior*, Hoboken, N.J, John Wiley & Sons.
- Mohd Yunus, N. Z., Wanatowski, D., Stace, R., Marto, A., Abdullah, R. A. & Mashros, N. 2014. A short review of the factors influencing lime-clay reactions. *Electronic Journal of Geotechnical Engineering*, 19 V, 6269-6282.

- Mooney, M. A. & Toohey, N. M. 2010. Accelerated curing and strength-modulus correlation for lime-stabilized soils. Colorado Department of Transportation, DTD Applied Research and Innovation Branch.
- Nalbantoglu, Z. & Tuncer, E. R. 2001. Compressibility and hydraulic conductivity of a chemically treated expansive clay. *Canadian Geotechnical Journal*, 38, 154-160.
- Nasrizar, A., Muttharam, M. & Illamparuthi, K. 2010. Effect of placement water content on the strength of temperature cured lime treated expansive soil. *GeoShanghai 2010*.
- Nasrizar, A. A., Ilamparuthi, K. & Muttharam, M. 2012. Quantitative Models for Strength of Lime Treated Expansive Soil. *American Society of Civil Engineers, GeoCongress*, 978-987.
- NLA. 2007. *Lime Terminology, Standards & Properties* [Online]. National Lime Association.  
Available:[http://lime.org/documents/publications/free\\_downloads/fact-properties2007rev.pdf](http://lime.org/documents/publications/free_downloads/fact-properties2007rev.pdf).
- Ochepo, J., Osinubi, K. J. & Sadeeq, J. A. Statistical Evaluation of the Effect of Elapse time on the Strength Properties of Lime-Bagasse Ash Treated Black Cotton Soil. 2013 2013. ESRSA Publications.
- Olphen, H. V. 1963. *An introduction to clay colloid chemistry, for clay technologists, geologists, and soil scientists*, J. Wiley, New York.
- Osinubi, K. J. 1998. Influence of Compactive Efforts and Compaction Delays on Lime-Treated Soil. *Journal of Transportation Engineering*, 124, 149-155.
- Osinubi, K. J. & Nwaiwu, C. M. O. 2006. Compaction delay effects on properties of lime-treated soil. *Journal of Materials in Civil Engineering*, 18, 250-258.
- Paige-Green, P. 2009. Reassessment of problems affecting stabilized layers in roads in South Africa.

- Pakbaz, M. S. & Farzi, M. 2015. Comparison of the effect of mixing methods (dry vs. wet) on mechanical and hydraulic properties of treated soil with cement or lime. *Applied Clay Science*, 105–106, 156-169.
- Pansu, M. & Gautheyrou, J. 2007. *Handbook of soil analysis: mineralogical, organic and inorganic methods*, Springer Science & Business Media.
- Petry, T. M. & Wohlgemuth, S. K. 1988. Effects of pulverization on the strength and durability of highly active clay soils stabilized with lime and Portland cement. *Transportation Research Board*, p. 38-45.
- Pomakhina, E., Deneele, D., Gaillot, A.-C., Paris, M. & Ouvrard, G. 2012. <sup>29</sup>Si solid state NMR investigation of pozzolanic reaction occurring in lime-treated Ca-bentonite. *Cement and concrete research*, 42, 626-632.
- Rao, S. M. & Shivananda, P. 2005. Role of curing temperature in progress of lime-soil reactions. *Geotechnical & Geological Engineering*, 23, 79-85.
- Ren, J., Shen, Z.-z., Yang, J., Zhao, J. & Yin, J.-n. 2014. Effects of Temperature and Dry Density on Hydraulic Conductivity of Silty Clay under Infiltration of Low-Temperature Water. *Arabian Journal for Science and Engineering*, 39, 461-466.
- Rogers, C. D. F. & Roff, T. E. J. 1997. Lime modification of clay soils for construction expediency. *Proceedings of the Institution of Civil Engineers - Geotechnical Engineering*, 125, 242-249.
- Saad, S., Mirzababaei, M., Mohamed, M. & Miraftab, M. Uniformity of density of compacted fibre reinforced clay soil samples prepared by static compaction. The 5th European Geosynthetics Congress. Valencia, Spain 2012.
- Saldanha, R. B. & Consoli, N. C. 2016. Accelerated Mix Design of Lime Stabilized Materials. *Journal of Materials in Civil Engineering*, 28, 06015012.
- Schanz, T. & Elsayy, M. B. D. 2015. Swelling characteristics and shear strength of highly expansive clay–lime mixtures: A comparative study. *Arabian Journal of Geosciences*, 8, 7919-7927.

- Schanz, T. & Tripathy, S. 2009. Swelling pressure of a divalent-rich bentonite: Diffuse double-layer theory revisited. *Water Resources Research*, 45.
- Shi, B., Jiang, H., Liu, Z. & Fang, H. Y. 2002. Engineering geological characteristics of expansive soils in China. *Engineering Geology*, 67, 63-71.
- Singh, J., Huang, P. M., Hammer, U. T. & Liaw, W. K. 1996. Influence of citric acid and glycine on the adsorption of mercury (II) by kaolinite under various pH conditions. *Clays and clay minerals*, 44, 41-48.
- Soltani, A., Deng, A., Taheri, A. & Mirzababaei, M. 2017. A sulphonated oil for stabilisation of expansive soils. *International Journal of Pavement Engineering*, 1-14.
- Sridharan, A. & Nagaraj, H. B. 2005. Plastic limit and compaction characteristics of finegrained soils. *Proceedings of the Institution of Civil Engineers - Ground Improvement*, 9, 17-22.
- Sridharan, A. & Prakash, K. 2000. Classification procedures for expansive soils. *Proceedings of the ICE-Geotechnical Engineering*, 143, 235-240.
- Sridharan, A., Rao, S. M. & Murthy, N. S. 1988. Liquid limit of kaolinitic soils. *Géotechnique*, 38, 191-198.
- Strawn, D. G., Bohn, H. L. & O'Connor, G. A. 2015. *Soil chemistry*, John Wiley & Sons.
- Sweeney, D. A., Wong, D. K. H. & Fredlund, D. G. 1988. Effect of lime on highly plastic clay with special emphasis on aging. *Transportation Research Record*, 1190, 13-23.
- Thyagaraj, T., Samuel, Z. & Kumar, K. S. R. 2016. Relative efficiencies of electrolytes in stabilization of an expansive soil. *International Journal of Geotechnical Engineering*, 10, 107-113.
- Toohey, N. M., Mooney, M. A. & Bearce, R. G. 2013. Stress-Strain-Strength Behavior of Lime-Stabilized Soils during Accelerated Curing. *Journal of Materials in Civil Engineering*, 25, 1880-1886.

- Tran, T. D., Cui, Y.-J., Tang, A. M., Audiguier, M. & Cojean, R. 2014. Effects of lime treatment on the microstructure and hydraulic conductivity of Héricourt clay. *Journal of Rock Mechanics and Geotechnical Engineering*, 6, 399-404.
- Verhasselt, A. F. 1990. The Nature of the Immediate Reaction of Lime in Treating Soils for Road Construction. *Physico-Chemical Aspects of Soil and Related Materials*.
- Villar, M. V. & Lloret, A. 2004. Influence of temperature on the hydro-mechanical behaviour of a compacted bentonite. *Applied Clay Science*, 26, 337-350.
- Villar, M. V. & Lloret, A. 2008. Influence of dry density and water content on the swelling of a compacted bentonite. *Applied Clay Science*, 39, 38-49.
- Vitale, E., Deneele, D., Paris, M. & Russo, G. 2017. Multi-scale analysis and time evolution of pozzolanic activity of lime treated clays. *Applied Clay Science*, 141, 36-45.
- Vitale, E., Deneele, D. & Russo, G. 2016a. Multiscale Analysis on the Behaviour of a Lime Treated Bentonite. *Procedia Engineering*, 158, 87-91.
- Vitale, E., Deneele, D., Russo, G. & Ouvrard, G. 2016b. Short-term effects on physical properties of lime treated kaolin. *Applied Clay Science*, 132-133, 223-231.
- Vitale, E., Russo, G. & Deneele, D. Multi-scale analysis on the effects of lime treatment on a kaolinite soil. 2016 2016c. 17-18.
- Whitlow, R. 2001. *Basic soil mechanics*, Harlow, Prentice Hall.
- Wild, S., Arabi, M. & Rowlands, G. O. 1987. Relation between pore size distribution, permeability, and cementitious gel formation in cured clay–lime systems. *Materials science and technology*, 3, 1005-1011.
- Yigzaw, Z. G., Cuisinier, O., Massat, L. & Masrouri, F. 2016. Role of different suction components on swelling behavior of compacted bentonites. *Applied Clay Science*, 120, 81-90.
- Zhang, D., Zhou, C.-H., Lin, C.-X., Tong, D.-S. & Yu, W.-H. 2010. Synthesis of clay minerals. *Applied Clay Science*, 50, 1-11.

Zhao, H., Liu, J., Guo, J., Zhao, C. & Gong, B.-w. 2015. Reexamination of Lime Stabilization Mechanisms of Expansive Clay. *Journal of Materials in Civil Engineering*, 27.